DOMENICA TORINO

DESIGN, SYNTHESIS, CONFORMATIONAL STUDY AND BIOLOGICAL EVALUATION OF STRUCTURAL ANALOGUES OF NATIVE BIOACTIVE PEPTIDES

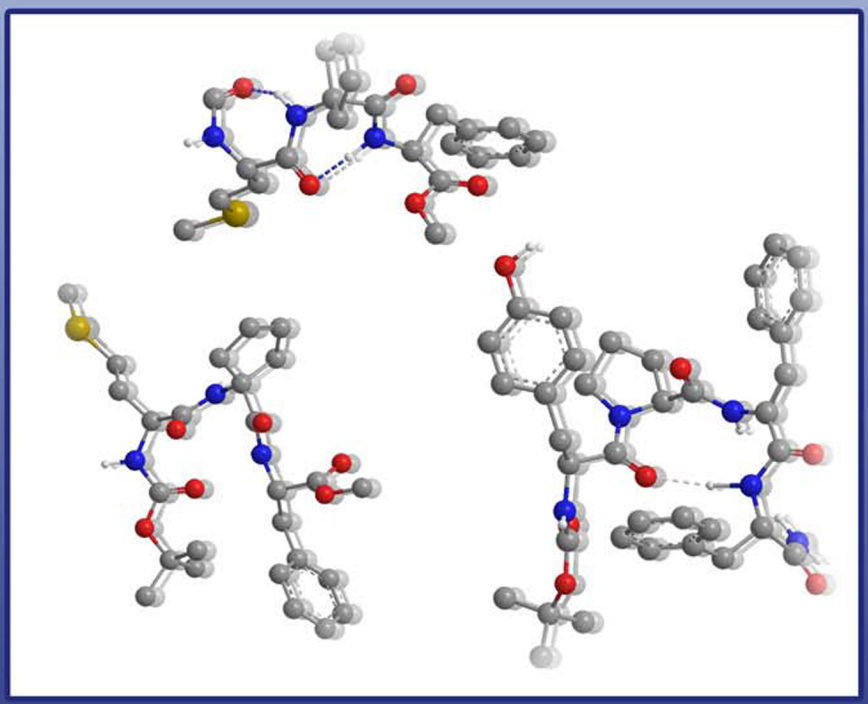

SAPIENZA
UNIVERSITÀ DI ROMA
facoltà di farmacia
Dipartimento di Chimica
e Tecnologie del Farmaco

PhD Thesis in Pharmaceutical Sciences
XXII cycle

Design, synthesis, conformational study and biological evaluation of structural analogues of native bioactive peptides

Tutors

Chiar.mo Prof. Gino LUCENTE
Chiar.mo Prof. Enrico MORERA

PhD student

Dr. Domenica TORINO

2006-2009

To my mother

Contents

INTRODUCTION

Peptides and peptidomimetics

Peptides play an important role in the organism as neurotransmitters, neuromodulators, hormones, antibiotics, growth promoters and inhibitors, cytokines, antigens, etc. They are known to influence essentially all vital physiological processes *via* inter- and intra-cellular communication, and signal transduction, mediated through various classes of receptors. The study of the peptides has acquired a key role in medicinal chemistry and a multitude of biologically active peptides have been discovered and characterized during the last decades.

The main objective of the peptide research is centered on elucidation and understanding of the relationships between the peptide three-dimensional structure (3D) and its biological activity. Since the initial event for the biological response is the molecular recognition, it is necessary that a portion of the surface of the ligand (*pharmacophore*), obtained by studying its 3D structure, can interact with a complementary surface of the acceptor/receptor molecule. The pharmacophore can involve both a continuous sequence of amino acids (*sychnologic* organization) or amino acid residues separated from each other within the primary structure (*rhegnylogic* organization) but near on the surface by the 3D structure of the polypeptide. In either cases, the peptide backbone functions as a scaffold for the key

side chain groups involved in the interaction and, in some cases, also acts as a hydrogen bond donor and/or acceptor in the molecular recognition (binding). In all cases, the side chain moieties involved directly in the binding are critical for the interaction, and their 3D architecture (topography) and stereoelectronic properties are needed for an efficient molecular recognition.[1]

Although native biologically active peptides have a great potential for therapeutical applications, their use as drugs is limited by different factors: a) low metabolic stability towards proteolysis in the grastrointestinal tract and in serum; b) poor absorption after oral ingestion, in particular due to their relatively high molecular weight and/or the lack of specific transport systems; c) rapid excretion through liver and kidneys.[2] Furthermore, a) the peptides generally are relatively small, conformationally flexible, molecule. Their interaction with different receptors can then cause undesired effects in several types of cells and organ systems. Peptide receptors and/or isoreceptors are in fact widely distributed in the organisms (Figure 1); b) the primary structure and conformation of most membrane-bound peptide receptors is still not known and efforts to clone these systems have a slow progress; c) the 3D structure of peptide ligands, either free or bound to the receptor/acceptor, is not generally known.[3]

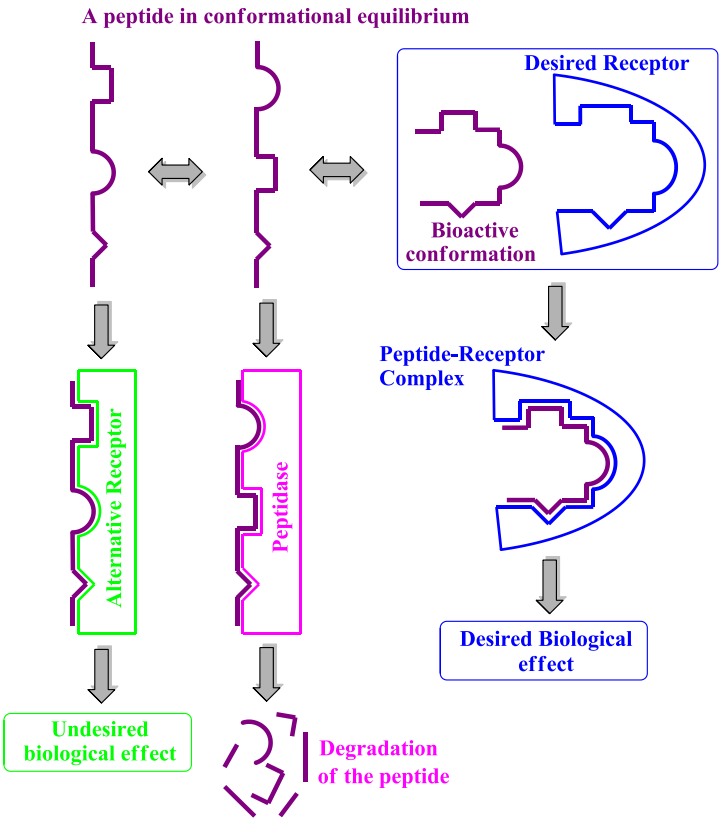

Figure 1. Peptide in conformational equilibrium.

In order to circumvent the above cited limitations, connected with the use of peptides as therapeutic agents, peptidomimetics also known "Trojan horses", can help to solve the problem. These compounds can be described, at the molecular level, as models designed so as to have pharmacophoric stereostructural elements able to mimic the correspondent 3D elements of native peptides in their 3D space. These structural features can improve, with equivalent or superior efficacy, the binding, the

biological activity as agonist (or antagonist), and the understanding of the structure-activity relationships. In comparison with native peptides, peptidomimetics may show higher receptor affinity and selectivity, higher metabolic stability, better bioavailability and enhanced duration of action.

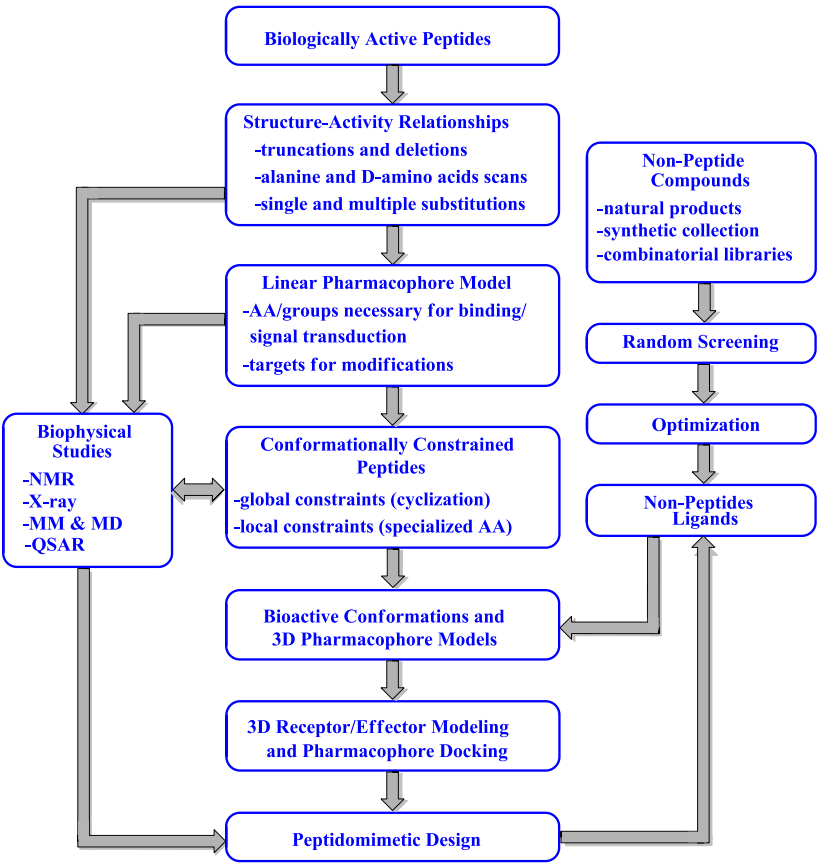

Scheme 1. Rational approach for peptidomimetics design.

During the past years, considerable progress has been made in the development of a rational approach to the design of peptide

ligands with specific conformational properties and highly potent biological activity (Scheme 1).[1]

Once the structure of the native peptide ligands has been elucidated, the first phase of this rational approach consists in the identification, through single amino acid replacement of the key amino acid residues required for receptor recognition. Further steps are aimed at the control of molecular flexibility. This is generally performed by adopting two different strategies: a) introduction of *local constraints* inside the ligand backbone in order to limit the range of the values adopted by ω, φ, ϕ torsion angles; b) introduction of *global constrain via* cyclization in order to make a rigid template for all the pharmacophoric structural elements. Models with rigid or semi-rigid conformations are thus produced, and the most active structures are selected by studying conformation-activity relationships. In the third phase a careful analysis of the 3D arrangement of side chains responsible for the activity is made. These studies often require complex experiments of NMR spectroscopy, X-ray analysis, circular dichroism data and, when possible, utilization of computational methods (molecular mechanics and molecular dynamics calculations). The results of the studies may lead to highly potent, effecacious and selective drug candidates which will be eventually the starting point for the design of ligands characterized by non-peptide nature (Scheme 1). This latter step is the most difficult and consists in

finding non-peptidic molecules suitable to replace the native crucial structural elements for receptor binding and recognition.

Strategies in the design of peptidomimetics

The design of peptidomimetics is based on different approaches. One of this consists in the N- and Cα -methylation or in the replacement of L-amino acids with their D-counterparts.[4,5]

Another approach, which increases the metabolic stability of biologically active peptides, is based on the introduction of amide bond isoster. These mimic the peptide bond and show higher stability toward enzymatic hydrolysis. Common examples of the class of amide bond surrogates can be found in sulphonamido peptides,[6] retro-inverso peptides[7] and azapeptides.[8]

Peptide analogs have also been obtained by introducing unusual residues, such as β-amino acids,[9] $C^{\alpha,\alpha}$ disubstituted amino acids[10] or N^{α}-C^{α} closed amino acids such as proline,[11] or hydroxy proline[12] and their analogues.

Turn inducer or helix inducer amino acids, such as dehydroamino acids can also be conveniently introduced in the backbone. The resulting molecules, which represent valid mimics of bioactive peptides, can efficiently interfere in several physiological processes.

Peptide cyclization, obtained by simple condensation of the *N*- and *C*-terminus or by connection of functionalized side chains, is also an useful approach in designing highly protease-resistant peptidomimetics. A very efficient method for preparing both small and macrocyclic rings is the ring-closing metathesis approach based on the use of the Grubb's catalyst.[13]

In order to overcome the low membrane permeability, which is a relevant obstacle for the drug bioavailability, suitable peptide analogues can be designed. Although the gut-barrier can be circumvented *via* non-oral administration of drugs, the blood-brain barrier (BBB) represents a problem which greatly reduces the time requested for the drug to reach the receptor site. Some of these limitations have been solved by masking polar groups within the peptide structure or by reducing hydrogen bonding potential (peptide lipidization). Other useful approaches are: the "prodrug approach" and the "vector-based strategy".The first is based on the coupling of a pharmacologically active moiety to a molecule with known transporters or to a lipophilicity enhancer, which is cleaved at or near the site of action. The "vector-based strategy" may involve the coupling of the peptide drug to a molecule that is normally transported through the BBB.[14]

Subject of present research

Some of the strategies reported above have been adopted in the studies performed during my PhD course. In this period the

interest was centered on the design and synthesis of analogues of biologically active peptides: endomorphins [EMs; Tyr-Pro-Trp-Phe-NH_2 (EM-1) and Tyr-Pro-Phe-Phe-NH_2 (EM-2)] and chemotactic *N*-formyl peptides.

The EMs are highly potent and selective μ-opioid receptor agonists and are considered the most effective "endogenous analgesics" released in response to pain stimuli.

The strong analgesic activity of EMs opens up the possibility to develop a novel class of painkillers based on their structure. Unfortunately, the exogenous application of these opioid peptides generally met with failure, owing to their biological instability and inability to be transmitted through the blood-brain barrier (BBB). In order to improve EMs properties as potential drugs as well as to better understand the key structural and conformational features on which receptor recognition and binding are based, a different number of their analogues were synthesized and evaluated.

We focused our attention on two different points:

a. the Pro at position 2 of EM-1 and EM-2, by replacing this residue with amino acids characterized by different constraints and structural features;
b. the Phe at position 3 and/or 4 of EM-2, by replacing with an α,β-unsaturated Phe residues.

Concerning chemotactic *N*-formyl peptides, they are involved in the defence mechanisms against bacterial infections through

binding with specific receptors located on neutrophil membrane. The interaction triggers, in addition to a rapid movement of the phagocytic cells towards the sites of infections (chemotaxis), a series of intracellular responses, relevant among which are lysosomal enzyme release and superoxide anion production.[15-18]

Despite extensive studies, both the essential cellular mechanisms controlling the neutrophil migration and the structure-activity relationships regulating the *N*-formyl peptide-receptor interactions, are not completely understood and are still under study.[18-20] However, since the discovery of *N*-formyl-methionyl peptides as agonists at the neutrophil receptors, the potent chemotactic agent *N*-formyl-Met-Leu-Phe-OH (fMLF) and its methyl ester (fMLF-OMe) have been chosen as the reference molecules and a variety of structural modifications have been performed on these tripeptides for systematic studies on biochemical mechanism and structure activity relationships.[21-25]

The main target of this research was:

a. to obtain information on structural and conformational properties which control biological activity;
b. to design potent and selective ligands by introducing unusual amino acids in place of Met or Leu residues;

c. to gain information on the consequences deriving from the alteration of the native side chain distances, through introduction of spacer residues.

References

1. Hruby, V. J. and Balse, P. M. *Curr. Med. Chem.* **2000**, *7*, 945 and refs. cited therein
2. Giannis, A.; Kolter, T. *Angew. Chem. Int. Ed. Engl.* **1993**, *32*, 1244.
3. Hruby, V. J.; Al-Obeidi, F.; Kazmierski, W. *Biochem. J.* **1990**, *268*, 249.
4. Yamazaki, T.; Ro, S.; Goodman, M.; Chung, N. N.; Schiller, P. W. *J. Med. Chem.* **1993**, *36*, 708.
5. Sagan, S.; Karoyan, P.; Lequin, O.; Chassaing, G.; Lavielle, S. *Curr. Med. Chem*., **2004**, *11*, 2799.
6. Giordano, C.; Lucente, G.; Masi, A.; Paglialunga Paradisi M.; Sansone, A.; Spisani S. *Bioorg. Med. Chem.* **2006**, *14*, 2642.
7. Fletcher, M. D.; Campbell, M. M. *Chem. Rev*. **1998**, *98*, 763.
8. Zega, A. *Curr. Med. Chem*. **2005**, *12*, 589.
9. Mollica, A.; Paglialunga Paradisi, M.; Torino, D.; Spisani, S.; Lucente, G. *Amino Acids* **2006**, *30*, 453.
10. Lucente, G.; Paglialunga Paradisi, M.; Giordano, C.; Sansone, A.; Torino, D.; Spisani, S. *Amino Acids* **2008**, *35*, 329.
11. Torino, D.; Mollica, A.; Pinnen, F.; Lucente, G.; Feliciani, F.; Davis, P.; Lai, J.; Ma, S-W.; Porreca, F.; Hruby, V. J. *Bioorg. Med. Chem. Lett.* **2009**, *19*, 4115.
12. Torino, D.; Mollica, A.; Pinnen, F.; Feliciani, F.; Spisani, S.; Lucente, G. *Bioorg. Med. Chem.* **2009**, *17*, 251.

13. Mollica, A.; Guardiani, G.; Davis, P.; Ma, S-W.; Porreca, F.; Lai, J.; Mannina, L.; Sobolev, A. P.; Hruby, V. J. *J. Med. Chem.* **2007**, *50*, 3138.
14. Gentilucci, L.; Tolomelli, A.; Squassabia, F. *Curr. Med. Chem.* **2006**, *13*, 2449 and refs. cited therein.
15. Freer, R. J.; Day, A. R.; Muthukumaraswamy, N.; Pinon, D.; Wu, A.; Showell, H. J.; Becker, E. L. *Biochemistry* **1982**, *21*, 257.
16. Toniolo, C.; Crisma, M.; Valle, G.; Bonora, G. M.; Polinelli, S.; Becker, E. L.; Freer, R. J.; Sudhanand, R.; Balaji Rao, P.; Balaram, P.; Sukumar, M. *Peptide Res.* **1989**, *2*, 275.
17. Le, Y.; Murphy, P. M.; Wang, J. M. *Trends Immunol.* **2002**, *23*, 541.
18. Cavicchioni, G.; Fraulini, A.; Falzarano, S.; Spisani, S. *Bioorg. Chem.* **2006**, *34*, 298.
19. Selvatici, R.; Falzarano, S.; Mollica, A.; Spisani, S. *Eur. J. Pharmacol.* **2006**, *534*, 1.
20. Fabbri, E.; Spisani, S.; Barbin, L.; Bondi, C.; Buzzi, M.; Traniello, S.; Pagani Zecchini, G.; Ferretti, M. E. *Cell. Signalling* **2000**, *12*, 391.
21. Miyazaki, M.; Kodama, H.; Fujita, I.; Hamasaki, Y.; Miyazaki, S.; Kondo, M. J. *Biochemistry* **1995**, *117*, 489.
22. Derian, C. K.; Solomon, H. F.; Higgins, J. D. III; Beblavy, M. J.; Santulli, R. J.; Bridger, G. J.; Pike, M. C.; Kroon, D. J.; Fischman, A. J. *Biochemistry* **1996**, *35*, 1265.
23. Higgins, J. D. III; Bridger, G. J.; Derian, C. K.; Beblavy, M. J.; Hernandez, P. E.; Gaul, F. E.; Abrams, M. J.; Pike, M. C.; Solomon, H. F. *J. Med. Chem.* **1996**, *39*, 1013.
24. Torrini, I.; Pagani Zecchini, G.; Paglialunga Paradisi, M.; Lucente, G.; Gavuzzo, E.; Mazza, F.; Pochetti, G.; Spisani, S.; Giuliani, A. L. *Int. J. Pept. Protein Res.* **1991**, *38*, 495.

25. Cavicchioni, G.; Turchetti, M.; Spisani, S. *J. Peptide Res.* **2002**, *60*, 223.

CHAPTER 1

Endomorphins (EMs) and their synthetic analogues

1.1 The pain

The International Association for the Study of Pain (IASP) defines pain as “an unpleasant sensory and emotional experience associated with actual or potential tissue damage, or described in terms of such damage”. Physiological pain is an important survival and protective mechanism designed to warn the animal of danger from potentially injurious stimuli from the external environment.

Precisely, the “pain system” should be called the “nociceptive system” because pain is a subjective result of nociception. Nociception is the encoding and processing of noxious stimuli in the nervous system. A noxious stimulus activates nociceptors (Aδ and C fibres) in the peripheral nerve (Figure 1).

Most of the nociceptors are polymodal, responding to noxious mechanical stimuli (painful pressure, squeezing or cutting of the tissue), noxious thermal stimuli (heat or cold), and chemical stimuli. Sensor molecules in the sensory endings of nociceptors transduce mechanical, thermal and chemical stimuli into a sensor potential, and when the amplitude of the sensor potential is sufficiently high, action potentials are triggered and conducted by the axon to the dorsal horn of the spinal cord or

the brainstem. Nociceptors can also exert efferent functions in the tissue by releasing neuropeptides [substance P, calcitonin gene-related peptide (CGRP)] from their sensory endings. Thereby, they induce vasodilatation, plasma extravasation and other effects, e.g. attraction of macrophages or degranulation of mast cells. Nociceptors activate synaptically nociceptive dorsal horn neurons (Figure 1). The latter are either ascending tract neurons or interneurons that are part of segmental motor or vegetative reflex pathways. Ascending axons in the spinothalamic tract activate the thalamocortical system that produces the conscious pain sensation. The pain sensation has a sensory discriminative aspect, i.e. the noxious stimulus is analysed for its location, duration and intensity. This is produced in the lateral thalamocortical system, which consists of relay nuclei in the lateral thalamus and the areas SI and SII in the postcentral gyrus. A second component of the pain sensation is the affective aspect, i.e. the noxious stimulus feels unpleasant and causes aversive reactions. This component is produced in the medial thalamocortical system, which consists of relay nuclei in the central and medial thalamus and the anterior cingulate cortex (ACC), the insula, and the prefrontal cortex. The spinal cord is under the influence of descending tracts that reduce or facilitate the nociceptive processing. Descending inhibition is formed by pathways that originate from brainstem nuclei (in particular, the periaqueductal grey, nucleus raphe

magnus) and descend in the dorsolateral funiculus of the spinal cord. This system is able to suppress nociceptive information processing via interneurons in the dorsal horn of the spinal cord.[1]

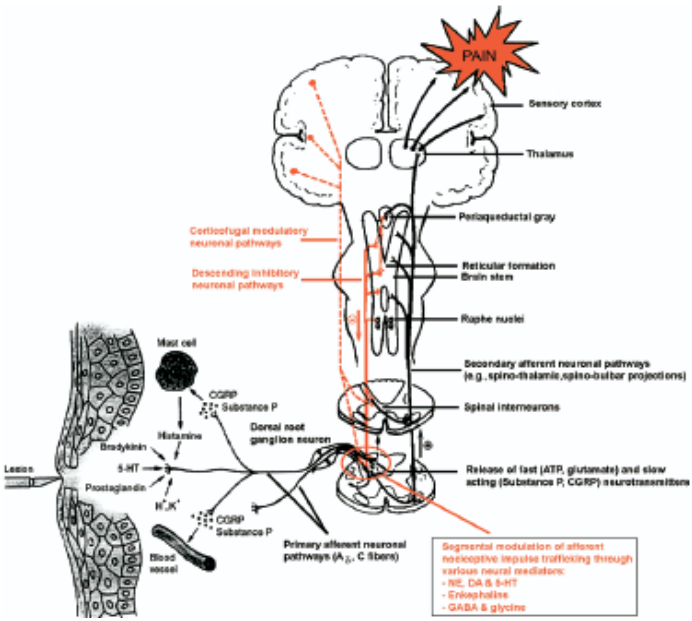

Figure 1. Ascending pathways of nociceptive impulses generated by peripheral sensory receptors (nociceptors) in response to noxious stimulation.

If persistent, physiological pain may progress to a pathological condition. Clinical pain is apparent when discomfort and abnormal sensitivity are present and is associated with three primary general features. Firstly, pain which may be dull, burning, or stabbing that is spontaneous. Secondly, pain responses to noxious stimuli are exaggerated (hyperalgesia). Thirdly, pain is produced by normally innocuous

stimuli (allodynia). Due to the differing pathophysiology, clinical pain is separated into inflammatory pain, associated with either tissue damage or an acute or chronic inflammatory condition, and neuropathic pain, which results from lesions to the peripheral or central nervous systems.[2]

The current treatment of pain remains highly reliant upon non-steroidal anti-inflammatory drugs (NSAIDs) and opioids. Chronic inflammatory pain is mainly treated by NSAIDs which have poor efficacy, and following chronic treatment can lead to serious problems including kidney failure, gastropathy and liver damage. For moderate to severe pain, opiates remain the preferred approach but many chronic pain conditions are refractory to opiate therapy and chronic dosing is associated with severe side effects.

It is possible to distinguish the opiates drugs from opioid. In the strict sense, opiates are drugs which are derived from opium and include the natural products morphine, codeine, thebaine and many semisynthetic congeners derived from them. In the wider sense, opiates are morphine-like drugs with non-peptidic structures. The old term opiates is now more and more replaced by the term opioids which applies to any substance, whether endogenous or synthetic, peptidic or non-peptidic, that produces morphine-like effects through an action on opioid receptors. Opioid systems comprise opiate alkaloids and the families of endogenous opioid peptides.[3]

1.1.1 Endogenous opioid peptides

For many centuries opium, the sticky exudates obtained from the poppy plant (*Papaver somniferum*) has been used as an effective painkiller. Opium contains a complex mixture of about 25 alkaloids. The main alkaloid of opium is morphine (Figure 2) that was isolated in 1803 by Sertürner and was found to be a particularly good analgesic and sedative, far more effective than crude opium.

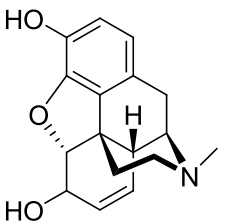

Figure 2. Structure of Morphine.

The rigid structural and stereochemical requirements essential for the analgesic action of morphine led to the theory that it produces its effect by interacting with a specific receptor in the mammalian brain, but the presence of an opiate-like system in the brain remained unproven. A particularly misleading observation was that the administration of the opioid antagonist naloxone to a normal animal produced little effect, although the drug was effective in reversing or preventing the effects of exogenous opiates.

The first physiological evidence suggesting an endogenous opioid system was the demonstration that analgesia produced by electrical stimulation of certain brain region was reversed by naloxone.[4-6] Pharmacological evidence for an opiate receptor also was building. In 1973, investigators in three laboratories demonstrated opiate binding sites in the brain.[7-10] This was the first use of radioligand binding assays to demonstrate the presence of membrane-associated neurotransmitter receptors in the brain.

Based on results of *in vivo* studies in dogs, Martin and colleagues postulated the existence of three main receptor types, μ, δ, and κ.[11] A fourth member of the opioid peptide receptor family, the *nociceptine/orphanine FQ* (N/FQ) receptor was cloned in 1994.[12-13]

Three distinct families of classical opioid peptides have been identified: the *enkefalins* (δ-selective), *endorphins* (non-selective) and *dynorphins* (κ-selective). Each family is derived from a distinct precursor polypeptide and has a characteristic anatomical distribution. These precursors, pre-proopiomelanocortin, pre-proenkefalin, and pre-prodynorphin, are encoding by three corresponding genes (Figure 3).

Each precursor is subject to complex cleavages and post-translational modifications resulting in the synthesis of multiple active peptides. The opioid peptides share the common amino-terminal sequence of Tyr-Gly-Gly-Phe- (Met or Leu), which has

been called the "opioid motif". This motif is followed by various *C*-terminal extensions yelding peptides ranging from 5 to 31 residues (Figure 4).

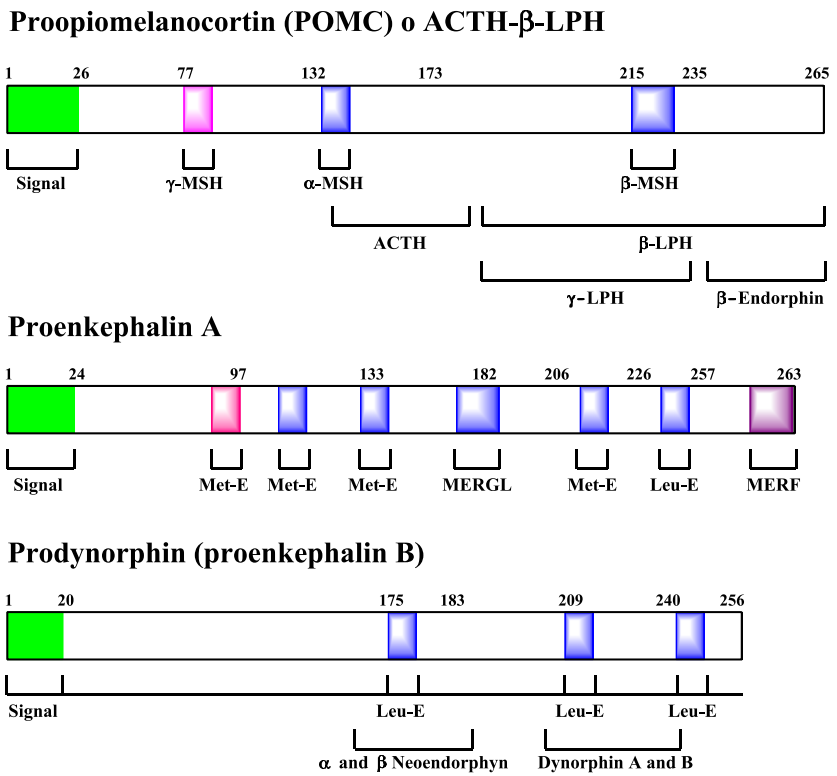

Figure 3. Peptide precursors.

A novel endogenous opioid peptide was cloned in 1995.[14-15] This peptide has a significant sequence homology to dynorphin A, with an identical length of 17 amino acids, identical carboxy-terminal residues, and a slight modification of amino-terminal opioid core (Phe-Gly-Gly-Phe instead of Tyr-Gly-Gly-Phe). The removal of hydroxyl phenolic group is sufficient to abolish

interactions with the three classical opioid-peptide receptors. This peptide was called *orphanin FQ* (OFQ) by one group of researchers and *nociceptin* (N) by another, because it lowered pain threshold under certain conditions. The N/OFQ system represents a new neuropeptide system with a high degree of sequence identity to the opioid peptides. However, the slight change in structure results in a profound alteration in function. N/OFQ has behavioural and pain modulatory properties distinct from those of the three classical opioid peptides.

Endogenous Opioid Peptides

Selected Endogenous Opioid Peptides	
[Leu^5]enkephalin	**Tyr-Gly-Gly-Phe-Leu**
[Met^5]enkephalin	**Tyr-Gly-Gly-Phe-Met**
Dynorphin A	**Tyr-Gly-Gly-Phe-Leu**-Arg-Arg-Ile-Arg-Pro-Lys-Leu-Lys-Trp-Asp-Asn-Gln
Dynorphin B	**Tyr-Gly-Gly-Phe-Leu**-Arg-Arg-Gln-Phe-Lys-Val-Val-Thr
α-Neoendorphin	**Tyr-Gly-Gly-Phe-Leu**-Arg-Lys-Tyr-Pro-Lys
β-Neoendorphin	**Tyr-Gly-Gly-Phe-Leu**-Arg-Lys-Tyr-Pro
β_h-Neoendorphin	**Tyr-Gly-Gly-Phe-Met**-Thr-Ser-Glu-Lys-Ser-Gln-Thr-Pro-Leu-Val-Thr-Leu-Phe-Lys-Asn-Ala Ile-Ile-Lys-Asn-Ala-Tyr-Lys-Lys-Gly-Glu
Novel Endogenous Opioid-Related Peptides	
Orphanin FQ/Nociceptin	Phe-**Gly-Gly-Phe**-Thr-Gly-Ala-Arg-Lys-Ser-Ala-Arg-Lys-Leu-Ala-Asn-Gln
Endomorphin-1	Tyr-Pro-Trp-Phe
Endomorphin-2	Tyr-Pro-Phe-Phe

Figure 4. Endogenous Opioid Peptides.

It is well established that morphine and related alkaloids elicit their analgesic effects when bound to the μ-opioid receptor. Intensive studies were undertaken to find a natural agonist for

that receptor in the nervous system. Several naturally occurring exogenous opioid peptides, which were shown to bind preferentially to the μ-receptor were isolated, such as *β*-casomorphin (Tyr-Pro-Phe-Pro-Gly-Pro-Ile) from digests of *β*-casein,[16] its shorter form, morphiceptin (Tyr-Pro-Phe-Pro-NH_2)[17-18] and hemorphin-4 (Tyr-Pro-Trp-Thr) from digests of haemoglobin.[19]

In early 1990 two peptides, Tyr-MIF-1 (Tyr-Pro-Leu-Gly-NH_2) and Tyr-W-MIF-1 (Tyr-Pro-Trp-Gly-NH_2) were found in the brain,[20-22] which displayed high selectivity for the μ-receptor sites, but their affinity was relatively low. The group of Zadina used Tyr-W-MIF-1 as a parent compound and systematically substituted each of the 20 natural amino acids for the Gly in position 4 and screened these analogs for binding to the *μ*-receptor. A biologically potent sequence, Tyr-Pro-Trp-Phe-NH_2 (Figure 5), was discovered and then identified in the bovine brain[23] and human cortex.[24] This new peptide, which was named endomorphin-1 (EM-1), showed remarkable affinity for the μ-opioid receptor and selectivity of 4000- and 15000-fold for the μ-opioid receptor over the δ- and κ-receptors, respectively. EM-1 was extremely potent in the guinea pig ileum assay, a classical test for the μ-opioid receptor agonist activity.[23] This peptide also had a potent and specific antinociceptive effect *in vivo*, as shown in the tail-flick test.[23,24] A second peptide, Tyr-Pro-Phe-Phe-NH_2 (Figure 5), which differed from EM-1 by only one amino acid,

was also isolated and named endomorphin-2 (EM-2). EM-2 was shown to be almost equally potent with EM-1.[23,24] Endomorphins (EMs) were the first peptides isolated from the brain that bind to the μ-opioid receptor with high affinity and selectivity and therefore were proposed as the most potent endogenous μ-opioid receptor ligands.

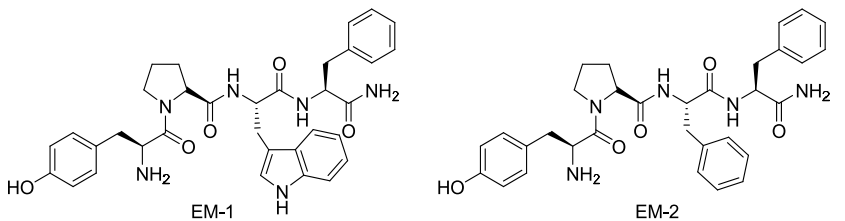

Figure 5. Structure of EM-1 and EM-2.

Despite the similar physiological effects, the structure of endomorphins is quite distinct from traditional opioid peptides; they are only four amino acid long, their *N*-terminal sequence is Tyr-Pro instead of Tyr-Gly-Gly-Phe, and their *C*-terminus is amidated, which seems to be essential for binding to the μ-opioid receptor. Endomorphins share common structural features with morphiceptin, hemorphin, Tyr-MIF-1, and Tyr-W-MIF-1.

1.1.2 Opioid receptors

Opioid receptors are most abundant in the central nervous system (CNS), but have also been localized in many peripheral

tissue of the mammalian organism. They belong to the big family of G-protein coupled receptors.

The G-protein coupled receptors (GPCRs) are also known as *metabotropic receptors* or *seven-transmembrane-spanning (heptaelical) receptors*. They are membrane receptors, that span the plasma membrane as a bundle of seven alpha helices, with an extracellular *N*-terminal domain of varying length and an intracellular *C*-terminal domain (Figure 6).

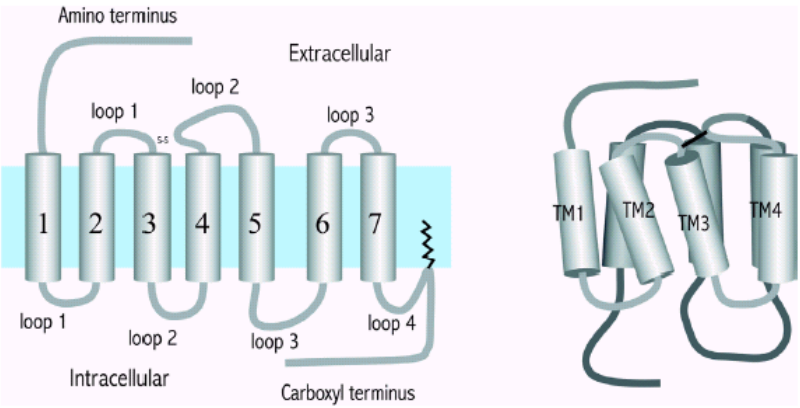

Figure 6. G-protein coupled receptor (GPCR).

They are coupled to intracellular effector systems via G-proteins that interact with the guanine nucleotides GTP and GDP. G-proteins are composed of three subunits, α, β and γ. Guanine nucleotides bind to the α-subunit, which has enzymic activity, catalysing the conversion of GTP to GDP; the β- and γ-subunits remain together as a $\beta\gamma$-complex. In the resting state, the G-protein exists as an unattached $\alpha\beta\gamma$-trimer, with GDP

occupying the site on the α-subunit (Scheme 1). When a GPCRs is occupied by an agonist molecule, a conformational change occurs, involving the citoplasmic domain of the receptor, causing it to acquire high affinity for the $\alpha\beta\gamma$-trimer. Association of $\alpha\beta\gamma$-trimer with the receptor causes the bound GDP to dissociate and to be replaced with GTP, which in turn causes dissociation of G-protein trimer, releasing α-GTP and $\beta\gamma$-subunits (Scheme 1); these are the active forms of the G-protein, which diffuse in the membrane and can associate with various enzymes and ion channels, causing activation or inactivation as the case may be. The process is terminated when the hydrolysis of GTP to GDP occurs through the GTPase activity of the α-subunit. The resulting α-GDP dissociates from

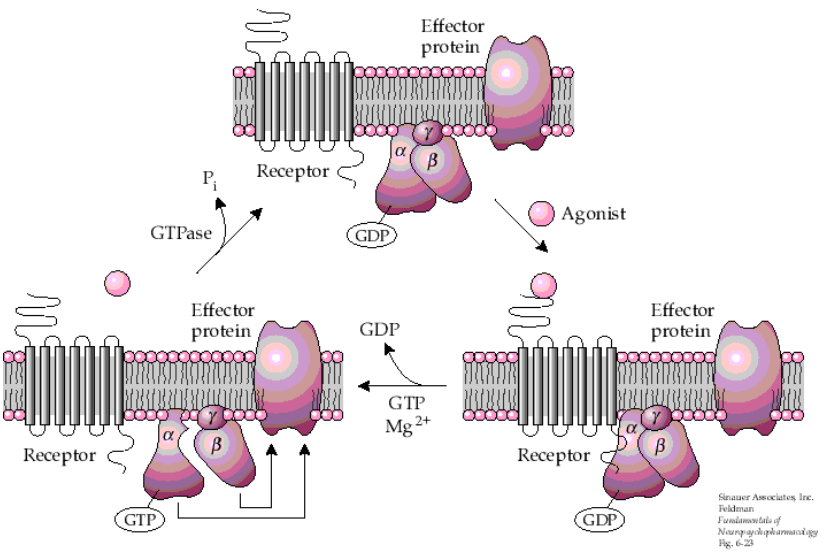

Scheme 1. Activation of G-protein coupled receptor.

the effector and reunites with the $\beta\gamma$-complex, completing the cycle. There are several types of G-protein, which interact with different receptors and control different effectors, e.g. the muscarinic acetylcholine receptor, adrenoceptors and neuropeptide receptors.

It is now well established that there are three well defined types of opioid receptors: the μ, δ and κ receptors.[25-27] Genes encoding for these receptors have been cloned.[28-31] The comparison of the amino acid sequences of three main opioid receptors revealed that they show extensive structural homology with each other. Physiological roles for each of the opioid receptors have not been clearly defined. Pain relief effects are mediated by all three receptor types, but in different degree: i) μ-receptor mediates the most potent antinociceptive effects, accompanied however by the development of dependence; ii) δ-receptor has lower efficacy in mediating pain relief, but might have a reduced addictive potential; iii) κ-receptor mediates analgesic effects in peripheral tissues.

It would be most useful to have the 3D structures of the opioid receptor to help study the mechanism of the new opioid receptor agonists, but there are no available 3D structures of opioid receptors determined by X-ray or NMR studies. Fortunately, the X-ray structure of bovine Rhodopsin, that belong to the GPCRs family, was solved (Figure 7)[32] and this

structure has been widely applied to homology modelling, based on the hypothesis of structural mimicry.[33]

Figure 7. Crystal structure model of bovine rhodopsin.

Indeed, several authors have recently developed alternative opioid receptor models using the rhodopsin X-ray structure as a template of these receptors.[34, 35]

1.2 Stucture-activity relationship studies and bioactive conformation of EMs

The EMs are highly active and selective MOR agonists, which possess several important biological effects and modulate a variety of physiological processes through the activation of membrane bound MOR. These tetrapeptides play a relevant role in the regulation of pain perception and in the analgesia;[23,36,37]

they show complex effects in the cardiovascular system;[38-41] they have gastrointestinal and respiratory functions;[37,42] they regulate the release of neurotransmitters;[43,44] furthermore, they display immunomodulatory properties.[45-47]

Due to the above-mentioned complex biological effects of EMs, it is important to identify the structural features of these tetrapeptides, which play a role in the formation of bioactive conformation and are responsible for the activity and selectivity toward MOR.

1.2.1 Pharmacophoric groups in EMs

From the structural point of view, the EMs can be divided into two biologically important parts,[48] which are the "message" and the "address" sequences. The "message" fragments are the *N*-terminal Tyr^1-Pro^2-Trp^3 and Tyr^1-Pro^2-Phe^3 tripeptide units, while the "address" fragment is the remaining *C*-terminal Phe^4-NH_2 unit (Figure 8). These two distinct sequences of EMs play a relevant role: the "message" sequence is required for the receptor binding and recognition and it is important in the formation of bioactive conformation; the "address" sequence is supposed to stabilize the bioactive conformation, among various conformations accessible to the *N*-terminal message sequence.

The data obtained from different studies pointed out that, for EM-1 and EM-2, the *N*-terminal amino (NH_2) group, the Tyr amino acid in position 1, and a further aromatic amino acids

(Trp or Phe) in position 3 or 4 can be considered as pharmacophore elements[49] (Figure 8). Since the aromatic side chain of Tyr^1, Trp^3/Phe^3, and Phe^4 amino acids rank among the putative pharmacophore elements of EMs, their conformations and orientation, as well as their relative spatial arrangements, are also important in the formation of bioactive conformation and in the binding to the receptor. Between the Tyr^1 and the other aromatic amino acids, Pro is located in position 2 as a spacer residue, which join(s) the pharmacophoric residues of the message sequence. Spacer residue plays a significant role in orienting the biologically important Tyr and Trp/Phe residues in the correct array necessary for opioid activity.

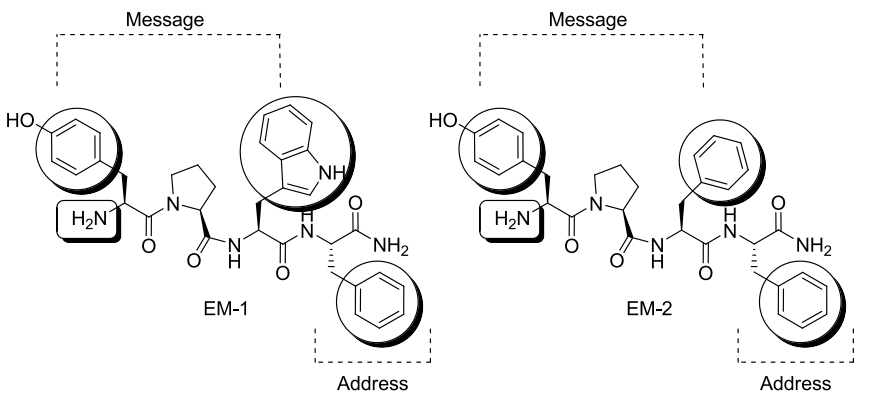

Figure 8. Message and address fragments as well as the putative pharmacophore elements of EM-1and EM-2.

Recent studies[50] established the importance of aromatic-aromatic or proline-aromatic interactions in the determination and stabilization of the structures of endomorphins. These

interactions may be also important in the association with the receptor and in ligand recognition.

Aromatic-aromatic interactions between different aromatic amino acids (Phe, Tyr and Trp) are important non-covalent interactions in proteins and peptides since determine and stabilize the three-dimensional structures and ligand bindings.

Both EMs contain aromatic amino acids (Tyr, Trp and Phe for EM-1, and Tyr and Phe for EM-2), which can interact with each other. The non-covalent interactions between residues with aromatic side-chains can stabilize the different conformers of EMs. Another important interaction in stabilizing protein structures which is also relevant in protein-protein, protein-peptide interactions and molecular recognition, is the C-H···π-interaction that can occur between a C-H-donor and a π-acceptor and can be treated as weak H-bond. One type of C-H···π-interaction, also found in peptides and proteins, is -in EMs- the interplay between the Pro and the aromatic amino acid side chains. It has been found that the C-H···π-interactions between side chains close to Pro and an aromatic amino acid can stabilize the *cis* peptide bond and may also be important in the stabilization of the structure of β-turns.[50]

1.2.2 Bioactive conformation of EMs

Determination of the bioactive conformation of endomorphins is an essential step to understand the action of

these peptides at their receptors. In small peptides such as endomorphins, the amino acid side-chains exhibit considerable conformational flexibility: it is difficult to establish the three-dimensional arrangement of endomorphins and the *cis*/*trans* rotamers of the amide linkage at Tyr-Pro allow endomorphins to exist as *cis*- and *trans*-isomers.[51] The question arises whether endomorphins adopt the *cis* or *trans* configuration of Tyr-Pro peptide bond, when bound to the receptor.

Recently, Gentilucci *et al.*[49] carried out different studies to establish the preferred conformation of EMs. Some studies performed on EM-1 indicated a biologically relevant conformation having Tyr^1 in proximity to Trp^2 and a *cis* Tyr^1-Pro^2 bond. On the other hand, other studies performed on EM-1 indicated a β-turn shaped geometry with a *trans* Tyr^1-Pro^2 bond. Concerning EM-2, both the *trans* and *cis* conformers adopted similar extended conformations, showing their backbones twisted at the Pro^2-Phe^3 moiety, except for the different orientation of Tyr respect Pro.

Then, several studies have been performed on EMs analogues and also these studies gave rise to distinct and contrasting models.

Keller *et al.*[52] synthesized analogs of EM-2 containing a dimethylated pseudoproline residue in place of Pro^2 that were all full μ-opioid agonists, showing good potency in functional assays and high μ-receptor binding affinities in the binding

assay. These results provided a direct evidence that EM-2 have the *cis*-configuration around Tyr-Pro peptide bond in the bioactive conformation. Similarly, a preference for the *cis*-configuration in the Dmt-Pro analogs was observed by Okada *et al.*.[53] All these data contradict the earlier findings by Podlogar *et al*.[51] and Eguchi *et al*.[54] who, based on NMR analyses, proposed an extended conformation of *trans* EM-1 as a potential bioactive form, and more recent report of In *et al*.,[55] who demonstrated, on the basis of 2D ^{1}H NMR and molecular docking, that EM-2 binds to the μ-opioid receptor in a *trans* Tyr-Pro conformation.

A different approach to increase the conformational flexibility at Tyr-Pro bond was represented by incorporating 1-aminocyclopentane-1-carboxylic acid (Ac_5c) and 1-aminocyclohexane-1-carboxylic acid (Ac_6c),[56] achiral analogs of α,α-disubstituted glycine. There is no rotational limitation on the *N*-Cα bond of Ac_5c and Ac_6c and the bulkiness of their aliphatic side-chains is similar to that of Pro. Incorporation of these amino acids into the sequence of EM-2 produced analogs with well conserved μ-affinities and retained selectivities. X-ray diffraction analysis revealed that [$(Ac_6c)^2$]EM-2 is folded into the *trans*-form for Tyr-Ac_6c. Since the selectivity of this analog was well conserved, it can be suggested that the folded form is important for the μ-selectivity. A different conclusion was presented by Shao *et al*.,[57] who studied conformational requirements of EM-2 analogs containing Phe-mimics,

phenylglycine (Phg) and homophenylalanine (Hfe). It has been suggested that the flexible side chains of aromatic amino acids in position 3 and/or 4 may cause the backbone of EM-2 analogs to adopt a folded structure, which results in weaker binding to the μ-opioid receptor.

1.3 Adopted structural modification strategies

Endomorphin-1 (EM-1) and endomorphin-2 (EM-2) are two endogenous opioid peptides with high affinity and selectivity for μ-opioid receptors.[23] Since the μ-opioid receptors mediate the most prominent pharmacological effects of morphine, the discovery of EM-1 and EM-2 has encouraged the application of natural and synthetic peptides as analgesics instead of morphine.[42,58,59] Indeed, both EM-1 and EM-2 exhibit potent antinociceptive effects in acute, inflammatory and neuropathic pain models without some of the undesirable side effects of morphine.[42,60,61] However, EMs as well as opioid peptides in general, show a poor bioavailability, mainly due to their inability to penetrate the gut-blood or the blood-brain barriers,[62,63] and rapid degradation *in vivo* by different proteases.[64] To circumvent these problems, different strategies have been adopted to modify opioid peptide properties.[52,65-67] Research efforts are focused on the design of analogues and peptidomimetics in order not only to improve EMs properties as potential drugs but also to better understand the key structural

and conformational features on which receptor recognition and binding are based.[68]

In several cases, peptide analogues or peptidomimetics have been found to possess much higher biological activity than that expected on the basis of simple binding studies or tissue bioassays. In this context, we have recently reported the synthesis, conformational study and pharmacological characterization of a series of EMs analogues characterized by the presence of conformationally constrained amino acid in position 2 of EM-1 and EM-2 and in position 3 and/or 4 in EM-2.

1.4 Synthesis and evaluation of new endomorphin analogues modified at the Pro^2 residue*

Several chemical modifications performed on EMs have been described previously and many of them were focused on the Pro at position 2.[56,58,65,69-74] The presence of Pro, the sole proteinogenic amino acid possessing a cyclic structure and a secondary amino group, represents a crucial factor in determining the structural and conformational properties of proteins and peptides. In the specific context of studies on EMs analogues, the Pro^2 is considered a stereochemical spacer,

*Torino, D.; Mollica, A.; Pinnen, F.; Lucente, G.; Feliciani, F.; Davis, P.; Lai, J.; Ma, S-W.; Porreca, F.; Hruby, V. J. *Bioorg. Med. Chem. Lett.* **2009**, *19*, 4115.

capable of favouring proper spatial orientation of the aromatic side chain groups, a key factor for ligand recognition and interaction with the receptor.[50,66]

Here we reports on the EM analogues given in Figure 9, which are obtained by replacing the Pro in position 2 with one of the four amino acid residues depicted in Figure 10. These amino acids, characterized by different constraints and structural features, can deeply alter the tetrapeptide backbone conformation and thus modulate in new ways the bioactivity of the peptide.

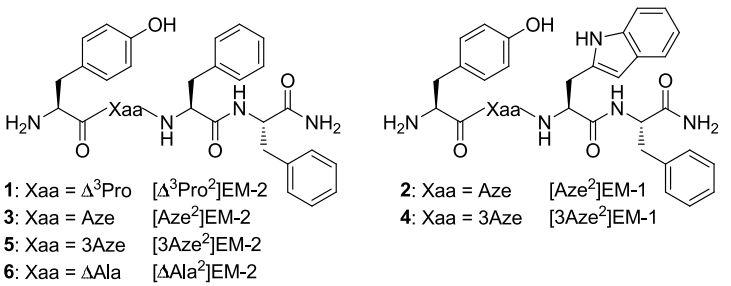

Figure 9. Molecular structure of the EM analogues **1**-**6**.

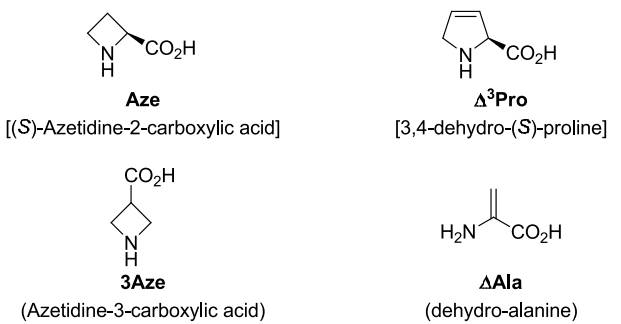

Figure 10. Molecular structure of the amino acids used to replace the native Pro[2] residue in endomorphins: (*S*)-azetidine-2-carboxylic acid (Aze); 3,4-dehydro-(*S*) proline (Δ^3Pro); azetidine-3-carboxylic acid (3Aze); dehydro-alanine (ΔAla).

A first modification, which leads to the EM-2 analogue **1**, is based on the introduction of the 3,4-dehydro-(*S*)-proline (Δ^3Pro) residue. This amino acid, as compared with Pro, has an almost planar and less flexible cyclic side chain ring, which does not allow rapid interconversion between ring-puckered forms typical of Pro residues and enhances, at the same time, the population of *cis* conformers around the CO-N tertiary amide bond.[75,76] In addition to this, the presence of the double bond may significantly improve, through π-π interactions, its binding to opioid receptors.[77,78] A related Δ^3Pro^2 containing EM-2 analogue, namely [Dmt^1, Δ^3Pro^2]EM-2, has been previously reported by Toth and Szemenyei[79] and utilised for the synthesis of the corresponding tritium labelled [$^3H_2$]Pro^2 analogue. Two of the other modified ligands here reported analogues contain a cyclic lower homologue of Pro. In particular, in analogues [Aze^2]EM-1 (**2)** and [Aze^2]EM-2 (**3)** the (*S*)-azetidine-2-carboxylic acid (Aze) has been incorporated. Literature data show that the four-membered ring system of *N*-acylated (*S*)-azetidine-2-carboxylic acid (Aze) is either planar or only slightly puckered[80-82] and presents, as compared with proline, reduced side chain steric effects, with increased backbone flexibility.[83] This latter property generates a larger number of low energy conformers with a population of the *cis* rotamers around the CO-N amide bond which has been suggested to be higher than that observed in Pro-containing peptides.[84]

Furthermore, the different ring size may significantly influence the type of folding with β-turns and γ-turns preferentially induced by Pro and Aze, respectively.[83]

The azetidine ring system also has been incorporated into the backbone of the analogues [3Aze^2]EM-1 (**4**) and [3Aze^2]EM-2 (**5**). Azetidine-3-carboxylic acid (3Aze) is an achiral conformationally restricted analogue of β-alanine which, although not used in opioid chemistry, has been employed for the synthesis of other pharmaceutical compounds.[85-87] As compared with Aze and Pro residues, 3Aze maintains the cyclic structure and the secondary amino group in the ring but is devoid of both chirality and restricted rotation around the N-Cα bond. Among 5-membered chiral β-residues related to 3Aze, both β-proline (pyrrolidine-3-carboxylic acid) and β-homoproline (2-pyrrolidineacetic acid) have already been used to replace Pro^2 in EM analogues.[58,65] Furthermore, EM-2 analogues containing cyclic 6-membered higher homologues of β-proline and 3Aze [viz nipecotic acid (piperidine-3-carboxylic acid) and isonipecotic acid (piperidine-4-carboxylic acid), respectively)] have been recently reported.[74]

The last analogue under study here is [ΔAla^2]EM-2 (**6**) which contains the rigid skeleton of dehydro-alanine (ΔAla). The local conformational restriction imposed on the backbone by the planar structure of ΔAla moiety, as well as its electronic distribution, significantly influences the properties of this

compound. Although a variety of molecular modifications performed on native EMs have been reported, analogues containing α,β-unsaturated amino acid residues are very scarce.[88] Thus, the reported data on compound **6** represent, to the best of our knowledge, the first information available in the literature on receptor binding affinity and selectivity of this type of EM analogues.

1.4.1 Chemistry

The solution phase synthesis of peptides **1-5** were performed following standard literature methods[89] which are given in Scheme 2.

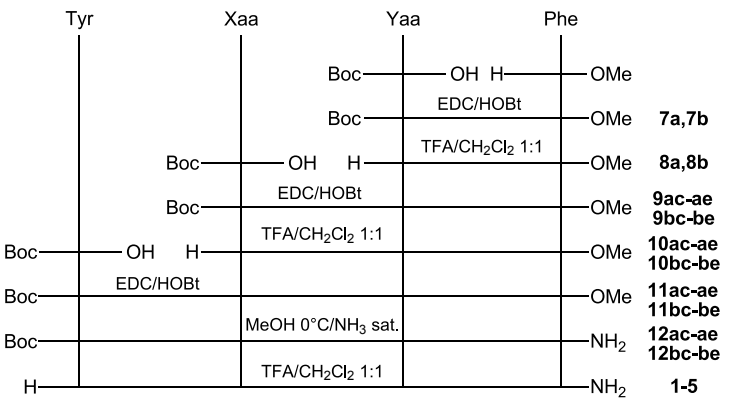

Scheme 2. Synthesis of EM analogues **1-5**. Xaa = Δ^3Pro; Yaa = Phe (**1**); Xaa = Aze; Yaa = Trp (**2**); Xaa = Aze; Yaa = Phe (**3**); Xaa = 3Aze; Yaa = Trp (**4**); Xaa = 3Aze; Yaa = Phe (**5**). Intermediates: Yaa = Phe = a; Yaa = Trp = b. Xaa = Δ^3Pro = c; Xaa = Aze = d; Xaa = 3Aze = e.

The synthesis of the dehydro-alanine-containing analogue **6**, was accomplished by exploiting the reactivity of the methylcysteine sulfoxide[90] as illustrated in Scheme 3.

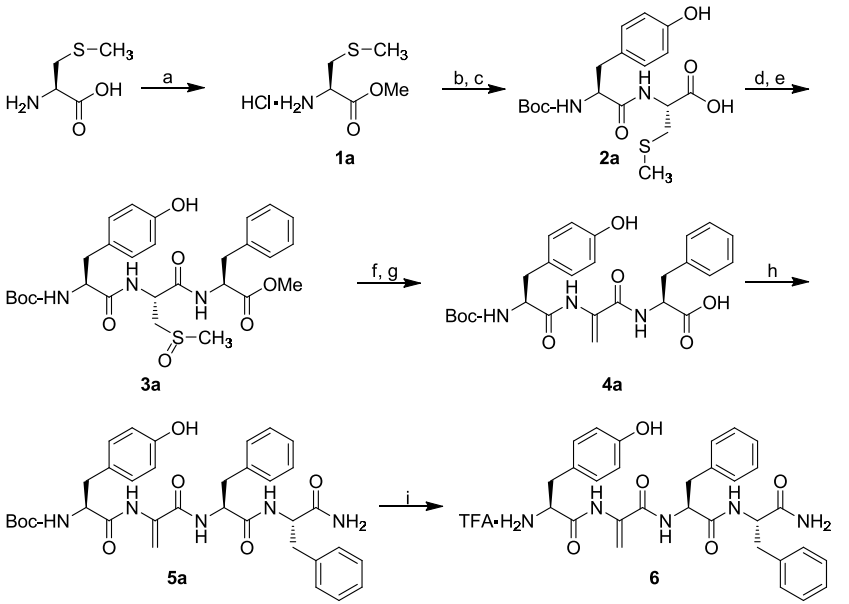

Scheme 3. Synthesis of EM-2 analogue **6**. *Reagents and conditions*: a) $SOCl_2$, MeOH, 15 min 0 °C, 3 h rt; b) Boc-Tyr-OH, EDC, HOBt, DIPEA, CH_2Cl_2 30 min 0 °C, 12 h rt; c) 1N NaOH, MeOH 5 h rt; d) HCl·H_2N-Phe-OMe, EDC, HOBt, DIPEA, CH_2Cl_2 30 min 0 °C, 12 h rt; e) $NaIO_4$, H_2O, dioxane 1 h 0 °C; f) DBU, MeOH, 1.5 h rt; g) 1N NaOH, MeOH 5 h rt; h) HCl·H_2N-Phe-NH_2, EDC, HOBt, DIPEA, CH_2Cl_2 30 min 0 °C, 12 h rt; i) TFA/CH_2Cl_2 1:1, 1.5 h rt under N_2.

1.4.2 Results and conclusions

As shown in Table 1 all analogues, except [3Aze^2]EM-1 (**4**), which can be considered a μ/δ mixed agonist, show high selectivity for μ-receptors and functional bioactivities in good agreement with the binding values. The highest affinity and selectivity is shown by the Aze-containing peptides **2** and **3**. This finding, together with the good activity of the [Δ^3Pro^2]EM-2 analogue **1**, confirms the role of the residue at position 2 as a stereochemical spacer.

Table 1. Binding affinity and *in vitro* activity for compounds **1-6**.

Compound	Receptor affinity[a,b] (nM)		Selectivity	Functional bioactivity	
	$K_i\delta$	$K_i\mu$	δ/μ	MVD[b] (IC_{50})	GPI[b] (IC_{50})
1 [Δ^3Pro^2]EM-2	n.c.[c]	6.5 ± 2.3	-	70 ± 12	14 ± 2.1
2 [Aze^2]EM-1	3500 ± 360	2.3 ± 0.23	1500	140 ± 21	7.9 ± 0.83
3 [Aze^2]EM-2	5100 ± 600	5.6 ± 1.2	920	150 ± 60	6.4 ± 1.2
4 [3Aze^2]EM-1	40 ± 8.5	34 ± 5.1	1.2	170 ± 32	140 ± 32
5 [3Aze^2]EM-2	6900 ± 1200	210 ± 51	32	13% at 1 μM	1400 ± 280
6 [ΔAla^2]EM-2	710 ± 130	34 ± 6.3	21	490 ± 150	170 ± 23
EM-1	-	4.55 ± 0.16	-	-	11.9 ± 0.69
EM-2	-	8.23 ± 0.48	-	-	9.67 ± 0.84

[a] Displacement of [^{3}H]DAMGO (μ-selective) and [^{3}H]DPDPE (δ-selective) from rat brain membrane binding sites.
[b] ± S.E.M.
[c] n.c.= not binding recorded.

The two analogues containing a β-residue, namely [3Aze^2]EM-1 (**4**) and [3Aze^2]EM-2 (**5**) exhibit highly different activity profiles (Table 1). The much lower activity shown by **5**, as compared to the Trp^3 containing analogue [3Aze^2]EM-1 (**4**), can be interpreted on the basis of the well recognised role of the aromatic residues on ligand-receptor interactions. Several studies on EM-1 and EM-2 clearly show that aromatic side chains with different size, distinct noncovalent interactions and H-bonding capability, can highly influence conformations[49] and binding.[50,51,91] Results of ligands **4** and **5** indicate that the beneficial effect on the activity, constantly observed in EM analogues containing the indole ring system at position 3, gives

results that are particularly efficient as compared to the Phe[3] residue in models containing the achiral 3Aze residue.

The low activity shown by [3Aze[2]]EM-2 (**5**) appears, however, is quite unexpected when compared to the high activity shown by EM analogues containing other cyclic β-residues in place of the native Pro[2]. In particular, among the recently examined EM-2 analogues containing positional isomers of the 6-membered piperidine-carboxylic acid, replacement of Pro[2] with the chiral nipecotic acid (viz piperidine-3-carboxylic acid) led, in accordance with the results concerning other related cyclic β-residues,[58,65] to a highly active analogue.[74] On the contrary, Pro[2] replacement with the achiral piperidine-4-carboxylic acid (viz isonipecotic acid) resulted, as in the case of the here reported analogue **5**, to a practically inactive ligand.[74] It can be argued that the high conformational restriction and the reduced flexibility of the 4-membered achiral 3Aze are detrimental features which prevail over the advantages which, in larger cyclic systems, derive from the presence of a β-positioned carboxylic group.

Peptide **6**, containing the rigid skeleton of ΔAla residue, has only modest affinity and bioactivity at the μ-opioid receptor, and this suggests that an efficient constraint at position 2 involves an amino acid residue with a cyclic structure.

1.4.3 Experimental section

Materials and methods. Boc-Aze-OH (purissimum, ≥99%), Boc-3Aze-OH (purissimum, ≥99%) and Boc-Δ^3Pro-OH (purissimum, ≥99%) were obtained commercially and used without further purification. Spectrograde solvents were purchased from Merck; all the other solvents and reagents were of the purest grade commercially available. Optical rotations were taken at 20 °C with a Schmidt-Haensch Polartronic D polarimeter (1 dm cell, *c* 1.0 in $CHCl_3$, unless otherwise specified). IR spectra were recorded in 1% $CHCl_3$ (unless otherwise specified) solution employing a Perkin-Elmer FT-IR Spectrum 1000 spectrometer. ^{1}H NMR experiments were performed at 400 MHz on a Bruker AM 400 spectrometer in $CDCl_3$ solution (unless otherwise specified), chemical shifts (δ) are quoted in parts per million (ppm) and were indirectly referred to TMS. TLC (thin layer chromatography) and PLC (preparative layer chromatography) were performed on silica gel Merck 60 F_{254} plates. The drying agent was sodium sulphate. All new compounds were also characterized by elemental analysis.

1.4.3.1 Chemistry. General procedures

A. Coupling with the carbodiimide method. To an ice-cooled mixture containing the required *N*-Boc-amino acid (1.0 mmol), HOBt (1.1 mmol), EDC (1.1 mmol) and NMM or DIPEA (2.2 mmol) in anhydrous CH_2Cl_2, the amino-derivative salt (1.1 mmol) was added. The

reaction mixture was allowed to warm to 0 °C for 10 min and then to room temperature. After 12 h the reaction mixture was diluted with EtOAc (20 mL) and washed with 5% citric acid (3 x 15 mL), $NaHCO_3$ ss (3 x 15 mL) and NaCl ss (2 x 15 mL). The organic layer was dried and evaporated under reduced pressure.

B. Deprotection of Boc-derivatives. The Boc group was removed by treatment with TFA in CH_2Cl_2 (1:1) for 1 h at room temperature. Removal of solvent and precipitation of the residue with diethyl ether gave the TFA salt that was used in the next step without further purification.

C. Preparation of peptide amides. The peptide methyl ester is allowed to stand in a pressure bottle at room temperature for 48 h in anhydrous MeOH previously saturated with ammonia gas at 0 °C. The solution is then concentrated to dryness in vacuo at a temperature not exceeding 40° C. Compounds were purified by PLC.

1.4.3.2 Synthesis

***N*-Boc-Phe-Phe-OMe (7a).** *N*-Boc-Phe-OH (0.895 g, 3.71 mmol) in CH_2Cl_2 (60 mL) was treated with $HCl{\cdot}H_2N$-Phe-OMe (0.727 g, 3.37 mmol) according to the general procedure A. The title compound was obtained as a white solid, pure on TLC (1.246 g, 87%); $[a]_D$ +34.28° (*c* 1, $CHCl_3$); IR ($CHCl_3$): ν 3423,

1742, 1677 cm^{-1}; ^1H NMR ($CDCl_3$): δ 1.42 [9H, s, $C(CH_3)_3$], 3.07 (4H, m, Phe^3 and Phe^4 β-CH_2), 3.70 (3H, s, $COOCH_3$), 4.35 (1H, m, Phe^3 α-CH), 4.81 (1H, m, Phe^4 α-CH), 4.93 (1H, br s, Phe^3 NH), 6.29 (1H, br s, Phe^4 NH), 7.00-7.30 (10H, m, aromatics). Anal. Calcd for $C_{24}H_{30}N_2O_5$: C, 67.59; H, 7.09; N, 6.57. Found: C, 67.86; H, 7.11; N, 6.59.

TFA·H_2N-Phe-Phe-OMe (8a). Deprotection of the *N*-Boc group was performed by adopting the general procedure B: **7a** (0.381 g, 0.89 mmol), CH_2Cl_2/TFA (6 mL) gave **8a** (0.392 g, quantitative yield).

***N*-Boc-Trp-Phe-OMe (7b).** *N*-Boc-Trp-OH (1.0 g, 3.62 mmol) in CH_2Cl_2 (58.6 mL) and DMF (10 mL) was treated with HCl·H_2N-Phe-OMe (0.71 g, 3.29 mmol) according to the general procedure A. The title compound was obtained as a white foam, pure on TLC (1.428 g, 93%); $[a]_D$ +16° (*c* 1, $CHCl_3$); IR ($CHCl_3$): ν 3477, 3418, 1742, 1673 cm^{-1}; ^1H NMR ($CDCl_3$): δ 1.44 [9H, s, $C(CH_3)_3$], 2.85-3.43 (4H, m, Trp and Phe^4 β-CH_2), 3.64 (3H, s, $COOCH_3$), 4.45 (1H, m, Trp α-CH), 4.75 (1H, m, Phe^4 α-CH), 5.14 (1H, br s, Trp NH), 6.22 (1H, br s, Phe^4 NH), 6.72-7.80 (10H, m, aromatics), 8.08 (1H, s, Trp Ind-NH). Anal. Calcd for $C_{26}H_{31}N_3O_5$: C, 67.08; H, 6.71; N, 9.03. Found: C, 67.28; H, 6.73; N, 9.05.

TFA·H_2N-Trp-Phe-OMe (8b). Deprotection of the *N*-Boc group was performed by adopting the general procedure B: **7b**

(0.26 g, 0.558 mmol), CH_2Cl_2/TFA (6 mL) gave **8b** (0.267 g, quantitative yield).

***N*-Boc-Aze-Phe-Phe-OMe (9ad).** *N*-Boc-Aze-OH (0.166 g, 0.83 mmol) in CH_2Cl_2 (15 mL) was treated with TFA·H_2N-Phe-Phe-OMe (0.330 g, 0.75 mmol) according to the general procedure A. Silica gel chromatography ($CHCl_2$/EtOAc 8:2) gave a pure product **9ad** as a white foam (0.302 g, 79%); $[a]_D$ -90° (*c* 1, $CHCl_3$); IR ($CHCl_3$): ν 3408, 1742, 1682 cm^{-1}; ^1H NMR ($CDCl_3$): δ 1.46 [9H, s, $C(CH_3)_3$], 2.10-2.40 (2H, br s, Aze C^3H_2), 2.93-3.19 (4H, m, Phe^3 β-CH_2 and Phe^4β-CH_2), 3.68 (3H, s, $COOCH_3$), 3.64 and 3.85 (2H, two m, Aze C^4H_2), 4.55 (1H, m, Aze α-CH), 4.67 (1H, m, Phe^3 α-CH), 4.81 (1H, m, Phe^4 α-CH), 6.55 (1H, br s, Phe^4 NH), 7.04-7.28 (10H, m, aromatics), 7.52 (1H, br s, Phe^3 NH). Anal. Calcd for $C_{28}H_{35}N_3O_6$: C, 65.99; H, 6.92; N, 8.25. Found: C, 66.05; H, 6.93; N, 8.26.

TFA·HN-Aze-Phe-Phe-OMe (10ad). Deprotection of the *N*-Boc group was performed by adopting the general procedure B: **9ad** (0.257 g, 0.505 mmol), CH_2Cl_2/TFA (6 mL) gave **10ad** (0.264 g, quantitative yield).

***N*-Boc-Tyr-Aze-Phe-Phe-OMe (11ad).** *N*-Boc-Tyr-OH (0.156 g, 0.555 mmol) in CH_2Cl_2 (10 mL) was treated with TFA·HN-Aze-Phe-Phe-OMe (0.264 g, 0.505 mmol) according to the general procedure A. Silica gel chromatography ($CHCl_3$/EtOAc 1:1) gave a pure product **11ad** as a white foam

(0.295 g, 90%); $[a]_D$ -14.7° (*c* 0.68, $CHCl_3$); IR ($CHCl_3$): ν 3429, 1741, 1670 cm^{-1}; ^1H NMR ($CDCl_3$): δ 1.43 [9H, s, $C(CH_3)_3$], 1.90-2.32 (2H, m, Aze C^3H_2), 2.65-2.90 (2H, m, Tyr β-CH_2), 2.91-3.34 (4H, m, Phe^3 β-CH_2 and Phe^4 β-CH_2) 3.70 (3H, s, $COOCH_3$), 3.68 and 4.01 (2H, two m, Aze C^4H_2), 4.25 (1H, m, Tyr α-CH), 4.60 (1H, m, Phe^3 α-CH), 4.69 (1H, m, Aze α-CH), 4.80 (1H, m, Phe^4 α-CH), 5.22 [1H, apparent t (the signals of two conformers are superimposed), Tyr NH], 6.67 (1H, d, *J* = 7.6 Hz Phe^4 NH), 6.72-7.33 (14H, m, aromatics), 7.54 (1H, d, *J* = 7.0 Hz Phe^3 NH). Anal. Calcd for $C_{37}H_{44}N_4O_8$: C, 66.05; H, 6.59; N, 8.33. Found: C, 66.12; H, 6.60; N, 8.35.

***N*-Boc-Tyr-Aze-Phe-Phe-NH_2 (12ad).** A solution of the peptide methyl ester **11ad** (0.15 g, 0.22 mmol) in MeOH/NH_3 sat. (6.3 mL) is allowed to stand in a pressure bottle at room temperature according to the general procedure C. The title compound was obtained as a white solid pure on TLC (0.139 g, 95%); ^1H NMR (DMSO-d_6): δ 1.45 [9H, s, $C(CH_3)_3$], 1.78 and 2.31 (2H, two m, Aze C^3H_2), 2.59-3.22 (6H, m, Phe^3 β-CH_2, Phe^4 β-CH_2 and Tyr β-CH_2), 3.77 and 4.10 (2H, two m, Aze C^4H_2), 3.99 (1H, m, Tyr α-CH), 4.45-4.50 (2H, m, Phe^3 α-CH and Phe^4 α-CH), 4.62 (1H, m, Aze α-CH), 6.60-7.34 (16H, m, aromatics and $CONH_2$), 8.01-8.28 (2H, m, Phe^3 NH, Phe^4 NH), 9.40 (1H, s, Tyr OH). Anal. Calcd for $C_{36}H_{42}N_4O_8$: C, 65.64; H, 6.43; N, 8.51. Found: C, 65.72; H, 6.44; N, 8.53.

TFA·H_2N-Tyr-Aze-Phe-Phe-NH_2 (3). Deprotection of the *N*-Boc group was performed by adopting the general procedure B: **12ad** (0.034 g, 0.052 mmol), CH_2Cl_2/TFA (6 mL) gave **3** (0.035 g, quantitative yield); ^{1}H NMR (DMSO-d_6): δ 1.78 and 2.31 (2H, two m, Aze C^3H_2), 2.59-3.22 (6H, m, Phe^3 β-CH_2, Phe^4 β-CH_2 and Tyr β-CH_2), 3.77 and 4.10 (2H, two m, Aze C^4H_2), 3.99 (1H, m, Tyr α-CH), 4.45-4.50 (2H, m, Phe^3 α-CH and Phe^4 α-CH), 4.62 (1H, m, Aze α-CH), 6.60-7.34 (16H, m, aromatics and $CONH_2$), 8.01-8.28 (5H, m, Phe^3 NH, Phe^4 NH and Tyr NH_3^+), 9.40 (1H, s, Tyr OH). Anal. Calcd for $C_{33}H_{36}F_3N_5O_7$: C, 59.01; H, 5.40; N, 10.43. Found: C, 59.24; H, 5.42; N, 10.40.

***N*-Boc-Aze-Trp-Phe-OMe (9bd).** *N*-Boc-Aze-OH (0.142 g, 0.709 mmol) in CH_2Cl_2 (13 mL) was treated with TFA·H_2N-Trp-Phe-OMe (0.309 g, 0.645 mmol) according to the general procedure A. Silica gel chromatography ($CHCl_3$/MeOH 99:1) gave a pure product **9bd** as a white foam (0.250 g, 71%); $[a]_D$ -92° (*c* 1, $CHCl_3$); IR ($CHCl_3$): ν 3428, 1742, 1681 cm^{-1}; ^{1}H NMR ($CDCl_3$): δ 1.44 [9H, s, $C(CH_3)_3$], 1.79-2.45 (2H, m, AzeC^3H_2), 2.85-3.10 (2H, m, Trp β-CH_2), 3.20-3.41 (2H, m, Phe β-CH_2), 3.52 (1H, m, Aze *H*C^4H), 3.64 (3H, s, $COOCH_3$), 3.92 (1H, m, Aze *H*C^4H), 4.58 (1H, m, Aze α-CH), 4.75 (2H, m, Phe α-CH and Trp α-CH), 6.90 and 7.82 [2H, br s (two conformers), Trp NH and Phe NH], 6.92-7.80 (10H, m, aromatics), 8.12 (1H,

s, Trp Ind-NH). Anal. Calcd for $C_{30}H_{36}N_4O_6$: C, 65.68; H, 6.61; N, 10.21. Found: C, 65.72; H, 6.62; N, 10.23.

TFA·HN-Aze-Trp-Phe-OMe (10bd). Deprotection of the *N*-Boc group was performed by adopting the general procedure B: **9bd** (0.218 g, 0.398 mmol), CH_2Cl_2/TFA (6 mL) gave **10bd** (0.224 g, quantitative yield).

***N*-Boc-Tyr-Aze-Trp-Phe-OMe (11bd).** *N*-Boc-Tyr-OH (0.123 g, 0.438 mmol) in CH_2Cl_2 (10 mL) was treated with compound **10bd** (0.224 g, 0.398 mmol) according to the general procedure A. Silica gel chromatography ($CHCl_3$/EtOAc 1:1) gave a pure product **11bd** as a white foam (0.145 g, 51%); $[a]_D$ -11° (*c* 1, $CHCl_3$); IR ($CHCl_3$): ν 3477, 3428, 1741, 1666 cm^{-1}; ^1H NMR ($CDCl_3$): δ 1.41 [9H, s, $C(CH_3)_3$], 2.15-2.25 (2H, m, AzeC^3H_2), 2.51-3.80 (2H, m, Tyr β-CH_2), 2.85-3.10 (2H, m, Trp β-CH_2), 3.15-3.36 (2H, m, Phe β-CH_2), 3.25 (1H, m, Aze *H*C^4H), 3.65 (3H, s, $COOCH_3$), 3.81 (1H, m, Aze *H*C^4H), 4.23 (1H, m, Tyr α-CH), 4.70 (3H, m, Aze α-CH, Phe α-CH and Trp α-CH), 5.21 (1H, d, *J* = 7.2 Hz Tyr NH), 6.50 (1H, d, *J* = 7.2 Hz Phe NH), 6.75 (1H, d, *J* = 7.6 Hz Trp NH), 6.60-7.80 (14H, m, aromatics), 8.38 (1H, s, Trp Ind-NH). Anal. Calcd for $C_{39}H_{45}N_5O_8$: C, 65.81; H, 6.37; N, 9.84. Found: C, 65.90; H, 6.38; N, 9.86.

***N*-Boc-Tyr-Aze-Trp-Phe-NH_2 (12bd).** A solution of the peptide methyl ester **11bd** (0.073 g, 0.103 mmol) in MeOH/NH_3 sat. (3 mL) is allowed to stand in a pressure bottle at room

temperature according to the general procedure C. The title compound was obtained as a white solid pure on TLC (0.063 g, 88%); ^{1}H NMR (DMSO-d_6): δ 1.45 [9H, s, C(CH$_3$)$_3$], 1.78 and 2.29 (2H, two m, Aze C^{3}H$_2$), 2.60-3.20 (6H, m, Phe β-CH$_2$, Trp β-CH$_2$ and Tyr β-CH$_2$), 3.67 and 4.04 (2H, two m, Aze C^{4}H$_2$), 3.94 (1H, m, Tyr α-CH), 4.41 (1H, m, Trp α-CH), 4.48 (1H, m, Phe α-CH), 4.60 (1H, m, Aze α-CH), 6.55-7.35 (17H, m, aromatics, Tyr NH and CONH$_2$), 8.00-8.25 (2H, m, Phe NH, Trp NH), 9.39 (1H, s, Tyr OH), 10.78 (1H, s, Trp Ind-NH). Anal. Calcd for $C_{38}H_{44}N_6O_7$: C, 65.50; H, 6.36; N, 12.06. Found: C, 65.69; H, 6.38; N, 12.09.

TFA·H$_2$N-Tyr-Aze-Trp-Phe-NH$_2$ (2). Deprotection of the *N*-Boc group was performed by adopting the general procedure B: **12bd** (0.030 g, 0.043mmol), CH_2Cl_2/TFA (6 mL) gave **2** (0.031 g, quantitative yield); ^{1}H NMR (DMSO-d_6): δ 1.78 and 2.29 (2H, two m, Aze C^{3}H$_2$), 2.60-3.20 (6H, m, Phe β-CH$_2$, Trp β-CH$_2$ and Tyr β-CH$_2$), 3.67 and 4.04 (2H, two m, Aze C^{4}H$_2$), 3.94 (1H, m, Tyr α-CH), 4.41 (1H, m, Trp α-CH), 4.48 (1H, m, Phe α-CH), 4.60 (1H, m, Aze α-CH), 6.55-7.35 (16H, m, aromatics and CONH$_2$), 8.00-8.25 (5H, m, Phe NH, Trp NH and Tyr NH$_3^+$), 9.39 (1H, s, Tyr OH), 10.78 (1H, s, Trp Ind-NH). Anal. Calcd for $C_{35}H_{37}F_3N_6O_7$: C, 59.15; H, 5.25; N, 11.82. Found: C, 59.27; H, 5.26; N, 11.83.

***N*-Boc-3Aze-Phe-Phe-OMe (9ae).** *N*-Boc-3Aze-OH (0.214 g, 1.067 mmol) in CH_2Cl_2 (16 mL) was treated with compound

8a (0.392 g, 0.89 mmol) according to the general procedure A. Silica gel chromatography ($CHCl_3$) gave a pure product **9ae** as a white foam (0.440 g, 97%); $[a]_D$ +21° (*c* 1, $CHCl_3$); IR ($CHCl_3$): ν 3406, 1742, 1682 cm^{-1}; ^1H NMR ($CDCl_3$): δ 1.46 [9H, s, $C(CH_3)_3$], 2.94-3.16 (5H, m, 3Aze α-CH, Phe^3 and Phe^4 β-CH_2), 3.70 (3H, s, $COOCH_3$), 3.90-4.07 (4H, m, 3Aze C^2H_2 and 3Aze C^4H_2), 4.64 (1H, m, Phe^3 α-CH), 4.75 (1H, m, Phe^4 α-CH), 6.08 (1H, d, *J* = 7.2 Hz Phe^4 NH), 6.14 (1H, d, *J* = 7.2 Hz Phe^3 NH) 7.00-7.30 (10H, m, aromatics). Anal. Calcd for $C_{28}H_{35}N_3O_6$: C, 65.99; H, 6.92; N, 8.25. Found: C, 66.25; H, 6.91; N, 8.28.

TFA·HN-3Aze-Phe-Phe-OMe (10ae). Deprotection of the *N*-Boc group was performed by adopting the general procedure B: **9ae** (0.405 g, 0.796 mmol), CH_2Cl_2/TFA (6 mL) gave **10ae** (0.416 g, quantitative yield).

***N*-Boc-Tyr-3Aze-Phe-Phe-OMe (11ae).** *N*-Boc-Tyr-OH (0.246 g, 0.876) in CH_2Cl_2 (14 mL) was treated with compound **10ae** (0.416 g, 0.796 mmol) according to the general procedure A. Silica gel chromatography ($CHCl_3$/EtOAc 9:1) gave a pure product **11ae** as a white foam (0.350 g, 65%); $[a]_D$ +26° (*c* 1, $CHCl_3$); IR ($CHCl_3$): ν 3426, 1741, 1661 cm^{-1}; ^1H NMR ($CDCl_3$): δ 1.46 [9H, s, $C(CH_3)_3$], 2.75-3.21 (11H, m, 3Aze C^2H_2, 3Aze C^4H_2, Tyr β-CH_2, Phe^3 β-CH_2, Phe^4 β-CH_2 and Phe^3 α-CH), 3.73 (3H, s, $COOCH_3$), 3.63-4.08 (1H, m, 3Aze α-CH), 4.15 (1H, m, Tyr α-CH), 4.75 (1H, m, Phe^4 α-CH), 5.80 (1H, br s, Tyr NH), 5.96 (1H, br s, Phe^3 NH), 6.61 (1H, d, *J* = 7.2 Hz

Phe^4 NH), 6.72-7.35 (14H, m, aromatics). Anal. Calcd for $C_{37}H_{44}N_4O_8$: C, 66.05; H, 6.59; N, 8.33. Found: C, 65.85; H, 6.57; N, 8.30.

***N*-Boc-Tyr-3Aze-Phe-Phe-NH$_2$ (12ae).** A solution of the peptide methyl ester **11ae** (0.12 g, 0.176 mmol) in MeOH/NH_3 sat. (5 mL) is allowed to stand in a pressure bottle at room temperature according to the general procedure C. The title compound was obtained as a white solid pure on TLC (0.11 g, 96%); ^{1}H NMR (DMSO-d_6): δ 1.46 [9H, s, C(CH$_3$)$_3$], 2.55-3.90 (11H, m, 3Aze C^{3}H$_2$, 3Aze C^{4}H$_2$, Tyr β-CH$_2$, Phe^3 β-CH$_2$, Phe^4 β-CH$_2$ and 3Aze α-CH), 3.99 (1H, m, Tyr α-CH), 4.47-4.53 (2H, m, Phe^3 α-CH and Phe^4 α-CH), 6.50 (1H, d, J = 7.2 Hz, Tyr NH), 6.61-7.36 (16H, m, aromatics and CONH$_2$), 8.00-8.31 (2H, m, Phe^3 NH and Phe^4 NH), 9.41 (1H, s, Tyr OH). Anal. Calcd for $C_{36}H_{43}N_5O_7$: C, 65.74; H, 6.59; N, 10.65. Found: C, 65.93; H, 6.60; N, 10.68.

TFA·H$_2$N-Tyr-3Aze-Phe-Phe-NH$_2$ (4). Deprotection of the *N*-Boc group was performed by adopting the general procedure B: **12ae** (0.049 g, 0.075 mmol), CH_2Cl_2/TFA (6 mL) gave **4** (0.050 g, quantitative yield); ^{1}H NMR (DMSO-d_6): δ 2.55-3.90 (11H, m, 3Aze C^{3}H$_2$, 3Aze C^{4}H$_2$, Tyr β-CH$_2$, Phe^3 β-CH$_2$, Phe^4 β-CH$_2$ and 3Aze α-CH), 3.99 (1H, m, Tyr α-CH), 4.47-4.53 (2H, m, Phe^3 α-CH and Phe^4 α-CH), 6.61-7.36 (16H, m, aromatics and CONH$_2$), 8.00-8.31 (5H, m, Phe^3 NH, Phe^4 NH and Tyr NH_3^+), 9.41 (1H, s, Tyr OH). Anal. Calcd for

$C_{33}H_{36}F_3N_5O_7$: C, 59.01; H, 5.40; N, 10.43. Found: C, 59.22; H, 5.41; N, 10.45.

***N*-Boc-3Aze-Trp-Phe-OMe (9be).** *N*-Boc-3-Aze-OH (0.123 g, 0.613 mmol) in CH_2Cl_2 (10 mL) was treated with compound **8b** (0.267 g, 0.558 mmol) according to the general procedure A. Silica gel chromatography ($CHCl_3$) gave a pure product **9be** as a white foam (0.244 g, 80%); $[a]_D$ +24° (*c* 1, $CHCl_3$); IR ($CHCl_3$): ν 3477, 1743, 1682 cm^{-1}; ^1H NMR ($CDCl_3$): δ 1.46 [9H, s, $C(CH_3)_3$], 2.88-3.45 (6H, m, 3Aze C^3H_2, Trp β-CH_2 and Phe^4 β-CH_2), 3.68 (3H, s, $COOCH_3$), 3.96-4.05 (2H, m, 3Aze C^4H_2), 4.01 (1H, m, 3Aze α-CH), 4.72 (2H, m, Phe α-CH and Trp α-CH), 6.00 (1H, br s, Trp NH), 6.35 (1H, br s, Phe^4 NH), 6.82-7.75 (10H, m, aromatics), 8.12 (1H, s, Trp Ind-NH). Anal. Calcd for $C_{30}H_{36}N_4O_6$: C, 65.68; H, 6.61; N, 10.21. Found: C, 65.74; H, 6.62; N, 10.23.

TFA·HN-3Aze-Trp-Phe-OMe (10be). Deprotection of the *N*-Boc group was performed by adopting the general procedure B: **9be** (0.217 g, 0.396 mmol), CH_2Cl_2/TFA (6 mL) gave **10be** (0.222 g, quantitative yield).

***N*-Boc-Tyr-3Aze-Trp-Phe-OMe (11be).** *N*-Boc-Tyr-OH (0.123 g, 0.436 mmol) in CH_2Cl_2 (10 mL) was treated with compound **10be** (0.222 g, 0.396 mmol) according to the general procedure A. Silica gel chromatography ($CHCl_3$/EtOAc 1:2) gave a pure product **11be** as a white foam (0.200 g, 71%); $[a]_D$ +10° (*c* 1, $CHCl_3$); IR ($CHCl_3$): ν 3475, 3424, 1741, 1656 cm^{-1};

^{1}H NMR ($CDCl_3$): δ 1.45 [9H, s, $C(CH_3)_3$], 2.72-3.23 (8H, m, 3Aze C^3H_2 Trp β-CH_2, Phe^4 β-CH_2 and Tyr β-CH_2), 3.57-3.99 (3H, m, 3Aze C^3H_2 and 3Aze α-CH), 3.67 (3H, s, $COOCH_3$), 4.01 (1H, m, 3Aze α-CH), 4.14 (1H, m, Tyr α-CH), 4.72 (2H, m, Phe α-CH and Trp α-CH), 5.45 (1H, m, Tyr NH), 6.23 (1H, br s, Trp NH), 6.68 and 7.63 (1H, two conformers, Phe NH), 6.82-7.63 (14H, m, aromatics), 8.74 (1H, s, Trp Ind-NH). Anal. Calcd for $C_{39}H_{45}N_5O_8$: C, 65.81; H, 6.37; N, 9.84. Found: C, 66.01; H, 6.38; N, 9.86.

***N*-Boc-Tyr-3Aze-Phe-Trp-NH_2 (12be).** A solution of the peptide methyl ester **11be** (0.07 g, 0.098 mmol) in MeOH/NH_3 sat. (3 mL) is allowed to stand in a pressure bottle at room temperature according to the general procedure C. The title compound was obtained as a white solid pure on TLC (0.058 g, 85%); ^{1}H NMR (DMSO-d_6): δ 1.43 [9H, s, $C(CH_3)_3$], 2.55-3.90 (11H, m, 3Aze C^3H_2, 3Aze C^4H_2, Tyr β-CH_2, Trp β-CH_2, Phe β-CH_2 and 3Aze α-CH), 3.99 (1H, m, Tyr α-CH), 4.42 (1H, m, Trp α-CH), 4.52 (1H, m, Phe α-CH), 6.58-7.59 (17H, m, aromatics, Tyr NH and $CONH_2$), 8.04-8.33 (2H, m, Trp NH, Phe NH), 9.40 (1H, s, Tyr OH), 10.79 (1H, s, Trp Ind-NH). Anal. Calcd for $C_{38}H_{44}N_6O_7$: C, 65.50; H, 6.36; N, 12.06. Found: C, 65.63; H, 6.24; N, 12.09.

TFA·H_2N-Tyr-3Aze-Trp-Phe-NH_2 (5). Deprotection of the *N*-Boc group was performed by adopting the general procedure B: **12be** (0.043 g, 0.062 mmol), CH_2Cl_2/TFA (6 mL) gave **5**

(0.044 g, quantitative yield); ^{1}H NMR (DMSO-d_6): δ 2.55-3.90 (11H, m, 3Aze C^{3}H$_2$, 3Aze C^{4}H$_2$, Tyr β-CH$_2$, Trp β-CH$_2$, Phe β-CH$_2$ and 3Aze α-CH), 3.99 (1H, m, Tyr α-CH), 4.42 (1H, m, Trp α-CH), 4.52 (1H, m, Phe α-CH), 6.58-7.59 (16H, m, aromatics and CONH$_2$), 8.04-8.33 (5H, m, Trp NH, Phe NH and Tyr NH$_3^+$), 9.40 (1H, s, Tyr OH), 10.79 (1H, s, Trp Ind-NH). Anal. Calcd for $C_{35}H_{37}F_3N_6O_7$: C, 59.15; H, 5.25; N, 11.82. Found: C, 59.29; H, 5.27; N, 11.78.

Boc-Δ^{3}Pro-Phe-Phe-OMe (9ac). *N*-Boc-Δ^{3}Pro-OH (0.118 g, 0.554 mmol) in CH_2Cl_2 (10 mL) was treated with compound **8a** (0.222 g, 0.504 mmol) according to the general procedure A. Silica gel chromatography ($CHCl_3$/EtOAc 1:2) gave a pure product **9ac** as a white foam (0.186 g, 71%); ^{1}H NMR ($CDCl_3$): δ 1.45 [9H, s, C(CH$_3$)$_3$], 2.83-3.09 (4H, m, Phe^3 β-CH$_2$, Phe^4 β-CH$_2$), 3.67 (3H, s, COOCH$_3$), 3.93-4.61 (4H, m, Phe^3 α-CH, Phe^4 α-CH and Δ^{3}Pro C^{5}H$_2$), 5.18 (1H, s, Δ^{3}Pro α-CH), 5.72 and 6.01 (2H, 2 br s, Δ^{3}Pro CH=CH), 6.09-7.36 (10H, m, aromatics), 8.12-8.25 (2H, m, Phe^3 NH and Phe^4 NH). Anal. Calcd for $C_{29}H_{35}N_3O_6$: C, 66.78; H, 6.76; N, 8.06. Found: C, 66.98; H, 6.78; N, 8.08.

TFA·HN-Δ^{3}Pro-Phe-Phe-OMe (10ac). Deprotection of the *N*-Boc group was performed by adopting the general procedure B: **9ac** (0.150 g, 0.288 mmol), CH_2Cl_2/TFA (6 mL) gave **10ac** (0.154 g, quantitative yield).

Boc-Tyr-Δ^3Pro-Phe-Phe-OMe (11ac). *N*-Boc-Tyr-OH (0.089 g, 0.317 mmol) in CH_2Cl_2 (10 mL) was treated with compound **10ac** (0.154 g, 0.288 mmol) according to the general procedure A. Silica gel chromatography ($CHCl_3$/EtOAc 1:2) gave a pure product **11ac** as a white foam (0.128 g, 65%); ^{1}H NMR ($CDCl_3$): δ 1.43 [9H, s, $C(CH_3)_3$], 2.83-3.09 (6H, m, Phe^3 β-CH_2, Phe^4 β-CH_2, Tyr β-CH_2), 3.67 (3H, s, $COOCH_3$), 3.93-4.61 (5H, m, Phe^3 α-CH, Phe^4 α-CH, Tyr α-CH and Δ^3Pro C^5H_2), 5.18 (1H, s, Δ^3Pro α-CH), 5.72 and 6.01 (2H, 2 br s, Δ^3Pro CH=CH), 6.09-7.36 (15H, m, aromatics and Tyr NH), 8.12-8.25 (2H, m, Phe^3 NH, Phe^4 NH), 9.51 (1H, s, Tyr OH). Anal. Calcd for $C_{38}H_{44}N_4O_8$: C, 66.65; H, 6.48; N, 8.18. Found: C, 66.84; H, 6.49; N, 8.20.

Boc-Tyr-Δ^3Pro-Phe-Phe-NH_2 (12ac). A solution of the peptide methyl ester **11ac** (0.090 g, 0.131 mmol) in MeOH/NH_3 sat. (6.3 mL) is allowed to stand in a pressure bottle at room temperature according to the general procedure C. The title compound was obtained as a white solid pure on TLC (0.061 g, 70%); ^{1}H NMR (DMSO-d_6): δ 1.43 [9H, s, $C(CH_3)_3$], 2.83-3.09 (6H, m, Phe^3 β-CH_2, Phe^4 β-CH_2, Tyr β-CH_2), 3.93-4.61 (5H, m, Phe^3 α-CH, Phe^4 α-CH, Tyr α-CH and Δ^3Pro C^5H_2), 5.18 (1H, s, Δ^3Pro α-CH), 5.72 and 6.01 (2H, 2 br s, Δ^3Pro CH=CH), 6.09-7.36 (17H, m, aromatics, Tyr NH and $CONH_2$), 8.12-8.25 (2H, m, Phe^3 NH and Phe^4 NH), 9.51 (1H, s, Tyr OH). Anal. Calcd

for $C_{37}H_{43}N_5O_7$: C, 66.35; H, 6.47; N, 10.46. Found: C, 66.54; H, 6.48; N, 10.49.

TFA·H_2N-Tyr-Δ^3Pro-Phe-Phe-NH_2 (1). Deprotection of the *N*-Boc group was performed by adopting the general procedure B: **12ac** (0.040 g, 0.06 mmol), CH_2Cl_2/TFA (6 mL) gave **1** (0.041 g, quantitative yield); ^{1}H NMR (DMSO-d_6): δ 2.83-3.09 (6H, m, Phe^3 β-CH_2, Phe^4 β-CH_2, and Tyr β-CH_2), 3.93-4.61 (5H, m, Phe^3 α-CH, Phe^4 α-CH, Tyr α-CH and Δ^3Pro C^5H_2), 5.18 (1H, s, Δ^3Pro α-CH), 5.72 and 6.01 (2H, 2 br s, Δ^3Pro CH=CH), 6.09-7.36 (16H, m, aromatics and $CONH_2$), 8.12-8.25 (5H, m, Phe^3 NH, Phe^4 NH and Tyr NH_3^+), 9.51 (1H, s, Tyr OH). Anal. Calcd for $C_{34}H_{36}F_3N_5O_7$: C, 59.73; H, 5.31; N, 10.24. Found: C, 59.55; H, 5.36; N, 10.30.

Boc-Tyr-Cys(Me)-OMe. *N*-Boc-Tyr-OH (0.834 g, 2.97 mmol) in CH_2Cl_2 (10 mL) was treated with HCl·H_2N-Cys(Me)-OMe (0.500 g, 2.70 mmol) according to the general procedure A. Silica gel chromatography ($CHCl_3$/EtOAc 1:1) gave a pure product as a white foam (0.845 g, 76%); ^{1}H NMR ($CDCl_3$): δ 1.45 [9H, s, $C(CH_3)_3$], 2.15 (3H, s, Cys CH_3), 2.72-3.01 (4H, m, Cys β-CH_2 and Tyr β-CH_2), 3.73 (3H, s, $COOCH_3$), 3.93 (1H, m, Tyr α-CH), 4.49 (1H, m, Cys α-CH), 6.62 (1H, d, J = 7.6 Hz, Tyr NH), 6.99 (1H, d, J = 8.0 Hz, Cys NH), 6.68 and 7.08 (4H, m, aromatics), 9.51 (1H, s, Tyr OH). Anal. Calcd for $C_{19}H_{28}N_2O_6S$: C, 55.32; H, 6.84; N, 6.79. Found: C, 55.48; H, 6.86; N, 6.81.

Boc-Tyr-Cys(Me)-Phe-OMe. *N*-Boc-Tyr-Cys(Me)-OH (0.772 g, 1.94 mmol), obtained by treatment with 1N NaOH (3 equiv.) in MeOH (10 mL), in CH_2Cl_2 (10 mL) was treated with $HCl \cdot H_2N$-Phe-OMe (0.378 g, 1.76 mmol) according to the general procedure A. Silica gel chromatography ($CHCl_3$/EtOAc 1:1) gave a pure product as a white foam (0.688 g, 70%); ^1H NMR ($CDCl_3$): δ 1.45 [9H, s, $C(CH_3)_3$], 2.15 (3H, s, Cys CH_3), 2.72-3.09 (6H, m, Cys β-CH_2, Phe β-CH_2 and Tyr β-CH_2), 3.73 (3H, s, $COOCH_3$), 3.93 (1H, m, Tyr α-CH), 4.49 (1H, m, Cys α-CH), 4.52 (1H, m, Phe α-CH), 6.62 (1H, d, J = 7.6 Hz, Tyr NH), 6.99 (1H, d, J = 8.0 Hz, Cys NH), 6.65-7.03 (10H, m, aromatics and Phe NH), 9.51 (1H, s, Tyr OH). Anal. Calcd for $C_{28}H_{37}N_3O_7S$: C, 60.09; H, 6.66; N, 7.51. Found: C, 60.27; H, 6.67; N, 7.53.

Boc-Tyr-Cys[(O)Me)]-Phe-OMe (3a). Sodium metaperiodate (0.251 g, 1.18 mmol) was dissolved in water (5 mL) and cooled to 0 °C. Boc-Tyr-Cys(Me)-Phe-OMe (0.600 g, 1.07 mmol) was dissolved in dioxane (10 mL) and added dropwise to the oxidant. Stirring was continued for 1 h. The reaction mixture was concentrated to remove organic solvent and the product extracted with CH_2Cl_2 (2 x 25 mL). The combined organic phases were washed with water (2 x 30 mL), brine (30 mL) and dried. Concentration of the organic phases in vacuo yielded both diastereoisomers of the title compound (0.609 g, 99%); ^1H NMR ($CDCl_3$): δ 1.45 [9H, s, $C(CH_3)_3$], 2.65

(3H, s, Cys-(O)CH_3), 2.72-3.09 (6H, m, Cys β-CH_2, Phe β-CH_2 and Tyr β-CH_2), 3.71 (3H, s, $COOCH_3$), 3.93 (1H, m, Tyr α-CH), 4.49 (1H, m, Cys α-CH), 4.52 (1H, m, Phe α-CH), 6.62 (1H, d, J = 7.6 Hz, Tyr NH), 6.99 (1H, d, J = 8.0 Hz, Cys NH), 6.65-7.03 (10H, m, aromatics and Phe NH), 9.51 (1H, s, Tyr OH). Anal. Calcd for $C_{28}H_{37}N_3O_8S$: C, 58.42; H, 6.48; N, 7.30. Found: C, 58.59; H, 6.49; N, 7.32.

Boc-Tyr-ΔAla-Phe-OMe. Compound **3a** (0.59 g, 1.03 mmol) was dissolved in MeOH (5 mL), DBU (0.313 g, 0.31 mL) added and the reaction mixture stirred at room temperature for 1.5 h. The reaction mixture was evaporated to dryness. The resulting compound was purified by column chromatography on silica gel (EtOAc/hexane 1:1) yielding the title compound as a colourless glass (0.505 g, 96% yield); ^{1}H NMR (DMSO-d_6): δ 1.45 [9H, s, $C(CH_3)_3$], 2.83-3.09 (4H, m, Phe β-CH_2 and Tyr β-CH_2), 3.71 (3H, s, $COOCH_3$), 3.93 (1H, m, Tyr α-CH), 4.52 (1H, m, Phe α-CH), 4.80 and 5.47 (2H, s, ΔAla CH_2), 6.62 (1H, d, J = 7.6 Hz, Tyr NH), 6.65-7.21 (9H, m, aromatics), 7.46 (1H, s, ΔAla NH), 8.11 (1H, d, J = 7.2 Hz, Phe NH), 9.51 (1H, s, Tyr OH). Anal. Calcd for $C_{27}H_{33}N_3O_7$: C, 63.39; H, 6.50; N, 8.21. Found: C, 63.58; H, 6.52; N, 8.23.

Boc-Tyr-ΔAla-Phe-OH (4a). Boc-Tyr-ΔAla-Phe-OMe (0.480 g, 0.94 mmol) was dissolved in MeOH (8 mL) and cooled on an ice bath whilst 1N NaOH (4.7 mL) was added dropwise. The reaction was allowed to warm to room

temperature over 1.5 h. The reaction mixture was concentrated, acidified to pH 4 with 2M $KHSO_4$ and the product extracted into CH_2Cl_2 (2 x 30 mL). The combined organics were washed with water, brine, dried and concentrated in vacuo yielding the desired compound **4a** as a white foam (0.467 g, quantitative yield).

Boc-Tyr-ΔAla-Phe-Phe-NH_2 (5a). Compound **4a** (0.450g, 0.905 mmol) in CH_2Cl_2 (10 mL) was treated with $HCl \cdot H_2N$-Phe-NH_2 (0.164 g, 0.822 mmol) according to the general procedure A. Silica gel chromatography ($CHCl_3$/EtOAc 1:2) gave a pure product **5a** as a white foam (0.264 g, 50%); ^{1}H NMR (DMSO-d_6): δ 1.45 [9H, s, $C(CH_3)_3$], 2.83-3.09 (6H, m, Phe^3 β-CH_2, Phe^4 β-CH_2 and Tyr β-CH_2), 3.93 (1H, m, Tyr α-CH), 4.47-4.53 (2H, m, Phe^3 α-CH and Phe^4 α-CH), 4.80 and 5.47 (2H, s, ΔAla CH_2), 6.62 (1H, d, J = 7.6 Hz, Tyr NH), 6.65-7.21 (16H, m, aromatics and $CONH_2$), 7.46 (1H, s, ΔAla NH), 8.11 (1H, d, J = 7.2 Hz, Phe^3 NH), 8.37 (1H, d, J = 7.2 Hz, Phe^4 NH), 9.51 (1H, s, Tyr OH). Anal. Calcd for $C_{35}H_{41}N_5O_7$: C, 65.30; H, 6.42; N, 10.88. Found: C, 65.49; H, 6.44; N, 10.91.

TFA·H_2N-Tyr-ΔAla-Phe-Phe-NH_2 (6). Deprotection of the *N*-Boc group was performed by adopting the general procedure B: **5a** (0.1 g, 0.155 mmol), CH_2Cl_2/TFA (6 mL) gave **6** (0.101 g, quantitative yield); ^{1}H NMR (DMSO-d_6): δ 2.74-3.07 (6H, m, Tyr β-CH_2, Phe^3 β-CH_2, Phe^4 β-CH_2), 4.24 (1H, m, Tyr α-CH), 4.50-4.58 (2H, m, Phe^3 α-CH and Phe^4 α-CH), 5.54 and 6.17

(2H, two s, ΔAla CH_2), 6.69-7.29 (16H, m, aromatics and $CONH_2$), 7.46 (1H, s, ΔAla NH), 8.09 (3H, br, Tyr NH_3^+), 8.18 and 8.56 (2H, two d, Phe^3 NH and Phe^4 NH), 9.69 (1H, s, Tyr OH). Anal. Calcd for $C_{32}H_{34}F_3N5O_7$: C, 58.44; H, 5.21; N, 10.65. Found: C, 58.37; H, 5.26; N, 10.61.

1.4.3.3 Biological assays

Receptor binding affinities to the δ- and μ-opioid receptors were performed using cell membrane preparations from transfected cells that stably express the respective receptors. The radiolabeled ligands used were [^{3}H]DPDPE and [^{3}H]DAMGO for δ- and μ-receptors, respectively (for more details about the procedure see Ref. 92). The *in vitro* tissue bioassays (MVD and GPI/LMMP) were performed as described previously.[93] IC_{50} values represent means of no less than four experiments. IC_{50} values, relative potency estimates, and their associated standard errors were determined by fitting the data to the Hill equation by a computerised non-linear least-squares method.

Acknowledgements

This research was supported in part by grants from the U.S. Public Health Service, National Institute of Drug Abuse DA06284 and DA13449 (V. J. H.).

1.5 Synthesis and evaluation of new endomorphin-2 analogues containing (Z)-α,β-dehydrophenilalanine (Δ^ZPhe) residues*

The alteration of the backbone sequence of native bioactive peptides through incorporation of unnatural amino acids or exogenous fragments of a different structure, is a common strategy adopted in medicinal chemistry in order to study their structure activity relationships and to obtain compounds with improved potency, selectivity, and potential therapeutic value.

Recent and significant examples of this approach can be found in the field of endomorphins, two endogenous neuropeptides [endomorphin-1: Tyr-Pro-Trp-Phe-NH_2 (EM-1) and endomorphin-2: Tyr-Pro-Phe-Phe-NH_2 (EM-2)], whose main proposed biological function is the pain control through activation, with high affinity and selectivity, of μ-opioid receptors.[23,24] A systematic evaluation of a variety of synthetic endomorphin analogues have provided insights into various structural and conformational features which are critical for the bioactivity of this family of neuropeptides.[94,95] The role exerted by the proline residue at position 2 of the tetrapeptide backbone as well as the spatial orientation adopted by the two Phe aromatic side chains at positions 3 and 4 appear to be

*Torino, D.; Mollica, A; Pinnen, F.; Feliciani, F.; Lucente, G.; Fabrizi, G.; Portalone, G.; Davis, P.; Lai, J.; Ma, S-W.; Porreca F.; Hruby, V. J. *J. Med. Chem.* (*submitted*)

particularly relevant.[50,68,91] Several papers, dealing with the incorporation at position 2 of EM with higher and lower homologues of proline,[74,96,97] and cyclic β-residues[58,65,69] document the attention dedicated to this first point. Also clearly documented is the influence that the mutual spatial orientation of the aromatic rings exerts on the interaction between EMs and their receptors.[57,98,99] The interest focused on this specific effect is based on the well recognized influence of the non bonded aromatic/aromatic and backbone/aromatic interactions on the conformational stability of the peptide.

In accordance with the above reported observations, a literature examination reveals that several papers, have described structural modifications performed on the EM native sequences, which specifically focused on replacement of the Phe^3 and Phe^4 residues. In Figure 11 most of the so far incorporated Phe mimic residues are illustrated.

Of particular interest appears the enhancement of activity and selectivity of EM analogues obtained through incorporation of β-methylated Phe residues (Figure 11) performed by Tomboly and coworkers.[102] The interesting rationale followed by these authors is based on the reduction of the conformational mobility of the Phe aromatic side chains by biasing, according to the original proposals of Hruby,[103,104] the population of the $\chi 1$ (torsion angle) rotamers. By following a related and still unexplored approach we decided to synthesize and investigate

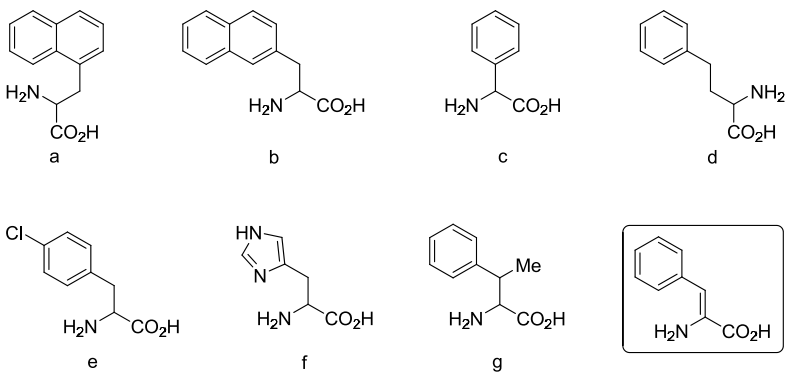

Figure 11. Structures **a-g** illustrate examples of aromatic amino acids so far used to replace native residues at positions 3 and/or 4 of endomorphins. The structure in the box refers to Δ^{Z}Phe, the achiral α,β-didehydro-amino acid adopted in the present study. (**a**): 3-(1-naphtyl)-alanine (1Nal);[70] (**b**): 3-(2-naphthyl)-alanine (2Nal);[70] (**c**): phenylglycine (Phg);[57,100] (**d**): homophenylalanine (Hfe);[100] (**e**): *p*-Cl phenylalanine;[101] (**f**): histidine;[98] (**g**): β-methyl-phenylalanine (β-MePhe).[102]

the properties of a series of EM analogues incorporating α,β-unsaturated phenylalanine residues at the position 3 and 4. In analogues with this structure the aromatic ring, and each of its two adjacent backbone amide groups, are bound to a sp^2 hybridized C^{β} or C^{α} atom, respectively. As a consequence, the achiral ΔPhe residue exerts conformational constraint on the backbone and restricts, at the same time, the β-aromatic substituent to the either (*Z*) or (*E*) orientation. These steric and stereochemical features, together with the chemical properties connected with the electronic distribution within the involved peptide bonds, render α,β-dehydroamino acids an appealing tool for the development of variants of naturally occurring bioactive peptides. The consequences of this structural alteration appear

quite relevant in the case of the tetrapeptidic EMs molecule. Here in fact three closely located aromatic side chains are present and their location involves both the "message" Tyr-Pro-Phe- *N*-terminal moiety and the Phe-NH_2 "address" *C*-terminal fragment.[105]

1.5.1 Chemistry

The syntheses of three EM-2 analogues Tyr-Pro-Δ^ZPhe-Phe-NH_2 {[Δ^ZPhe^3]EM-2} (**1**), Tyr-Pro-Phe-Δ^ZPhe-NH_2 {[Δ^ZPhe^4]EM-2} (**2**) and Tyr-Pro-Δ^ZPhe-Δ^ZPhe-NH_2 {[Δ^ZPhe^{3,4}]EM-2} (**3**) are here reported. Incorporation of the Δ^ZPhe residue has been accomplished by performing an acetic anhydride mediated azlactonization-dehydration reaction on dipeptide or tripeptide units containing *C*-terminal β-hydroxy-D,L-phenylalanine.[106] Scheme 4 outlines the synthesis of the [Δ^ZPhe^3] and [Δ^ZPhe^{3,4}] EM-2 analogs. The common intermediate Boc-Pro-Δ^ZPhe-azlactone **5** is used to obtain both the final tetrapeptides **1** and **3**. Ring opening of the *C*-terminal unsaturated azlactone **5** with the sodium salt of β-hydroxy-D,L-phenylalanine, followed by azlactonization and subsequent treatment with MeOH/DMAP is the key step for the incorporation of the two consecutive Δ^ZPhe residues in the tetrapeptide **3**. An analogous synthetic pathway is illustrated in Scheme 5 where the synthesis of [Δ^ZPhe^4]EM-2 (**2**) is outlined.

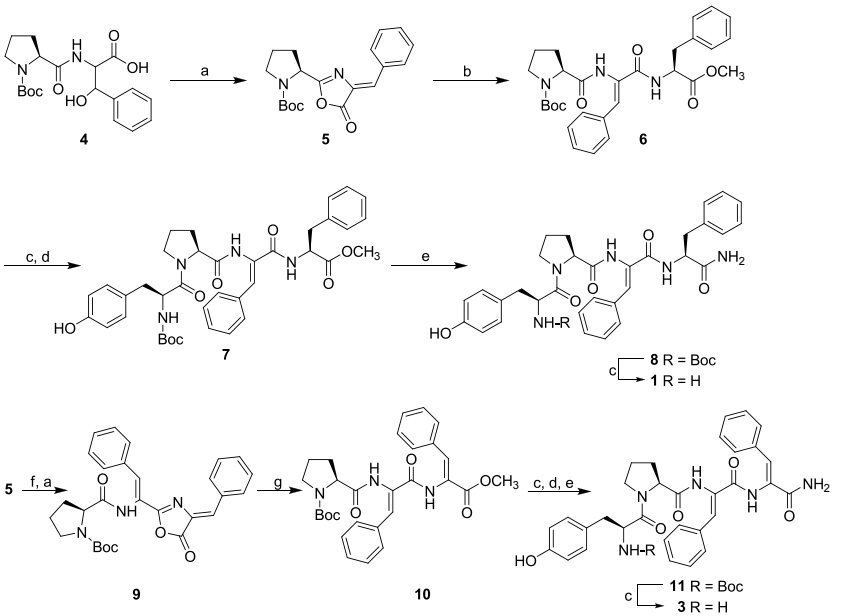

Scheme 4. Synthesis of compound **1-3**. *Reagents and conditions*: a) $(CH_3CO)_2O/CH_3COONa$, 24 h rt; b) $HCl{\cdot}H_2N$-Phe-OMe, DIEA, DMAP, CH_2Cl_2, 12 h rt; c) TFA/CH_2Cl_2 1:1, 1 h rt; d) Boc-Tyr-OH, EDC, HOBt, NMM, CH_2Cl_2, 30 min 0 °C, 12 h rt; e) NH_3/MeOH, 48 h rt; f) DL-3-β-(OH)Phe-OH, 1N NaOH, acetone, 12 h rt; g) DMAP, MeOH, 12 h rt.

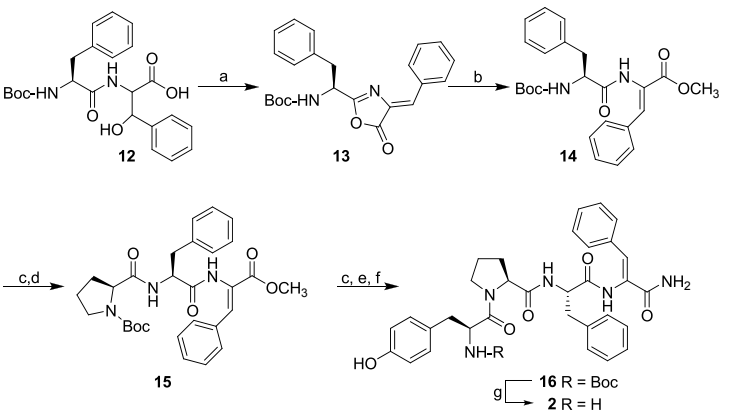

Scheme 5. Synthesis of compound **2**. *Reagents and conditions*: a) $(CH_3CO)_2O/CH_3COONa$, 24 h rt; b) DMAP, MeOH, 12 h rt; c) TFA/CH_2Cl_2 1:1, 1 h rt; d) Boc-Pro-OH, EDC, HOBt, NMM, CH_2Cl_2, 30 min 0 °C, 12 h rt; e) Boc-Tyr-OH, EDC, HOBt, NMM, CH_2Cl_2, 30 min 0 °C, 12 h rt; f) NH_3/MeOH, 48 h rt.

1.5.2 Results and discussion

Table 2 summarizes binding affinity and functional bioactivity for μ and δ opioid receptors of the here studied EM-2 analogues. Data reported indicate that [Δ^{Z}Phe^{3}]EM-2 (**1**) and [Δ^{Z}Phe^{3,4}]EM-2 (**3**) bind weakly to μ receptors ($K_i\mu$ = 202 nM and 128 nM, respectively) and are, although with a certain μ selectivity, weakly active in the GPI assay. Conversely, the analogue [Δ^{Z}Phe^{4}]EM-2 (**2**) shows potent μ binding affinity and high μ versus δ selectivity ($K_i\delta$ /$K_i\mu$ = 1200 ca.) with high potency in the GPI assay, comparable to the parent EM-2. Thus, binding and bioassays data indicate that, the incorporation of the Δ^{Z}Phe at position 3 or at positions 3 and 4 simultaneously, are both detrimental structural modifications. The corresponding alteration, performed at position 4 only, leads to the ligand **2** which maintains high affinity and activity together with the μ selectivity typical of the native ligand.

Table 2. Binding affinity and *in vitro* activity for compounds **1-3** and **EM-2**.

	Receptor affinity[a,b] (nM)		Selectivity	Functional bioactivity	
Compound	$K_i\delta$	$K_i\mu$	δ/μ	MVD[b] (IC_{50})	GPI[b] (IC_{50})
EM-2	-	8.23 ± 0.48	-	-	9.67 ± 0.84
1 [Δ^{Z}Phe^{3}]EM-2	n.c.[c]	200 ± 16	-	1953 ± 430	170 ± 13
2 [Δ^{Z}Phe^{4}]EM-2	>10000	8.4 ± 1.2	>1200	390 ± 87	25 ± 2.8
3 [Δ^{Z}Phe^{3,4}]EM-2	7300 ± 890	130 ± 36	57	1060 ± 120	330 ± 59

[a] Displacement of [^{3}H]DAMGO (μ-selective) and [^{3}H]DPDPE (δ-selective) from rat brain membrane binding sites.
[b] ± S.E.M.
[c] n.c. = not binding recorded.

In order to gain further information on the preferred conformation of the new ligands we examined the 2D ^{1}H NMR structures of the new ligands **1-3**, the conformation adopted in solution, and in the crystal structure of **8,** the N^{α}-Boc derivative of **1**, namely Boc-Tyr-Pro-Δ^{Z}Phe-Phe-NH_2 (see Scheme 4).

Single crystals of **8** were successfully obtained by slow evaporation from a solution in MeOH. The molecule (Figure 12 and Table 3) presents a *trans* Tyr-Pro amide bond and adopts a H-bond stabilized β-turn structure with the Pro and Δ^{Z}Phe residues at the *i*+1 and *i*+2 corner positions, respectively, of the turn. As for the endomorphin μ-receptor agonists, only two other crystal structures have been reported, i.e. [D-Tic^2]EM-2[107] and [Chx^2]EM-2[56] in addition to the *C*-terminal free acid Tyr-Pro-Phe-Phe-OH,[55] this latter completely devoid of μ-opioid receptor agonist activity. The X-ray crystal structure of **8** gives then the first available information on the solid state conformation adopted by an *N*-protected EM analogue. As shown in Table 4 and Figure 13 [Δ^{Z}Phe^3]EM-2 (**1**) and its N^{α}-Boc protected derivative **8** show strong sequential NOEs Pro C^{α}H···Δ^{Z}Phe^3 NH. This effect is observed, for both **1** and **8**, by two interresidue NOEs which are not found in the case of [Δ^{Z}Phe^4]EM-2 (**2**) and [Δ^{Z}Phe^{3,4}]EM-2 (**3**): the first between the NH groups of Δ^{Z}Phe^3 and Phe^4 and the second between Pro C^{α}H and Phe^4 NH (i.e. between the "*i*+2 and *i*+3" and "*i*+1 and *i*+3" residues, respectively, of a β-turn).

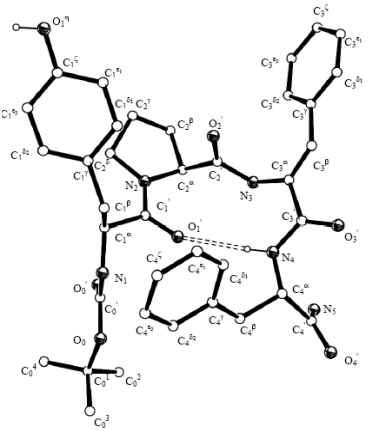

Figure 12. X-ray crystal structure of Boc-Tyr-Pro-Δ^{Z}Phe-Phe-NH_2 (**8**), with numbering of the atoms. The intramolecular H-bond is shown as a dashed double line.

Table 3. Main backbone and side chains torsion angles (°) of the X-ray crystal structure of **8**[a].

Backbone		
O_0-C_0'-$N_1C_1^{\alpha}$	ω_0	177.5(4)
C_0'-N_1-C_1^{α}-C_1'	φ_1	-62.7(6)
N_1-C_1^{α}-C_1'-N_2	ψ_1	150.3(4)
C_1^{α}-C_1'-N_2-C_2^{α}	ω_1	175.5(5)
C_1'-N_2-C_2^{α}-C_2'	φ_2	-59.4(6)
N_2-C_2^{α}-C_2'-N_3	ψ_2	127.9(4)
C_2^{α}-C_2'-N_3-C_3^{α}	ω_2	-175.5(4)
C_2'-N_3-C_3^{α}-C_3'	φ_3	113.8(5)
N_3-C_3^{α}-C_3'-N_4	ψ_3	-14.2(7)
C_3^{α}-C_3'-N_4-C_4^{α}	ω_3	-179.3(5)
C_3'-N_4-C_4^{α}-C_4'	φ_4	-78.1(6)
N_4-C_4^{α}-C_4'-N_5	ψ_4	-19.3(6)
Side chains		
N_1-C_1^{α}-C_1^{β}-C_1^{γ} (Tyr)	$\chi_1^{1,1}$	-156.2(4)
N_2-C_2^{α}-C_2^{β}-C_2^{γ} (Pro)	$\chi_2^{1,1}$	18.2(6)
N_3-C_3^{α}-C_3^{β}-C_3^{γ} (Δ^{Z}Phe)	$\chi_3^{1,1}$	-8.0(11)
N_4-C_4^{α}-C_4^{β}-C_4^{γ} (Phe)	$\chi_4^{1,1}$	-72.6(5)

[a] Numbers in parenthesis are e.s.d. values.

Table 4. Observed NOE cross peaks and intensities of analogs **1**-**3** and **8**[a] in DMSO-d_6.

	1	**2**	**3**	**8**
Δ^zPhe^3 NH··· Phe^4 NH	m	-	-	m
Pro C$^\alpha$H··· Phe^4 NH	m[b]	-	-	m
Pro C$^\alpha$H··· Δ^zPhe^3 NH	s[b]	-	s	s
Pro C$^\alpha$H··· Phe^3 NH	-	s	-	-
Phe C$^\alpha$H··· Δ^zPhe^4 NH	-	m	-	-
Tyr C$^\alpha$H··· Pro C$^\delta$H$_2$	m	m	m	m

[a] NOE intensities are classified as weak (1.6 - 5.0 Å), medium (1.6 - 3.6 Å) and strong (1.6 - 2.9 Å). [b] The Pro C$^\alpha$H is partially overlapped with Phe C$^\alpha$H.

These data strongly suggest that the N^α-Boc derivative **8** maintains in DMSO-d_6 solution the folded conformation found in the crystal and that the same conformational preference is also shown by its *N*-terminal free analog **1**. It is worth noting that findings on **1** and **8** are those expected on the basis of literature on peptides containing α,β-didehydro amino acid where the strong tendency of the Δ^ZPhe residue to occupy the *i*+2 position of β-turns is well documented.[108,109] No NOEs indicative of folded structures could be found in the spectra of the two peptides [Δ^ZPhe^4]EM-2 (**2**) and [Δ^ZPhe^{3,4}]EM-2 (**3**). Furthermore, the presence of the sequential NOEs Pro C$^\alpha$H···Phe NH and Phe NH···Δ^ZPhe NH in the spectrum of **2** are consistent with an extended structure.

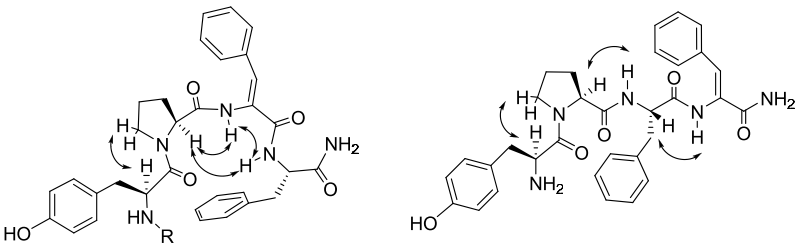

Figure 13. Relevant interproton correlations as deduced by ROESY experiments of compounds **1**, **2** and **8**.

1.5.3 Conclusions

As revealed by literature data the tetrapeptidic molecule of EMs is characterized by considerable conformational flexibility involving both the backbone and the aromatic side chains. Although the optimal three-dimensional arrangement of the EM pharmacophoric elements favouring selectivity and potency as μ agonist is not yet resolved, the relevant role of a proper spatial orientation of the aromatic rings, and in particular of the benzylic side chains at position 3 and 4, is well established. Here we have examined the properties of new EM analogues in which Phe mimics, with the aromatic ring blocked in the (*Z*) spatial orientation, have been incorporated. A remarkable difference is observed in the receptor affinity and functional bioactivity between [Δ^{Z}Phe^{4}]EM-2 (**2**), possessing the aromatic at position 3 free to adopt a proper spatial orientation, and the analogue [Δ^{Z}Phe^{3}]EM-2 (**1**) in which the Phe at position 3 is forced to the rigid (*Z*) orientation imposed by the olefinic geometry of the

residue. These results underline the importance of the correct orientation of the aromatic rings, and suggest, at the same time, that the performed modification of Phe^3, in the Tyr-Pro-Phe- "message" moiety, leads to the ligand **1** in which both the folded conformation of the backbone and the third aromatic ring spatial orientation are unfavourable features for proper interaction with the receptor. The [$\Delta^Z$$Phe^4$]EM-2 (**2**) analogue**,** which maintains unchanged the native EM "message" sequence and an extended backbone conformation exhibits a high activity, comparable to that of EM-2. In this analogue the aromatic side chain at position 3 is not forced to a Δ^Z orientation and can adopt a proper orientation in the receptor pocket. This interpretation appears to be in agreement with the previously described EM analogues containing β-MePhe stereoisomers.[102] Here, the highest activity is shown by the ligand Tyr-Pro-Phe-(2*S*,3*S*)-β-MePhe-NH_2 which maintains the native Phe^3 residue and possesses at position 4 an aromatic side chain properly oriented by the stereochemistry of the β-MePhe residue.

1.5.4 Experimental section

Materials and methods. Spectrograde solvents were purchased from Merck; all the other solvents and reagents were of the purest grade commercially available. TLC (thin layer chromatography) and PLC (preparative layer chromatography) were performed on silica gel Merck 60 F_{254} plates. The drying

agent was sodium sulphate. All 1D and 2D ^{1}H NMR experiments were performed at 400 MHz on a Bruker Avance 400 NMR spectrometer with a constant temperature at 298 K. The ROESY spectra were obtained using standard pulse programs, with a mixing times of 300 ms. The 2D NMR matrixes were created and analyzed using the TOPSPIN 3.0a computer program (Bruker Biospin - 2009). Each two-dimensional spectrum was acquired in a 1024 x 1024 data matrix complex points in F_1 and F_2. Zero filling in F_1 and sine windows in both dimensions were applied before Fourier transformation. Chemical shifts (δ) are quoted in parts per million (ppm) downfield from tetramethylsilane, and values of coupling constants are given in Hz. The purity of all tested compounds was determined by combustion analysis and they are ≥ 95% pure. HRMS data of final products are also reported.

1.5.4.1 Chemistry. General procedures

A. Coupling with the carbodiimide method. To an ice-cooled mixture containing the required *N*-Boc-amino acid (1.0 mmol), HOBt (1.1 mmol), EDC (1.1 mmol) and NMM (2.2 mmol) in anhydrous CH_2Cl_2, the amino-derivative salt (1.1 mmol) was added. The reaction mixture was allowed to warm to 0 °C for 10 min and then to room temperature. After 12 h the reaction mixture was diluted with EtOAc (20 mL) and washed

with 5% citric acid (3 x 15 mL), $NaHCO_3$ ss (3 x 15 mL) and NaCl ss (2 x 15 mL). The organic layer was dried over Na_2SO_4 and evaporated under reduced pressure.

B. Deprotection of Boc-derivatives. The Boc group was removed by treatment with TFA in CH_2Cl_2 (1:1) for 1 h at room temperature. Removal of solvent and precipitation of the residue with diethyl ether gave the TFA salt that was used in the next step without further purification.

C. Preparation of peptide amides. The peptide methyl ester is allowed to stand in a pressure bottle at room temperature for 48 h in anhydrous methanol previously saturated with ammonia gas at 0 °C. The solution is then concentrated to dryness in vacuo at a temperature not exceeding 40 °C.

1.5.4.2 Synthesis

***N*-Boc-Pro-*β*-(OH)Phe-OH (4).** To a precooled solution (-10 °C) of Boc-Pro-OH (2 g, 9.3 mmol) in THF, NMM (9.3 mmol) and *i*BuOCOCl (9.3 mmol) were added. After 10 min of stirring, a solution of DL-(*β*-OH)Phe (2.22 g, 11.16 mmol) in 1N NaOH (11.1 mL) was added and the mixture stirred at 0 °C for 2 h and at room temperature overnight. The organic solvent was removed under reduced pressure and the acqueous phase was

acidified with solid citric acid to pH 3 and extracted with EtOAc (3 x 15 mL). EtOAc layer was washed with water, dried and evaporated under reduced pressure to give TLC pure title product **4** as colourless oil (2.89 g, 82%).

***N*-Boc-Pro-Phe-azlactone (5).** To a solution of **4** (2.89 g, 7.65 mmol) in acetic anhydride (11.7 mL) was added freshly fused sodium acetate (0.627 g, 7.65 mmol) and the mixture was left overnight at room temperature. The reaction mixture was poured over crushed ice and stirred. Then was extracted with EtOAc and organic layer was washed with 10% $NaHCO_3$, water and dried under reduced pressure. The azlactone **5** (2.48 g, 95%) was used for preparation of **6** without further purification.

***N*-Boc-Pro-Δ^ZPhe-PheOMe (6).** To a stirred solution of azlactone **5** (2.48 g, 7.24 mmol) and HCl·H_2N-Phe-OMe in CH_2Cl_2 (20 mL), DIEA (1.24 mL, 7.24 mmol) and DMAP (0.035 g, 0.04 mmol, 4 mol %) were added at 0 °C and the reaction mixture was stirred overnight at room temperature. Then the reaction mixture was diluted with CH_2Cl_2 and the organic layer was washed by saturated acqueous $NaHCO_3$, water and brine. The organic layer was dried and evaporated under reduced pressure to give TLC pure title product **6** as white foam (3.23 g, 86%); ^{1}H NMR (DMSO-d_6): δ 1.41 [9H, s, $C(CH_3)_3$], 1.70-2.19 (4H, m, Pro C^3H_2 and Pro C^4H_2), 3.05-3.10 (2H, m, Phe β-CH_2), 3.56 (3H, s, $COOCH_3$), 3.40-3.60 (2H, m, Pro C^5H_2), 4.27 (1H, m, Pro α-CH), 4.54 (1H, m, Phe α-CH), 7.18-

7.61 (11H, m, aromatics and Δ^ZPhe β-CH), 8.02 (1H, d, *J* = 7.2 Hz, Phe NH), 9.69 (1H, s, Δ^ZPhe NH).

***N*-Boc-Tyr-Pro-Δ^zPhe-Phe-OMe (7).** The Boc group of **6** was removed in according to general procedure B to give a quantitative yield of TFA·HN-Pro-Δ^ZPhe-Phe-OMe. *N*-Boc-Tyr-OH (0.924 g, 3.28 mmol) in CH_2Cl_2 (20 mL) was treated with TFA·HN-Pro-Δ^ZPhe-Phe-OMe (1.597 g, 2.98 mmol) according to the general procedure A. Silica gel chromatography (CH_2Cl_2/MeOH 98:2) gave a pure product **7** as a white foam (0.816 g, 40%); ^{1}H NMR ($CDCl_3$): δ 1.3 [9H, s, $C(CH_3)_3$], 1.61-2.15 (4H, m, Pro C^3H_2 and Pro C^4H_2), 2.80-3.20 (4H, m, Phe β-CH_2 and Tyr β-CH_2), 3.30 and 3.75 (2H, m, Pro C^5H_2), 3.71 (3H, m, $COOCH_3$), 4.57 (1H, m, Pro α-CH), 4.70 (1H, m, Tyr α-CH), 4.89 (1H, m, Phe α-CH), 5.22 (1H, d, *J* = 8.8 Hz, Tyr NH), 6.60-7.55 (16H, m, aromatics, Δ^ZPhe β-CH and Δ^ZPhe NH), 7.09 (1H, d, *J* = 4.4 Hz, Phe NH).

***N*-Boc-Pro-Δ^zPhe-Phe-azlactone (9).** Prepared as above described for compound **5**. The azlactone **9** (1.13 g, 99%) was used for preparation of **10** without further purification.

***N*-Boc-Pro-Δ^zPhe-Δ^zPhe-OMe (10).** To a stirred solution of azlactone **9** (0.28 g, 0.70 mmol) in MeOH (10 mL), DMAP (0.085 g, 0.70 mmol) was added at room temperature and the reaction mixture was stirred at room temperature overnight. Then the reaction mixture was acidified with saturated aqueous citric acid to pH 4, the organic solvent was evaporated and the

acqueous phase was extracted with Et_2O (3 x 15 mL). Et_2O layer was washed with citric acid 5% and brine, dried and evaporated under reduced pressure. Silica gel chromatography (CH_2Cl_2/EtOAc 8:2) gave a pure product **10** as a white foam (0.720 g, 60%); ^{1}H NMR ($CDCl_3$): δ 1.31 [9H, s, $C(CH_3)_3$], 1.70-2.35 (4H, m, Pro C^3H_2 and Pro C^4H_2), 3.44 (2H, m, Pro C^5H_2), 3.88 (3H, s, $COOCH_3$), 4.30 (1H, m, Pro α-CH), 7.20-7.68 (12H, m, aromatics, Δ^ZPhe^3 β-CH and Δ^ZPhe^4 β-CH), 7.84 (1H, s, Δ^ZPhe^4 NH), 8.54 (1H, s, Δ^ZPhe^3 NH).

***N*-Boc-Tyr-Pro-Δ^ZPhe-Δ^ZPhe-OMe.** The Boc group of **10** was removed in according to general procedure B to give a quantitative yield of TFA·HN-Pro-Δ^ZPhe-Δ^ZPhe-OMe. *N*-Boc-Tyr-OH (0.202 g, 0.72 mmol) in CH_2Cl_2 (10 mL) was treated with TFA·HN-Pro-Δ^ZPhe-Δ^ZPhe-OMe (0.344 g, 0.65 mmol) according to the general procedure A. Silica gel chromatography (CH_2Cl_2/EtOAc 7:3) gave a pure product as a white foam (0.198 g, 44%); ^{1}H NMR ($CDCl_3$): δ 1.40 [9H, s, $C(CH_3)_3$], 1.60-1.93 (4H, m, Pro C^3H_2 and Pro C^4H_2), 2.62-2.69 (2H, m, Tyr β-CH_2), 3.12 and 3.68 (2H, m, Pro C^5H_2), 3.85 (3H, s, $COOCH_3$), 4.44 (1H, m, Pro α-CH), 4.65 (1H, m, Tyr α-CH), 5.13 (1H, d, J = 8.0 Hz, Tyr NH), 6.50-7.63 (16H, m, aromatics, Δ^ZPhe^3 β-CH and Δ^ZPhe^4 β-CH), 7.68 (1H, s, Δ^ZPhe^4 NH), 8.37 (1H, s, Δ^ZPhe^3 NH).

***N*-Boc-Phe-*β*-(OH)Phe-OH (12).** Prepared as above described for compound **4**. Pure on TLC (quantitative yield).

***N*-Boc-Phe-Phe-azlactone (13).** Prepared as above described for compound **5**. The azlactone **13** (0.276 g, 75%) was used for preparation of **14** without further purification.

***N*-Boc-Phe-Δ^ZPhe-OMe (14).** Prepared as above described for compound **10**. Pure on TLC (0.284 g, 95%); ^{1}H NMR ($CDCl_3$): δ 1.37 [9H, s, $C(CH_3)_3$], 3.02 and 3.15 (2H, m, Phe $C^\beta H_2$), 3.77 (3H, s, $COOCH_3$), 4.46 (1H, m, Phe α-CH), 4.93 (1H, d, *J* = 8.4 Hz, Phe NH), 7.00-7.40 (11H, m, aromatics and Δ^ZPhe^4 β-CH), 7.61 (1H, s, Δ^ZPhe^4 NH).

***N*-Boc-Pro-Phe-Δ^ZPhe-OMe (15).** The Boc group of **14** was removed in according to general procedure B to give a quantitative yield of TFA·H_2N-Phe-Δ^ZPhe-OMe. *N*-Boc-Pro-OH (0.159 g, 0.74 mmol) in THF (10 mL) was treated with TFA·H_2N-Phe-Δ^ZPhe-OMe (0.293 g, 0.67 mmol) according to the general procedure A. Silica gel chromatography (CH_2Cl_2/EtOAc 9:1) gave a pure product **15** as a white foam (0.155 g, 44%); ^{1}H NMR ($CDCl_3$): δ 1.37 [9H, s, $C(CH_3)_3$], 1.60-2.10 (4H, m, Pro C^3H_2 and Pro C^4H_2), 3.20 (4H, m, Phe β-CH_2 and Pro C^5H_2), 3.83 (3H, s, $COOCH_3$), 4.14 (1H, m, Pro α-CH), 4.86 (1H, m, Phe α-CH), 6.67 (1H, d, *J* = 8.0 Hz, Phe NH), 7.19-7.51 (11H, m, aromatics and Δ^ZPhe^4 β-CH), 8.25 (1H, s, Δ^ZPhe^4 NH).

***N*-Boc-Tyr-Pro-Phe-Δ^{Z}Phe-OMe.** The Boc group of **15** was removed in according to general procedure B to give a quantitative yield of TFA·HN-Pro-Phe-Δ^{Z}Phe-OMe. *N*-Boc-Tyr-OH (0.078 g, 0.28 mmol) in CH_2Cl_2 (10 mL) was treated with TFA·HN-Pro-Phe-Δ^{Z}Phe-OMe (0.135 g, 0.25 mmol) according to the general procedure A. Silica gel chromatography (CH_2Cl_2/EtOAc 3:2) gave a pure product as a white foam (0.068 g, 40%); ^{1}H NMR ($CDCl_3$): δ 1.37 [9H, s, $C(CH_3)_3$], 1.60-1.90 (4H, m, Pro C^3H_2 and Pro C^4H_2), 2.71-3.62 (6H, m, Phe β-CH_2, Tyr β-CH_2 and Pro C^5H_2), 3.83 (3H, s, $COOCH_3$), 4.48 (1H, m, Pro α-CH), 4.50 (1H, m, Tyr α-CH), 4.71 (1H, m, Phe α-CH), 5.10 (1H, d, *J* = 8.8 Hz, Tyr NH), 6.08 (1H, d, *J* = 7.6 Hz, Phe NH), 6.50-7.51 (15H, m, aromatics and $\Delta^{Z}Phe^4$ β-CH), 8.12 (1H, s, Tyr OH), 8.51 (1H, s, $\Delta^{Z}Phe^4$ NH).

***N*-Boc-Tyr-Pro-Δ^{Z}Phe-Phe-NH_2 (8).** A solution of the peptide methyl ester **15** (0.020 g, 0.029 mmol) in MeOH/NH_3 sat. (3 mL) is allowed to stand in a pressure bottle at room temperature according to the general procedure C. The title compound **8** was purified by crystallization from MeOH (0.018 g, 95%); mp = 228-232 °C; ^{1}H NMR (DMSO-d_6): δ 1.30 [9H, s, $C(CH_3)_3$], 1.85-2.31 (4H, m, Pro C^3H_2 and Pro C^4H_2), 2.58-3.20 (4H, m, Phe^3 β-CH_2 and Tyr β-CH_2), 3.58-3.70 (2H, m, Pro C^5H_2), 4.17 (1H, m, Tyr α-CH), 4.39 (1H, m, Pro $C^{\alpha}H$), 4.50 (1H, m, Phe^3 α-CH), 6.60-7.55 (18H, m, aromatics, Tyr NH,

Δ^ZPhe^4 β-CH and $CONH_2$), 7.90 (1H, d, J = 8.4 Hz, Phe^3 NH), 9.18 (1H, s, Tyr OH), 9.70 (1H, s, Δ^ZPhe^4 NH); HRMS for $[M+H]^+$: *m/z* calcd 670.3241; found 670.3248.

***N*-Boc-Tyr-Pro-Phe-Δ^ZPhe-NH_2 (16).** A solution of the peptide methyl ester (0.106 g, 0.155 mmol) in MeOH/NH_3 sat. (7 mL) is allowed to stand in a pressure bottle at room temperature according to the general procedure C. The title compound **16** was purified by PLC ($CHCl_3$/MeOH 95:5); (0.058 g, 55%); ^{1}H NMR (DMSO-d_6): δ 1.30 [(9H, s, $C(CH_3)_3$], 1.70-2.00 (4H, m, Pro C^{3}H$_2$ and Pro C^{4}H$_2$), 2.50-3.10 (4H, m, Phe^4 β-CH_2 and Tyr β-CH_2), 3.48 and 3.58 (2H, m, Pro C^{5}H$_2$), 4.21 (1H, m, Tyr α-CH), 4.32 (1H, m, Pro α-CH), 4.53 (1H, m, Phe^4 α-CH), 6.60-7.51 (18H, m, aromatics, Tyr NH, Δ^ZPhe^3 β-CH and $CONH_2$), 8.31 (1H, d, J = 7.2 Hz, Phe^4 NH), 9.66 (1H, s, Δ^ZPhe^3 NH), 9.45 (1H, s, Tyr OH); HRMS for $[M+H]^+$: *m/z* calcd 670.3241; found 670.3238.

***N*-Boc-*T*yr-Pro-Δ^ZPhe-Δ^ZPhe-NH_2 (11).** A solution of the peptide methyl ester (0.112 g, 0.16 mmol) in MeOH/NH_3 sat. (7 mL) is allowed to stand in a pressure bottle at room temperature according to the general procedure C. The title compound **11** was purified by PLC ($CHCl_3$/MeOH 95:5); (0.061 g, 55%); ^{1}H NMR (DMSO-d_6): δ 1.30 [(9H, s, $C(CH_3)_3$], 1.71-2.26 (4H, m, Pro C^{3}H$_2$ and Pro C^{4}H$_2$), 2.62-2.75 (2H, m, Tyr β-CH_2), 3.48-3.72 (2H, m, Pro C^{5}H$_2$), 4.25 (1H, m, Tyr α-CH), 4.46 (1H, m,

Pro α-CH), 6.60-7.80 (19H, m, aromatics, Tyr NH, Δ^{Z}Phe^{3} β-CH, Δ^{Z}Phe^{4} β-CH and $CONH_2$), 9.22 (1H, s, Tyr OH), 9.52 (1H, s, Δ^{Z}Phe^{4} NH), 10.12 (1H, s, Δ^{Z}Phe^{3} NH); HRMS for $[M+H]^+$: *m/z* calcd 668.3084; found 668.3091.

TFA·H_2N-Tyr-Pro-Δ^{Z}Phe-Phe-NH_2 (1). Deprotection of the *N*-Boc group was performed by adopting the general procedure B: **8** (0.030 g, 0.046 mmol), CH_2Cl_2/TFA (5 mL) gave **1** (0.031 g, quantitative yield); ^{1}H NMR (DMSO-d_6): δ 1.85-2.13 (4H, m, Pro C^{3}H$_2$ and Pro C^{4}H$_2$), 2.70-3.20 (4H, m, Phe^4 β-CH_2 and Tyr β-CH_2), 3.41 and 3.61 (2H, m, Pro C^{5}H$_2$), 4.21 (1H, m, Tyr α-CH), 4.50 (2H, m, Phe^4 α-CH and Pro α-CH), 6.60-7.60 (17H, m, aromatics, Δ^{Z}Phe^{3} β-CH and $CONH_2$), 7.77 (1H, d, J = 8.0 Hz, Phe^4 NH), 8.09 (3H, br, Tyr NH_3^+), 9.36 (1H, s, Tyr OH), 9.82 (1H, s, Δ^{Z}Phe^{3} NH); HRMS for $[M+H]^+$: *m/z* calcd 684.2645; found 684.2652. Anal. Calcd for $C_{34}H_{36}F_3N_5O_7$: C, 59.73; H, 5.31; N, 10.24. Found: C, 59.96; H, 5.33; N, 10.28.

TFA·H_2N-Tyr-Pro-Phe-Δ^{Z}Phe-NH_2 (2). Deprotection of the *N*-Boc group was performed by adopting the general procedure B: **16** (0.020 g, 0.036 mmol), CH_2Cl_2/TFA (5 mL) gave **2** (0.0205 g, quantitative yield); ^{1}H NMR (DMSO-d_6): δ 1.69-2.08 (4H, m, Pro C^{3}H$_2$ and Pro C^{4}H$_2$), 2.70-3.20 (4H, m, Phe^3 β-CH_2 and Tyr β-CH_2), 3.40-3.68 (2H, m, Pro C^{5}H$_2$), 4.17 (1H, m, Tyr α-CH), 4.41 (1H, m, Pro α-CH), 4.63 (1H, m, Phe^3 α-CH), 6.60-7.55 (17H, m, aromatics, Δ^{Z}Phe^{4} β-CH and $CONH_2$), 8.09

(3H, br, Tyr NH_3^+), 8.30 (1H, d, J = 7.8 Hz, Phe^3 NH), 9.38 (1H, s, Tyr OH), 9.70 (1H, s, Δ^zPhe^4 NH); HRMS for $[M+H]^+$: *m/z* calcd 684.2645; found 684.2639. Anal. Calcd for $C_{34}H_{36}F_3N_5O_7$: C, 59.73; H, 5.31; N, 10.24. Found: C, 59.49; H, 5.28; N, 10.19.

TFA·H_2N-Tyr-Pro-Δ^zPhe-Δ^zPhe-NH_2 (3). Deprotection of the *N*-Boc group was performed by adopting the general procedure B: **11** (0.028 g, 0.042 mmol), CH_2Cl_2/TFA (5 mL) gave **3** (0.0286 g, quantitative yield); ^{1}H NMR (DMSO-d_6): δ 1.71-2.20 (4H, m, Pro C^{3}H$_2$ and Pro C^{4}H$_2$), 2.68-3.07 (2H, m, Tyr β-CH$_2$), 3.40-3.68 (2H, m, Pro C^{5}H$_2$), 4.17 (1H, m, Tyr α-CH), 4.53 (1H, m, Pro α-CH), 6.60-7.80 (18H, m, aromatics, Δ^ZPhe^3 β-CH, Δ^ZPhe^4 β-CH and $CONH_2$), 8.09 (3H, br, Tyr NH_3^+), 9.35 (1H, s, Tyr OH), 9.42 (1H, s, Δ^ZPhe^4 NH), 10.13 (1H, s, Δ^ZPhe^3 NH); HRMS for $[M+H]^+$: *m/z* calcd 682.2489; found 682.2496. Anal. Calcd for $C_{34}H_{34}F_3N_5O_7$: C, 59.91; H, 5.03; N, 10.27. Found: C, 59.67; H, 5.01; N, 10.22.

1.5.4.3 X-ray crystallographic data for 8

Crystal Data

$C_{37}H_{43}N_5O_7$, FW = 669.76. Monoclinic, space group $P2_1$, a = 13.401(4), b = 8.9611(15), c = 15.027(4) Å, β = 103.31(3)°, V = 1756.0(8) Å^3, Z = 2, ρ_{calc} = 1.267 Mg m^{-3}, λ = Mo $K\alpha$, μ = 0.09 mm^{-1}.

Data Collection and Refinement

A clear colourless 0.15 x 0.10 x 0.10 mm crystal was mounted on an Oxford Diffraction Xcalibur diffractometer equipped with a CCD detector. Lattice parameters were obtained using CrysAlis CCD from 1162 reflections in the range $3 < \theta < 29°$. 2785 reflections (1959 independent) were collected at room temperature and corrected for Lorentz, polarization and absorption effects. The structure was solved with SIR97 and refined with the aid of SHELXL-97. In the final full-matrix least-squares calculations 455 parameters were refined. H atoms were included using a riding model [C-H bond distances in the range 0.93 - 0.97 Å, $U_{iso}(H)$ equal to 1.2 or 1.5 $U_{eq}(C)$]. Final residuals were $R1 = 0.036$ for the 1372 reflections having $F_o > 4\sigma(F_o)$ and 0.060 for all data. Final difference Fourier excursions were 0.10 and -0.12 eÅ^3.

1.5.4.4 Biological Assays

Receptor binding affinities to δ- and μ-opioid receptors were performed using cell membranes preparations from transfected cells that stably express the respective receptors. The radiolabeled ligands used were [^{3}H]DPDPE and [^{3}H]DAMGO for δ- and μ- receptors, respectively.[92] The *in vitro* tissue bioassays (MVD and GPI/LMMP) were performed as described previously.[93] IC_{50} values represent means of no less than four experiments. IC_{50} values, relative potency estimates, and their associated standard errors were determined by fitting the data to

the Hill equation by a computerized non-linear least-squares method.

Acknowledgments

This research was supported in part by grants of the U. S. Public Health Service, National Institutes of Health.

References

1. Schaible, H-G.; Richter, F. *Curr. Conc. Clinical Surgery*, **2004**, *389*, 237.
2. Seminars in *Cell & Developmental Biology*, **2006**, *17*, 541.
3. Offermanns, S.; Rosenthal, W. In *Encyclopedic Reference of Molecular Pharmacology*. Springer-Verlag Berlin Heidelberg **2004**.
4. Akil, H.; Mayer, D. J.; Liebeskid, J. C. *C. R. Acad. Sci. Hebd. Seances Acad. Sci. Ser. D.* **1972**, *274*, 3603.
5. Akil, H.; Mayer, D. J.; Liebeskid, J. C. *Science* **1976**, *191*, 961.
6. Akil, H.; Shiomi, H.; Matthews, J. *Science* **1985**, *227*, 424.
7. Pert, C. B.; Snyder, S. H. *Science* **1973**, *179*, 1011.
8. Pfeiffer, A.; Brantl, V. Herz, A.; Emrich, H. M. *Science* **1986**, *233*, 774.
9. Simon, E. J.; Hiller, J. M.; Eldman, I. *Proc. Natl., Sci. U.S.A*. **1973**, *70*, 1947.
10. Terenius, L. *Acta Pharmacol. Toxicol.* **1973**, *32*, 317.
11. Martin, W. R.; Eades, C. G.; Thompson, J. A.; Huppler, R. E.; Gilbert, P. E. *J. Pharmacol. Exp. Ther*. **1976**, *197*, 517.
12. Bunzow, J. R.; Grandy, D. K. *FEBS Lett*. **1994,** *347*, 279.

13. Mollereau, C.; Parmentier, M.; Mailleux, P.; Butour J. L.; Moisand, C.; Chalon, P.; Caput, D.; Vassart, G.; Meunier, J. C. *FEBS Lett.* **1994**, *341*, 33.
14. Meunier, J. C.; Mollereau, C.; Toll, L.; Suaudeau, C.; Moisand, C.; Alvinerie, P.; Butour, J-L.; Guillemot, J. C.; Ferrara, P.; Monsarrat, B. *Nature* **1995**, *377*, 532.
15. Reinscheid, R. K.; Nothacker, H. P.; Bourson, A.; Ardati, A.; Henningsen, R. A.; Bunzow, J. R. *Science* **1995**, *270*, 792.
16. Henschen, A.; Lottspeich, F.; Brantl, V.; Teschemacher, H. *Hoppe-Seyler's Z Physiol Chem.* **1979**, *360*, 1217.
17. Chang, K.-J.; Killian, A.; Hazum, E.; Cuatrecasas, P.; Chang, J-K. *Science* **1981**, *121*, 75.
18. Chang, K-J.; Su, I.F.; Brent, D. A.; Chang, J-K. *Science* **1985**, *250*, 9706.
19. Brantl, V.; Gramsh, C.; Lottspeich, F.; Mertz, R.; Jaeger, K-H.; Herz, A. *Eur J Pharmacol*. **1986**, *125*, 309.
20. Horvath, A.; Kastin, A. J. *Int. J. Pept. Protein Res.* **1990**, *36*, 281.
21. Erchegyi, J.; Kastin, A. J.; Zadina, J. E. *Peptides* **1992**, *13*, 623.
22. Hackler, L.; Kastin, A. J.; Erchegyi, J.; Zadina, J. E. *Neuropeptides* **1993**, *24*, 159.
23. Zadina, J. E.; Hackler, L.; Ge, L-J.; Kastin, A. J. *Nature* **1997**, *386*, 499.
24. Hackler, L.; Zadina, J. E.; Ge, L-J.; Kastin, A. J. *Peptides* **1997**, *18*, 1635.
25. Harrison, L. M.; Kastin, A. J.; Zadina, J. E. *Peptides* **1998**, *19*, 1603.
26. Kieffer, B. L. *Trends Pharmacol. Sci.* **1999**, *20*, 19.
27. Clark, J. A.; Liu, L.; Price, M.; Hersh, B.; Edelson, M.; Pasternak, G. W. *J. Pharmacol. Exp. Ther.* **1989**, *251*, 461.
28. Evans, C. J.; Keith, D. E. Jr.; Morrison, H.; Magendzo, K.; Edwards, R. H. *Science*, **1992**, *258*, 1952.

29. Kieffer, B. L.; Befort, K.; Gaveriaux-Ruff, C.; Hirth, C. G. *Proc. Natl. Acad. Sci. USA* **1992**, *89*, 12048.
30. Chen, Y.; Mestek, A.; Liu, J.; Hurley, J. A.; Yu, L. *Mol. Pharmacol.* **1993**, *44*, 8.
31. Minami, M.; Toya, T.; Katao, Y.; Maekawa, K.; Nakamura, S.; Onogi, T.; Kaneko, S.; Satoh, M. *FEBS Lett.* **1993**, *329*, 291.
32. Okada, T.; Sugihara, M.; Bondar, A. N.; Elstner, M.; Entel, P.; Buss, V.; *J. Mol. Biol.* **2004**, *342*, 571.
33. Hillisch, A.; Pineda, L. F.; Hilgenfeld, R. *Drug Discov. Today* **2004**, *9*, 659.
34. Mosberg, H. I.; Fowler, C. B. *J. Peptide Res.* **2002**, *60*, 329.
35. Liu X.; Kai, M.; Jin, L.; Wang, R. *J. Comput. Aided. Mol. Des.* **2009**, *23*, 321.
36. Stone, L. S.: Fairbanks, C. A.; Laughlin, T. M.; Nguyen, H. O.; Bushy, T. M.; Wessendorf, M. W.; Wilcox, G. L. *Neuroreport* **1997**, *8*, 3131.
37. Goldberg, I. E.; Rossi, G. C.; Letchworth, S. R.; Mathis, J. P.; Ryan-Moro, J.; Leventhal, L.; Su, W.; Emmel, D.; Bolan, E. A.; Pasternak, G. W. *J. Pharmacol. Exp. Ther.* **1998**, *286*, 1007.
38. Champion, H. C.; Zadina, J. E.; Kastin, A. J.; Hackler, L.; Ge, L-J.; Kadowitz, P. *J. Biochem. Biophys. Res. Commun.* **1997**, *235*, 567.
39. Champion, H. C.; Zadina, J. E.; Kastin, A. J.; Hackler, L.; Ge, L-J.; Kadowitz, P. J. *Peptides* **1997**, *18*, 1393.
40. Champion, H. C.; Zadina, J. E.; Kastin, A. J.; Kadowitz, P. J. *Peptides* **1998**, *19*, 925.
41. Czapla, M. A.; Champion, H. C.; Zadina, J. E.; Kastin, A. J.; Hackler, L.; Ge, L-J.; Kadowitz, P. J. *Life Sci.* **1998**, *62*, 175.
42. Czapla, M. A.; Gozal, D.; Alea, O. A.; Beckerman, R. C.; Zadina, J. E. *Am. J. Respir. Crit. Care Med.* **2000**, *162*, 994.

43. Nishiwaki, H.; Saitoh, N.; Nishio, H.; Takeuchi, T.; Hata, F. *Jpn. J. Pharmacol.* **1998**, *78*, 83.
44. Patel, H. J.; Enkatesan, P. V.; Halfpenny, J. M.; Acoub, H. Y.; Fox, A.; Barnes, P. J.; Belvisi, M. G. *Eur. J. Pharmacol.* **1999**, *374*, 21.
45. Azuma, Y.; Wang, P-L.; Shinohara, M.; Ohura, K. *Immunol. Lett.* **2000**, *75*, 55.
46. Azuma, Y.; Ohura, K.; Wang, P-L.; Shinohara, M. *J. Neuroimmunol.* **2001**, *119*, 51.
47. Azuma, Y.; Ohura, K.; Wang, P-L.; Shinohara, M. *Immunol. Lett.* **2002**, *81*, 31.
48. Yamazaki, T.; Ro, S.; Goodman, M.; Chung, N. N.; Schiller, P. W. *J. Med. Chem.* **1993**, *36*, 708.
49. Gentilucci, L.; Tolomelli, A. *Curr. Top. Med. Chem.* **2004**, *4*, 105.
50. Leitgeb, B.; Tóth, G. *Eur. J. Med. Chem.* **2005**, *40*, 674 and refs. cited therein.
51. Podlogar, B. L.; Paterlini, M. G.; Ferguson, D. M.; Leo, G. C.; Demeter, D. A.; Brown, F. K.; Reitz, A. B. *FEBS Lett.* **1998**, *439*, 13.
52. Keller, M.; Boissard, C.; Patiny, L.; Chung, N. N.; Lemieux, C.; Mutter, M.; Schiller, P. W. *J. Med. Chem.* **2001**, *44*, 3896.
53. Okada, Y.; Fujita, Y.; Motoyama, T.; Tsuda, Y.; Yokoi, T.; Li, T.; Sasaki, Y.; Ambo, A.; Jinsmaa, Y.; Bryant, S. D.; Lazarus, L. H. *Bioorg. Med. Chem.* **2003**, *11*, 1983.
54. Eguchi, M.; Shen, R. Y.; Shea, J. P.; Lee, M. S.; Kahn, M. *J. Med. Chem.* **2002**, *45*, 1395.
55. In, Y.; Minoura, K.; Tomoo, K.; Sasaki, Y.; Lazarus, L. H.; Okada, Y.; Ishida, T. *FEBS J.* **2005**, *272*, 5079.
56. Doi, M.; Asano, A.; Komura, E.; Ueda, Y. *Biochem. Biophys. Res. Commun*. **2002**, *297*, 138.

57. Shao, X.; Gao, Y.; Zhu, C.; Liu, X.; Yao, J.; Cui, Y.; Wang, R. *Bioorg. Med. Chem.* **2007**, *15*, 3539.
58. Cardillo, G.; Gentilucci, L.; Melchiorre, P.; Spampinato, S. *Bioorg. Med. Chem. Lett.* **2000**, *10*, 2755.
59. Foran, S. E.; Carr, D. B.; Lipkowski, A. W.; Maszczynska, I.; Marchand, J. E.; Misicka, A.; Beinborn, M.; Kopin, A. S.; Kream, R. M. *J. Pharmacol. Exp. Ther.* **2000**, *295*, 1142.
60. Sakurada, S.; Watanabe, H.; Hayashi, T.; Yuhki, M.; Fujimura, T.; Murayama, K.; Sakurada, C.; Sakurada, T. *Br. J. Pharmacol.*, **2002**, *137*, 1143.
61. Wilson, A. M.; Soignier, R. D.; Zadina, J. E.; Kastin, A. J.; Nores, W. L.; Olson, R. D.; Olson, G. A. *Peptides* **2000,** *21*, 1871.
62. Meisenberg, G.; Simmons, W. H. *Life Sci.* **1983**, *32*, 2611.
63. Begley, D. J. *J. Pharm. Pharmacol.* **1996**, *48*, 136.
64. Tömböly, C.; Pèter, A.; Tòth, G. *Peptides* **2002**, *23*, 1573.
65. Cardillo, G.; Gentilucci, L.; Qasem, A.R.; Sgarzi, F.; Spampinato, S. *J. Med. Chem.* **2002**, *45*, 2571.
66. Okada, Y.; Fukumizu, A.; Takahashi, M.; Shimizu, Y.; Tsuda, Y.; Yokoi, T.; Bryant, S. D.; Lazarus, L. H. *Biochem. Biophys. Res. Comm.* **2000**, *276*, 7.
67. Paterlini, M. G.; Avitabile, F.; Ostrowski, B. G.; Ferguson, D. M.; Portoghese, P. S. *Biophys. J.* **2000**, *78*, 590.
68. Leitgeb, B. *Chem. Biodiv*. **2007**, *4*, 2703.
69. Keresztes, A.; Szűcs, M.; Borics, A.; Kövér, K. E.; Forró, E.; Fülöp, F.; Tömböly, C.; Péter, A.; Páhi, A.; Fábián, G.; Murányi, M.; Tóth, G. *J. Med. Chem.* **2008**, *51*, 4270.
70. Fichna, J.; Do Rego, J-C.; Chung, N. N.; Lemieux, C.; Schiller, P. W.; Poels, J.; Broeck, J. V.; Costentin, J.; Janecka, A. *J. Med. Chem.* **2007**, *50*, 512.

71. Cardillo, G.; Gentilucci, L.; Tolomelli, A.; Calienni, M.; Qasem, A. R.; Spampinato, S. *Org. Biomol. Chem.* **2003**, *1*, 1498.
72. Yamada, T.; Iino, M.; Matsuoka, N.; Yanagihara, R.; Miyazawa, T.; Shirasu, N.; Shimohigashi, Y. *Pept. Sci.* **1999**, *36*, 441.
73. Tóth, G.; Keresztes, A.; Tömböly, C.; Péter, A.; Fülöp, F.; Tourwé, D.; Navratilova, E.; Varga, É.; Roeske, W. R.; Yamamura, H. I.; Sz}ucs, M.; Borsodi, A. *Pure Appl. Chem.* **2004**, *76*, 951.
74. Staniszewska, R.; Fichna, J.; Gach, K.; Toth, G.; Poels, J.; Vanden Broeck, J.; Janecka, A. *Chem. Biol. Drug Des.* **2008**, *72*, 91.
75. Benedetti, E.; Di Blasio, B.; Pavone, V.; Pedone, C.; Felix, A.; Goodman, M. *Biopolymers* **1981**, *20*, 283.
76. Flores-Ortega, A.; Casanovas, J.; Zanuy, D.; Nussinov, R.; Alemán, C. *J. Phys. Chem. B.* **2007**, *111*, 5475.
77. Moore, S.; Felix, A. M.; Meienhofer, J. *J. Med. Chem.* **1977**, *20*, 495.
78. Werner, S.; Kasi, D.; Brummond, K. M. *J. Comb. Chem.* **2007**, *9*, 677.
79. Szemenyei, E.; Toth, G. J. *Labelled. Compd. Radiopharm.* **2007**, *50*, 1148.
80. Toniolo, C. *Int. J. Pept. Protein Res.* **1990**, *35*, 287.
81. Zagari, A.; Némethy, G.; Scheraga, H. A. *Biopolymers* **1990**, *30*, 951.
82. Shuman, R. T.; Rothenberger, R. B.; Campbell, C. S.; Smith, G. F.; Gifford-Moore, D.; Paschal, J. W.; Gesellchen, P. D. *J. Med. Chem.* **1995**, *38*, 4446.
83. Baeza, J. L.; Gerona-Navarro, G.; Pérez de Vega, M. J.; García-López, M. T.; González-Muñiz, R.; Martín-Martínez, M. *J. Org. Chem.* **2008**, *73*, 1704.
84. Kern, D.; Schutkowski, M.; Drakenberg, T. *J. Am. Chem. Soc.* **1997**, *119*, 8403.

85. Macdonald, S. J. F.; Dowle, M. D.; Harrison, L. A.; Clarke, G. D. E.; Inglis, G. G. A.; Johnson, M. R.; Shah, P.; Smith, R. A.; Amour, A.; Fleetwood, G.; Humphreys, D. C.; Molloy, C. R.; Dixon, M.; Godward, R. E.; Wonacott, A. J.; Singh, O. M.; Hodgson, S. T.; Hardy, G. W. *J. Med. Chem.* **2002**, *45*, 3878.
86. Fish, P.; Barber, C. G.; Brown, D. G.; Butt, R.; Collis, M. J.; Dickinson, R. P.; Henry, B. T.; Horne, V. A.; Huggins, J. P.; King, E.; O'Gara, M.; McCleverty, D.; McIntosh, F.; Phillips, C.; Webster, R. *J. Med. Chem.* **2007**, *50*, 2341.
87. Klein, S. I.; Czekaj, M.; Molino, B. F.; Chu, V. *Bioorg. Med. Chem. Lett.* **1997**, *7*, 1773.
88. Brown, W.; Dimaio, J.; Schiller, P.; Martel, R. World Patent WO 9522557, 1995, CAN, 124:30439.
89. Bodansky, M. *In Principles of Peptide Synthesis*; Springer: Berlin, **1984**.
90. Burrage, S.; Raynham, T.; Williams, G.; Essex, J. W.; Allen, C.; Cardno, M.; Swali,V.; Bradley, M. *Chem. Eur. J.* **2000**, *6*, 1455.
91. Yu, Y.; Shao, X.; Cui, Y.; Liu, H-M.; Wang, C-L.; Fan, Y-Z.; Liu, J.; Dong, S-L.; Cui, Y-X.; Wang, R. *Chem. Med. Chem.* **2007**, *2*, 309.
92. Wang, Z.; Gardell, L. R.; Ossipov, M. H.; Vanderah, T. W.; Brennan, B. B.; Hochgeschwender, U.; Hruby, V. J.; Malan, T. P. Jr.; Lai, J.; Porreca, F. *J. Neurosci.* **2001**, *21*, 1779.
93. Kramer, T. H.; Davis, P.; Hruby, V. J.; Burks, T. F.; Porreca, F. *J. Pharmacol. Exp. Ther.* **1993**, *266*, 577.
94. Janecka, A.; Staniszewska, R.; Fichna, J. *Curr. Med. Chem*. **2007**, *14*, 3201.
95. Fichna, J.; Janecka, A.; Costentin, J.; do Rego, J-C. *Pharmacol. Rev*. **2007**, *59*, 88.

96. Perlikowska, R.; Gach, K.; Fichna, J.; Toth, G.; Walkowiak, B.; do Rego, J-C.; Janecka, A. *Bioorg. Med. Chem*. **2009**, *17*, 3789.
97. Torino, D.; Mollica, A.; Pinnen, F.; Lucente, G.; Feliciani, F.; Peg, D.; Lai, J.; Ma, S-W.; Porreca, F.; Hruby, V. J. *Bioorg. Med. Chem. Lett*. **2009**, *19*, 4115.
98. Honda, T.; Shirasu, N.; Isozaki, K.; Kawano, M.; Shigehiro, D.; Chuman, Y.; Fujita, T.; Nose, T.; Shimohigashi, Y. *Bioorg. Med. Chem.* **2007**, *15*, 3883.
99. Del Borgo, M. P.; Blanchfield, J. T.; Toth, I. *Bioorg. Med. Chem. Lett*. **2008**, *16*, 4341.
100. Gao, Y.; Liu, X.; Liu, W.; Qi, Y.; Liu, X.; Zhou, Y.; Wang, R. *Bioorg. Med. Chem. Lett*. **2006**, *16*, 3688.
101. Fichna, J.; do-Rego, J-C.; Kosson, P..; Costentin, J.; Janecka, A. *Biochem. Pharmacol.* **2005**, *69*, 179.
102. Tömböly, C.; Kövér, K. E.; Péter, A.; Tourwé, D.; Biyashev, D.; Benyhe, S.; Borsodi, A.; Al-Khrasani, M.; Rónai, A. Z.; Tóth, G. *J. Med. Chem*. **2004**, *47*, 735.
103. Hruby, V. J.; Al-Obeidi, F.; Kazmierski, W. *Biochem. J.* **1990**, *268*, 249.
104. Hruby, V. J.; Li, G.; Haskell-Luevano, C.; Shenderovich, M. *Biopolymers* **1997**, *43*, 219.
105. Schwyzer, R. *Ann. N. Y. Acad. Sci.* **1977**, *297*, 3.
106. Goel, V. K.; Guha, M.; Baxla, A. P.; Dey, S.; Singh, T. P. *J. Mol. Struct.* **2003**, *658*, 135.
107. Flippen-Anderson, J. L.; Deschamps, J. R.; George, C.; Reddy, P. A.; Lewin, A. H.; Brine, G. A.; Sheldrick, G.; Nikiforovich, G. *J. Pept. Res*. **1997**, *49*, 384.
108. Piazzesi, A. M.; Bardi, R.; Crisma, M.; Bonora, G. M.; Toniolo, C.; Chauhan, V. S.; Kaur, P.; Uma, K.; Balaram, P. *Gazz. Chim. Ital*. **1991**, *121*, 1.

109. Ramagopal, U. A.; Ramakumar, S.; Joshi, R. M.; Chauhan, V. S. *J. Pept. Res.* **1998**, *52*, 208.

CHAPTER 2

Chemotactic *N*-formyl peptides

2.1 Chemotaxis

Chemotaxis, the reaction by which the direction of migration of cells is determined by substances, called chemotactic agents, in their environment, is one of the fundamental responses of prokaryotic and eukaryotic cells to external stimuli.[1] Prokaryotic microorganisms such as bacteria use it to search for food and avoid toxins. In vertebrates, chemotaxis is generally accepted as a major process bringing leukocytes from the blood to the tissue sites of inflammation.

Various families of chemoattractant agents have been described over the years. These include the large family of chemokines, complement fragments (C5a, C3a), cathelicidins and defensins, chemerin, lipid mediators (platelet activating factor, leukotriene B4, etc), and a host of pathogen-derived molecules.

Human neutrophils represent the major subset (50 to 60%) of circulating leukocytes, and are phagocytic cells specialized in the "first line of defence" against infectious agents or "non-self" substances which penetrate the body's physical barriers.[2] They are also the major cell type associated with acute inflammatory reactions. Their targets include bacteria, fungi, protozoa, viruses, virally infected cells and tumor cells.

Neutrophils circulate in the bloodstream, and can be recruited in high numbers in infected or inflamed tissues along the concentration gradients of chemoattractants either released by the microorganisms themselves, or arising from inflammatory reaction in the infected tissue.

Various inflammatory mediators, including the *N*-formyl-methionyl peptides derived from bacterial metabolism or from disrupted mitochondria, are capable of activating neutrophils via specific receptors.[3,4] The *N*-formyl tripeptide for-Met-Leu-Phe-OH (fMLF) (Figure 1) is the main chemotactic factor produced by *Escherichia coli*[5] and, with its synthetic methyl ester derivative, for-Met-Leu-Phe-OMe (fMLF-OMe) (Figure 1), is the highly potent chemoattractant for phagocytes.

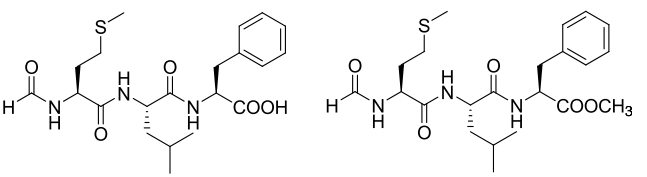

Figure 1. *N*-formyl tripeptide and its methyl ester.

2.1.1 The role of neutrophils in acute inflammation

Leukocytes, such as neutrophils, continuously patrol the vasculature, monitoring for signals of bacterial infection or inflammation. Substances released from pathogens, such as lipopolysaccharide (LPS) or classical chemoattractants e.g. fMLF, and tissue damage, such as tumor necrosis factor-α

(TNF-α), upregulate the expression of adhesion molecules on vascular endothelium, and this, in turn, initiates the extravasation of leukocytes to the inflamed area.

Leukocyte extravasation from blood into tissues involves several steps called *random contact*, *rolling*, *sticking*, *diapedesis* and *chemotaxis*[6] (Figure 2). When the leukocytes approach the post-capillary venules in areas of subendothelial inflammation, the initial *random contact* changes into *rolling*, which can be described as low affinity adhesive interaction between leukocytes and the endothelium, and defined as leukocyte movement through vessels.

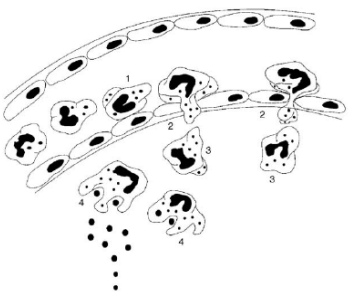

Figure 2. Activation of neutrophil functions in the inflammatory process: (1) margination: the adhesion of neutrophils to endothelium causes them to aggregate along the vessel walls, owing to the upregulation of the expression of adhesion molecules in both neutrophils and endothelial cells; (2) diapedesis: transmigration of neutrophils across the endothelial barrier; (3) chemotaxis: after leaving nearby blood vessels, neutrophils are attracted to the inflammatory sites up a gradient of chemicals factors. They lose their round configuration and assume a polarized morphology with an anterior lamellipodium extended in the direction of movement; (4) phagocytosis: once the neutrophil has arrived at the site of inflammation, it ceases to move and at the high concentrations of chemoattractants found here, the cell begins to phagocyte foreign particles.

After firm attachment (*sticking*, the more stable adhesion), leukocytes start migrating across the endothelium (*diapedesis*) via intercellular junctions into the subendothelial space. Finally, leukocytes are attracted to the inflammatory sites (chemotaxis) through the production of exogenous and endogenous chemoattractant mediators. Exogenous chemotaxins include bacterial oligopeptides of the fMLF type, lectins, denatured proteins, some lipids and lipopolysaccharides. Endogenous chemotaxins are produced by the host organism and are of humoral (complement fragment C5a, C5a-des-Arg and C3a, fibrinopeptides, kallikrein and plasminogen activator) or cellular type (from different cells: leukotriene B4, platelet activated factor, chemotactic cytokines etc.).[7,8] Once the neutrophil has arrived at the site of inflammation, it ceases to move, probably due to the lack of defined chemoattractant gradient. At the high concentrations of chemoattractants found here, the cell begins phagocytosis and killing (oxygen independent and dependent) of foreign particles.[9] Phagocytosis is accompanied by lysosomal enzyme secretion and production of two types of free radicals by neutrophils: a) reactive oxygen intermediates which are formed in neutrophils by the activity of NADPH oxidase, the membrane associated enzyme of the respiratory burst;[10] b) reactive nitrogen intermediates, the first of which, nitric oxide, is produced by nitric oxide synthase.[11] These, together with the contents of neutrophil granules, have an extensive killing capacity.[12]

2.1.2 Formyl peptide receptors (FPRs)

FMLF, together with its synthetic methyl ester derivative, fMLF-OMe, is used as a model chemoattractant due to its highly effective ability to activate all physiological functions of neutrophils through cell surface receptors coupled to intracellular effectors through guanine nucleotide regulatory proteins (G proteins). The interaction of fMLF with its receptor expressed on neutrophils activates signal transduction pathways. This activation is known to provoke various biochemical responses which contribute to physiological defence against bacterial infection and cell disruption. In fact, it has long been known that the signal transduction pathway underlying the chemotactic response differs from those responsible for cytotoxic functions, and several previous experiments carried out utilizing pharmacological manipulation of the signal transduction pathway have highlighted the fact that distinct mechanisms are involved in each of these neutrophil responses. This can be rationalized on the basis of the existence of at least two different functional receptor subtypes or isoforms; low doses of a full agonist (or "pure" chemoattractant) are required to interact with a high-affinity receptor subtype, FPR, which activates the signal transduction pathway responsible for the chemotactic response, while the increase in full agonist concentration (typical of infection sites) allows binding with its low-affinity subtype, FPRL1, which is able to activate the signal

transduction pathways responsible for superoxide anion production and lysozyme release.

The classic fMLF chemoattractant exerts its effects by binding to FPRs, which are classical G-protein coupled receptors characterized by seven hydrophobic transmembrane segments connected by hydrophilic domains; potential *N*-linked glycosylation or phosphorylation sites are present on the extracellular or intracellular receptor surface, respectively.[13]

Human FPR was first defined biochemically in 1976 as a high-affinity binding site for the prototype fMLF on the surface of neutrophils. It was then cloned in 1990, by Boulay *et al*., from a differentiated HL-60 myeloid leukaemia-cell cDNA library.[14] Two additional human genes, designated FPRL1 (FPR like-1) and FPRL2 (FPR like-2), were subsequently isolated by low-stringency hybridization using FPR cDNA as a probe.[15-17]

Physiologically, the FPR is predominantly if not exclusively coupled to pertussis toxin (PTX)-sensitive G-proteins of the G*i*-family,[18-21] although in recombinant systems, the FPR also possesses the potential to couple to the PTX-insensitive G-proteins Gα15 and Gα16.[22] G*i* proteins are the most abundant and important G proteins in phagocytes as they mediate most, if not all, of the stimulatory effects of chemoattractants.

It is generally accepted that FPRL1 shares signal transduction features with FPR, since both receptors are sensitive to pertussis

toxin (PTX) and possess a high degree of amino acid identity in the cytoplasmic signaling domains.

Following ligand binding (Figure 3), FPRs undergo a conformational change that enables them to interact with the PTX-sensitive G*i* proteins. After binding of its agonists, the receptor activates the heterotrimeric G protein, which dissociates into α and βγ subunits. Upon activation, the receptor triggers exchange of GDP to GTP binding in the α subunit. $G i\alpha_{\text{-GTP}}$ is capable of inhibiting certain adenylyl cyclase isoforms,[23] but adenylyl cyclase inhibition is of little, if any, importance in phagocytes.[21]

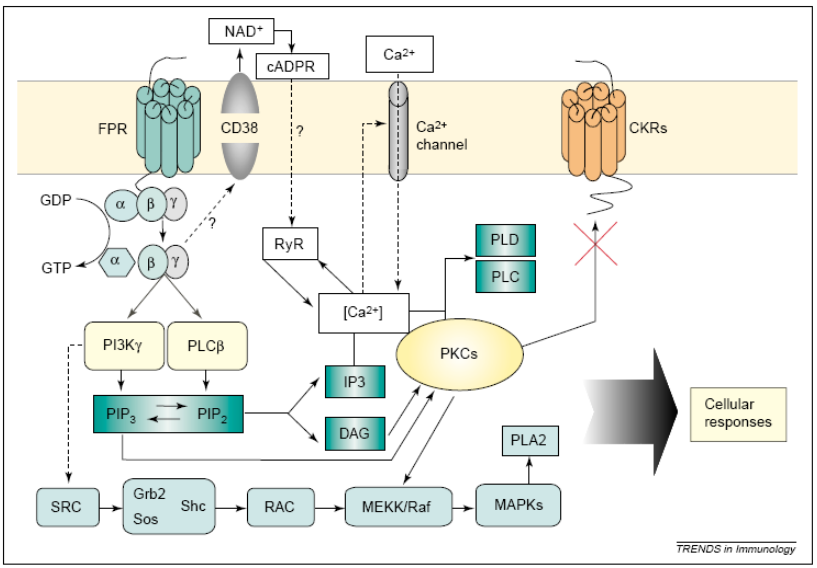

Figure 3. Schematic signaling pathways of an activated formyl peptide receptor (FPR).

Rather, the βγ-complex activates phospholipase C (PLC) isoenzymes β2 and β3[24,25] and phosphoinositide 3-kinase-γ (PI3Kγ).[26] Gene knock-out studies in the mouse revealed that phospholipases C-β2 and β3 as well as phosphoinositide 3-kinase-γ play crucial roles in the activation of down-stream phagocyte functions, e.g. chemotaxis and oxygen radical formation.[27-29]

PI3K converts the membrane phosphatidylinositol 4,5 bisphosphate (PIP_2) into phosphatidylinositol-3,4,5 trisphosphate (PIP_3). PIP_3 is catabolized by PLC to the secondary messengers inositol trisphosphate (IP_3) and diacylglycerol (DAG). While IP_3 regulates the mobilization of Ca^{2+} from intracellular stores, DAG activates protein kinase C (PKC). Calcium enhancement appears to occur in two stages: an initial transient release from intracellular storage sites followed by a more delayed influx across the plasma membrane. Increase in Ca^{2+} cytosolic levels has been postulated to be a necessary condition for neutrophil response to formyl peptides, as it is one of the earliest detectable events induced by cell exposure to fMLF. The release of Ca^{2+} from internal stores induces the opening of the store-operated Ca^{2+} channel in the plasma membrane and a sustained influx of Ca^{2+} takes place.[30] Other intracellular effectors coupled to FPR signaling cascade include phospholipases A_2, D, mitogen-activated protein kinase (MAPK),[31,32] and the tyrosine kinase lyn.[33] Following activation

by ligand, FPR undergoes rapid serine and threonine phosphorylation, and is desensitized and internalized.[34,35] However, FPR internalization can occur in the absence of desensitization, indicating that desensitization and internalization are controlled by distinct mechanisms.[36,37]

Further studies[38] suggest that FPR internalization is mediated by mechanisms independent of the actions of arrestin, dynamin and clathrin, which, on the other hand, are involved in the internalization of some other G protein-coupled receptors such as the β-adrenergic receptor.

Unlike FPR, the signal transduction pathways mediated by FPRL1 have not been extensively studied. Nevertheless, it is suggested that FPRL1 may share many signaling characteristics observed with FPR based on their high level of homology, sensitivity to PTX, and mediation of potent phagocyte activation by agonists. In addition to its role in bacterial host defense, the FPR may play a more general role in inflammatory reactions. This notion is supported by the fact that the FPR is also expressed in cell types other than classic phagocytes such as astrocytes, hepatocytes, epithelial cells, T lymphocytes, neuroblastoma cells and microvascular endothelial cells.[39,40] Moreover, formyl peptides released from damaged mitochondria activate the FPR.[41]

Furthermore, various non-formylated peptides, specifically human immunodeficiency virus-1 envelope protein-derived

peptides, annexin I and annexin I-derived peptides are FPR agonists.[40,42] Annexin I peptides have been recently reported as novel, endogenous fMLF receptor ligands able to induce anti-inflammatory effects.[43]

2.2 Structure-activity relationship of fMLF

In spite of the numerous studies into the biological responses of human neutrophils arising from their interaction with the chemotactic fMLF,[44-52] nobody has yet clarified which chemical mechanisms are involved in the binding of this ligand to its receptor. The receptor has been studied in order to understand its position in the membrane and the steric characteristics which allow the best biological responses,[16,53-56] but not to establish how the ligand hooks into its receptor pocket.

The tripeptide fMLF together with fMLF-OMe, is a potent chemoattractant for phagocytes and is also generally adopted as the reference model for evaluating the activity of newly synthesized analogues. In addition to its high lipophilic character, due to the presence of the three hydrophobic side chains, this compound is characterized by a pronounced conformational flexibility of the backbone, which appears to be an important feature for establishing efficient interactions with the FPR.[57]

Several fMLF-OMe analogues have been synthesized and utilized in different laboratories with the aim of characterizing

formyl peptide interaction in phagocytes, as well as in cellular activation.[30,58-63]

In the working model of the portion of the receptor accommodating the tripeptide, five critical areas in the receptor that interact with the peptide were identified. Further studies have also revealed that the ligand binding pocket is large enough to accommodate a fourth amino acid residue,[64,65] up to 5 amino acids in length.[66]

N-Formyl group (H-CO)

As regards prototype fMLF, it is ascertained that *N*-formylation is necessary for optimal activity, simulating the situation at the amino end of proteins produced by bacteria such as *E. coli*.

Furthermore, the formyl group (H-CO) on the *N*-terminal methionine is small enough to reach the bottom of the binding cavity; it participates as hydrogen donor in linking to the receptor and it seems that its role in this interaction cannot be ruled out. Relevant is the observation that modifications centred at this function can modulate the neutrophil biological responses. Indeed, the presence of a free amino group and acetylation at the *N*-terminus of MLF both result in drastic losses in agonist activity as compared to fMLF.[45] Both urea and carbamate derivatized fMLF analogues, among which Boc-Met-Leu-Phe-OMe, containing the bulky *t*BuOCO (Boc) group in

place of the native H-CO (For), have been studied and found active as antagonists.[67,68]

The development of FPR antagonist is therefore of considerable interest, in particular for their potential use as therapeutic agent in the treatment of inflamation-related disorders. Indeed, in several pathological conditions the inappropriate activation of neutrophils can cause tissue damage.

Methionine residue (Met)

An important area of interaction is the hydrophobic cavity in the receptor occupied by the Met side chain. This cavity is of limited depth: side chains larger than four carbon atoms show no further increase in activity. In addition, a discrete area of positive charge in this cavity was postulated as complementary to the relatively electron-rich sulphur atom of the Met residue.[69]

Leucine residue (Leu)

The central hydrophobic Leu, although critical for backbone conformation, results to be the most tolerant towards replacement and modification.[70]

It was proposed a hydrophobic pocket in the receptor where leucine fits. Indications and conformational analyses have revealed that it is a rather large hydrofobic pocket, which fits from four up to seven carbon atoms. Full activity is reached only when the pocket is filled, so several analogues have been

prepared, where Leu has been replaced by, for example, α,α-disubstituted amino acids.[71,72]

Other several fMLF analogues modified at position-2 with high activity and selectivity have been described.[73,74]

Phenylalanine residue (Phe)

Studies have also determined that the *C*-terminal amino acid should be aromatic, Phe being the preferred choice.[45,75,76] Leu and Phe side-chain, are accommodated in a hydrophobic pocket.

Carboxylic group (Phe C=O)

Several studies demonstrated the necessity of a carboxylic group, both free and esterified, to trigger a biological response in human neutrophils. Esterification (e.g. methylation) of the *C*-terminal carboxylic group does not result in a reduction of activity.[77] A critical interaction of the Phe C=O group with the receptor, possibly via hydrogen bonding, has also been hypothesized.[46,78]

Several years ago my research group and then I, during my PhD, initiated a research program based on the synthesis of new fMLF-OMe analogues in order to: (i) obtain more effective and selective ligands; (ii) gain information on the structural features and conformational preferences of chemotactic formyl tripeptides.

2.3 Hybrid α/β-peptides: For-Met-Leu-Phe-OMe analogues containing geminally disubstituted $\beta^{2,2}$- and $\beta^{3,3}$-amino acids at the central position*

Neutrophils are involved in the first line of defence mechanism against pathogen microorganisms. They migrate from blood to sites of infection by following the concentration gradients of chemoattractants such as the cleavage products of bacterial and mitochondrial proteins. The hydrophobic *N*-formyl tripeptide For-Met-Leu-Phe-OH (fMLF) and its synthetic methyl ester (fMLF-OMe) are among the early recognized and highly potent chemotactic agents. Their binding to specific receptors located on the neutrophil plasma membrane gives rise, in addition to the directed migration (chemotaxis), to a cascade of biochemical responses including activation of radical oxygen production and release of proteolytic enzymes.[42,75]

A number of primary structure–activity studies, based on structurally modified fMLF analogues, have been performed and several fundamental points concerning the key role of the *N*-terminal protecting group in modulating the activity as well as the nature of the constituent amino acids have been established.[45,46,68] A more complex picture emerges from the analysis of the literature data analyzing conformation–activity

*Mollica, A.; Paglialunga Paradisi, M.; Torino, D.; Spisani, S.; Lucente G. *Amino Acids* **2006**, *30*, 453.

relationships. Here different tridimensional structures have been proposed as representatives of optimal interaction with the neutrophil formyl peptide receptors.[79] However, both structure–activity and conformation–activity studies[62,80,81] on fMLF analogues highlight the role exerted on the activity by the nature of the central residue. Suitable replacements of the native Leu can in fact give rise to stabilized folded or extended conformations[82,83] and allow at the same time key interactions with the central hydrophobic site which is known to be an important modulator of the biological functions[50,59] of *N*-formyl chemotactic tripeptides.

In accordance with the above reported observations several papers have examined synthesis and activity of fMLF analogues characterized by replacements at the central position. Particular attention has been paid to For-Met-Xaa-Phe-OMe models incorporating $C^{\alpha,\alpha}$-dialkylated glycines with linear [e.g., α-aminoisobutyric acid (Aib); di-*n*-propylglycine (Dpg)] and cyclic [e.g., 1-aminocycloalkane-1-carboxylic acids (Acnc)] alkyl side chains at position 2 (Figure 4).[50,62,81]

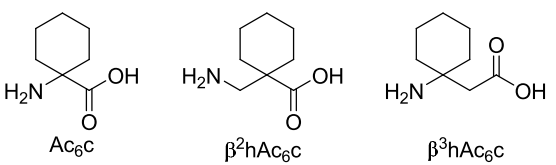

Figure 4. Geminally disubstituted α- and β-amino acids containing a cyclohexyl side chain.

These α,α-disubstituted aminoacidic residues significantly restrict the available range of backbone conformations and the derived conformationally constrained peptides represent useful probes to get informations on the biological active conformations. In particular, the chemoattractant tripeptides For-Met-Ac_nc-Phe-OMe (with n = 6 and 7), containing 1-aminocycloalkane-1-carboxylic acids in place of native Leu, were found to be very interesting ligands which exhibit both high activity and H-bond stabilized folded conformation.[50]

By taking into account the above considerations and as part of our previous research aimed at exploring the consequences of incorporating β-residues and higher homologues into short α-peptide sequences,[84-86] we report here studies on the two new fMLF analogues For-Met-β^3hAc_6c-Phe-OMe **6** and For-Met-β^2hAc_6c-Phe-OMe **12** (Figure 5) in which the central Leu has been replaced by two positional isomers of a geminally disubstituted β-residue[87] which shares with the Ac_6c the presence of a cyclohexyl side chain (Figure 4).

It should be noted here that although hybrid α/β-peptides are less studied as compared with the well known class of β-amino acid oligomers (β-peptides),[88,89] they represent an emerging approach for generating analogues of α-peptide endowed with selected resistance to proteolysis and specific conformational properties.[90,91] In particular we have focused our interest on these two unnatural amino acids by taking into account the

possibility to combine different points of interest: the improvement of the bioactivity due to the lipophilic side chain; the influence of the different spatial positioning of the side chain on the peptide backbone; the stabilization of folded conformations.

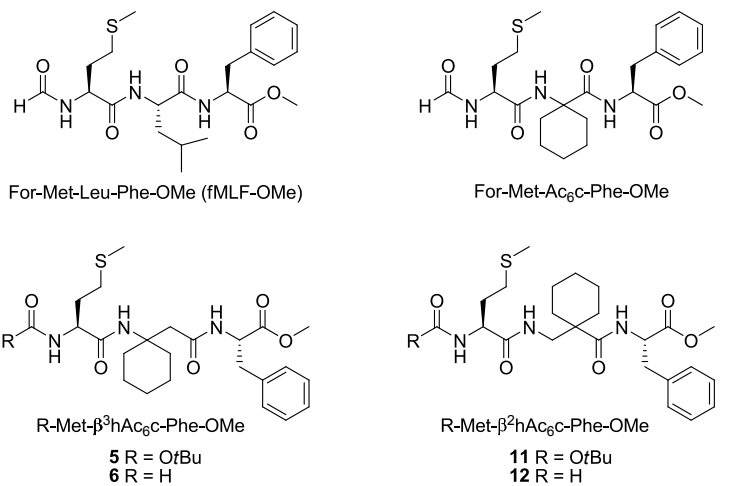

Figure 5. Structures of the relevant compounds investigated in this study.

2.3.1 Chemistry

The synthesis of Boc-Met-β^3hAc$_6$c-Phe-OMe (**5**) and Boc-Met-β^2hAc$_6$c-Phe-OMe (**11**) has been performed by following two different strategies shown in Schemes 1 and 2. A direct transformation of the *N*-Boc derivatives **5** and **11** into the corresponding *N*-formyl analogues **6** and **12** was performed by following the procedure of Lajoie and Kraus.[92] Tripeptide **5** containing the β^3hAc$_6$c residue was synthesized starting from methylenecyclohexane by using chlorosulphonyl isocyanate to

give the spirolactame **1** (Scheme 1).[93] A different strategy[87] was used to obtain the β^2hAc$_6$c-containing tripeptide **11** by using methyl cyanoacetate as key reagent (Scheme 2).

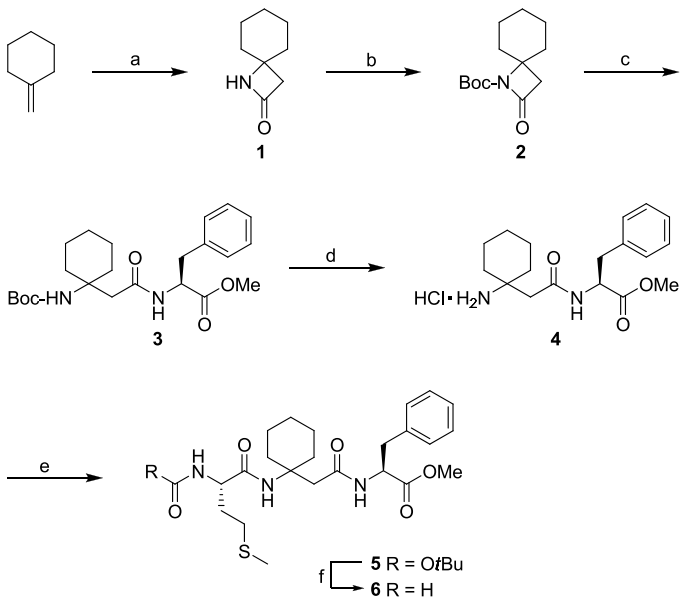

Scheme 1. Synthesis of the β^3hAc$_6$c-containing peptide derivatives **5** and **6**. *Reagents and conditions*: a) Chlorosulphonyl isocyanate, Et_2O, 10 min 0 °C then Na_2SO_3, 1h rt; b) Boc_2O, DMAP, CH_3CN, 15 min 0 °C, overnight rt; c) H_2N-Phe-OMe, KCN, DMF dry, 16h 50 °C under N_2; d) $SOCl_2$, MeOH, 40 min -15 °C, 3h 45°C; e) Boc-Met-OH, *i*BuOCOCl, NMM, CH_2Cl_2/DMF, 30 min -15 °C, overnight rt; f) HCOOH, overnight rt then EEDQ, $CHCl_3$, 24h rt.

2.3.2 Conformational studies

In order to ascertain the involvement of the NH groups of *N*-formyl analogues **6** and **12** in intramolecular H-bonds, a ^{1}H NMR solvent perturbation experiment was undertaken. In Figure 6, the chemical shift dependence of the three NH groups of each compound is reported as a function of increasing

DMSO-d_6 concentration in $CDCl_3$ solution (10 mM). The results clearly show the different behaviors of the two models **6** and **12**. The NH groups of the two external residues of **6** (Figure 6A) interact freely with the DMSO while the NH of the central β^3hAc$_6$c is slightly shielded and then probably involved in a weak intramolecular H-bond (the $\Delta\delta$ ppm values shown by the three NH groups are 0.75, 0.31, and 0.50 for Met, β^3hAc$_6$c, and Phe, respectively). However, when the IR spectrum in $CHCl_3$ of **6** was examined, the absorptions in the 3400-3300 cm^{-1} stretching region, where the intramolecular H-bonds commonly appear, were found to be very weak.

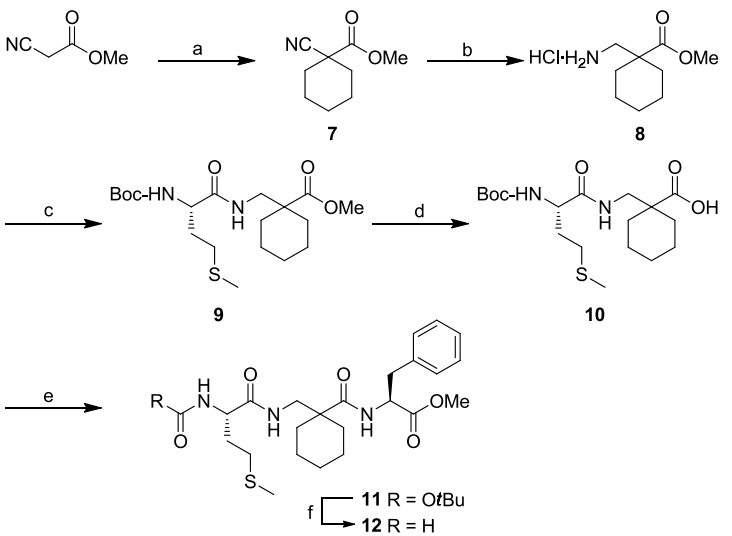

Scheme 2. Synthesis of the β^2hAc$_6$c containing peptide derivatives **11** and **12**. *Reagents and conditions:* a) K_2CO_3, 1,5-dibromo-pentane, DMF, 5h rt; b) H_2-Pd/C 10%, 10N HCl, MeOH, 6h rt; c) Boc-Met-OH, *i*BuOCOCl, NMM, CH_2Cl_2/DMF, overnight rt; d) 1N LiOH, THF/H_2O 5:1, overnight rt; e) HCl·H_2N-Phe-OMe, EDC, HOBt, NMM, CH_2Cl_2, 30 min 0 °C, overnight rt; f) HCOOH, overnight rt then EEDQ, $CHCl_3$, 24h rt.

The tripeptide **12** (Figure 6B) exhibits a strong H-bonding involvement of the NH of the central β^2hAc$_6$c together with that of the C-terminal Phe, while the NH of the *N*-terminal Met appears completely free (the Δδ ppm values are 1.21, -0.16, and 0.21 for Met, β^2hAc$_6$c, and Phe, respectively). In contrast to the IR spectrum of **6**, that of **12** in $CHCl_3$ shows strong absorption bands in the 3400-3300 cm^{-1} stretching region.

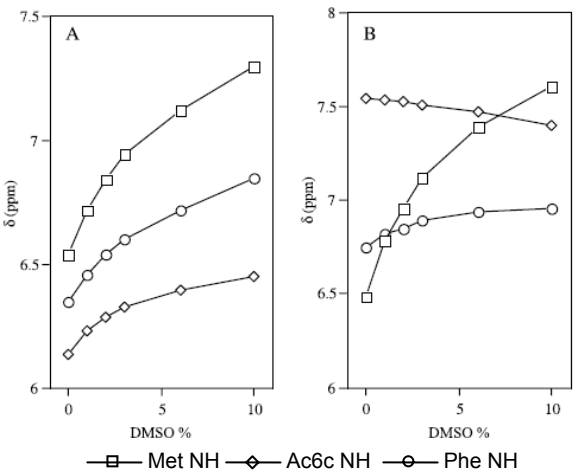

Figure 6. Delineation of hydrogen-bonded NH groups in tripeptides **6** and **12**. Chemical shift dependence of the NH resonances as a function of the DMSO-d_6 concentration (% v/v) in $CDCl_3$ solution. Peptide concentration 10 mM. (**A**) HCO-Met-β^3hAc$_6$c-Phe-OMe **6**; (**B**) HCO-Met-β^2hAc$_6$c-Phe-OMe **12**.

For the β^3hAc$_6$c-containing model **6**, the above reported data suggest, in addition to a large amount of unfolded conformations, the occurrence of a limited population of folded structures centered at the β-residue (C6 conformation) and

associated with a weak intraresidue electrostatic interaction which is not clearly detected by IR spectroscopy.[94] In the case of the β^2hAc$_6$c- containing model **12**, the strong involvement in H-bonding of the β-residue NH is accompanied by an analogous, albeit less pronounced behavior of the Phe *C*-terminal NH. A reasonable interpretation of these data indicates a system of t\wo consecutive local foldings centered at the β^2hAc$_6$c (C8 conformation; pseudo γ-turn)[95] and at the Met residue (C7 conformation; γ-turn) as depicted in Figure 7. In this case, both the intramolecular H-bonds are not highly distorted and clearly revealed by IR spectroscopy.

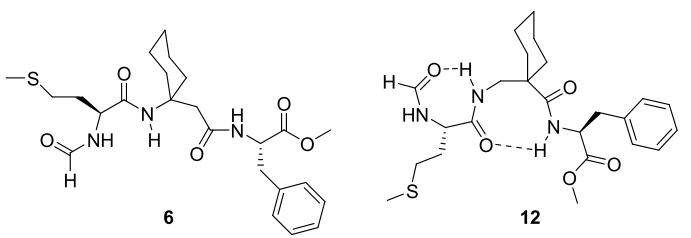

Figure 7. Representation of the molecular structure of the products **6** and **12**.

2.3.3 Biological results

The agonistic activity of the new ligands has been determined on human neutrophils and compared with that of the standard tripeptide fMLF-OMe; directed migration (chemotaxis), superoxide anion production, and lysozyme release have been measured.

Except for a modest activity shown as chemoattractants (Figure 8A) and lysozyme releasers (Figure 8C), the two *N*-Boc derivatives **5** and **11** are completely inactive in the superoxide anion production (Figure 8B). On the contrary, both the *N*-For-tripeptides **6** and **12** have been found highly active in inducing neutrophil chemotaxis exhibiting an analogous peak which at a concentration of 10^{-10} M reaches the activity of the reference molecule (chemotactic index, 1.0) (Figure 8A).

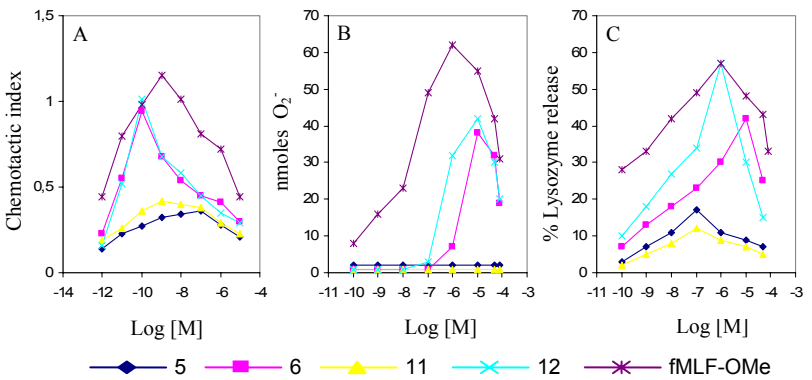

Figure 8. Biological activity of the tripeptides **5-12** compared with the reference ligand fMLF-OMe. (**A**) Chemotactic index; (**B**) Superoxide anion production; (**C**) Release of neutrophil granule enzymes evaluated by determining lysozyme activity.

Analogues **6** and **12** exhibit a comparably weak activity in the superoxide anion production (Figure 8B). However, for the lysozyme release activity (Figure 8C) the tripeptide **12** containing the β^2hAc$_6$c residue is notably more potent and efficient than the positional isomer **6** containing the β^3hAc$_6$c residue.

2.3.4 Discussion and conclusions

As previously mentioned, studies on chemotactic tripeptides indicate that the substitution at the central position of fMLF-OMe is critical for the activity. Concerning replacements related with the here examined analogues, it can be recalled that the incorporation of a central β-Ala or β^3hLeu leads to inactive or scarcely active ligands. The present results show, however, that the geminal substitution at the β-residue with the cyclohexyl side chain, regardless of the $\beta^{2,2}$ or the $\beta^{3,3}$ location, restores the activity in accordance with the effects produced by the same cyclic side chain on Ac_6c-containing α-peptides. Only in the case of the activity connected with the lysozyme release, the two positional isomers **6** and **12** exhibit clearly different behaviors. In fact, as previously mentioned, the $\beta^{2,2}$ isomer **12** is sensibly both more efficient and more potent than the $\beta^{3,3}$ and at a concentration of 10^{-6} M shows a peak reaching that of the reference molecule (Figure 8C). Finally, the conformational behavior exhibited in $CDCl_3$ solution by **6** and **12** shows the effects exerted by the different location of the side chain on the β-residue. However, despite the distinct preferred conformations, the two molecules show substantially comparable biological responses, except for the secretagogue activity. This suggests an induced fit mechanism operative during the interaction of this type of ligands with the human neutrophil receptors.

2.3.5 Experimental section

Materials and methods. Boc-Met-OH (purum, ≥98%) and HCl·H_2N-Phe-OMe (purissimum, ≥99%) were purchased from Fluka. Spectrograde solvents were purchased from Merck; all the other solvents and reagents were of the purest grade commercially available. Melting points were determined with a Büchi B 540 apparatus and are uncorrected. Optical rotations were taken at 20 °C with a Schmidt-Haensch Polartronic D polarimeter (1 dm cell, *c* 1.0 in $CHCl_3$, unless otherwise specified). IR spectra were recorded in 1% $CHCl_3$ (unless otherwise specified) solution employing a Perkin-Elmer FT-IR Spectrum 1000 spectrometer. ^{1}H NMR experiments were performed at 400 MHz on a Bruker AM 400 spectrometer in $CDCl_3$ solution (unless otherwise specified) and chemical shifts (δ) are quoted in parts per million (ppm) and were indirectly referred to TMS. TLC (thin layer chromatography) and PLC (preparative layer chromatography) were performed on silica gel Merck 60 F_{254} plates. The drying agent was sodium sulphate. Light petroleum refers to the 40-60 °C bp fraction. Elemental analyses were performed in the laboratories of the Servizio Microanalisi del CNR, Area della Ricerca di Roma, Montelibretti, Italy, and were within ±0.4% theoretical values. The abbreviations used are as follows: β^3hAc$_6$c, (1-aminocyclohexyl)-acetic acid; β^2hAc$_6$c, 1-(aminomethyl)-cyclohexanecarboxylic acid; Boc, *tert*-butyloxycarbonyl;

Boc_2O, di-*tert*-butyl dicarbonate; DMF, dimethylformamide; EEDQ, ethyl 2-ethoxy-1,2-dihydro-1-quinolinecarboxylate; EDC, *N*-(3-dimethylaminopropyl)-*N'*-ethylcarbodiimide hydrochloride; Et_2O, diethyl ether; HOBt, 1-hydroxybenzotriazole; *i*BuOCOCl, *iso*-butyl chloroformate 97%; KRPG, Krebs–Ringer phosphate containing 0.1% (w/v) d-glucose; NMM, *N*-methylmorpholine; PLC, preparative-layer chromatography; TEA, triethylamine; TLC, thin-layer chromatography.

2.3.5.1 Synthesis

***N*-Boc-β^{3}hAc$_6$c-Phe-OMe (3).** KCN (1 mmol) and freshly prepared H_2N-Phe-OMe (1.2 mmol) were added to a solution of **2**[87] in dry DMF (6 mL). The mixture was stirred at 50 °C under N_2 atmosphere for 16 h, then the solvent was evaporated in vacuo and the residue diluted with $CHCl_3$, washed with 5% citric acid, $NaHCO_3$ ss, and NaCl ss. The organic layer was dried, filtered and evaporated in vacuo to give crude **3**. The product was purified by silica gel chromatography using a gradient of $CHCl_3$/EtOAc as eluant to afford 0.32 g of pure **3** (76%) as an oil; $[a]_D$ +18° (*c* 1.0, $CHCl_3$); IR ($CHCl_3$): ν 3439, 2935, 1742, 1704, 1666, 1498 cm^{-1}; ^1H NMR ($CDCl_3$): δ 1.37-1.97 [19H, m, $C(CH_3)_3$ and Ac$_6$c side chain], 2.63 (2H, m, CH_2-CO), 3.02-3.16 (2H, A and B of an ABX, *J* = 5.9, 7.2, and 14.0 Hz, Phe β-CH_2), 3.72 (3H, s, $COOCH_3$), 4.49 (1H, s, Ac$_6$c NH),

4.87 (1H, m, Phe α-CH), 6.17 (1H, d, *J* = 7.8 Hz, Phe NH), 7.15-7.33 (5H, m, aromatics).

***N*-Boc-Met-β^{3}hAc$_6$c-Phe-OMe (5).** The mixture of Boc-Met-OH (0.67 mmol) in 5 mL of CH_2Cl_2 was cooled at -15 °C for 10 min, then *i*BuOCOCl (0.75 mmol) and NMM (0.75 mmol) were added and the mixture was stirred for 10 min at the same temperature. To the solution of **4** (0.67 mmol) in CH_2Cl_2, 10% DMF and NMM (0.75 mmol) were added. After 15 min at -15 °C, the mixture was kept at room temperature overnight. The mixture was diluted with $CHCl_3$, washed with 5% citric acid, $NaHCO_3$ ss and NaCl ss. The combined organic layers were dried and filtered and the solvent was removed in vacuo to afford 0.35 g of crude **5**. This was purified by silica gel column chromatography using a gradient of $CHCl_3$/EtOAc as eluant to give 0.240 g of pure **5** as colorless oil (65%); $[a]_D$ +12° (*c* 0.5 $CHCl_3$); IR (c 0.5% $CHCl_3$): ν 3420, 3360, 2936, 1737, 1671 cm^{-1}; ^{1}H NMR ($CDCl_3$): δ 1.27-1.90 [19H, m, $C(CH_3)_3$ and Ac$_6$c side chain], 1.87-2.58 (6H, m, β^{3}hAc$_6$c CH_2CO, Met β-CH_2 and Met γ-CH_2), 2.13 (3H, s, SCH_3), 3.00-3.25 (2H, m, Phe β-CH_2), 3.74 (3H, s, $COOCH_3$), 4.20 (1H, m, Met α-CH), 4.86 (1H, m, Phe α-CH), 5.34 (1H, d, *J* = 7.7 Hz, Met NH), 6.27 (1H, s, β^{3}hAc$_6$c NH), 6.40 (1H, d, *J* = 7.3 Hz, Phe NH), 7.15-7.34 (5H, m, aromatics).

***N*-Boc-Met-β^{2}hAc$_6$c-OMe (9).** The mixture of Boc-Met-OH (0.814 mmol) in 5 mL of CH_2Cl_2 was cooled at -15 °C for 15

min, then *i*BuOCOCl (0.82 mmol) and NMM (0.9 mmol) were added and the mixture was stirred for 15 min at the same temperature. Then a solution of **8** (0.814 mmol) in CH_2Cl_2 (4 mL) and DMF (0.4 mL) was added. After 10 min at -15 °C, the mixture was kept at room temperature overnight. The mixture was diluted with CH_2Cl_2 and washed with of 10% citric acid, $NaHCO_3$ ss, and NaCl ss. The combined organic layers were dried, and filtered and the solvent removed in vacuo to obtain crude **9**. The product was purified by PLC, with EtOAc/$CHCl_3$ (1:1) as eluant to give pure **9** (90%); $[a]_D$ -15° (*c* 1.0, $CHCl_3$); IR (c 0.5% $CHCl_3$): ν 3433, 3029, 1712, 1678, 1496 cm^{-1}; ^1H NMR ($CDCl_3$): δ 1.26-1.58 (19H, m, $C(CH_3)_3$ [s at 1.46] and β^2hAc_6c side chain), 1.95-2.58 (7H, m, S-CH_3, [s at 2.13] Met β-CH_2 and Met γ-CH_2), 3.39 (2H, m, β_2hAc_6c NHC*H*$_2$), 3.71 (3H, s, $COOCH_3$), 4.22 (1H, m, Met α-CH), 5.21 (1H, d, *J* = 7.3 Hz, Met NH), 6.52 (1H, m, β^2hAc_6c NH).

***N*-Boc-Met-β^{2}hAc$_6$c-OH (10).** 1N LiOH (1.43 mL) was added to the solution of **9** (0.7 mmol) in THF/H_2O (5:1) (3 mL), stirred at 0 °C for 15 min and then left at room temperature overnight. The mixture was concentrated in vacuo and extracted with Et_2O. The aqueous phase was acidified with 1N HCl and extracted with EtOAc. The organic layer was washed with NaCl ss, dried and evaporated in vacuo to give 0.13 g (50%) of crude product. The obtained **10** was used into the next step without further purification.

***N*-Boc-Met-β^{2}hAc$_6$c-Phe-OMe (11).** Product **10** (0.4 mmol) was added at rt to a mixture of EDC (0.4 mmol) and HOBt (0.4 mmol) and NMM (0.8 mmol) in 20 mL of dry CH_2Cl_2. After 10 min, HCl·H_2N-Phe-OMe (0.36 mmol) was added. The reaction flask was kept at room temperature under N_2 atmosphere overnight. The mixture was concentrated in vacuo, diluted with EtOAc, and washed with 5% citric acid, $NaHCO_3$ ss, and NaCl ss. The combined organic layers were dried, filtered and the solvent was removed in vacuo to obtain the crude **11**. The product was purified by PLC using CH_2Cl_2/MeOH (95:5) as eluant to give 0.16 g of a pure **11** as colorless oil (72%); ^{1}H NMR ($CDCl_3$): δ 1.25-1.90 (21H, m, $C(CH_3)_3$, [s at 1.46] Met β-CH_2 and β^{2}hAc$_6$c side chain), 2.10 (3H, s, SCH_3), 2.53 (2H, m, Met γ-CH_2), 3.10-3.30 (2H, A and B of an ABX, *J* = 4.4, 11.0 and 14.0 Hz, Phe β-CH_2), 2.70 and 3.70 (2H, two m, β^{2}hAc$_6$c NHC*H$_2$*), 3.81 (3H, s, $COOCH_3$), 4.08 (1H, m, Met α-CH), 4.88 (1H, m, Phe α-CH), 5.16 (1H, d, *J* = 8.4 Hz, Met NH), 7.01 (1H, d, *J* = 8.4 Hz, Phe NH), 7.10-7.30 (5H, m, aromatics), 7.70 (1H, br s, β^{2}hAc$_6$c NH).

For-Met-β^{3}hAc$_6$c-Phe-OMe (6). [a]$_D$ +16° (*c* 0.5 $CHCl_3$); IR($CHCl_3$): ν 3423, 3032, 2400, 1739, 1675, 1510 cm^{-1}; ^{1}H NMR ($CDCl_3$): δ 1.27-2.32 [17H, m, β^{3}hAc$_6$c side chain and CH_2CO, Met β-CH_2, SCH_3 (s at 2.15)], 2.57 (2H, m, Met γ-CH_2), 3.07 and 3.11 (2H, A and B of ABX, *J* = 5.5, 7.5, 14.0

Hz, Phe β-CH_2), 3.75 (3H, s, $COOCH_3$), 4.59 (1H, m, Met α-CH), 4.83 (1H, m, Phe α-CH), 6.02 (1H, s, β^3hAc_6c NH), 6.35 (1H, d, *J* = 8.2 Hz, Phe NH), 6.55 (1H, d, *J* = 7.5 Hz, Met NH), 7.15-7.35 (5H, m, aromatics), 8.20 (1H, s, HCO).

For-Met-β^2hAc_6c-Phe-OMe (12). $[a]_D$ -29.5° (*c* 0.17 $CHCl_3$); IR (c 0.5%, $CHCl_3$) 3429, 3369, 3337, 2934, 1728, 1673, 1498 cm^{-1}; ^1H NMR ($CDCl_3$): δ 1.15-2.05 (12H, m, Met β-CH_2 and β^2hAc_6c side chain), 2.15 (3H, s, SCH_3), 2.60 (2H, m, Met γ-CH_2), 3.15-3.27 (2H, A and B of an ABX, *J* = 4.6, 10.0, 14.0 Hz, Phe β-CH_2), 2.86 and 3.75 (2H, m, β^2hAc_6c NHC*H*$_2$), 3.84 (3H, s, $COOCH_3$), 4.48 (1H, m, Met α-CH), 4.83 (1H, m, Phe α-CH), 6.50 (1H, d, *J* = 7.6 Hz Met NH), 6.77 (1H, d, *J* = 8.0 Hz, Phe NH), 7.20-7.35 (5H, m, aromatics), 7.56 (1H, br s, NH), 8.18 (1H, s, HCO).

2.3.5.2 Biological assays

Cell preparation

Cells were obtained from the blood of healthy subjects, and human peripheral blood neutrophils were purified by using the standard techniques of dextran (Pharmacia, Uppsala, Sweden) sedimentation, centrifugation on Ficoll-Paque (Pharmacia), and hypotonic lysis of contaminating red cells. Cells were washed twice and resuspended in Krebs-Ringer phosphate (KRPG), pH 7.4, at final concentration of 50 x 10^6 cells/mL and kept at room temperature until used. Neutrophils were 98-100% viable, as

determined using the Trypan Blue exclusion test. The study was approved by the local Ethics Committee and informed consent was obtained from all participants.

Random locomotion

Random locomotion was performed with 48-well microchemotaxis chamber (Bio Probe, Milan, Italy) and migration into the filter was evaluated by the leading-front method.[96] The actual control random movement is 35 ± 3 μm (mean with standard error) of 10 separate experiments performed in duplicate.

Chemotaxis

Each peptide was added to the lower compartment of the chemotaxis chamber. Peptides were diluted from a stock solution with KRPG containing 1 mg/mL of bovine serum albumin (BSA) (Orha Behringwerke, Germany) and used at concentrations ranging from 10^{-12} to 10^{-5} M. Data were expressed in terms of chemotactic index (CI), which is the ratio of the difference of migration toward test attractant minus migration toward the buffer to the migration toward the buffer; the values are the means of six separate experiments performed in duplicate. Standard errors are in the 0.02-0.09 CI range.

Superoxide anion production

Superoxide anion was measured by the superoxide dismutase-inhibitable reduction of ferricytochrome *c* (Sigma) modified for microplate-based assays. Tests were carried out in a final volume of 200 mL containing 4 x 10^5 neutrophils, 100 nmoles cytochrome *c*, and KRPG. At zero time, different amounts (1 x 10^{-10} to 8 x 10^{-5} M) of each peptide were added and the plates were incubated into a microplate reader (Ceres 900, Bio-TeK Instruments, Inc.) with the compartment temperature set at 37 °C. Absorbance was recorded at 550 and 468 nm. The difference in absorbance at the two wavelengths was used to calculate nanomoles of O_2^- produced using an absorptivity for cytochrome *c* of 18.5 mM^{-1} cm^{-1}. Neutrophils were incubated with 5 μg/mL cytochalasin B (Sigma) for 5 min prior to activation by peptides. Results were expressed as net nanomoles of O_2^- per 1 x 10^6 cells per 5 min and are the means of six separate experiments performed in duplicate. Standard errors are in 0.1-4 nanomoles O_2^- range.

Enzyme assay

The release of neutrophil granule enzymes was evaluated by determination of lysozyme activity, modified for microplate based assays. Cells, 3 x 10^6/well, were first incubated in triplicate wells of microplates with 5 μg/mL cytochalasin B at 37 °C for 15 min and then in the presence of each peptide at a final concentration of 1 x 10^{-10} to 8 x 10^{-5} M for a further 15

min. The plates were then centrifuged at 400 x g for 5 min and the lysozyme was quantified nephelometrically by the rate of lysis of cell wall suspension of Micrococcus lysodeikticus. The reaction rate was measured using a microplate reader at 465 nm. Enzyme release was expressed as the net percentage of total enzyme content released by 0.1% Triton X-100. Total enzyme activity was 85 x 1mg per 1 x 10^7 cells/min. The values are the means of five separate experiments done in duplicate. Standard errors are in the range of 1-6%.

2.4 Chemotactic tripeptides incorporating at position 2 α-amino acid residues with unsaturated side chains*

Directed migration of neutrophils along an increasing chemical gradient (chemotaxis) from blood to inflammatory sites is the first line of defence against bacterial infections. Chemotaxis depends upon the interaction of a variety of extracellular messengers with specific receptors located on neutrophil plasma membrane. Several chemically unrelated substances, such as arachidonic acid metabolites, complement fragment C5a, bacterial or mitochondrial protein-derived *N*-formyl peptides and a number of chemokines have the ability to initiate the migratory response.[97] Binding of these ligands with

*Lucente, G.; Paradisi Paglialunga, M.; Giordano, C.; Sansone, A.; Torino, D.; Spisani, S. *Amino Acids* **2008**, *35*, 329.

neutrophil receptors gives rise, in addition to chemotaxis, to a series of connected biochemical events consisting primarily in particle phagocytosis, superoxide anion production and release of proteolytic enzymes. Among chemotactic agents, highly specific for human neutrophils, *N*-For-Met-Leu-Phe-OH (fMLF) and its methyl ester (fMLF-OMe) are recognized as the reference molecules for studies aimed at elucidating the structure-activity relationships. These tripeptide ligands bind to at least two G protein coupled receptors, the high-affinity FPR and its low-affinity variant FPRL1.[98] It has been shown that complex intracellular signal transduction systems exist in human neutrophils.[99,100] However, although several studies deal with this topic, the relationships between intracellular signalling and the different biological activities are still not well established. Thus, design and synthesis of fMLF analogues capable to exhibit selective behaviour,[101] represent very useful tools for studying signal transduction systems.

The effects of native amino acid substitutions on fMLF sequence, as well as the biological consequences of the backbone conformation modifications, have been extensively studied.[102] While the sulphur containing *N*-terminal For-Met-moiety and the aromatic side chain at the *C*-terminal position are crucial for both binding and receptor activation, the hydrophobic Leu residue at the position 2, although critical for backbone conformation, results to be the most tolerant towards

replacements and modifications.[70] In accordance with this observation, several studies on position 2 fMLF analogues have been performed with particular attention focused on: i) the control of the backbone conformations and ii) the production of ligands capable to exhibit selective behaviour towards the other cellular functions associated with the chemotaxis. Well known examples of the conformational control are the position 2 analogues containing $C^{\alpha,\alpha}$ disubstituted residues with linear or cyclic side chains, characterized by extended structure[62,83] and β-turn folding,[50] respectively. Representative of a selectively acting analogue is the tripeptide $[\Delta^{Z}Leu]^{2}$fMLF-OMe containing an α,β-didehydro residue replacing the native Leu; this compound is practically inactive as chemoattractant and highly active in the superoxide anion generation and lysozyme release.[103]

Based on the above observations indicating that peptide-receptor interactions in the specific area involving the position 2 of the *N*-formyl tripeptides are important modulators of the biological effects and as prosecution of our previous research in this field,[71] we report here on a series of new fMLF-OMe analogues characterized by the presence at position 2 of three different types of synthetic α-aminoacids (Figure 9), all containing γ-δ-didehydro side chains. (Alg = (*S*)-allylglycine; Dag = diallylglycine; Cpg = 1-aminocyclopent-3-ene-1-carboxylic acid).

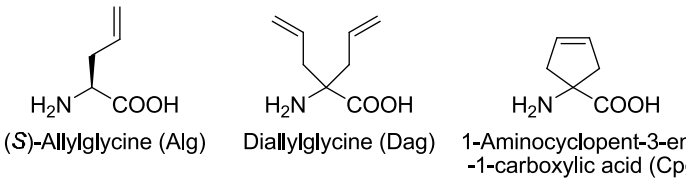

Figure 9. Synthetic γ-δ-didehydro-α-amino acid residues replacing native (*S*)-Leucine in the here reported fMLF-OMe analogues.

It can be noted that whereas C^{α}-allylglycine has been frequently used in peptide chemistry as starting residue for ring-closing metathesis (RCM) reactions, no data seem at the present available on biological activity of peptides incorporating the Dag or the Cpg residue. Model peptides containing a Boc protected *N*-terminal Cpg residue have been recently described.[104]

2.4.1 Chemistry

The synthesis of the Boc-peptides and the corresponding *N*-formyl analogues was performed according to Schemes 3-5. Fmoc-Alg-Phe-OMe (**1**) was obtained by coupling Fmoc-Alg-OH with HCl·H_2N-Phe-OMe using EDC/HOBt. After *N*-deprotection of **1** by pyperidine treatment, the dipeptide **2** was acylated (EDC/HOBt) by Boc-Met-OH to give Boc-Met-Alg-Phe-OMe (**3**).

Coupling of Boc-Met-OH with Dag-OEt (BOP/HOBT) or Cpg-OEt (EDC/HOBt) afforded Boc-Met-Dag-OEt (**5**) and Boc-Met-Cpg-OEt (**8**), respectively. *C*-deprotection by hydrolysis of **5** and **8** gave the free acids which were coupled (EDC/HOBt)

with HCl·H_2N-Phe-OMe to give Boc-Met-Dag-Phe-OMe (**6**) and Boc-Met-Cpg-Phe-OMe (**9**), respectively.

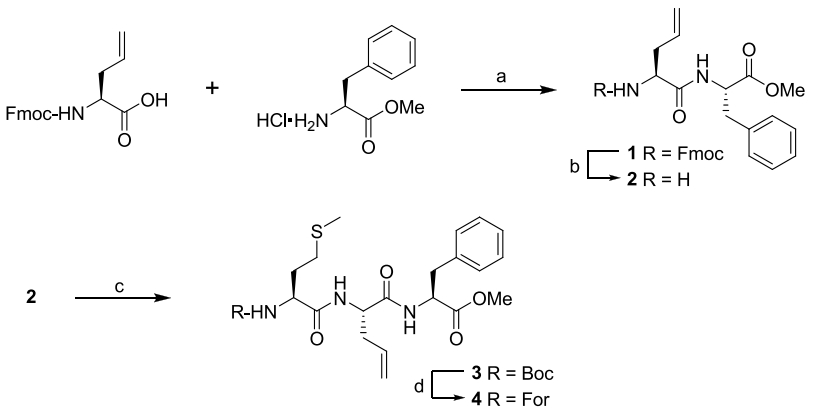

Scheme 3. Synthesis of (*S*)-Allylglycine (Alg) containing tripeptides **3** and **4**. *Reagents and conditions*: a) HOBt, EDC, TEA, EtOAc, 30 min 0 °C, 12h rt; b) piperidine, CH_2Cl_2, 1/2h rt; c) Boc-Met-OH, HOBt, EDC, TEA, EtOAc 30 min 0 °C, 12h rt; d) HCOOH, overnight, rt then EEDQ, $CHCl_3$ 24h rt.

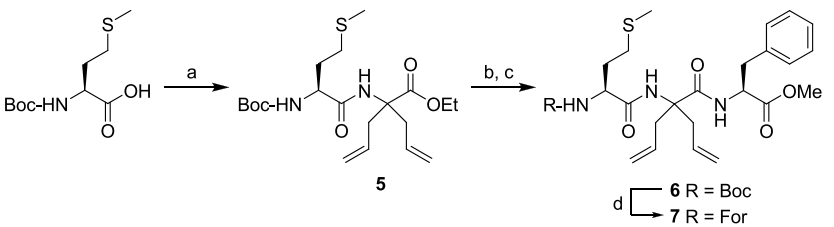

Scheme 4. Synthesis of Diallylglycine (Dag) containing tripeptides **6**-**7**. *Reagents and conditions*: a) Dag-OEt, BOP, HOBt, NMM, EtOAc, 30 min 0 °C, 12h rt; b) 2N LiOH, MeOH, overnight rt; c) HCl·H_2N-PheOMe, BOP, HOBt, NMM, EtOAc, 30 min 0 °C, 12h rt; d) HCOOH, overnight rt then EEDQ, $CHCl_3$, 24h rt.

RCM reaction by using second generation Grubbs catalyst performed on the tripeptide **6** containing central Dag afforded in good yields the Cpg analogue **9**. Direct transformation of the *N*-Boc derivatives **3**, **6**, and **9** into the corresponding *N*-formyl

analogs **4**, **7** and **10** was performed by treatment of the *N*-Boc derivatives with formic acid followed by EEDQ.[92]

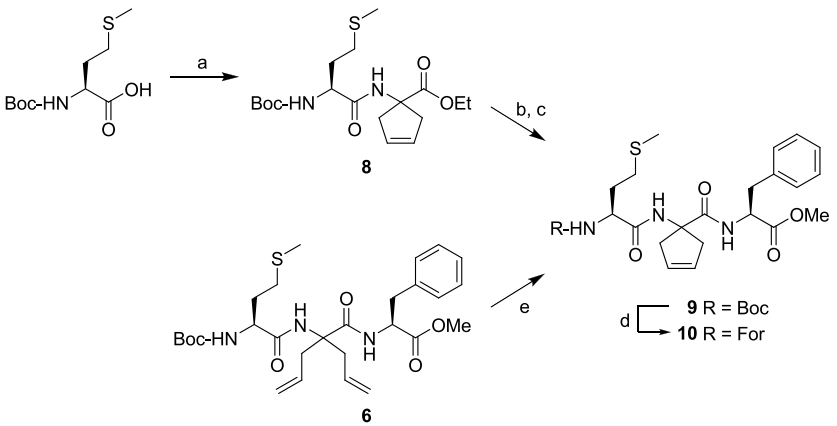

Scheme 5. Synthesis of 1-Aminocyclopent-3-ene-1-carboxylic acid (Cpg) containing tripeptides **9** and **10**. *Reagents and conditions*: a) Cpg-OEt, EDC, HOBt, TEA, EtOAc, 30 min 0 °C, 12h rt; b) 1N NaOH, MeOH, overnight rt; c) HCl·H_2N-Phe-OMe, EDC, HOBt, TEA, EtOAc, 30 min 0 °C, 12h rt; d) HCOOH, overnight rt then EEDQ, $CHCl_3$, 24h rt; e) Grubbs catalyst, CH_2Cl_2, 5h rt.

2.4.2 Conformational studies

^{1}H NMR

Information on the conformational preferences of the tripeptides **7**, **9** and **10** containing the stereochemically constrained residues of Dag and Cpg has been obtained by examining the involvement of the NH groups in intramolecular H-bonds by using ^{1}H NMR titration experiments.

In Figure 10 the chemical shift dependence of the shift values as a function of increasing DMSO-d_6 concentrations in $CDCl_3$ solution (10 mM) is reported. In Table 1 the solvent exposure of

the NH groups is expressed as the difference (Δδ, ppm) between the chemical shift observed in neat $CDCl_3$ and in a $CDCl_3$ solution containing 10% DMSO-d_6. High values of Δδ correspond to efficient H bonding interaction of the NH groups with the DMSO-d_6 while low values indicate scarce sensibility to solvent composition variation and presumable involvement in intramolecular H-bonds.

The values of here studied peptides reported in Table 1 are compared with the data previously observed for the related models Boc-Met-Ac_5c-Phe-OMe[50] and HCO-Met-Dpg-Phe-OMe[62] containing 1-amino-1-cyclopropane carboxylic acid (Ac_5c) residue and di-*n*-propylglycine (Dpg), respectively.

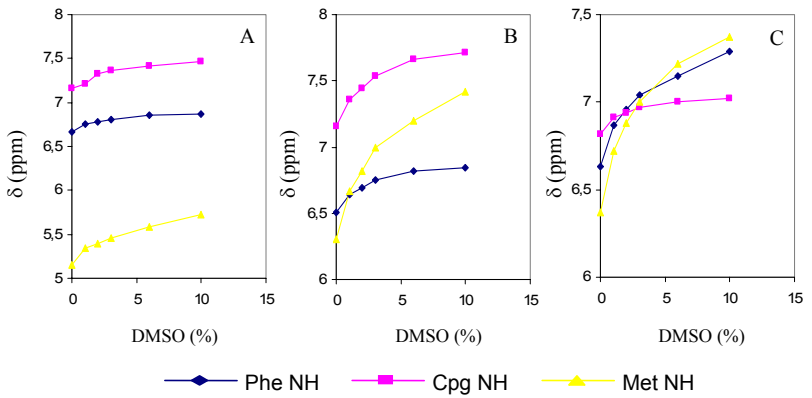

Figure 10. Delineation of NH chemical shifts as a function of increasing percentage of DMSO-d_6 to the $CDCl_3$ solution (vol/vol) for (**A**): Boc-Met-Cpg-Phe-OMe (**9**); (**B**): For-Met-Cpg-Phe-OMe (**10**); (**C**): For-Met-Dag-Phe-OMe (**7**).

The solvent perturbation experiments performed on Cpg containing models **9** and **10** indicate that the Phe and the Cpg

NH (Table 1) are scarcely affected by the change of the solvent composition ($\Delta\delta$ = 0.20 and 0.30 ppm for **9** and 0.33 and 0.55 for **10**, respectively).

Table 1. Solvent-composition effects on NH chemical shifts of peptides. Values reported are the differences ($\Delta\delta$, ppm) between NH proton chemical shifts observed in $CDCl_3$ solution containing 10% DMSO-d_6 and neat $CDCl_3$.

Compound	Met NH	Central NH	Phe NH
HCO-Met-Dag-Phe-OMe (**7**)	1.00	0.20	0.66
HCO-Met-Cpg-Phe-OMe (**10**)	1.12	0.55	0.33
Boc-Met-Cpg-Phe-OMe (**9**)	0.57	0.30	0.20
Boc-Met-Ac$_5$C-Phe-OMe[a]	1.00	0.94	0.15
HCO-Met-Dpg-Phe-OMe[b]	1.40	0.25	1.30

[a] See reference: Toniolo et al. (1989)
[b] See reference: Dentino et al. (1991)

The *N*-terminal Met NH shows, on the other hand, a value of 1.12 ppm for the HCO-NH of **10** and 0.57 for the Boc-NH of **9**. To properly evaluate the solvent shielding exhibited by the Met NH of **9** it should be recalled that the bulky *t*-butyloxycarbonyl group significantly hinders the interaction of the NH with the solvent.[105] Thus, the $\Delta\delta$ value found for **9**, lower than that expected for a free NH group, is only in part attributable to the participation to intramolecular H-bonding since the effect of the *N*-Boc must be considered. By taking into account this latter consideration it can be assumed that both **9** and **10** are characterized by a similar conformer population characterized by the central Cpg and the *N*-terminal Phe NH groups not freely

interacting with the solvent and then presumably involved in intramolecular H-bonds.

It is interesting to note that the above reported **9** and **10** titration data differ significantly from those exhibited by the tripeptide Boc-Met-Ac_5c-Phe-OMe.[50] In this case (Table 2) both the *C*-terminal Met and the central Ac_5c NH groups interact efficiently with the solvent ($\Delta\delta$ = 1.0 and 0.94 ppm, respectively) while the Phe NH appears sensibly unaffected by the solvent composition ($\Delta\delta$ = 0.15 ppm).

Table 2. Observed nuclear Overhauser effects (NOEs) in the Noesy spectrum of HCO-Met-Cpg-Phe-OMe **10**.

HCO · · · Met NH	m	Cpg NH · · · Met $C^{\alpha}H$	s
Met NH · · · Met $C^{\alpha}H$	w	Cpg $C^{\gamma}H$ · · · Cpg $C^{\beta}H_2$	s
Met $C^{\alpha}H$ · · · $C^{\beta}H_2$	m	Cpg $C^{\delta}H$ · · · Cpg $C^{\varepsilon}H_2$	s
Phe NH · · · Phe $C^{\alpha}H$	m	Cpg $C^{\beta}H_2$ · · · Phe NH	m
Phe $C^{\alpha}H$ · · · Phe $C^{\beta}H_2$	m	Cpg $C^{\varepsilon}H$ · · · Phe NH	m

s strong; *m* medium; *w* weak.

Thus, the preferred solution conformation of the Ac_5c containing tripeptide has been described as a type-II β-turn (C10 ring) stabilized by a single intramolecular H-bond involving the Boc CO and the *C*-terminal Phe NH. In the case of the analogues **9** and **10**, containing the central Cpg residue, the picture is less clearly defined since both the Cpg NH and the *C*-terminal Phe NH, appear not completely free to interact with the solvent. Thus, a conformation which takes into account this situation should be considered.

In order to get further information on the preferred conformation induced by the central Cpg residue, a two dimensional NMR experiment was carried out on the tripeptide **10**. Detection of nuclear Overhauser effects (NOEs) in the NOESY spectra are related to the through-space proximity of the protons of the molecule. The estimates of the cross-peak relative intensities found for **10** are summarized in Table 2 on an arbitrary scale. The interresidue NOE HCO···Met NH is in accordance with the *cis* configuration of the two H atoms of the H-CO-NH group, as always found in the crystal structures of *N*-formyl peptides. Noteworthy is the absence of the NOE between the NH groups of the (*i* + 2) and (*i* + 3) residue (i.e. Cpg NH···Phe NH) which is diagnostic of a β-turn structure. Furthermore, the observation of NOEs between the Phe NH and the Cpg β- and ε-CH_2 groups, does not support the hypothesis of the C_{10} conformation and suggests that the Phe NH interacts with the Met-CO thus stabilizing a γ-turn centred at the Cpg residue. Concerning the Cpg NH···Met $C^{\alpha}H$ spatial connectivity it can be observed that this finding, taken together with the partial solvent inaccessibility shown by the Cpg NH ($\Delta\delta$ = 0.30 ppm), suggests the presence, although in limited extent, of a second γ-turn structure[106,107] centred at the Met residue and involving the formylic carbonyl and the Cpg NH (Figure 11).

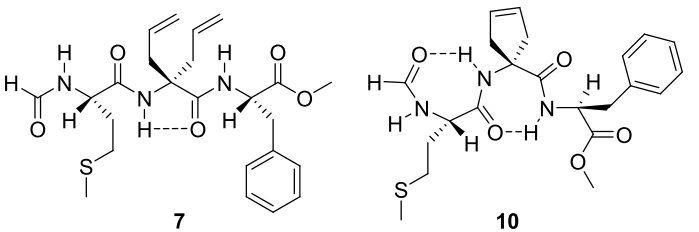

Figure 11. Preferred conformation adopted by *N*-formyl tripeptides **7** and **10** in $CDCl_3$ solution. The intraresidue H-bond in the C5 conformation of **7** and in the two consecutive γ-turns (C7 structures) of **10** are indicated by dotted lines.

The titration experiments were then extended to the analogue HCO-Met-Dag-Phe-OMe (**7**) containing the di-allylglycine residue in place to the native (*S*)-leucine (Figure 2C). In this case the NH of the central residue presents a pronounced solvent inaccessibility ($\Delta\delta = 0.20$, Table 1) while the Met and, in less extent, the Phe NH groups interact efficiently with the solvent. In accordance with literature these data suggest the presence in $CDCl_3$ solution of a significant population of the peptide molecules in an extended conformation with the Dag NH involved in a C_5 intraresidue H bond (Figure 3). An analogue behaviour has been previously observed[62] for the corresponding saturated formyl tripeptide HCO-Met-Dpg-Phe-OMe in which the NH of the central $C^{\alpha,\alpha}$ tetrasubstituted residue is strongly solvent shielded while the Met and Phe NH groups are completely free (see Table 1).

IR

The presence in the tripeptides under study of intramolecularly H bonded NH groups has also been studied by the examining the IR absorptions in the NH stretching region ($CHCl_3$, 5 mM). In the spectrum of *N*-Boc derivative **9** two bands are observed at 3428 and 3375 cm^{-1} corresponding to free and H bonded groups, respectively. An analogue outcome is shown by the corresponding formyl derivative **10** which exhibits a shoulder at 3378 cm^{-1} partially superimposed to the band at 3411 cm^{-1} due to the free NH stretching. In the spectrum of **7** two bands are observed at 3416 and 3368 cm^{-1}; the band at lower frequency can be assigned to the intraresidue H bonded Dag NH group. Finally a strong absorption band at 3416 cm^{-1}, attributable to free NH stretching, is exhibited by the *N*-formyl tripeptide **4** which presents a weak large band centered at 3320 cm^{-1}. This suggests that, at variance with derivatives **7**, **9** and **10**, only weak intramolecular H-bonds occur in the $CHCl_3$ solution of **4**.

2.4.3 Biological results

The biological activity of the *N*-formyl analogues **4**, **7**, and **10**, together with that of the corresponding *N*-Boc derivatives **3**, **6** and **9** has been determined on human neutrophils and compared with that of the reference ligand fMLF-OMe. Directed migration (chemotaxis), superoxide anion production and lysozyme release have been measured. The results of the

agonistic chemotactic activity of the three *N*-formyl tripeptides, expressed as chemotactic index (C.I.), are summarized in Figure 12A. It can be seen that the three formyl tripeptides **4**, **7**, and **10** are able to significantly stimulate neutrophil chemotaxis although with lower potency than the parent ligand fMLF-OMe. Notably, the Cpg containing analogue **10** reaches the same potency of the parent at a concentration value of 10^{-7} M. Both the Alg and Dag containing models **4** and **7** show an activity peak (C.I. = 0.78 and 0.82, respectively) centred at a lower concentration (10^{-10} M) than that of the parent (10^{-9} M). Furthermore, at very low concentration (10^{-13} M) the Alg containing model **4** shows higher activity than the parent molecule (C.I. = 0.44 against 0.33), thus exhibiting higher efficacy. As also shown in Figure 12A all the *N*-Boc derivatives **3**, **6**, and **9** exhibit a very similar common behaviour with an activity peak centred at 10^{-9} M and a very modest activity.

As shown in Figure 12B the three formyl peptides **4**, **7**, and **10** are highly active in stimulating superoxide anion production with the Alg containing analogue **4** showing the activity peak at the same concentration of the parent although with lower activity. Both the other two analogues **7** and **10** induce the same maximal anion production at concentration 10^{-5} M with a value corresponding to that of the fMLF-OMe. Figure 12C reports the results concerning the lysozyme release. Here all the three *N*-formyl derivatives exhibit a similar profile of

activity with a maximum centred at concentration 10^{-5} M and a rank of potency: **10** = **4** >**7**.

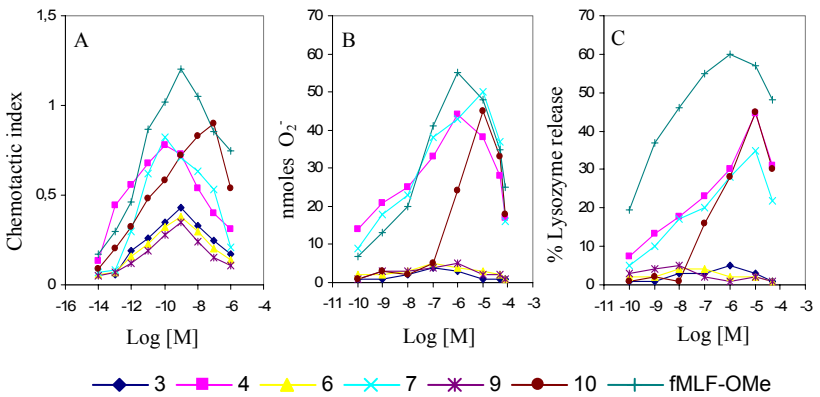

Figure 12. Biological activity of centrally modified *N*-For and *N*-Boc MLF-OMe analogues **3**, **4**, **6**, **7**, **9** and **10**. (**A**) Chemotactic index; (**B**) Superoxide anion production and (**C**) Release of neutrophil granule enzyme evaluated by determining lysozyme activity.

As generally found and as shown in Figures 12B and C the three *N*-Boc derivatives **3**, **6** and **9**, at variance with the corresponding *N*-formyl analogues, are completely unable to elicit superoxide anion and lysozyme release.

2.4.4 Conclusions

In summary we have described synthesis, conformational preferences and activity of a new group of fMLF-OMe analogues structurally related by the common presence at position 2 of residues bearing unsaturated side chains. As reported in Figure 12 all the three *N*-For analogues **4**, **7** and **10** are capable to elicit high to moderate values of chemotaxis as

well as of superoxide anion production and lysozyme release. These findings confirm the versatility of the fMLF-OMe to accept structural modifications at the central position.

The preferred conformations of the models incorporating the $C^{\alpha,\alpha}$-disubstituted residues Dag and Cpg (Figure 11) indicate that an analogous effect is induced by the Dag and the corresponding saturated residue. It is found in fact that the tripeptide **7**, containing two linear allylic side chains at position 2, adopts the expected C_5 extended conformation also found in the case of the di-*n*-propylglycine (Dpg) containing tripeptide.[62] On the other hand, the conformation of the tripeptide **10**, incorporating the Cpg residue differs from the β-turn structure found in the case of the related model containing the cyclopentane ring.[50]

The last reported finding underlines the interest to further explore the ability of Cpg to induce specific conformations into peptide backbones in which this residue is incorporated. In addition to this, the chemical reactivity of the unsaturated 5-membered ring must be considered. This property appears particularly interesting in the light of recent transformation reactions performed on *N*-protected Cpg esters such as hydroboration-oxidation reactions[108] and 1,3-dipolar additions.[109] These data and the concomitant lack of information on the biochemical consequences of the incorporation of the Cpg residue into native peptides, stimulate further studies on

this unsaturated cyclic $C^{\alpha,\alpha}$-disubstituted amino acid and on peptides containing residues with cyclopentenyl side chains.

2.4.5 Experimental section

Materials and methods. Cpg-OEt has been synthesized starting from *cis*-1,4-dichloro-2-butene and the Schiff base obtained by reacting ethyl glycinate with 4-bromobenzaldehyde.[110] Dag-OEt was synthesized starting from ethyl isocyanoacetate and allyl bromide under phase transfer catalysis conditions.[111] All other starting materials and reagents were obtained commercially and used without further purification. Melting points were determined with a Büchi B 540 apparatus and are uncorrected. Optical rotations were taken at 20 °C with a Schmidt-Haensch Polartronic D polarimeter (1 dm cell, *c* 1.0 in $CHCl_3$, unless otherwise specified). IR spectra were recorded in 1% $CHCl_3$ solution (unless otherwise specified) employing a Perkin-Elmer FT-IR Spectrum 1000 spectrometer. ^1H NMR experiments were performed at 400 MHz on a Bruker AM 400 spectrometer in $CDCl_3$ solution and chemical shifts (δ) are quoted in parts per million (ppm) and were indirectly referred to TMS. NOESY spectra were recorded in $CDCl_3$ on Avance 400 Bruker console with a 800 msec mixing time and displayed in the phase-sensitive mode. Usually 256 x 1024 data points were collected and for each block 64 transients were collected for two-dimensional experiments. The

data sets were linearly predicted to 512 x 1024 data points. A Gaussian window was applied in both dimensions. Zero filling was used for a final spectrum of 1024 x 1024 data points. TLC thin layer chromatography) were performed on silica gel Merck 60 F_{254} plates. The drying agent was sodium sulphate. Elemental analyses were performed in the laboratories of the Servizio Microanalisi del CNR, Area della Ricerca di Roma, Montelibretti, Italy, and were within ±0.4% of the theoretical values.

2.4.5.1 Chemistry. General procedure

A. Coupling with the carbodiimide method. To an ice-cooled mixture containing the required *N*-Boc- or *N*-Fmoc-amino acid (1.0 mmol), the amino-derivative·HCl (1.0 mmol), HOBt (1.2 mmol), and TEA (2.2 mmol) in anhydrous EtOAc (6 mL), EDC (1.2 mmol) was added and the reaction mixture was allowed to warm to room temperature. After 12 h the reaction mixture was diluted with EtOAc (20 mL) and washed with 1M $KHSO_4$ (2 x 15 mL), saturated aqueous $NaHCO_3$ (2 x 15 mL) and brine (15 mL). The organic phase was dried and evaporated under reduced pressure.

B. Preparation of the *N*-formyl derivatives. The *N*-Boc derivative (1.0 mmol) was dissolved in formic acid (3 mL) and the mixture was allowed to stand at room

temperature overnight. After removal of the excess formic acid under vacuum, the residue was dissolved in dry CH_2Cl_2 (10 mL) or dry DMF (2 mL). EEDQ 97% (1.2 mmol) was added and the solution was stirred at room temperature for 24 h. Evaporation under reduced pressure afforded the crude *N*-formyl derivative.[92]

2.4.5.2 Synthesis

Fmoc-Alg-Phe-OMe (1). Fmoc-Alg-OH (0.5 g, 1.48 mmol) was treated with $HCl \cdot H_2N$-Phe-OMe (0.320 g, 1.48 mmol) according to the carbodiimide coupling general procedure. Crystallization from EtOAc/Hexane gave the title product as a white solid (0.670 g, 90%); mp 150-153 °C; $[a]_D$ +14° (*c* 1 $CHCl_3$); IR ($CHCl_3$): ν 3421, 1739, 1680 cm^{-1}; ^1H NMR ($CDCl_3$): δ 2.30 (2H, br s, CH_2-CH=CH_2), 2.74-3.00 (2H, m, Phe β-CH_2), 3.50 (3H, s, $COOCH_3$), 3.88-4.30 (4H, m, CH-CH_2 and Alg α-CH), 4.50 (1H, m, Phe α-CH), 4.70-4.90 (2H, m, CH_2-CH=CH_2), 5.30-5.50 (1H, m, CH_2-CH=CH_2), 6.63 (1H, br s, Phe NH), 6.80 (1H, br s, Alg NH), 7.00-7.50 (13H, m, aromatics). Anal. Calcd for $C_{30}H_{34}N_2O_5$: C, 71.69; H, 6.82; N, 5.57. Found: C, 71.58; H, 6.77; N, 5.58.

H_2N-Alg-Phe-OMe (2). Fmoc-Alg-Phe-OMe (0.670 g, 1.34 mmol) in CH_2Cl_2 (4 mL) was *N*-deprotected by treatment with piperidine (4 mL) for 1/2 h. The reaction solution was diluted with CH_2Cl_2 (2 x 15 mL) and washed with 1N HCl (2 x 15 mL).

The aqueous phase was basified with $NaHCO_3$ and the product extracted with CH_2Cl_2. Resulting H_2N-Alg-Phe-OMe **2** was used without further purification.

***N*-Boc-Met-Alg-Phe-OMe (3).** The above prepared H_2N-Alg-Phe-OMe **2** was acylated with Boc-Met-OH (0.284 g, 1.14 mmol) according to the carbodiimide coupling general procedure. Silica gel flash chromatography (CH_2Cl_2/MeOH 98:2) gave a pure product as a white solid (0.430 g, 64%); $[a]_D$ +2° (*c* 0.5, $CHCl_3$); IR ($CHCl_3$): ν 3414, 1741, 1670 cm^{-1}; ^1H NMR ($CDCl_3$): δ 1.45 [9H, s, $C(CH_3)_3$], 1.85-2.11 [5H, m, Met β-CH_2 and S-CH_3 (s at 2.10)], 2.45-2.57 (4H, m, Met γ-CH_2 and CH_2-CH=CH_2), 3.05 and 3.17 (2H, A and B of an ABX, J = 5.6, 10.4 and 6.0 Hz, Phe β-CH_2), 3.72 (3H, s, $COOCH_3$), 4.23 (1H, m, Met α-CH), 4.40 (1H, m, Alg α-CH), 4.83 (1H, m, Phe α-CH), 5.07-5.18 (3H, m, CH_2-CH=CH_2 and Met NH), 5.61-5.68 (1H, m, CH_2-CH=CH_2), 6.46 (1H, br s, Phe NH), 6.70 (1H, d, J = 7.2 Hz, Alg NH) 7.01-7.5 (5H, m, aromatics). Anal. Calcd for $C_{25}H_{37}N_3O_6S$: C, 59.15; H, 7.35; N, 8.28. Found: C, 59.13; H, 7.31; N, 8.09.

***N*-Boc-Met-Dag-OEt (5).** To a solution of Boc-Met-OH (0.476 g, 0.19 mmol) in anhydrous EtOAc (20 mL), BOP (0.955 g, 0.216 mmol), HOBt (0.357 g, 0.264 mmol) and few drops of DMF were added. The solution was then ice cooled for few minutes and a suspension of HCl·H_2N-Dag-OEt (0.500 g, 2.16 mmol) and NMM (0.7 mL, 6.48 mmol) in EtOAc (2 mL) was

added. After 12 h at room temperature the reaction mixture was diluted with EtOAc (20 mL) and washed with 1M $KHSO_4$ (2 x 15 mL), saturated aqueous $NaHCO_3$ (2 x 15 mL) and brine (15 mL). The organic phase was dried and evaporated under reduced pressure. Silica gel chromatography ($CHCl_3$) gave the pure product as pale yellow oil (0.7 g, 86%); $[a]_D$ -15° (*c* 1, $CHCl_3$); IR ($CHCl_3$): ν 3423, 1799, 1677 cm^{-1}; ^1H NMR ($CDCl_3$): δ 1.25 (3H, m, $COOCH_2CH_3$), 1.43 [9H, s, $C(CH_3)_3$], 1.72-2.11 [5H, m, Met β-CH_2 and SCH_3 (s, at 2.09)], 2.48-2.65 (4H, m, Met γ-CH_2 and CH_2-CH=CH_2), 2.99-3.25 (2H, m, CH_2-CH=CH_2), 4.10-4.22 (2H, m, $COOCH_2CH_3$ and Met α-CH), 4.99-5.30 (5H, m, Met NH and two CH_2-CH=CH_2), 5.49-5.73 (2H, m, two CH_2-CH=CH_2), 6.95 (1H, s, Dag NH). Anal. Calcd for $C_{20}H_{34}N_2O_5S$: C, 57.94; H, 8.27; N, 6.76. Found: C, 57.03; H, 8.28; N, 6.57.

***N*-Boc-Met-Dag-OH.** Boc-Met-Dag-OEt (0.7 g, 1.64 mmol) was treated with 2N LiOH (2 mL) and MeOH (7 mL) and left overnight at room temperature. MeOH was removed at reduced pressure, water (10 mL) was added and the solution extracted with Et_2O (2 x 25 mL). The aqueous phase was then acidified with 1N $KHSO_4$ and extracted with EtOAc (3 x 20 mL). The organic phases were washed with brine, dried and evaporated. A white foam (0.406 g, 60%), pure on TLC was obtained and used without further purification.

***N*-Boc-Met-Dag-Phe-OMe (6).** To a solution of Boc-Met-Dag-OH (0.406 g, 0.98 mmol) in anhydrous EtOAc (20 mL), BOP (0.490 g, 1.1 mmol), HOBt (0.185 g, 1.36 mmol) and few drops of DMF were added. The solution was cooled for few minutes and a suspension of $HCl \cdot H_2N$-Phe-OMe (0.240 g, 1.11 mmol) and NMM (0.32 mL, 2.94 mmol) in EtOAc (1 mL) was added. The reaction mixture was allowed to stand overnight at room temperature. EtOAc (20 mL) was then added and the solution washed with 1M $KHSO_4$ (2 x 15 mL), saturated acqueous $NaHCO_3$ (2 x 15 mL) and brine (15 mL). The organic phase was dried and evaporated under reduced pressure. Silica gel chromatography (EtOAc/Hexane 3:7) and crystallization from EtOAc/Hexane gave the pure title product **6** as white solid (0.3 g, 53%); IR ($CHCl_3$): ν 3432, 1741, 1667 cm^{-1}; ^1H NMR ($CDCl_3$): δ 1.44 [9H, s, $C(CH_3)_3$], 1.89-2.10 [5H, m, Met β-CH_2 and S-CH_3 (s, at 2.09)], 2.50-2.63 (4H, m, Met γ-CH_2 and CH_2-$CH{=}CH_2$), 2.76 (2H, m, CH_2-$CH{=}CH_2$), 3.05-3.14 (2H, m, Phe β-CH_2), 3.70 (3H, s, $COOCH_3$), 4.15 (1H, m, Met α-CH), 4.83 (1H, m, Phe α-CH), 5.00-5.08 (5H, m, two CH_2-$CH{=}CH_2$ and Met NH), 5.45-5.57 (2H, m, two CH_2-$CH{=}CH_2$), 6.81 (1H, br s, Phe NH), 6.88 (1H, s, Dag NH), 7.00-7.50 (5H, m, aromatics). Anal. Calcd for $C_{28}H_{41}N_3O_6S$: C, 61.40; H, 7.55; N, 67.00. Found: C, 61.26; H, 7.77; N, 67.25.

***N*-Boc-Met-Cpg-OEt (8).** Boc-Met-OH (0.268 g, 1.07 mmol) was coupled with Cpg-OEt (0.152 g, 0.980 mmol)

according to the carbodiimide coupling general procedure. The title compound was obtained as a foam, pure on TLC (0.221 g, 58%); $[a]_D$ +1.1° (*c* 1, $CHCl_3$); IR ($CHCl_3$): ν 3422, 1739, 1660 cm^{-1}; ^1H NMR ($CDCl_3$): δ 1.27 (3H, t, *J* = 7.6 Hz, $COOCH_2CH_3$), 1.46 [9H, s, $C(CH_3)_3$], 1.90-2.15 [5H, m, Met β-CH_2 and S-CH_3 (s at 2.13)], 2.58-2.69 (4H, m, Met γ-CH_2 and CH_2-CH=CH), 3.10 (2H, apparent t, CH_2-CH=CH), 4.21 (2H, q, $COOCH_2CH_3$), 4.27 (1H, m, Met α-CH), 5.18 (1H, br s, Met NH), 5.68 (2H, sharp m, CH=CH), 6.89 (1H, s, Cpg NH). Anal. Calcd for $C_{18}H_{30}N_2O_5S$: C, 55.94; H, 7.82; N, 7.25. Found: C, 56.22; H, 7.77; N, 7.22.

***N*-Boc-Met-Cpg-OH** Boc-Met-Cpg-OEt (0.210 g, 0.54 mmol) was treated with 1N NaOH (2.17 mL) and MeOH (10 mL) and left at room temperature overnight. MeOH was evaporated under vacuum, water (10 mL) was added and the solution extracted with diethyl ether (2 x 25 mL). The aqueous phase was then acidified with 1N $KHSO_4$ and the product extracted with EtOAc (3 x 20 mL). The organic phases were washed with brine, dried and evaporated to give TLC pure title product as white foam (0.190 g, quantitative yield). Anal. Calcd for $C_{16}H_{26}N_2O_5S$: C, 53.61; H, 7.31; N, 7.84. Found: C, 53.77; H, 7.49; N, 8.38.

***N*-Boc-Met-Cpg-Phe-OMe (9).** Boc-Met-Cpg-OH (0.195 g, 0.54 mmol) was treated with HCl·H_2N-Phe-OMe (0.117 g, 0.54 mmol) according to the carbodiimide coupling general

procedure. Crystallization from EtOAc gave the title pure product as a colourless crystals (0.181 g, 64%). **Boc-Met-Cpg-Phe-OMe (9)** was also prepared by using the ring-closing methatesis (RCM) reaction: (20 mg, 0.045 mmol) of Boc-Met-Dag-Phe-OMe **6** in CH_2Cl_2 (2 mL) was treated with 2nd generation Grubbs catalyst (benzylidene[1,3-bis(2,4,6-trimethylphenyl)-2-imidazolidinylidene]-dichloro(phenylmethy-lene)-(tricyclohexylphosphine) ruthenium) (10% mol) and the reaction mixture was left at room temperature for 5 h. The solvent was evaporated and the crude product was purified by PLC (EtOAc/$CHCl_3$ 1:1) to give 11 mg (47%) of product which resulted to be identical to Boc-Met-Cpg-Phe-OMe obtained by coupling the above reported Boc-Met-Cpg-OH with H_2N-Phe-OMe; mp 148.1-148.9 °C; IR ($CHCl_3$): ν 3428, 1742, 1667 cm^{-1}; ^1H NMR ($CDCl_3$): δ 1.46 [9H, s, $C(CH_3)_3$], 1.87-2.14 [5H, m, Met β-CH_2 and S-CH_3 (s at 2.11)], 2.47-2.62 (2H, m, Met γ-CH_2), 2.72-2.92 (4H, m, two CH_2-CH=CH), 3.08 and 3.18 (2H, A and B of an ABX, J = 5.6, 6.8 and 14.0 Hz, Phe β-CH_2) 3.74 (3H, s, $COOCH_3$), 4.22 (1H, m, Met α-CH), 4.84 (1H, m, Phe α-CH), 5.16 (1H, br s, Met NH), 5.71 (2H, m, CH=CH), 6.67 (1H, br s, Phe NH), 7.16 (1H, s, Cpg NH), 7.09-7.33 (5H, m, aromatics). Anal. Calcd for $C_{26}H_{37}N_3O_6S$: C, 60.09; H, 7.18; N, 8.09. Found: C, 59.98; H, 7.11; N, 7.78.

For-Met-Alg-Phe-OMe (4). From Boc-Met-Alg-Phe-OMe (0.100 g, 0.19 mmol) in dry DMF according to the general

procedure for preparation of the *N*-formyl derivatives. Silica gel flash chromatography (CH_2Cl_2/MeOH 98:2) gave the pure product as a white solid (0.07 g, 86%); $[a]_D$ +3° (*c* 1, $CHCl_3$); IR ($CHCl_3$): ν 3414, 1741, 1670 cm^{-1}; ^1H NMR ($CDCl_3$): δ 1.91-2.11 [5H, m, Met β-CH_2 and S-CH_3 (s, at 2.09)], 2.40-2.61 (4H, m, Met γ-CH_2 and CH_2-CH=CH_2), 3.09 and 3.14 (2H, A and B of an ABX, *J* = 5.6, 6.0 and 13.6 Hz, Phe β-CH_2), 3.70 (3H, s, $COOCH_3$), 4.54 (1H, m, Alg α-CH), 4.73 (1H, m, Met α-CH), 4.81 (1H, m, Phe α-CH), 5.10 (2H, m, CH_2-CH=CH_2), 5.60 (1H, m, CH_2-CH=CH_2), 6.72 (2H, apparent d, Phe NH and Met NH), 6.93 (1H, d, *J* = 7.2 Hz, Alg NH), 7.02-7.5 (5H, m, aromatics), 8.17 (1H, s, HCO). Anal. Calcd for $C_{21}H_{29}N_3O_5S$: C, 57.91; H, 6.71; N, 9.65. Found: C, 57.37; H, 6.76; N, 9.71.

For-Met-Dag-Phe-OMe (7). From Boc-Met-Dag-Phe-OMe (0.100 g, 0.17 mmol) in dry DMF according to the general procedure for preparation of the *N*-formyl derivatives. Silica gel flash chromatography (CH_2Cl_2/MeOH 98:2) gave the pure product as a colourless oil (0.06 g, 70%); IR ($CHCl_3$): ν 3414, 1741, 1670 cm^{-1}; ^1H NMR ($CDCl_3$): δ 1.87-2.11 [5H, m, Met β-CH_2 and S-CH_3 (s, at 2.09)], 2.48-2.65 (4H, m, Met γ-CH_2 and CH_2-CH=CH_2), 2.81-2.90 (2H, m, CH_2-CH=CH_2), 3.09 and 3.14 (2H, A and B of an ABX, *J* = 5.6, 7.2 and 14.0 Hz, Phe β-CH_2), 3.70 (3H, s, $COOCH_3$), 4.57 (1H, m, Met α-CH), 4.83 (1H, m, Phe α-CH), 4.97-5.10 (4H, m, two CH_2-CH=CH_2),

5.45-5.57 (2H, m, two CH_2-CH=CH_2), 6.37 (2H, d, *J* = 7.0 Hz, Met NH), 6.63 (1H, d, *J* = 7.2 Hz, Phe NH), 6.93 (1H, s, Dag NH), 7.10-7.30 (5H, m, aromatics), 8.13 (1H, s, HCO). Anal. Calcd for $C_{24}H_{33}N_3O_5S$: C, 60.61; H, 6.99; N, 8.84. Found: C, 60.64; H, 6.95; N, 8.65.

For-Met-Cpg-Phe-OMe (10). From Boc-Met-Cpg-Phe-OMe (0.06 g, 0.11 mmol) in CH_2Cl_2 according to the general procedure for preparation of the *N*-formyl derivatives. Silica gel flash chromatography (EtOAc/$CHCl_3$ 7:3) gave the pure product as a colourless oil (0.05 g, 98%); IR ($CHCl_3$): ν 3411, 1742, 1670 cm^{-1}; ^1H NMR ($CDCl_3$): δ 1.90-2.11 [5H, m, Met β-CH_2 and S-CH_3 (s at 2.11)], 2.45-2.63 (2H, m, Met γ-CH_2), 2.71-2.98 (4H, m, two CH_2-CH=CH), 3.08 and 3.17 (2H, A and B of an ABX, *J* = 5.6, 6.8 and 14.0 Hz, Phe β-CH_2), 3.74 (3H, s, $COOCH_3$), 4.64 (1H, m, Met α-CH), 4.83 (1H, m, Phe α-CH) 5.71 (2H, m, CH=CH), 6.57 (1H, d, *J* = 7.6 Hz, Met NH), 6.61 (1H, d, *J* = 7.6 Hz, Phe NH), 7.08-7.34 (6H, m, aromatics and Cpg NH), 8.13 (1H, s, HCO). Anal. Calcd for $C_{25}H_{29}N_3O_5S$: C, 59.34; H, 6.53; N, 9.39. Found: C, 59.01; H, 6.55; N, 9.42.

2.4.5.3 Biological assays

Cell preparation

Cells were obtained from the blood of healthy subjects, and human peripheral blood neutrophils were purified by using the standard techniques of dextran (Pharmacia, Uppsala, Sweden)

sedimentation, centrifugation on Ficoll-Paque (Pharmacia), and hypotonic lysis of contaminating red cells. Cells were washed twice and resuspended in Krebs-Ringer phosphate (KRPG), pH 7.4, at final concentration of 50 x 10^6 cells/mL and kept at room temperature until used. Neutrophils were 98-100% viable, as determined using the Trypan Blue exclusion test. The study was approved by the local Ethics Committee and informed consent was obtained from all participants.

Random locomotion

Random locomotion was performed with 48-well microchemotaxis chamber (Bio Probe, Milan, Italy) and migration into the filter was evaluated by the leading-front method.[96] The actual control random movement is 35 ± 3 μm SE of 10 separate experiments performed in duplicate.

Chemotaxis

Each peptide was added to the lower compartment of the chemotaxis chamber. Peptides were diluted from a stock solution with KRPG containing 1 mg/mL of bovine serum albumin (BSA; Orha Behringwerke, Germany) and used at concentrations ranging from 10^{-12} to 10^{-5} M. Data were expressed in terms of chemotactic index (CI), which is the ratio (migration toward test attractant minus migration toward the buffer/migration toward the buffer); the values are the mean of

six separate experiments performed in duplicate. Standard errors are in the 0.02-0.09 CI range.

Superoxide anion (O_2^-) production

This anion was measured by the superoxide dismutase-inhibitable reduction of ferricytochrome *c* (Sigma, USA) modified for microplate-based assays. Tests were carried out in a final volume of 200 mL containing 4 x 10^5 neutrophils, 100 nmoles cytochrome *c* and KRPG. At zero time different amounts (10^{-10} -8 x 10^{-5} M) of each peptide were added and the plates were incubated into a microplate reader (Ceres 900, Bio-TeK Instruments, Inc.) with the compartment temperature set at 37 °C. Absorbance was recorded at 550 and 468 nm. The difference in absorbance at the two wavelengths was used to calculate nmoles of O_2^- produced using an absorptivity for cytochrome *c* of 18.5 mM^{-1} cm^{-1}. Neutrophils were incubated with 5 μg/mL cytochalasin B (Sigma) for 5 min prior to activation by peptides. Results were expressed as net nmoles of O_2^- per 1 x 10^6 cells per 5 min and are the mean of six separate experiments performed in duplicate. Standard errors are in 0.1-4 nmoles O_2^- range.

Enzyme assay

The release of neutrophil granule enzymes was evaluated by determination of lysozyme activity, modified for microplate-based assays. Cells, 3 x 10^6/well, were first incubated in

triplicate wells of microplates with 5 μg/mL cytochalasin B at 37 °C for 15 min and then in the presence of each peptide at a final concentration of 10^{-10} -8 x 10^{-5} M for a further 15 min. The plates were then centrifuged at 400 x g for 5 min and the lysozyme was quantified nephelometrically by the rate of lysis of cell wall suspension of Micrococcus lysodeikticus. The reaction rate was measured using a microplate reader at 465 nm. Enzyme release was expressed as a net percentage of total enzyme content released by 0.1% Triton X-100. Total enzyme activity was 85 ± 1 mg per 1 x 10^7 cells/min. The values are the mean of five separate experiments done in duplicate. Standard errors are in the range of 1-6%.

2.5 X-ray crystal structure and conformation of *N*-(*tert*-butyloxycarbonyl)-L-methionyl-(1-aminocyclo-pent-3-ene-1-carbonyl)-L-phenylalanine methylester (Boc^0-Met^1-Cpg^2-Phe^3-OMe)*

Owing to the capacity to induce conformational restrictions and stability towards enzymatic degradation to peptides, the replacement of natural α-amino acids with synthetic C^α-tetrasubstitued (quaternary) residues is the object of considerable attention in the design of synthetic peptides suitable for the use as therapeutical agents.[112-114] Since the conformational restrictions imposed by C^α-tetrasubstitued

*Mura, P.; Camalli, M.; Campi, G.; Lucente, G.; Giordano, C.; Mollica, A.; Sansone, A.; Torino, D. *Z. Kristallogr.* **2009**, *224*, 225.

residues on peptide backbones vary and generally increase when the quaternary α-carbon atom makes part of a ring structure (as compared with models containing two free-rotating side chains at the C^{α}-atom), synthetic α-aminoacidic residues, such as 1-aminocycloalkane-1-carboxylic acids (Ac_nc)[115-117] and related heterocyclic counterparts,[113, 118] are the object of special interest.

Here we report the structure and conformation adopted in the crystal by a position-2 modified analogue of the antagonistic chemotactic agent *N*-Boc-Met-Leu-Phe-OMe.[100] In the model under study (Figure 13) the native central Leu has been replaced by the achiral 1-aminocyclopent-3-ene- 1-carboxylic acid (Cpg), the unsaturated analogue of the extensively studied Ac_5c residue. It is worth noting here that, whereas the conformational consequences of the incorporation in the peptide skeleton of Ac_nc residues and related heterocyclic ring strucures have been extensively studied,[50,105,115-118] data on organic compounds, including peptides, containing the synthetic 5-membered-ring cycloalkenic Cpg residue are very scarce.[72,104] The here reported structure gives the first information on the conformation adopted

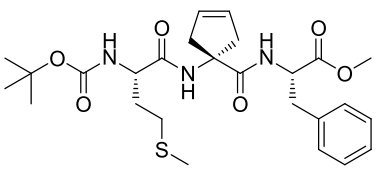

Figure 13. Chemical structure of the title tripeptide derivative Boc-Met-Cpg-Phe-OMe.

in the crystal by a Cpg containing tripeptide model. Synthesis, preferred conformation in $CDCl_3$ solution and biological activity of the title compound Boc-Met-Cpg-Phe-OMe have been previously reported.[72]

2.5.1 Crystal state conformational analysis

The molecular structure of the peptide Boc-Met-Cpg-Phe-OMe together with the atom-labelling is reported in Figure 14.

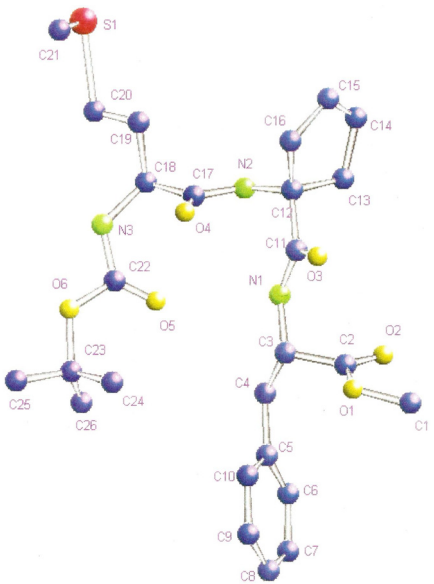

Figure 14. Geometry[126] of Boc-Met-Cpg-Phe-OMe, hydrogen atoms are omitted for clarity, thermal ellipsoids are drawn at 30% probability level.

Selected bond lengths (Å) and angles (°) are reported in Table 3. The backbone of the *N*-protected tripeptide adopts a folded β-turn conformation (Figure 15). The ϕ, ω dihedral angles (Table 4) relative to the Met (ϕ_{i+1} = -49.3° and ω_{i+1} =

142.6°) and Cpg (ϕ_{i+2} = 61.0° and ω_{i+2} = 32.8°) residues are in line with the values assigned to the two aminoacids occupying the central positions (*i* + 1 and *i* + 2) of a sequence of four residues which adopts an ideal type-II (see Figure 15) β-turn (ϕ_{i+1} = -60°, ω_{i+1} = 120°; ϕ_{i+2} = 80°, ω_{i+2} = 0).[119] The folding,

Table 3. Selected bond lengths (Å) and bond angles (°) in Boc-Met-Cpg-Phe-OMe (esd's are given in parentheses).

Bond lengths		N_1 — C_3	1.453(7)
O_6 — C_{23}	1.485(12)	C_3 — C_4	1.511(6)
O_6 — C_{22}	1.349(9)	C_3 — C_2	1.525(9)
C_{22} — N_3	1.342(9)		
N_3 — C_{18}	1.455(10)	Bond angles	
C_{17} — C_{18}	1.572(9)	C_{25} — C_{23} — O_6	102.4(9)
N_2 — C_{17}	1.344(10)	C_{23} — O_6 — C_{22}	121.4(5)
N_2 — C_{12}	1.433(8)	C_{12} — C_{16} — C_{15}	101.8(9)
C_{12} — C_{16}	1.575(8)	C_{13} — C_{12} — C_{16}	105.2(5)
C_{15} — C_{16}	1.471(10)	C_{14} — C_{15} — C_{16}	114.4(7)
C_{14} — C_{15}	1.284(13)	C_{13} — C_{14} — C_{15}	112.8(7)
C_{13} — C_{14}	1.504(9)	C_{12} — C_{13} — C_{14}	102.2(6)
C_{12} — C_{13}	1.542(11)	N_1 — C_3 — C_2	109.5(5)
C_{11} — C_{12}	1.540(7)	N_2 — C_{12} — C_{11}	110.8(4)
N_1 — C_{11}	1.324(7)	N_3 — C_{18} — C_{17}	108.4(5)

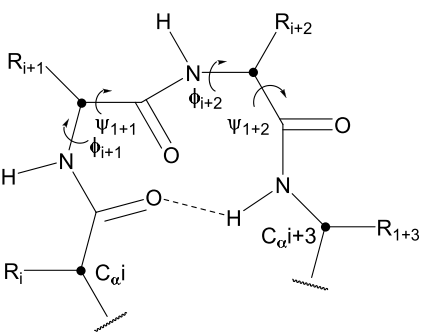

Figure 15. Schematic illustration of a peptide backbone folded in a *β*-turn (C10) structure. Torsion angles ϕ and ψ at the two corner residues *i* + 1 and *i* + 2 are shown. The dashed line indicates the (*i* + 3) → (*i*) NH···CO hydrogen-bond which frequently stabilizes the folding.

Table 4. Main torsion angles (°) of the tripeptide methyl ester Boc^0-Met^1-Cpg^2- Phe^3-OMe.

Backbone		
C_{18} — N_3 — C_{22} — O_6		168.5(6)
C_{23} — O_6 — C_{22} — N_3		-173.6(7)
C_{22} — N_3 — C_{18} — C_{17}	ϕ_{i+1}	-49.3(8)
N_2 — C_{17} — C_{18} — N_3	ψ_{i+1}	142.6(5)
C_{12} — N_2 — C_{17} — C_{18}	ω_1	170.6(5)
C_{17} — N_2 — C_{12} — C_{11}	ϕ_{i+2}	61.0(8)
N_1 — C_{11} — C_{12} — N_2	ψ_{i+2}	32.8(10)
C_3 — N_1 — C_{11} — C_{12}	ω_2	176.9(7)
C_{11} — N_1 — C_3 — C_2		-57.7(9)
O_1 — C_2 — C_3 — N_1		132.5(5)
C_1 — O_1 — C_2 — C_3		177.5(5)
Side chains Met		
N_3 — C_{18} — C_{19} — C_{20}	$\chi_{i+1}{}^1$	-54.3(12)
C_{18} — C_{19} — C_{20} — S_1	$\chi_{i+1}{}^2$	
C_{19} — C_{20} — S_1 — C_{21}	$\chi_1{}^3$	
Cpg		
N_2 — C_{12} — C_{16} — C_{15}	$\chi_2{}^1$	-99.3(7)
N_2 — C_{12} — C_{13} — C_{14}	$\chi_2{}^{1'}$	101.8(5)
C_{14} — C_{15} — C_{16} — C_{12}		-12.5(9)
C_{12} — C_{13} — C_{14} — C_{15}		11.1(8)
Phe		
N_1 — C_3 — C_4 — C_5	$\chi_3{}^1$	-178.2(5)
C_3 — C_4 — C_5 — C_6	$\chi_3{}^2$	-132.5(6)
C_3 — C_4 — C_5 — C_{10}	$\chi_3{}^{2'}$	49.1(8)
C_2 — C_3 — C_4 — C_5		61.6(6)
O_2 — C_2 — C_3 — N_1		-51.2(8)

which gives rise to a changement of the backbone direction of approximately 180° as compared with an extended conformation, is characterized by a weak electrostatic interaction between N_1 (the Phe NH) and the urethane carbonylic oxygen O_5 (Figure 15). This generates a ten-membered pseudo-ring system with the $N_1 \cdots O_5$ distance

(3.356(8) Å) which is slightly beyond the highest values observed in the statistical distribution (2.5-3.2 Å) of the intramolecular bond distances.[120] The degree of the backbone folding can be also evaluated by considering the distance separating the C^{α} carbon atoms of the first (*i*) and the fourth (*i* + 3) residue which, in standard β-turns, does not exceed 7 Å.[121] In the molecule under study the distance observed between O_6 (here replacing the C^{α}_{i}) and the Phe C^{α} carbon atom (C^{α}_{i+3}) is 5.49(1) Å in perfect accordance with a β-turn folding not accompanied by the $i + 3 \rightarrow i$ intramolecular H-bond.

As shown in Figure 15 and Table 4 the Met-Cpg (ω_1) and Cpg-Phe (ω_2) amide bonds are in the expected trans conformation. Whereas the Cpg-Phe junction is practically planar (ω_2 = 176.9°), the central Met-Cpg shows a sensible deviation from planarity (ω_1 = 170.6°). At the *N*-terminal moiety the torsion angles around the O_6-C_{22} and C_{22}-N_3 bonds (-173.6° and 168.5°, respectively) indicate that the urethane *tert*-Bu-O-CO-NH- chain adopts a slightly distorted type *b* *trans-trans* planar conformation[122] with the O_6-C_{23}-C_{25} valence angle (102.4°) (Table 3) smaller by about 7° than the tetrahedral value; both these findings are in accordance with the geometrical and conformational peculiarities derived from crystallographic investigations on peptides containing the *tert*-butyloxycarbonylamino group.[122] At the esterified *C*-terminus the carbonylic oxygen O_2 points toward the preceding Cpg

carbonyl O_3 with the planar CO-OMe methyl ester fragment adopting a gauche arrangement (the O_2-C_2-C_3-N_1 torsion angle being -51.2°).

The cyclopentene ring points toward the methionine side chain and adopts an envelope conformation (Cs) with the C^{α} carbon C_{12} displaced 0.309(8) Å from the plane of the other four ring atoms. Thus, a pseudo-mirror plane, bisecting the olefinic bond and passing through the carbon at the flap, can be individuated. Due to the constraint imposed by the unsaturated 5-membered ring all the endocyclic bond angles are significantly lower than the theoretical values. The highest deviation from the tetrahedral geometry is shown by the angle at C_{16} (101.8° versus 109.5°) while the two olefinic bond angles at C_{14} and C_{15} deviate of 5.6 and 7.2° respectively from the regular value of 120°.

Mention should be made of the value adopted by the exocyclic valence angle (τ angle) at the (C^{α} carbon atom C_{12}) of the Cpg residue. The analysis of the basic geometry of the amino acid residues of protein structures has demonstrated the almost invariability of all bond lengths and bond angles except for τ, the backbone angles at the C^{α} carbon atoms (N-C^{α}-C').[123] This latter angle can be widened or contracted significantly from the tetrahedral geometry to accomodate various strains in the structure and, owing to its dependence by the local backbone conformation, its deviation represents an useful parameter in

peptide and protein studies.[124] In the case of C^{α}-tetrasubstituted residues it is highly sensible to the type of the adopted local conformation and it is smaller than the tetrahedral value in the fully extended conformations (typical values: 102-107°). The opposite trend is observed in the folded conformations and the value here found (τ = 110.8(4)°; Table 3) for the Cpg residue, 1.3° larger than the tetrahedral value, corresponds to that typically adopted by the Ac_nc containing folded peptides.

2.5.2 Conclusions

The conformational analysis described here shows that the unusual synthetic amino acid Cpg maintains, when introduced into a peptide backbone, the strong tendency, characteristic of the C^{α}-tetrasubstituted residues, to induce folded conformations. This result appears of interest since, at variance with the saturated counterparts (i.e. residues of the Ac_nc type), the chemical reactivity offered by the olefinic bond present in the Cpg molecule, represents a suitable point of attack for a variety of chemical trasformations.

2.5.3 Experimental section

2.5.3.1 X-ray crystallography

A crystal of the *N*-(*tert*-butyloxycarbonyl)-L-methionyl-(1-aminocyclopent-3-ene-1-carbonyl)-L-phenylalanine methylester was sealed in a glass capillary. Diffraction data sets of the

crystal were collected at room temperature on the XRD1 beamline at the ELETTRA Synchrotron Light Laboratory (Trieste, Italy) by using a horizontal single axis goniostat diffractometer and a 165 mm MarResearch CCD X-ray detector positioned at 40 mm distance from the crystal; ϕ scans with 3° steps were performed to obtain the data. Diffraction data were processed and scaled by using the CCP4 program package.[125] Unit cell parameters were determined and refined from 15 frames and the data collection consisted of 120 frames. The structure was solved by direct methods and refined using Sir2008 (part of Il Milione suite).[126] Of the 34.513 reflections which were collected, 4851 were independent. All non-hydrogen atoms were refined by a full-matrix least squares method with anisotropic thermal parameters. The hydrogen atoms were idealized (C-H = 0.96 Å); each of them was assigned 1.3 of the equiv. isotropic temperature factor of the parent atom and allowed to ride on it. The final cycle of full-matrix least-squares refinement on F was based on 3433 observed reflections [$F > 3\sigma(F)$]; a final R factor of 0.102, wR = 0.111 and a goodness of fit of 0.84 have been obtained for 320 parameters. The final difference Fourier map, with a root-mean-square deviation of electron density of 0.04 e $Å^{-3}$ showed minimum and maximum values of -0.18 and 0.40, respectively. Crystal and data collection details together with structure refinement are summarized in Table 5.

Table 5. Crystal data and refinement of Boc-Met-Cpg-Phe-OMe.

Empirical formula	$C_{26}H_{37}N_3O_6S$
Formula weight	519.66
Crystal system	Monoclinic
Space group	$P2_1$ (No. 4)
a	5.867(7) Å
b	23.54(2) Å
c	10.34(1) Å
β	99.74(5)°
V	1407(2) $Å^3$
Z	2
D(calc)	1.227 $g \cdot cm^{-3}$
Absorption coefficient	0.145 mm^{-1}
F(000)	556
Crystal size	0.03 x 0.05 x 0.15 mm
Temperature (K)	293
Radiation (Å)	0.68880
Data collection range	$4.2° < \theta < 31.8°$
Index ranges	$0 \le h \le 8$; $0 \le k \le 35$; $-15 \le l \le 15$
Refl. Collected/Unique	34,514/4867 [*R*(int) = 0.07]
Completeness	91% (θ = 31.8°)
Refinement method	full-matrix, least-squares on *F*
Observed data	[$F > 3.0\sigma(F)$] 3433
Number of parameters	320
R, *wR*, GOF	0.1020, 0.1110, 0.84
Weight	$w = 1/(307.9798 + 1.00F_o + 0.00F_o^2$
Max. and Av. Shift/Error	0.12, 0.02
Largest diff. peak/hole	-0.18, 0.40 $e/Å^{-3}$

2.5.3.2 Synthesis

The synthesis is reported in the Ref. 72. Needle crystals were obtained by slow evaporation of an ethyl acetate solution, after four days, at room temperature.

2.6 Synthesis and bioactivity of chemotactic tetrapeptides: fMLF-OMe analogues incorporating spacer amino acids at the lateral positions*

Natural and synthetic chemoattractant *N*-formyl tripeptides continue to stimulate a great deal of interest due to their ability to bind to specific G-protein-coupled receptors (FPRs) primarily expressed on neutrophil and monocyte membranes. In addition to *N*-formyl tripeptides several FPR ligands of different origin and molecular structure have been identified over the past years. However, due to its simple structure and high agonistic potency *N*-formyl-Met-Leu-Phe-OH (fMLF) and its methyl ester (fMLF-OMe) remain the reference molecules for studies on peptidic chemoattractants derived from cleavage of bacterial or mitochondrial proteins.

Binding of *N*-formyl peptides to leucocyte FPRs activates a variety of cell functions including migration towards the inflammation sites, generation of free radicals and release of granule contents.

In addition to the above cited biochemical events, which concern the role played by FPR in the host defense against invading microorganisms, a further relevant point has been recently evidenced. Studies from several groups firmly establish in fact that the distribution of FPR is not limited to neutrophil and monocytes but is widely extended to different tissues and

*Lucente, G.; Giordano, C.; Sansone, A.; Torino, D.; Spisani, S. *Amino Acids* **2009**, *37*, 285.

organs.[39,127] Thus, it is now clear that the family of chemoattractant receptors, together with a variety of microbial and endogenous ligands, forms a complex system whose pathophysiological functions involve several and probably determinant roles in both inflammatory and immunological diseases. The above reported findings have enlarged the interest on *N*-formyl peptide chemoattractants well beyond the host defence against microbial infection and have underlined, at the same time, the relevance of FPRs as potential target for the development of new therapeutic strategies.[128] However, in spite of these data, several aspects concerning the structural basis of receptor/agonists interaction and the signalling mechanisms[100] still remain to be elucidated.[129]

Previous investigations based on fMLF backbone modification give clear evidence that the sulphur-containing *N*-terminal For Met-moiety and the aromatic side chain at the *C*-terminal position of the tripeptide are crucial for both binding and receptor activation. The central hydrophobic Leu, on the other hand, appears to be quite tolerant of modification[70] and several fMLF analogues modified at position-2 with high activity and selectivity have been described.[73,74] Finally, it is now well known that key interactions between ligands and FPRs involve in addition to the Met and Phe hydrophobic side chains specific hydrogen bonding established by the *N*-terminal formylic group. Relevant is the observation that modifications

centred at this function can modulate the neutrophil biological responses and open the way to FPR antagonists whose interest for the use in diagnostic and therapeutic applications is well known. In particular both urea and carbamate derivatized fMLF analogues, among which Boc-Met-Leu-Phe-OMe, containing the bulky *t*BuOCO (Boc) group in place the native H-CO (For), have been studied and found active as antagonists.[67,68]

In accordance with the observed versatility towards structural modifications at position-2 of fMLF we reported previously studies on *N*-For and *N*-Boc analogues characterized by the presence of linear achiral ω-amino acids as spacers, in place of the central Leu.[85] These tripeptides maintain the two native Met and Phe side chains but are characterized by different distances on the backbone between side chains at position-1 and position-3 depending upon the ω-amino acid residue used as spacer. As prosecution of these studies we report here the results of a new approach in which *N*-For and *N*-Boc tetrapeptidic analogues of fMLF-OMe are examined. At variance with previous approaches, the here reported analogues have been designed so as to maintain intact all the three native residues present in the reference ligand and to possess a backbone sequence altered by the presence of a spacer amino acid inserted between the Met and the Leu (tetrapeptide models of the Xaa^2 type) or between Leu and Phe (tetrapeptide models of Xaa^3 type) as depicted in Figure 16.

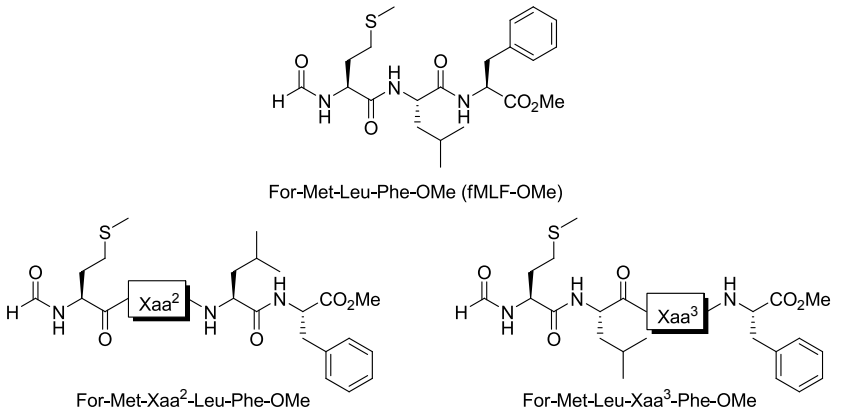

Figure 16. Structure of fMLF-OMe and its Xaa^2 and Xaa^3 tetrapeptide analogues reported in the present study. The spacer amino acid Xaa represents in all cases a residue of Gly, β-Ala or Pro.

The aim of this study is to get preliminary information on the consequences that the variation of the disposition and distance, relating the two critical side chains present in the native ligand, has on the interaction with the complementary pockets of the FPR receptor. In order to investigate this point three different spacers have been used. Two of these are the achiral and side chain devoid residues of Gly and β-Ala while the third is the chiral residue of Pro. This latter shares with the achiral Gly and β-Ala residues the absence of the characteristic side chain present in all natural amino acids and, under this aspect, can be related to Gly of which can be considered a ring-constrained analogue.

2.6.1 Chemistry

The synthesis of the *N*-Boc-tetrapeptides and the corresponding *N*-formyl derivatives was performed in solution according to the strategy reported in Schemes 6 and 7.

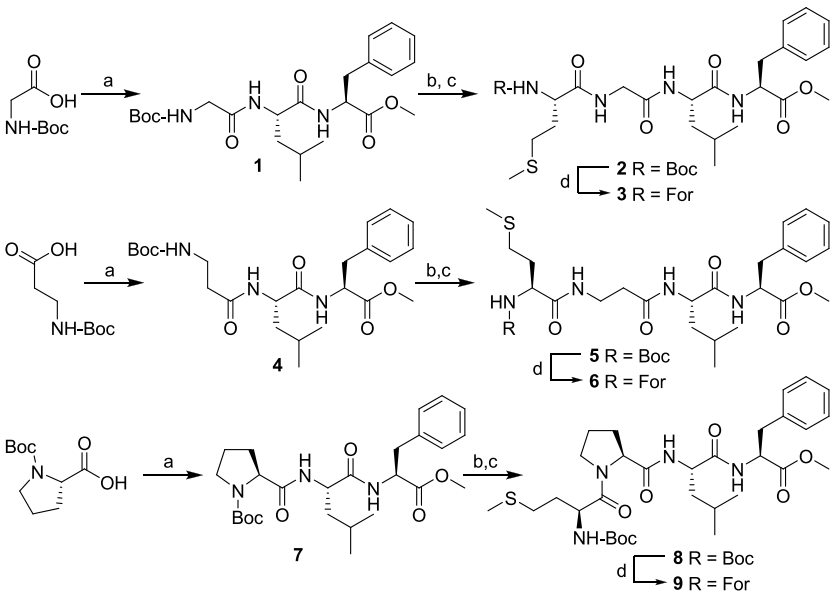

Scheme 6. Synthesis of *N*-protected tetrapeptides of the Xaa[2] type (**2-3**: Xaa = Gly; **5-6**: Xaa = β-Ala; **8-9**: Xaa = Pro). *Reagents and conditions*: a) TFA·H_2N-Leu-Phe-OMe, TEA, HOBt, EDC, dry EtOAc, 30 min 0 °C, 12h rt; b) TFA/CH_2Cl_2 1:1, 1h rt; c) Boc-Met-OH, HOBt, TEA, EDC, dry EtOAc, 30 min 0 °C, 12h rt; d) HCOOH, overnight rt then EEDQ, $CHCl_3$, 24h rt.

Analogues of the Xaa[2] type were obtained by coupling the *N*-Boc-Xaa-OH derivatives with the *N*-terminal dipeptide fragment thus giving the three tripeptides Boc-Xaa-Leu-Phe-OMe (**1**, **4** and **7**). These were then deprotected and coupled with Boc-Met-OH to give the three tetrapeptides Boc-Met-Xaa-Leu-Phe-OMe **2**, **5** and **8**.

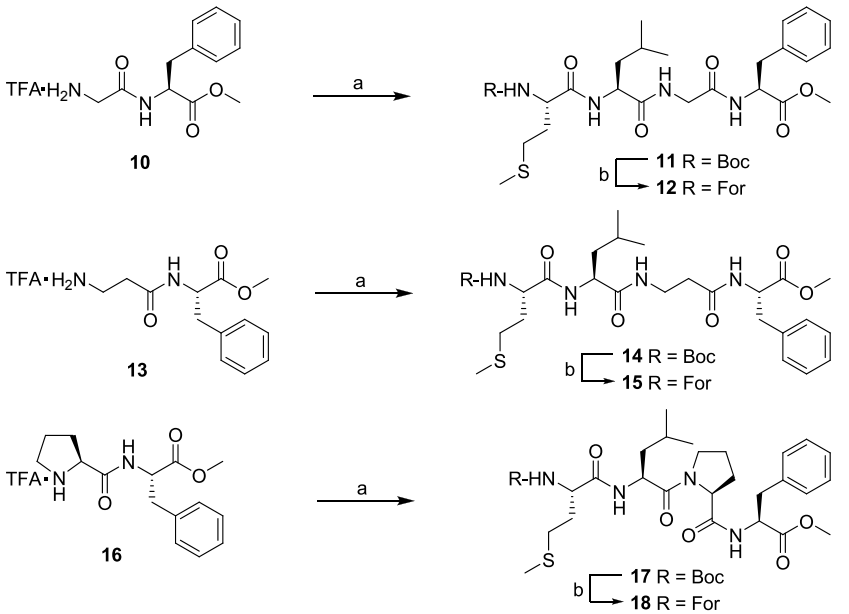

Scheme 7. Synthesis of *N*-protected tetrapeptides of the Xaa[3] type (**11-12**: Xaa = Gly; **14-15**: Xaa = β-Ala; **17-18**: Xaa = Pro). *Reagents and conditions*: a) Boc-Met-Leu-OH, HOBt, TEA, EDC, dry EtOAc; b) HCOOH, overnight rt then EEDQ, $CHCl_3$, 24h rt.

A different strategy was adopted for the synthesis of the Xaa[3] models (see Scheme 7) where the three dipeptide derivatives Boc-Xaa-Phe-OMe were firstly synthesized; *N*-deprotection to **10**, **13** and **16** was followed by coupling with the common dipeptide fragment Boc-Met-Leu-OH to give the tetrapeptides *N*-Boc-Met-Leu-Xaa-Phe-OMe **11**, **14** and **17**. Direct transformation of all the *N*-Boc derivatives (Schemes 6, 7) into the corresponding *N*-formyl analogues **3**, **6**, **9**, **12**, **15** and **18** was performed by treatment of each *N*-Boc derivative with formic acid and then with EEDQ.[92]

2.6.2 Biological results

The activity of the *N*-For and *N*-Boc tetrapeptide derivatives reported in Schemes 6 and 7 has been determined on human neutrophils. Directed migration (chemotaxis), superoxide anion production and lysozyme release have been measured. In the first set of experiments (see Figures 17, 18) the agonistic activity was measured and compared to that of the standard tripeptide fMLF-OMe. In the second set (see Figures 19, 20) the antagonistic activity of the *N*-Boc tetetrapeptides, which have been found inactive as agonists, have been examined as antagonists by measuring their ability to inhibit the effect stimulated by an optimal dose of fMLF-OMe.

As shown in Figures 17A and 18A all the *N*-For tetrapeptide analogues maintain moderate to high capacity to induce chemotaxis with dose-response curves showing an optimal concentration value around 10^{-9} M. The three models of Xaa^2 type Gly^2 (**3**), β-Ala^2 (**6**) and Pro^2 (**9**) (Figure 17A) exhibit moderate activity and very similar behaviour with the Pro^2 model **9** with about the same potency but with lower efficiency (peptide concentration at which maximal activity is observed) than the β-Ala^2 (**6**) and Gly^2 (**3**). The activity of the Xaa^3 type analogues, on the other hand, is greatly influenced by the nature of the spacer residue (Figure 18A). Thus, while the tetrapeptide **15**, containing β-Ala as spacer, is a very potent chemotactic agent-nearly as active as the reference molecule-compound **12**,

containing Gly as spacer, is only moderately active with a maximum value comparable to those shown by the models of the Xaa^2 type.

Figures 17B and 18B illustrate the ability of the Xaa^2 and Xaa^3 models, respectively, to trigger superoxide anion production. Also in this case all tetrapeptides maintain moderate to good activity with values of 50 and 53 nmoles at 10^{-6} M for β-Ala containing models **6** (Figure 17B) and **15** (Figure 18B), respectively. Notable is also the dose-response curve exhibited by the Pro^3 tetrapeptide **18** (Figure 17B) with a peak value of 56 nmoles at concentration 10^{-5} M. This result is opposite to that observed in the Xaa^2 series where the Pro^2 incorporation produces the least active model (compound **9** in Figure 17B).

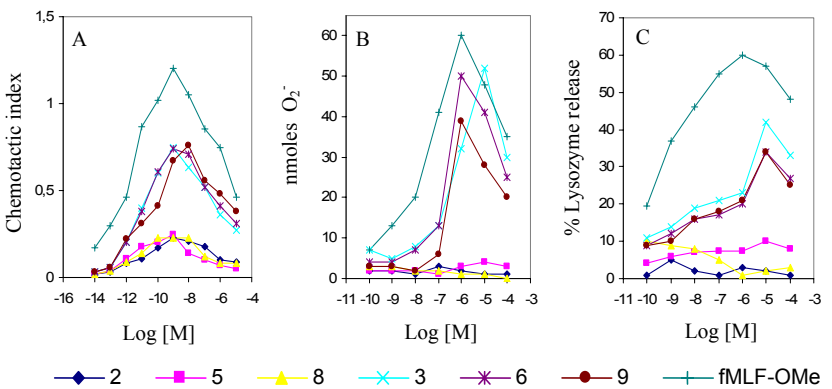

Figure 17. Biological activity towards human neutrophils of *N*-For (**3**, **6** and **9**) and *N*-Boc (**2**, **5** and **8**) tetrapeptide analogues of Xaa^2 type (see Scheme 6) compared with the reference ligand fMLF-OMe. (**A**) Chemotactic index; (**B**) Superoxide anion production; (**C**) Release of granule enzymes evaluated by determining lysozyme release. Points are single representative experiments carried in duplicate

As for the enzyme secretagogue activity (Figures 17C, 18C) all the tetrapeptides show dose-response curves with the same maximum value centred at 10^{-5} M and lysozyme release moderately higher in the Xaa^3 series, with values ranging between 46-49% and 34-42% for the Xaa^3 and Xaa^2 models, respectively.

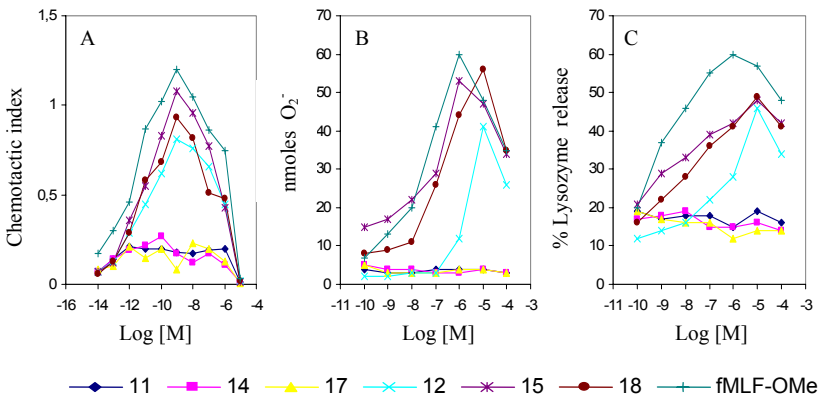

Figure 18. Biological activity towards human neutrophils of *N*-For (**12**, **15** and **18**) and *N*-Boc (**11**, **14** and **17**) tetrapeptide analogues of Xaa^3 type (see Scheme 7) compared with the reference ligand fMLF-OMe. (**A**) Chemotactic index; (**B**) Superoxide anion production; (**C**) Release of granule enzymes evaluated by determining lysozyme release. Points are single representative experiments carried in duplicate

As shown in Figures 17 and 18 the agonistic activity values shown by the *N*-Boc derivatives, regardless the nature of the spacer residue and its location on the backbone, are not statistically significant for all the three biological functions tested. These compounds have been examined as antagonists by measuring their ability to inhibit the effect stimulated by an optimal dose of the reference peptide fMLF-OMe. The influence

of increasing concentrations of *N*-Boc tetrapeptides of Xaa^2 type (Gly^2: **2**; β-Ala^2: **5**; Pro^2: **8**) and Xaa^3 type (Gly^3: **11**; β-Ala^3: **14**; Pro^3: **17**) on the three examined functional acivities are reported in Figures 19 and 20, respectively. It can be seen that the *N*-Boc tetrapeptides of both the series exert significant dose-dependent inhibition (50% ca. at 10^{-9} M) of the CI with a similar profile of activity (Figures 19A, 20A). Conversely, no significant inhibition is observed for the *N*-Boc tetrapeptides on both the superoxide anion production (Figures 19B, 20B) and lysozyme release (Figure 20C), except a very weak effect shown by the Xaa^2 tetrapeptides on lysozyme release (Figure 19C) where a 50% inhibition is reached only at high concentrations (10^{-6} to 10^{-5} M).

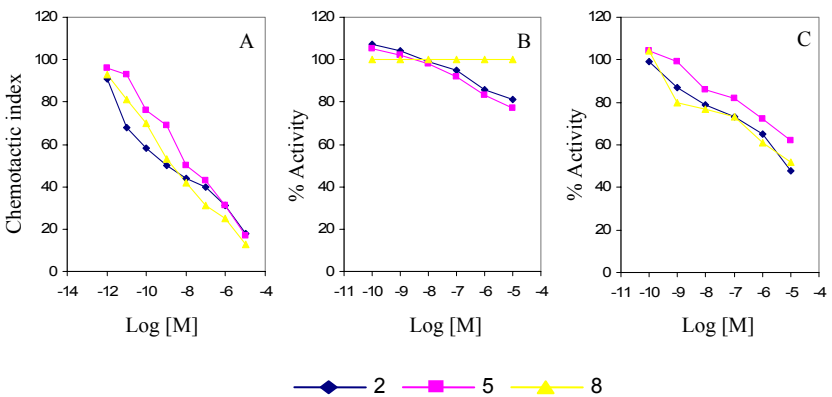

Figure 19. Effect of *N*-Boc tetrapeptides of Xaa^2 type (Gly^2: **2**; β-Ala^2: **5**; Pro^2: **8**) on human neutrophil activities triggered by fMLF-OMe. (**A**) Chemotactic index; (**B**) Superoxide anion production; (**C**) Release of granule enzymes.

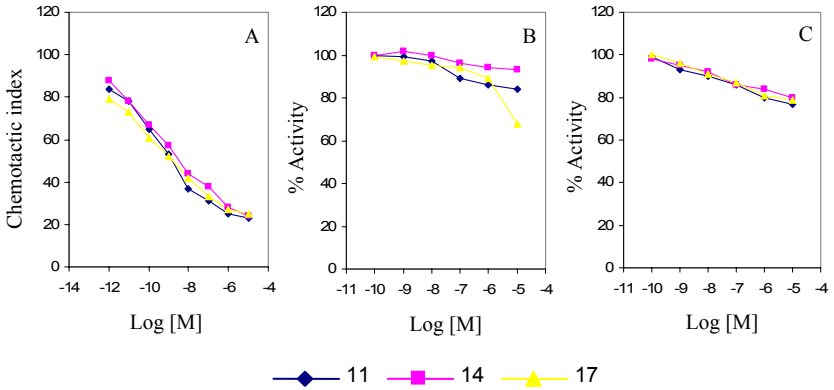

Figure 20. Effect of *N*-Boc tetrapeptides of Xaa^3 type (Gly^3: **11**; β-Ala^3: **14**; Pro^3: **17**) on human neutrophil activities triggered by fMLF-OMe. (**A**) Chemotactic index; (**B**) Superoxide anion production; (**C**) Release of granule enzymes.

2.6.3 Conclusions

The results reported here give for the first time information on the properties of a series of tetrapeptidic fMLF-OMe analogues obtained by performing incorporation of spacer residues in the molecule of the reference ligand and leaving at the same time intact the original stereochemistry and succession on the backbone of the three native amino acid residues of the reference ligand. This approach differs from previously reported studies in which one or more residues of fMLF have been replaced.[129] As shown in Figures 17A and 18A all *N*-For tetrapeptides maintain the ability to elicit high to moderate values of chemotaxis. However, when the chemotatic index of the two series of tetrapeptides is compared two points can be evidenced: (1) the incorporation of the Xaa^2 spacer between the

Met and Leu (Figure 17A is generally more detrimental for the activity than the corresponding Xaa^3 modification involving Leu and Phe (Figure 3A). Remarkable is the activity shown by the β-Ala^3 containing model **15** (Figure 18A) which reaches an activity comparable to that of fMLF-OMe; (2) at variance with Xaa^3 series, the nature of the incorporated spacer does not affect appreciably the activity of Xaa^2 models which exhibit very close dose-response curves (Figure 17A). Only the Pro^2 analogue **9** shows a slightly different behaviour with a peak of activity centred at higher concentration than the Gly^2 **3** and β-Ala^2 **6** models. This effect can be related to the well known influence of the Pro residue on hydrogen bonding and backbone conformation. On the basis of these findings it can be speculated that the Met and Leu binding pockets on the receptor are more critically related and probably more nearly located than those relating Leu and Phe. The sensibly higher chemotactic activity of the β-Ala^3 analogue **15**, as compared with the corresponding Gly^3 containing model **12** (Figure 18A), seems in accordance with this preliminary interpretation.

With regard to the superoxide anion production (Figures 17B, 18B) it can be noted the general good agonist activity shown by both the Xaa^2 and Xaa^3 series of analogues as compared with the only modest activity exhibited by the same models for the lysozyme release (Figures 17C, 18C). It can be observed here that the best results are obtained with the β-Ala containing

models in both the Xaa^2 and Xaa^3 series (model **6** and **15** in Figure 17B, 18B, respectively). Thus, the incorporation of the β-Ala residue at position 3 leads to tetrapeptide ligands with high activity for both chemotaxis and generation of reactive oxygen species. These findings stimulate further research on fMLF-OMe analogues obtained through incorporation of β-residues and in particular of achiral higher homologues of β-Ala. Models of this type, designed according the results reported in Figures 17B and 18A-B, appear in fact well suited to give highly active new tetrapeptides as well as information on the interaction with receptor hydrophobic pockets.

As shown in Figures 17 and 18 the presence of the bulky *N*-Boc protecting group does not modify the expected inactivity as agonists of the new analogues. These compounds have been then tested as antagonists. Figures 19 and 20 clearly show that the incorporation of a spacer gives rise, almost regardless the nature of the incorporated amino acid residue and its position on the backbone, to ligands characterized by relevant inhibition against migratory activity (Figures 19A, 20A). A different result is observed in the case of the other two biological functions tested (Figures 19B-C, 20B-C) where all the performed modifications do not produce appreciable inhibitory effects at physiological concentrations. Thus, the elongation of the fMLF-OMe backbone, through spacer incorporation at the two lateral positions, combined with the presence of a bulky *N*-protecting

group, leads to effective antagonists which can be selective for the chemotactic function.

Taken together the here reported results indicate that the adopted approach of modification of the prototype of the family of chemotactic peptides gives rise to an articulate picture of data which represent a promising basis for the study of the FPR receptor and for the design of new ligands with both agonistic and selective antagonistic activity.

2.6.4 Experimental section

Materials and methods. Melting points were determined with a Büchi B 540 apparatus and are uncorrected. Optical rotations were taken at 20 °C with a Schmidt-Haensch Polartronic D polarimeter (1 dm cell, *c* 1.0 in $CHCl_3$, unless otherwise specified). IR spectra were recorded in 1% $CHCl_3$ solution (unless otherwise specified) employing a Perkin-Elmer FT-IR Spectrum 1000 spectrometer. ^1H NMR experiments were performed at 400 MHz on a Bruker AM 400 spectrometer in $CDCl_3$ solution and chemical shifts (δ) are quoted in parts per million (ppm) and were indirectly referred to TMS. TLC (thin layer chromatography) were performed on silica gel Merck 60 F_{254} plates. The drying agent was sodium sulphate. Elemental analyses were performed in the laboratories of the Servizio Microanalisi del CNR, Area della Ricerca di Roma,

Montelibretti, Italy, and were within ±0.4% of the theoretical values.

Protected amino acids were purchased from Bachem and Fluka. Coupling and *N*-Boc deprotection procedures were performed according general protocols[130] and checked for purity by TLC, HPLC and elemental analysis. *N*-Formylation was attained starting from the corresponding *N*-Boc derivatives.[92]

2.6.4.1 Chemistry. General procedure

A. Coupling with the carbodiimide method. To an ice-cooled mixture containing the required *N*-Boc-amino acid (1.0 mmol), the amino-derivative salt (1.0 mmol), HOBt (1.2 mmol), and TEA (2.2 mmol) in anhydrous EtOAc (6 mL), EDC (1.2 mmol) was added and the reaction mixture was allowed to warm to room temperature. After 12 h the reaction mixture was diluted with EtOAc (20 mL) and washed with 1M $KHSO_4$ (2 x 15 mL), saturated aqueous $NaHCO_3$ (2 x 15 mL) and brine (15 mL). The organic phase was dried and evaporated under reduced pressure.

B. Preparation of the *N*-formyl derivatives. The *N*-Boc derivative (1.0 mmol) was dissolved in formic acid (3 mL) and the mixture was allowed to stand at room temperature overnight. After removal of the excess formic acid under vacuum, the residue was dissolved in

dry CH_2Cl_2 (10 mL) or dry DMF (2 mL). EEDQ 97% (1.2 mmol) was added and the solution was stirred at room temperature for 24 h. Evaporation under reduced pressure afforded the crude *N*-formyl derivatives.[92]

2.6.4.2 Synthesis

Boc-Met-Gly-Leu-Phe-OMe (2). From Boc-Met-OH (0.058 g, 0.23 mmol) and TFA·H_2N-Gly-Leu-Phe-OMe (0.107 g, 0.23 mmol)[131] according to the general procedure A. Crystallization from hexane gave the pure product as white solid (0.100 g, 75%); mp 134.3-136.5°C; $[a]_D$ +2.0° (*c* 1, $CHCl_3$); IR ($CHCl_3$): ν 3421, 1710, 1676 cm^{-1}; ^1H NMR ($CDCl_3$): δ 0.87-0.90 [6H, m, Leu CH-(C*H*$_3$)$_2$], 1.45 [9H, s, C(CH_3)$_3$], 1.48-1.93 [5H, m, Met β-CH_2 and Leu C*H*$_2$-C*H*-(CH_3)$_2$], 2.12 (3H, s, SCH_3), 2.57 (2H, m, Met γ-CH_2), 3.01 and 3.18 (2H, A and B of an ABX, *J* = 6.0, 5.6 and 14.0 Hz, Phe β-CH_2), 3.71 (3H, s, $COOCH_3$), 3.78-3.99 (2H, m, Gly α-CH_2), 3.98 (1H, m, Met α-CH), 4.44 (1H, m, Leu α-CH), 4.83 (1H, m, Phe α-CH), 5.37 (1H, d, *J* = 7.6 Hz, Met NH), 6.74 (2H, m, Phe NH and Leu NH), 6.96 (1H, br s, Gly NH), 7.12-7.29 (5H, m, aromatics). Anal. Calcd for $C_{28}H_{44}N_4O_7S$: C, 57.91; H, 7.64; N, 9.65. Found: C, 58.14; H, 7.61; N, 9.68.

For-Met-Gly-Leu-Phe-OMe (3). From Boc-Met-Gly-Leu Phe-OMe (0.1 g, 0.17 mmol) according to the general procedure B. Crystallization from EtOAc/Hexane. White solid (0.080 g,

93%); mp 175-177.9 °C; $[a]_D$ +2.0° (*c* 1, $CHCl_3$); IR ($CHCl_3$): ν 3671, 3426, 1652 cm^{-1}; ^1H NMR ($CDCl_3$): δ 0.87-0.90 [6H, m, Leu CH-(C*H*$_3$)$_2$], 1.48-1.93 [5H, m, Met β-CH_2 and Leu C*H*$_2$-C*H*-$(CH_3)_2$], 2.12 (3H, s, SCH_3)], 2.57 (2H, m, Met γ-CH_2), 3.01 and 3.18 (2H, A and B of an ABX, *J* = 6.3, 5.6, 13.8 Hz, Phe β-CH_2), 3.71 (3H, s, $COOCH_3$), 3.78-3.99 (2H, m, Gly α-CH_2), 4.30 (1H, m, Met α-CH), 4.44 (1H, m, Leu α-CH), 4.83 (1H, m, Phe α-CH), 5.37 (1H, d, *J* = 8.0 Hz, Met NH), 6.74 (2H, m, Phe NH and Leu NH), 6.96 (1H, br s, Gly NH), 7.12-7.29 (5H, m, aromatics), 8.04 (1H, s, HCO). Anal. Calcd for $C_{24}H_{36}N_4O_6S$: C, 56.67; H, 7.13; N, 11.02. Found: C, 56.81; H, 7.16; N, 11.05.

Boc-β-Ala-Leu-Phe-OMe (4). From Boc-β-Ala-OH (0.080 g, 0.42 mmol) and TFA·H_2N-Leu-Phe-OMe (0.170 g, 0.42 mmol) according to the general procedure A. The title compound was obtained as a white solid, pure on TLC (0.170 g, 87%); $[a]_D$ -7.0° (*c* 1, $CHCl_3$); IR ($CHCl_3$): ν 3427, 3011, 1741, 1631 cm^{-1}; ^1H NMR ($CDCl_3$): δ 0.89-0.98 [6H, m, Leu CH-(C*H*$_3$)$_2$], 1.47 [9H, s, $C(CH_3)_3$], 1.77-1.88 [5H, m, Leu C*H*$_2$-C*H*-$(CH_3)_2$ and β-Ala α-CH_2], 2.90 and 3.15 (2H, A and B of an ABX, *J* = 6.1, 5.6 and 14.0 Hz, Phe β-CH_2), 3.20-3.50 (2H, m, β-Ala β-CH_2), 3.70 (3H, s, $COOCH_3$), 4.50 (1H, m, Leu α-CH), 4.75 (1H, m, Phe α-CH), 5.20 (1H, d, *J* = 7.2 Hz, β-Ala NH), 6.20 (1H, d, *J* = 7.6 Hz, Phe NH), 6.75 (1H, d, *J* = 7.3 Hz, Leu

NH), 7.01-7.45 (5H, m, aromatics). Anal. Calcd for $C_{24}H_{37}N_3O_6$: C, 62.18; H, 8.04; N, 9.06. Found: C, 62.33; H, 8.07; N, 9.09.

Boc-Met-β-Ala-Leu-Phe-OMe (5). From Boc-Met-OH (0.0645 g, 0.26 mmol) and TFA·H_2N-β-Ala-Leu-Phe-OMe (0.123 g, 0.26 mmol), this latter obtained from deprotection of Boc-β-Ala-Leu-Phe-OMe, according to the general procedure A. Colourless oil (0.170 g, 87%); mp 133.5-135 °C; $[a]_D$ +42° (*c* 1, $CHCl_3$); IR ($CHCl_3$): ν 3427, 1741, 1631 cm^{-1}; ^{1}H NMR ($CDCl_3$): δ 0.85-0.91 [6H, m, Leu CH-(C*H*$_3$)$_2$], 1.45 [9H, s, C(CH_3)$_3$], 1.53-1.66 [3H, m, Leu C*H*$_2$-C*H*-(CH_3)$_2$], 1.68-1.84 (2H, m, Met β-CH_2), 2.10 (3H, s, SCH_3), 2.28-2.51 (4H, m, β-Ala α-CH_2 and γ-Met CH_2), 3.04-3.19 (3H, m, β-Ala β-C*H*H and Phe β-CH_2), 3.75 (3H, s, $COOCH_3$), 3.85-3.90 (2H, m, β-Ala β-C*H*H and Met α-CH), 4.37 (1H, m, Leu α-CH), 4.99 (1H, m, Phe α-CH), 5.21 (1H, d, *J* = 8.0 Hz, Met NH), 6.68-6.72 (2H, m, Phe NH and Leu NH), 7.14-7.26 (5H, m, aromatics), 7.66 (1H, apparent t, β-Ala NH). Anal. Calcd for $C_{29}H_{46}N_4O_7S$: C, 58.56; H, 7.80; N, 9.42. Found: C, 58.79; H, 7.83; N, 9.44.

For-Met-β-Ala-Leu-Phe-OMe (6). From Boc-Met-β-Ala-Leu-Phe-OMe (0.1 g, 0.168 mmol) according to the general procedure B. Crystallized from hexane. White solid (0.050 g, 57%); mp 157.7-161.3 °C. $[a]_D$ -16.0° (*c* 1, $CHCl_3$); IR ($CHCl_3$): ν 3671, 3424, 1734, 1670 cm^{-1}; ^{1}H NMR ($CDCl_3$): δ 0.85-0.91 [6H, m, Leu CH-(C*H*$_3$)$_2$], 1.53-1.66 (3H, m, Leu C*H*$_2$-C*H*-

(CH_3)$_2$, 1.68-1.84 (2H, m, Met β-CH_2), 2.10 (3H, s, SCH_3), 2.28-2.51 (4H, m, β-Ala α-CH_2 and Met γ-CH_2), 3.04-3.19 (3H, m, β-Ala β-C*H*H and Phe β-CH_2), 3.75 (3H, s, $COOCH_3$), 3.85-3.90 (2H, m, β-Ala β-C*H*H and Met α-CH), 4.37 (1H, m, Leu α-CH), 4.99 (1H, m, Phe α-CH), 5.21 (1H, d, *J* = 8.0 Hz, Met NH), 6.68-6.72 (2H, m, Phe NH and Leu NH), 7.14-7.26 (5H, m, aromatics), 7.66 (1H, br s, β-Ala NH), 8.01 (1H, s, HCO). Anal. Calcd for $C_{25}H_{38}N_4O_6S$: C, 57.45; H, 7.33; N, 10.72. Found: C, 57.58; H, 7.30; N, 10.74.

Boc-Pro-Leu-Phe-OMe (7). From Boc-Pro-OH (0.07 g, 0.325 mmol) and TFA·H_2N-Leu-Phe-OMe (0.132 g, 0.325 mmol) according to the general procedure A. White foam, pure on TLC (0.160 g, 90%); [a]$_D$ -49.05° (*c* 1, $CHCl_3$); IR ($CHCl_3$): ν 3422, 1760, 1676 cm^{-1}; ^{1}H NMR ($CDCl_3$): δ 0.87-0.98 [6H, m, Leu CH-(C*H*$_3$)$_2$], 1.51 [9H, s, C(CH_3)$_3$], 1.70-2.50 [(8H, m, Pro β-CH_2, Pro γ-CH_2, Pro δ-C*H*H, and Leu C*H*$_2$-C*H*-(CH_3)$_2$)], 3.10-3.30 (2H, m, Phe β-CH_2), 3.30-3.50 (1H, m, Pro δ-C*H*H), 3.70 (3H, s, $COOCH_3$), 4.30-4.60 (3H, m, Pro α-CH, Leu α-CH and Phe α-CH), 6.50-6.70 (2H, m, Leu NH and Phe NH), 7.01-7.50 (5H, m, aromatics). Anal. Calcd for $C_{26}H_{39}N_3O_6$: C, 63.78; H, 8.03; N, 8.58. Found: C, 63.52; H, 8.01; N, 8.54.

Boc-Met-Pro-Leu-Phe-OMe (8). From Boc-Met-OH (0.0676 g, 0.27 mmol) and TFA·HN-Pro-Leu-Phe-OMe (0.110 g, 0.27 mmol), this latter obtained from Boc-Pro-Leu-Phe-OMe,

according to the general procedure A. Silica gel chromatography (CH_2Cl_2/MeOH 98:2) and crystallization from EtOAc/Hexane gave the pure title product as a white solid (0.120 g, 70%); mp 112.5-114 °C; $[a]_D$ -42° (*c* 1, $CHCl_3$); IR ($CHCl_3$): ν 3419, 1741, 1676 cm^{-1}; ^1H NMR ($CDCl_3$): δ 0.88-0.97 [6H, m, Leu CH-(CH_3)$_2$], 1.48 [9H, s, $C(CH_3)_3$], 1.61-1.65 (4H, m, Pro β-CH_2 and Pro γ-CH_2), 1.84-2.14 [8H, m, Met β-CH_2, Leu CH_2-CH-$(CH_3)_2$ and SCH_3 (s at 2.13)], 2.30 (1H, m, Pro δ-CHH), 2.58 (2H, m, Met δ-CH_2), 3.10 and 3.21 (2H, A and B of an ABX, *J* = 6.0, 5.6 and 13.6 Hz, Phe β-CH_2), 3.64 (1H, m, Pro δ-CHH) 3.75 (3H, s, $COOCH_3$), 4.35 (1H, m, Met α-CH), 4.53 (1H, m, Pro α-CH), 4.63 (1H, m, Leu α-CH), 4.87 (1H, m, Phe α-CH), 5.30 (1H, d, *J* = 9.6 Hz, Met NH), 6.63 (1H, d, *J* = 6.8 Hz, Phe NH), 7.02 (1H, d, *J* = 7.6 Hz, Leu NH), 7.14-7.33 (5H, m, aromatics). Anal. Calcd for $C_{31}H_{48}N_4O_7S$: C, 59.98; H, 7.79; N, 9.02. Found: C, 60.15; H, 7.82; N, 9.05.

For-Met-Pro-Leu-Phe-OMe (9). From Boc-Met-Pro-Leu-Phe-OMe (0.08 g, 0.127 mmol) according to the general procedure B. The mixture was purified on silica gel chromatography ($CHCl_3$/MeOH 99:1). Colourless oil (0.068 g, 95%); $[a]_D$ -13.0° (*c* 1, $CHCl_3$); IR ($CHCl_3$): ν 3417, 1743, 1677 cm^{-1}; ^1H NMR ($CDCl_3$): δ 0.88-0.97 [6H, m, Leu CH-(CH_3)$_2$], 1.61-1.65 (4H, m, Pro β-CH_2 and Pro γ-CH_2), 1.84-2.14 [8H, m, Met β-CH_2, Leu CH_2-CH-$(CH_3)_2$ and SCH_3 (s at 2.13)], 2.30

(1H, br s, Pro δ-C*H*H), 2.58 (2H, m, Met δ-CH_2), 3.10 and 3.21 (2H, A and B of an ABX, *J* = 6.3, 5.7 and 13.5 Hz, Phe β-CH_2), 3.64 (1H, m, Pro δ-C*H*H) 3.75 (3H, s, $COOCH_3$), 4.35 (1H, m, Leu α-CH), 4.53 (1H, m, Pro α-CH), 4.63 (1H, m, Met α-CH), 4.87 (1H, m, Phe α-CH), 5.30 (1H, d, *J* = 8.2 Hz, Met NH), 6.63 (1H, d, *J* = 7.6 Hz, Phe NH), 7.02 (1H, d, *J* = 6.8 Hz, Leu NH), 7.14-7.33 (5H, m, aromatics), 8.03 (1H, s, HCO). Anal. Calcd for $C_{27}H_{40}N_4O_6S$: C, 59.10; H, 7.35; N, 10.21. Found: C, 59.29; H, 7.38; N, 10.25.

Boc-Met-Leu-Gly-Phe-OMe (11). From Boc-Met-Leu-OH (0.107 g, 0.297 mmol),[132] and TFA·N_2H-Gly-Phe-OMe **10** (0.104 g, 0.297 mmol), obtained from Boc-Gly-Phe-OMe,[133] according to the general procedure A. The mixture was purified on silica gel chromatography (CH_2Cl_2/EtOAc 2:8). White foam (0.121 g, 70%); $[a]_D$ +1.0° (*c* 1, $CHCl_3$); IR ($CHCl_3$): ν 3419, 1735, 1678 cm^{-1}; ^{1}H NMR ($CDCl_3$): δ 0.96-0.99 [6H, m, Leu CH-(C*H*$_3$)$_2$], 1.45 [9H, s, C(CH_3)$_3$], 1.55-1.69 [3H, m, Leu C*H*$_2$-C*H*-(CH_3)$_2$], 1.88-2.11 [5H, m, Met β-CH_2 and SCH_3 (s, at 2.09)], 2.55 (2H, m, Met γ-CH_2), 3.05 and 3.17 (2H, A and B of an ABX, *J* = 6.0, 5.6 and 14.0 Hz, Phe β-CH_2), 3.70 (3H, s, $COOCH_3$), 3.86-4.03 (2H, m Gly α-CH_2), 4.26 (1H, m, Met α-CH), 4.45 (1H, m, Leu α-CH), 4.85 (1H, m, Phe α-CH), 5.45 (1H, br s, Met NH), 6.98 (1H, d, *J* = 8.0 Hz, Leu NH), 7.03 (1H, d, *J* = 7.2 Hz, Phe NH), 7.12-7.29 (6H, m, aromatics and Gly

NH). Anal. Calcd for $C_{28}H_{44}N_4O_7S$: C, 57.91; H, 7.64; N, 9.65. Found: C, 58.14; H, 7.61; N, 9.68.

For-Met-Leu-Gly-Phe-OMe (12). From Boc-Met-Leu-Gly-Phe-OMe (0.07 g, 0.12 mmol) according to the general procedure B. The reaction mixture was purified on silica gel chromatography ($CHCl_3$/MeOH 95:5). White foam (0.059 g, 97%); $[a]_D$ +0.5° (*c* 0.7, $CHCl_3$); IR ($CHCl_3$): ν 3415, 1740, 1670 cm^{-1}; ^1H NMR ($CDCl_3$): δ 0.96-0.99 [6H, m, Leu CH-(C*H*$_3$)$_2$], 1.54-1.68 [3H, m, Leu C*H*$_2$-C*H*-$(CH_3)_2$], 1.87-2.11 [5H, m, Met β-CH_2 and SCH_3 (s, at 2.06)], 2.51 (2H, m, Met γ-CH_2), 3.03 and 3.18 (2H, A and B of an ABX, *J* = 6.0, 5.7 and 13.6 Hz, Phe β-CH_2), 3.71 (3H, s, $COOCH_3$), 3.96-4.20 (2H, m, Gly CH_2), 4.94 (1H, m, Met α-CH), 4.71 (1H, m, Leu α-CH), 4.86 (1H, m, Phe α-CH), 7.09-7.31 (6H, m, aromatics and Met NH), 7.42 (1H, br s, Phe NH), 7.62 (1H, br s, Gly NH), 7.75 (1H, br s, Leu NH), 8.14 (1H, s, HCO). Anal. Calcd for $C_{24}H_{36}N_4O_6S$: C, 56.67; H, 7.13; N, 11.02. Found: C, 56.84; H, 7.15; N, 11.05.

Boc-Met-Leu-β-Ala-Phe-OMe (14). From Boc-Met-Leu-OH (0.128 g, 0.354 mmol) and TFA·H_2N-β-Ala-Phe-OMe **13** (0.129 g, 0.354 mmol), this latter obtained from Boc-β-Ala-Phe-OMe,[85] according to the general procedure A. Amorphous solid, pure on TLC (0.155 g, 74%); $[a]_D$ +23.0° (*c* 1, $CHCl_3$); IR ($CHCl_3$): ν 3421, 1738, 1673 cm^{-1}; ^1H NMR ($CDCl_3$): δ 0.93-0.96 [6H, m, Leu CH-(C*H*$_3$)$_2$], 1.41 [9H, s, $C(CH_3)_3$], 1.48-1.70

[3H, m, Leu C*H*$_2$-C*H*-(CH$_3$)$_2$], 1.91-2.15 [5H, m, Met β-CH$_2$ and SCH$_3$ (s, at 2.12)], 2.30 (2H, m, β-Ala α-CH$_2$), 2.63 (2H, m, Met γ-CH$_2$), 2.99-3.22 (3H, m, β-Ala β-C*H*H and Phe β-CH$_2$), 3.78 (3H, s, COOCH$_3$), 3.79-3.86 (1H, m, β-Ala β-C*H*H), 4.25 (1H, m, Met α-CH), 4.27 (1H, m, Leu α-CH), 4.84 (1H, m, Phe α-CH), 5.18 (1H, br s, Met NH), 6.72 (1H, br s, Leu NH), 7.05 (1H, d, *J* = 8.0 Hz, Phe NH), 7.22-7.33 (6H, m, aromatics and β-Ala NH). Anal. Calcd for C$_{29}$H$_{46}$N$_4$O$_7$S: C, 58.56; H, 7.80; N, 9.42. Found: C, 58.79; H, 7.83; N, 9.44.

For-Met-Leu-β-Ala-Phe-OMe (15). From Boc-Met-Leu-β-Ala-Phe-OMe (0.056 g, 0.095 mmol) according to the general procedure B. The mixture was purified on silica gel flash chromatography (CHCl$_3$/MeOH 95:5). Amorphous solid (0.039 g, 79%); [a]$_D$ -55.3° (*c* 0.38, MeOH); IR (CHCl$_3$): ν 3421, 1743, 1648 cm^{-1}; ^{1}H NMR (CDCl$_3$): δ 0.84-0.91 [6H, Leu CH-(C*H*$_3$)$_2$], 1.34-1.60 [3H, m, Leu C*H*$_2$-C*H*-(CH$_3$)$_2$], 1.70-2.05 [5H, m, Met β-CH$_2$ and SCH$_3$ (s, at 2.02)], 2.22 (2H, m, β-Ala α-CH$_2$), 2.42 (2H, m, Met γ-CH$_2$), 3.05-3.25 (2H, m, β-Ala β-CH$_2$), 2.83-3.04 (2H, m, Phe β-CH$_2$), 3.58 (3H, s, COOCH$_3$), 4.21 (1H, m, Leu α-CH), 4.40 (1H, m, Met α-CH), 4.46 (1H, m, Phe α-CH), 7.17-7.30 (5H, m, aromatics), 7.87 (1H, br s, β-Ala NH), 8.00 (1H, br s, Leu NH), 8.01 (1H, s, HCO), 8.29 (1H, br s, Met NH), 8.39 (1H, d, *J* = 7.2 Hz, Phe NH),). Anal. Calcd for C$_{25}$H$_{38}$N$_4$O$_6$S: C, 57.45; H, 7.33; N, 10.72. Found: C, 57.30; H, 7.30; N, 10.67.

Boc-Met-Leu-Pro-Phe-OMe (17). From Boc-Met-Leu-OH (0.115 g, 0.319 mmol) and TFA·HN-Pro-Phe-OMe **16** (0.124 g, 0.319 mmol), this latter obtained from Boc-Pro-Phe-OMe,[80] according to the general procedure A. The mixture was purified on silica gel chromatography (CH_2Cl_2/EtOAc 1:1). Colourless oil (0.115 g, 58%); $[a]_D$ -52.0° (*c* 0.94, $CHCl_3$); IR ($CHCl_3$): ν 3421, 1743, 1678 cm^{-1}; ^1H NMR ($CDCl_3$): δ 0.92-0.96 [6H, m, Leu CH-(C*H*$_3$)$_2$], 1.46 [9H, s, C(CH_3)$_3$], 1.56-1.72 [3H, m, Leu C*H*$_2$-C*H*-(CH_3)$_2$], 1.86-2.36 [9H, m, Met β-CH_2, SCH_3 (s, at 2.12) and Pro β-CH_2 and Pro γ-CH_2], 2.58 (2H, m, Met γ-CH_2), 3.02-3.20 (2H, m, Phe β-CH_2), 3.42-3.51 (1H, m, Pro δ-*H*CH), 3.61-3.69 (1H, m, Pro δ–*H*CH), 3.72 (3H, s, $COOCH_3$), 4.29 (1H, m, Met α-CH), 4.55 (1H, m, Pro α-CH), 4.73 (1H, m, Leu α-CH), 4.78 (1H, m, Phe α-CH), 5.17 (1H, d, *J* = 8.4 Hz, Met NH), 6.74 (1H, br s, Leu NH), 6.99 (1H, d, *J* = 7.6 Hz, Phe NH), 7.11-7.33 (5H, m, aromatics). Anal. Calcd for $C_{31}H_{48}N_4O_7S$: C, 59.98; H, 7.79; N, 9.02. Found: C, 59.80; H, 7.76; N, 9.00.

For-Met-Leu-Pro-Phe-OMe (18). From Boc-Met-Leu-Pro-Phe-OMe (0.071 g, 0.114 mmol) according to the general procedure B. The mixture was purified on silica gel flash chromatography ($CHCl_3$/MeOH 98:2). Colourless oil (0.058 g, 93%); $[a]_D$ -43.2° (*c* 0.95, $CHCl_3$); IR ($CHCl_3$): ν 3417, 1743, 1673 cm^{-1}; ^1H NMR ($CDCl_3$): δ 0.93-0.95 [6H, m, Leu CH-(C*H*$_3$)$_2$], 1.25-1.40 [3H, m, Leu C*H*$_2$-C*H*-(CH_3)$_2$], 1.58-2.31

[9H, m, Met β-CH_2, SCH_3 (s, at 2.11), Pro β-CH_2 and Pro γ-CH_2], 2.58 (2H, m, Met γ-CH_2), 3.02 and 3.15 (2H, A and B of an ABX, J = 6.4, 5.6 and 13.6 Hz, Phe β-CH_2), 3.51 (1H, m, Pro δ-C*H*H), 3.67 (1H, m, Pro δ-C*H*H), 3.69 (3H, s, $COOCH_3$), 4.62 (1H, m, Pro α-CH), 4.76 (1H, m, Leu α-CH), 4.77 (1H, m, Phe α-CH), 4.85 (1H, m, Met α-CH), 6.55 (1H, d, J = 8.0 Hz, Met NH), 7.09 (1H, d, J = 7.2 Hz, Phe NH), 7.23 (1H, d, J = 7.6 Hz, Leu NH), 7.08-7.30 (5H, m, aromatics), 8.18 (1H, s, HCO). Anal. Calcd for $C_{27}H_{40}N_4O_6S$: C, 59.10; H, 7.35; N, 10.21. Found: C, 59.29; H, 7.38; N, 10.25.

2.6.4.3 Biological assays

Cell preparation

Cells were obtained from the blood of healthy subjects, and human peripheral blood neutrophils were purified by using the standard techniques of dextran (Pharmacia, Uppsala, Sweden) sedimentation, centrifugation on Ficoll-Paque (Pharmacia), and hypotonic lysis of contaminating red cells. Cells were washed twice and resuspended in Krebs-Ringer phosphate (KRPG), pH 7.4, at final concentration of 50 X 10^6 cells/mL and kept at room temperature until used. Neutrophils were 98-100% viable, as determined using the Trypan Blue exclusion test. The study was approved by the local Ethics Committee and informed consent was obtained from all participants.

Random locomotion

Random locomotion was performed with 48-well microchemotaxis chamber (Bio Probe, Milan, Italy) and migration into the filter was evaluated by the leading-front method.[96] The actual control random movement is 35 ± 3 μm SE of ten separate experiments performed in duplicate.

Chemotaxis

Each peptide was added to the lower compartment of the chemotaxis chamber. Peptides were diluted from a stock solution with KRPG containing 1 mg/mL of bovine serum albumin (BSA; Orha Behringwerke, Germany) and used at concentrations ranging from 10^{-12} to 10^{-5} M. Data were expressed in terms of chemotactic index (CI), which is the ratio: (migration towards test attractant minus migration towards the buffer/migration towards the buffer); the values are the mean of six separate experiments performed in duplicate. Standard errors are in the 0.02-0.09 CI range.

Superoxide anion (O_2^-) production

This anion was measured by the superoxide dismutase-inhibitable reduction of ferricytochrome *c* (Sigma, USA) modified for microplate-based assays. Tests were carried out in a final volume of 200 μl containing 4 x 10^5 neutrophils, 100 nmoles cytochrome *c* and KRPG. At zero time different

amounts (10^{-10} -8 x 10^{-5} M) of each peptide were added and the plates were incubated into a microplate reader (Ceres 900, Bio-TeK Instruments, Inc.) with the compartment temperature set at 37 °C. Absorbance was recorded at 550 and 468 nm. The difference in absorbance at the two wavelengths was used to calculate nmoles of O_2^- produced using a molar extinction coefficient for cytochrome *c* of 18.5 mM^{-1} cm^{-1}. Neutrophils were incubated with 5 μg/mL cytochalasin B (Sigma) for 5 min prior to activation by peptides. Results were expressed as net nmoles of O_2^- per 1 x 10^6 cells per 5 min and are the mean of six separate experiments performed in duplicate. Standard errors are in 0.1-4 nmoles O_2^- range.

Enzyme assay

The release of neutrophil granule enzymes was evaluated by determination of lysozyme activity, modified for microplate-based assays. Cells, 3 x 10^6/well, were first incubated in triplicate wells of microplates with 5 μg/mL cytochalasin B at 37 °C for 15 min and then in the presence of each peptide at a final concentration of 10^{-10} -8 x 10^{-5} M for a further 15 min. The plates were then centrifuged at 400xg for 5 min and the lysozyme was quantified nephelometrically by the rate of lysis of cell wall suspension of Micrococcus lysodeikticus. The reaction rate was measured using a microplate reader at 465 nm. Enzyme release was expressed as a net percentage of total

enzyme content released by 0.1% Triton X-100. Total enzyme activity was 85 ± 1 mg per 1 x 10^7 cells/min. The values are the mean of five separate experiments done in duplicate. Standard errors are in the range 1-6%.

Antagonist assay

Antagonist activity was determined by measuring the ability of a derivative to inhibit chemotaxis, superoxide anion production or granule enzyme release as induced by fMLF-OMe. Antagonist activity data (percentage of activity) were obtained by comparing the CI, nanomoles of O_2^- or percentage of lysozyme release in the absence (100%) and in the presence of the derivative. CI of 10 nM fMLF-OMe was 1.15 ± 0.10 SE. O_2^- generation produced by 1 μM fMLF-OMe was 62 ± 2 nmol/1 x 10^6 cells/5 min. Enzyme activity triggered by 1 μM fMLF-OMe was 54 ± 5%/3 x 10^6 cells/min. Derivatives were added to neutrophils 10 min before the incubation step for cellular functionality. Each value represents an average of six separate experiments done in duplicate. Standard errors are within 10% of the mean value.

Statistical analysis

The non-parametric Wilcoxon test was used in the statistical evaluation of differences between groups. Differences were considered to be statistically significant at $P \leq 0.05$.

Acknowledgments

This work was supported by grants from Fondazione Cassa di Risparmio di Ferrara. We are grateful to Banca del Sangue of Ferrara for providing fresh blood.

2.7 Novel chemotactic For-Met-Leu-Phe-OMe (fMLF-OMe) analogues based on Met residue replacement by 4-amino-proline scaffold: Synthesis and bioactivity*

Due to their key role in the body's physiological defence against bacterial infections chemotactic *N*-formyl peptides, which are products of bacterial metabolism, continue to stimulate the interest of chemists and biochemists. They act by binding at highly specific G-protein-coupled formyl peptide receptors (FPRs) located on the membrane of neutrophils. The interaction triggers, in addition to a rapid movement of the phagocytic cells towards the sites of infections (chemotaxis), a series of intracellular responses, relevant among which are lysosomal enzyme release and superoxide anion production.[46,50,40,129] Despite extensive studies, both the essential cellular mechanisms controlling the neutrophil migration and the structure-activity relationships regulating the *N*-formyl peptide-receptor study interactions, are not completely understood and

*Torino, D.; Mollica, A.; Pinnen, F.; Feliciani, F.; Spisani, S.; Lucente, G. *Bioorg. Med. Chem.* **2009**, *17*, 251.

still under.[100,129,134] However, since the discovery of *N*-formyl-methionyl peptides as agonists at the neutrophil receptors, the potent chemotactic agent *N*-formyl-Met-Leu-Phe-OH (fMLF) and its methyl ester (fMLF-OMe) have been chosen as the reference molecules and a variety of structural modifications have been performed on these tripeptides for systematic studies on biochemical mechanism and structure activity relationships.[58, 63, 67, 68,101]

Examination of the above cited studies indicate that both receptor recognition and agonistic activity of fMLF-OMe analogues are highly sensible to alterations centred at the *N*-terminal formyl group and/or at the sulphur-containing Met side chain. However, both the aromatic *C*-terminal residue and the central Leu isobutyl side chain are more tolerant towards replacement or modification and several analogues of fMLF-OMe modified at these two residues have been examined. Thus, a remarkable degree of specificity is postulated for the region of FPRs devoted to the accommodation of the *N*-terminus portion of fMLF-OMe ligand and its analogues.[46,67] This property has been related to the presence in the involved receptor region of (i) a hydrophobic pocket containing an area of positive charge suitable to interact with the electron rich methylthio group of Met side chain and (ii) a small cavity capable to bind through a hydrogen bonding system the formyl H-CO-NH group. It is also relevant to note in this context that the replacement of the small

N-formyl group with the bulkier substituents such as *t*-butyloxycarbonyl (Boc) transforms fMLF-OMe and several of its active analogues into inactive or weakly active agonists, generally endowed with antagonistic activity.[50,67]

In order to get information on the factors responsible for the critical role exerted by the receptor area interacting with the *N*-terminal elements of the chemotactic *N*-formyl tripeptide ligands, we reported recently results obtained by studying new fMLF-OMe analogues incorporating the two epimeric proline-methionine chimera residues *cis*-4(*S*)-methylthio-(*S*)-proline (cMtp) and *trans*-4(*R*)-methylthio-(*S*)-proline (tMtp) at *N*-terminal position (Figure 21).[135] In these tripeptide analogues the presence of the pyrrolidine scaffold, combined with the different stereochemistry at position 4 of the ring, allowed the examination of ligands with restricted spatial orientation of the *N*-protecting groups (*N*-formyl or *N*-Boc) with respect to the *S*-methyl at position 4 and the amide junction at position 2 of the ring. No other analogues of this type, involving the Met residue, have been reported so far. Examination of these new models showed, quite unexpectetly, that the two *N*-For tripeptides are practically inactive while the *N*-Boc derivatives show significant chemotactic activity with cMtp containing analogue almost equipotent with the reference ligand fMLF-OMe. It seems that in these models the interaction of the *N*-terminal functional groups with the involved receptor area leads to a different type

of accommodation as compared with usual ligands. This strongly suggests that studies based on conformationally restricted analogues of this type may shed light on a critical and still unclear point concerning the ligand-receptor interaction. Based on this consideration we decided to examine a group of new and unusual fMLF-OMe derivatives in which the sulfurated Met side chain is omitted and the 4(*S*) and 4(*R*) 4-amino-(*S*)-proline (cAmp and tAmp, respectively) (Figure 21) are used as a quite rigid skeleton on which the *N*-For and *N*-Boc acylating groups can be attached in different combinations.

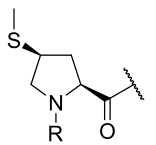

I (cMtp-)

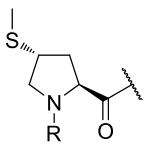

II (tMtp-)

Residues of **I**): ***cis***-(2*S*,4*S*)-4-methylthio- and **II**): *trans*-(2*S*,4*R*)-4-methylthio-proline (R = For, Boc)

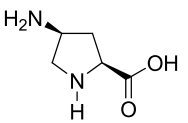

cis-(2*S*,4*S*)-4-amino-proline (cAmp)

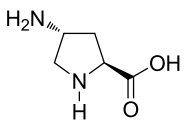

trans-(2*S*,4*R*)-4-amino-proline (tAmp)

Figure 21. Chemical structure of proline scaffolds cited in the text.

2.7.1 Chemistry

The synthesis of the *N*-protected 4-amino prolines **6** and **14** and the target tripeptides **17-19** are reported in Schemes 8-10.

Examination of the literature shows that efficient approaches can be followed to obtain different 4-substituted prolines starting from the commercially available *trans*-4-hydroxy-L-proline. *cis*-isomers can be easily formed by direct Mitsunobu reaction[136,137] or by nucleophilic SN_2 displacement performed on *trans*-4-*O*-tosyl or 4-*O*-mesyl *N*-protected derivatives.[135,138-140]

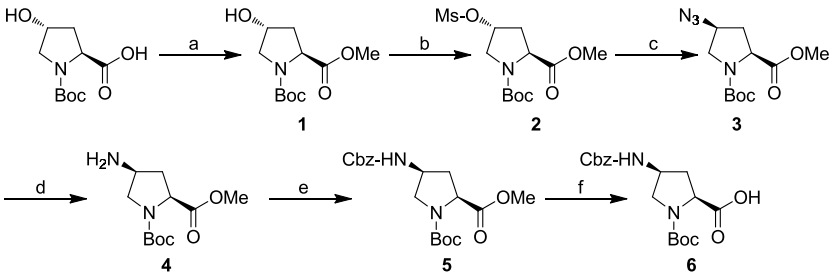

Scheme 8. Synthesis of compound **6**. *Reagents and conditions*: a) ethereal diazomethane/MeOH; b) MsCl, TEA, CH_2Cl_2, 0 °C 3 h; c) NaN_3/DMF, 55 °C overnight; d) H_2-Pd/C, MeOH, 6h rt; e) Cbz-Cl, TEA, CH_2Cl_2, 2h 0 °C, 1h rt; f) 1N NaOH, MeOH, 30 min 0 °C, overnight, rt.

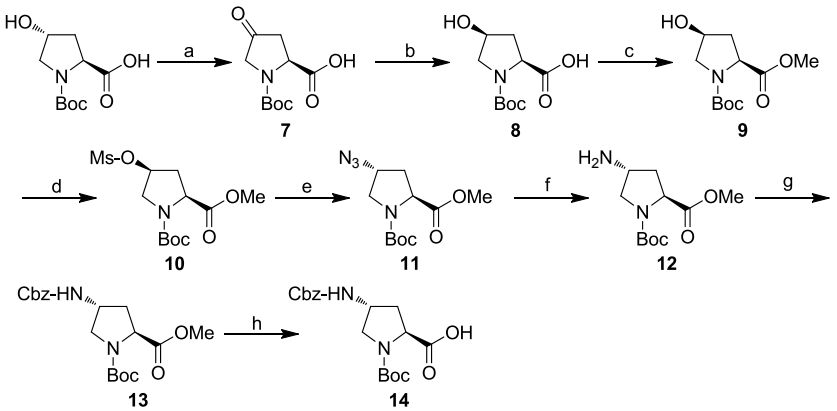

Scheme 9. Synthesis of compound **14**. *Reagents and conditions*: a) CrO_3/Py; b) $NaBH_4/H_2O$, MeOH; c) ethereal diazomethane/MeOH; d) MsCl, TEA, CH_2Cl_2, 30 min 0 °C; e) NaN_3/DMF, 55 °C, overnight; f) H_2-Pd/C, MeOH, 6h rt,; g) Cbz-Cl,TEA,CH_2Cl_2, 2h 0 °C, 1h rt; h) 1N NaOH, MeOH, 30 min 0 °C, overnight, rt.

An alternative synthetic strategy, based on *N*-protected 4-hydroxy-L-prolines, involves the oxidation of the 4-OH group and the stereoselective reduction of the resultant ketone with $NaBH_4$. This useful stereoselective reduction, originally observed by Patchett and Witkop,[141] gives exclusively the *cis* isomer and is frequently used in the synthesis of peptides containing 4-substituted proline analogues.[136,142]

According to the above reported literature data, commercially available *N*-Boc-*trans*-(2*S*,4*R*)-4-hydroxyproline was used as starting material for the synthesis of the *N*-Boc-*cis*-(2*S*,4*S*)-4-benzyloxycarbonylamino-proline [Boc-cAmp(Cbz)-OH] **6** (Scheme 8). Mesylation of the 4-OH, followed by inversion of the absolute configuration by nucleophilic substitution with NaN_3[140] gave, after reduction and amino protection, the desired precursor amino acid derivative **6**. A more complex strategy was adopted for the synthesis of *N*-Boc-*trans*-(2*S*,4*R*)-4-benzyloxycarbonylamino-proline [Boc-tAmp(Cbz)-OH] **14**, the diastereoisomeric analogue of **6**. In this case (Scheme 9) the *N*-Boc-*trans*-(2*S*,4*R*)-4-hydroxyproline was initially oxidized to give the 4-oxo derivative **7**. This was stereoselectively reduced[141,142] to *N*-Boc-*cis*-(2*S*,4*S*)-4-hydroxyproline **8** and esterified with ethereal diazomethane to give the methyl ester **9** as a single product on TLC. The same sequence of reactions, already followed to obtain compound **6**, led to the final *N*-Boc-tAmp(Cbz)-OH **14**.

The above described precursors **6** and **14** were used for the synthesis of two series of fMLF-OMe analogues. Each series contains, as reported in Scheme 10, cAmp (compounds **17a-19a**) or tAmp (compounds **17b-19b**) as *N*-terminal residue. The tripeptides were obtained by using the Leu-Phe-OMe dipeptide as common *C*-terminal fragment to provide the orthogonally protected key precursors **15a-b**. Hydrogenolytic deprotection of the Cbz-NH- bound at the 4-amino group of the proline residue gave the two *N*-Boc tripeptides **16a-b** from which the two couples of target substrates **17a-b** and **18a-b** were obtained by *N*-Boc protection or *N*-formylation, respectively, of the free proline 4-amino group.

In order to synthesize the last couple of substrates **19a-b**, characterized by the presence of a formyl group bound at each of the two amino functions of the prolinic scaffold, Boc deprotection followed by *N*-formylation of **16a-b** is required. When the deprotection was performed with trifluoroacetic acid and the resulting tripeptidic bis-trifluoroacetates were used for the subsequent formylation reaction low yields and rather complex reaction mixtures were obtained. This reaction sequence was sensibly improved when HCOOH, instead of the usual trifluoroacetic acid, was used for *N*-Boc deprotection and the resulting bis-formates were formylated by adopting the mixed anhydride strategy.

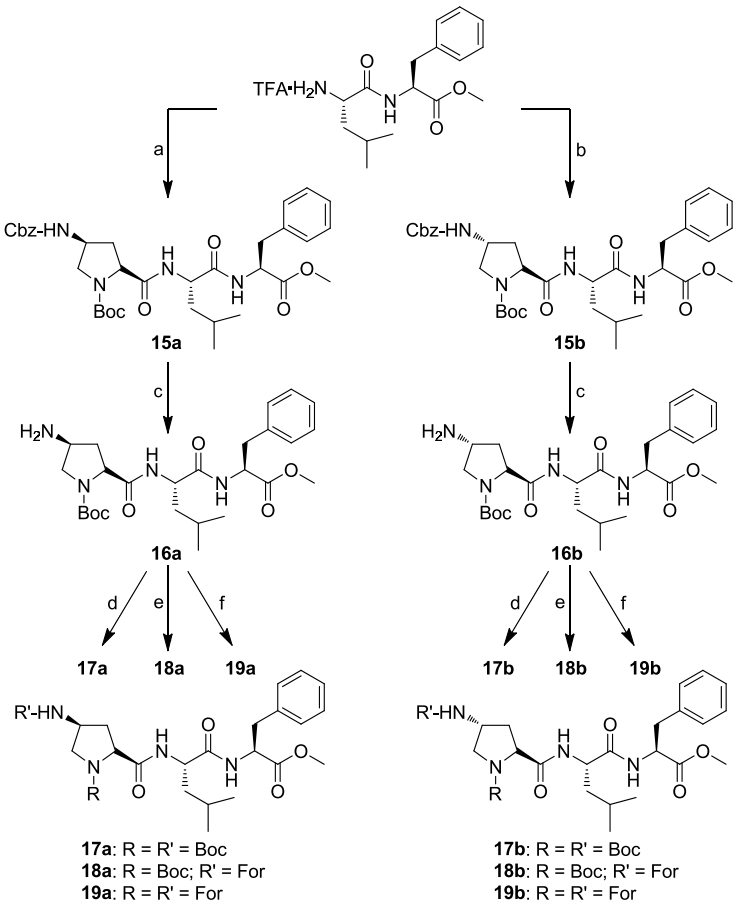

Scheme 10. Synthesis of compounds **17a,b-19a,b**. *Reagents and conditions*: a) Boc-cAmp(Cbz)-OH, *i*BuOCOCl, NMM, CH_2Cl_2, 30 min -15 °C, overnight rt; b) Boc-tAmp(Cbz)-OH, *i*BuOCOCl, NMM, CH_2Cl_2, 30 min -15 °C, overnight rt; c) H_2-Pd/C, MeOH, 3h rt; d) Boc_2O, TEA, EtOAc, 1h rt; e) HCOOH, *i*BuOCOCl, NMM, CH_2Cl_2, 30 min -15 °C, overnight rt; f) HCOOH, *i*BuOCOCl, NMM, CH_2Cl_2, 30 min -15 °C, overnight rt.

2.7.2 Biological results

2.7.2.1 Agonism

The biological activity of the six models under study has been determined on human neutrophils and compared with that

of the parent tripeptide fMLF-OMe.[143,144] The analogues of the two series (**17-19a** and **17-19b**) were evaluated for their ability to activate directed migration (chemotaxis), stimulate production of superoxide anion radicals (O_2^-) and induce lysozyme release from granules of human neutrophils. Results are plotted in Figure 22 and the activity values exhibited at the optimal peptide concentration are summarized in Table 6. All the four models containing the bulky *N*-Boc protecting group (i.e: compounds **17a**, **18a** and **17b**, **18b**) show moderate chemotactic activity with the highest value (0.45 C.I.) reached by the tAmp containing peptide **17b** at the optimal concentration of 10^{-10}M (Table 6 and Figure 22A). Highly active chemotactic agonists are the two peptides **19a** and **19b**, both characterized by the presence of a *N*-For acylating group at both the amino groups of the proline scaffold. At very low concentration (about 10^{-12} M) these models equal the activity of the reference molecule and reach maximal activity (0.75 C.I.) at a concentration (10^{-10} M), lower than that where the fMLF-OMe peak (10^{-9} M) appears (Table 6).

All the models examined are practically inactive as superoxide anion producers (Figure 22B) and only very weak secretagogue agents (Figure 22C). The highest value for this latter function (24% of lysozyme release at concentration 10^{-6} M) is shown by the peptide **19a** containing two *N*-For acylating group at the cAmp residue.

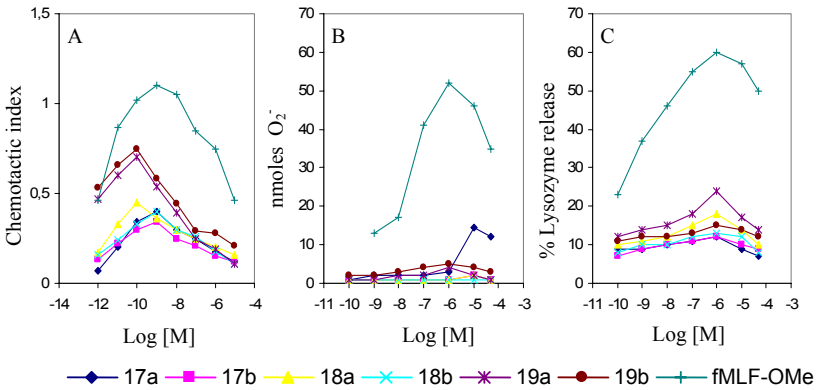

Figure 22. Biological activities of tripeptide derivatives **17a,b-19a,b** and fMLF-OMe. (**A**) Chemotactic index; (**B**) Superoxide anion production; (**C**) Release of neutrophil granule enzymes evaluated by determining lysozyme activity.

Table 6. Chemotactic activity, superoxide anion production and lysozyme release of fMLF-OMe derivatives.

Peptides	Chemotactic index[a]	O_2^-[a] (nmol)	% Lysozyme release[a]
fMLF-OMe	1.10 ± 0.08 (10^{-9} M)	52 ± 4 (10^{-6} M)	60 ± 4 (10^{-6} M)
17a	0.40 ± 0.02 (10^{-9} M)	14.6 ± 1 (10^{-5} M)	12 ± 1 (10^{-6} M)
18a	0.34 ± 0.02 (10^{-9} M)	2.0 ± 0.5 (10^{-5} M)	12 ± 1 (10^{-6} M)
19a	0.70 ± 0.01 (10^{-10} M)	4.0 ± 0.5 (10^{-6} M)	24 ± 2 (10^{-6} M)
17b	0.45 ± 0.01 (10^{-10} M)	2.0 ± 0.5 (10^{-5} M)	18 ± 1 (10^{-6} M)
18b	0.40 ± 0.02 (10^{-9} M)	1.0 ± 0.5 (10^{-5} M)	13 ± 1 (10^{-6} M)
19b	0.75 ± 0.02 (10^{-10} M)	5.0 ± 0.5 (10^{-6} M)	15 ± 1 (10^{-6} M)

[±] Standard errors of the mean (SEM); optimal concentration values in parentheses.
[a] Values indicate the efficacy (activity at the optimal peptide concentrations).

2.7.2.2 Antagonism

All models under study were tested for their ability to inhibit the three biological functions, except for the chemotaxis of compounds **19a-b** which are good agonists in this function. The antagonism was determined by measuring the ability to inhibit

the activity stimulated by fMLF-OMe on human neutrophils. The influence of an increasing concentration of **17a-b** and **18a-b** on chemotaxis induced by 10 nM fMLF-OMe, which is the optimal dose for chemotaxis activation, is shown in Figure 23A.

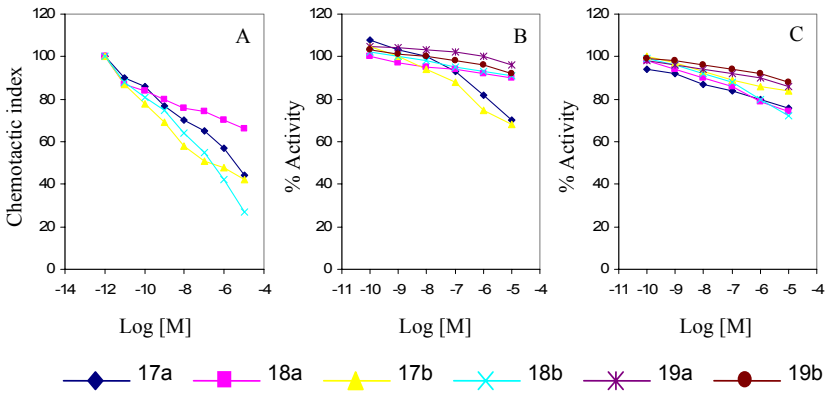

Figure 23. Effect of *N*-Boc-protected tripeptides **17a,b-19a,b** on the neutrophil activities triggered by fMLF-OMe. (**A**) Chemotactic index; (**B**) Superoxide anion production; (**C**) Release of neutrophil granule enzymes evaluated by determining the lysozyme activity.

A significant dose-dependent inhibition of the chemotactic index, which reaches the value of 73% at the highest concentration, is observed for compound **18b** containing the 4-NH For substituent at the *N*-Boc-tAmp residue. Interestingly, the epimeric model **18a**, containing the cAmp residue, is only a very modest antagonist. Good chemotactic antagonism and almost identical values (about 60% inhibition at the maximum concentration) are also shown by **17a** and **17b** containing two *N*-Boc groups at the cAmp and tAmp residue, respectively. As can be deduced by Figure 23B and C, which refer to the superoxide

anion production and inhibition of lysozyme release, only the two latter mentioned analogues (**17a** and **17b**) exhibit a modest activity in the superoxide anion production inhibition, with a maximum value of 30% at 10^{-5} M concentration (Figure 23B). None of the other tripeptides show significant antagonism towards both superoxide anion production and lysozyme release (Figures 23B and C).

2.7.3 Conclusions

In the present study, we tried to evaluate the functional group requirements of the FPRs in the critical region devoted to the interaction with the *N*-terminal residue of fMLF and related *N*-formyl tripeptide ligands. Peptide models used in this effort are of an unusual type and contain the pyrrolidine ring of 4-amino L-proline in place of the native methionine. The crucial formyl group has been bound at either of the amino groups of the proline scaffold which also supports the bulky *N*-Boc protecting group. Contrary to our expectation, suggested in part by results obtained with fMLF-OMe analogues containing the *N*-Boc-4-methylthio-proline at the *N*-terminal position, all the synthesized tripeptides characterized by the presence of the Boc group, including the two models **18a-b** bearing a *N*-formylic group at the 4-amino-proline scaffold, display only modest chemotactic activity, with a maximum value of 0.45 of the chemotactic index (Table 6) shown by tripeptide **17b**. Conversely, the derivatives

19a and **19b**, in which both the *N*-terminal amino groups are formylated, are potent agonists with comparable potency. These latter models are among the first fMLF analogues which, although devoid of the sulfur-containing Met side chain, exhibit good chemotactic activity. It seems then that the absence of bulky groups at the *N*-terminal position, combined with the presence of the *N*-For groups at the rigid scaffold, may lead to a right fitting with the receptor even if the methylthio group of the Met side chain is absent. Connected with the chemotactic activity of **19a** and **19b** is the antagonism displayed by the *N*-Boc-tripeptide **18b** and, with reduced potency, by **17a-b** (Figure 23A). It can be seen here that the replacement of the formylic group with a bulky substituent leads to the same change of activity from agonism to antagonism, primarily observed on passing from fMLF-OMe to Boc-MLF-OMe. This behaviour is not observed in the case of the fMLF-OMe analogues containing proline-methionine chimera residues at the *N*-terminal position. Finally, concerning the different stereochemistry at the 4-amino-proline residue, characterizing the three couples of the examined tripeptides, this feature does not influence appreciably the biological functions tested, regardless of the presence of *N*-Boc or *N*-For substituents. However, as can be seen by the values summarized in Table 6 the *trans* models are in any case slightly more active than the epimeric *cis* models.

A final observation concerns the agonistic activity of the tripeptides under study toward the superoxide anion production and lysozyme release (Figure 22B and C). With the exception of the low values observed for the secretagogue activity in the case of **19a** (24% as maximum value at 10^{-6} M concentration; Table 6 and Figure 22B) all the other compounds are practically inactive toward these two biological functions. Thus, the here reported structural modification at the *N*-terminal residue of fMLF-OMe may represent an useful basis for the design of ‘‘pure” chemotactic agonists. As it is well known,[99,100,145] agonists of this type capable to select or modulate the different neutrophil responses (distinct from “full” agonists), are of great utility as probes to gain information on the complex biochemical mechanisms regulating the signal transduction pathways.[129]

In conclusion, in this study a new type of fMLF-OMe tripeptide analogues, obtained by replacing the critical native Met residue with a 4-amino-proline scaffold bearing different substituents, have been described. This synthetic strategy leads to molecules which, depending upon the nature of the acylating groups at the *N*-terminal position, exhibit significant chemotactic agonism or antagonism with selectivity towards the neutrophil biological functions.

2.7.4 Experimental section

Materials and methods. Optical rotations were taken at 20 °C with a Schmidt-Haensch Polartronic D polarimeter (1 dm cell, *c* 1.0 in $CHCl_3$ except otherwise specified). Anhydrous solvents were prepared by distillation over sodium metal or calcium hydride prior to use. TLC (thin-layer chromatography) and PLC (preparative layer chromatography) were performed on Merck 60 F_{254} silica gel plates. The drying agent was sodium sulphate. ^1H NMR experiments were performed at 400 MHz on a Bruker AM 400 spectrometer in $CDCl_3$ solution and chemical shifts (δ) are quoted in parts per million (ppm) and were indirectly referred to TMS. Coupling constants are in Hz. Most of the reactions were carried out under inert atmosphere of nitrogen. The reported yields are for purified materials but were not optimized.

2.7.4.1 Chemistry. General procedure

A. Catalytic hydrogenolysis. A solution of the compound in MeOH and 10% Pd on C (10%) was vigorously stirred at room temperature and atmospheric pressure for 2-6 h (TLC control) under a slow stream of hydrogen. The catalyst was removed by filtration and washed with MeOH. The filtrate was evaporated under reduced pressure and used for the subsequent reaction.

B. Coupling with the mixed anhydride method. To a mixture cooled at -15 °C containing the required *N*-

protected amino acid (1.0 mmol) in CH_2Cl_2 were added isobutyl chloroformate (IBCF; 1.0 mmol) and NMM (1.1 mmol). The mixture was stirred for 10 min at the same temperature and then the required amino-derivative salt (1.0 mmol) and NMM (1.1 mmol) were added. After 15 min at -15 °C the mixture was kept at room temperature overnight. After removal of the solvent under reduced pressure, the residue was dissolved in EtOAc and washed with 5% citric acid (2 x 15 mL), $NaHCO_3$ ss (2 x 15 mL) and NaCl ss (15 mL). The organic layer was dried over Na_2SO_4 and evaporated under reduced pressure.

2.7.4.2 Synthesis

***N*-Boc-*trans*-(4-hydroxy)-L-proline methyl ester (1).** To a solution of *N*-Boc-*trans*-4-hydroxy-L-proline (1 g, 4.33 mmol) in MeOH (10 mL) an ethereal diazomethane solution was added until a yellow colour persisted. The solution was evaporated under reduced pressure to give title compound, pure on TLC (quantitative yield); $[a]_D$ -65° (*c* 0.6, $CHCl_3$); ^{1}H NMR ($CDCl_3$): δ 1.49 [9H, s, $C(CH_3)_3$], 2.05-2.31 (2H, m, Pro C^3H_2), 3.48-3.67 (2H, m, Pro δ-C^5H_2), 3.75 (3H, s, $COOCH_3$), 4.39-4.51 (2H, m, Pro α-CH and Pro C^4H). Anal. Calcd for $C_{11}H_{19}NO_5$: C, 53.87; H, 7.81; N, 5.71. Found: C, 53.81; H, 7.82; N, 5.75.

***N*-Boc-*trans*-(4-mesyloxy)-L-proline methyl ester (2).** To an ice-cooled solution of the methyl ester **1** (1.06 g, 4.33 mmol) in dry CH_2Cl_2 (10 mL), TEA (0.73 mL, 5.2 mmol) and MsCl (0.4 mL, 5.2 mmol) were added. The resulting mixture was stirred for 3 h at 0 °C. The mixture was diluted with CH_2Cl_2 and washed with 1N HCl, $NaHCO_3$ ss and brine. The organic layer was dried and evaporated under reduced pressure to yield 1.34 g (96%) of pure **2** as a pale yellow oil; $[a]_D$ -52° (*c* 1.6, $CHCl_3$); ^1H NMR ($CDCl_3$): δ 1.41 [9H, s, $C(CH_3)_3$], 2.21-2.67 (2H, m, Pro C^3H_2), 2.98 (3H, s, CH_3SO_2), 3.70-3.85 (5H, m, Pro C^5H_2 and $COOCH_3$), 4.44 (1H, m, Pro α-CH), 5.24 (1H, m, Pro C^4H). Anal. Calcd for $C_{12}H_{21}NO_7S$: C, 44.57; H, 6.55; N, 4.33. Found: C, 44.67; H, 6.58; N, 4.31.

***N*-Boc-*cis*-(4-azido)-L-proline methyl ester (3).** A solution of **2** (0.806 g, 2.49 mmol) and NaN_3 (0.194 mg, 2.98 mmol) in dry DMF (5 mL) was stirred at 55 °C overnight. After removal of the solvent under reduced pressure, the residue was dissolved in EtOAc and washed with water and NaCl ss. The organic layer was dried and evaporated under reduced pressure. The residue was purified by silica gel chromatography (petroleum ether/EtOAc 5:1) to give pure **3** as a colourless oil (0.496 g, 73%).

***N*-Boc-cAmp-OMe (4).** Reduction of the azido group was performed by adopting the general procedure above reported for the catalytic hydrogenolysis: **3** (0.496 g, 1.84 mmol), MeOH

(16.5 mL) and Pd/C (0.0496 g) gave **4** (0.34 g, 76%) after 6 h at room temperature.

***N*-Boc-cAmp(Cbz)-OMe (5).** To an ice-cooled solution of **4** (0.359 g, 1.47 mmol) in CH_2Cl_2/DMF 9:1 (20 mL) TEA (0.62 mL, 4.41 mmol) and Cbz-Cl (0.29 mL, 1.76 mmol) were added. The resulting mixture was stirred for 2 h at 0 °C and 1 h at room temperature. After removal of the solvent under reduced pressure, the residue was dissolved in EtOAc and washed with 5% citric acid, $NaHCO_3$ ss and NaCl ss. The organic layer was dried and evaporated under reduced pressure. The residue was purified by silica gel chromatography ($CHCl_3$/EtOAc 7:3) to give pure **5** as a colourless oil (0.308 g, 55%); $[a]_D$ -13.9° (*c* 0.3, $CHCl_3$); IR ($CHCl_3$): ν 3434, 1743, 1698 cm^{-1}; ^1H NMR ($CDCl_3$): δ 1.45 [9H, s, $C(CH_3)_3$], 1.89-2.03 and 2.39-2.60 (2H, m, Pro C^3H_2), 3.40-3.81 (2H, m, Pro C^5H_2), 3.71 (3H, s, $COOCH_3$), 4.21-4.50 (2H, m, Pro α-CH, Pro C^4H), 5.18 (2H, s, C_6H_5-CH_2), 5.75 (1H, d, J = 8.0 Hz, Z-NH), 7.03-7.45 (5H, m, aromatics). Anal. Calcd for $C_{19}H_{26}N_2O_6$: C, 60.30; H, 6.93; N, 7.40. Found: C, 60.47; H, 6.90; N, 7.43.

***N*-Boc-cAmp(Cbz)-OH (6).** To an ice-cooled solution of methyl ester **5** (0.145 g, 0.38 mmol) in MeOH, 1N NaOH (1.14 mL) was added dropwise and the mixture was stirred at slow stream of hydrogen. The catalyst was removed by filtration and washed with MeOH. The filtrate was evaporated under reduced pressure and used for the subsequent reaction.

***N*-Boc-(4-oxo)-L-proline (7).** To a mixture of pyridine (8.8 mL) and dry CH_2Cl_2 (20 mL) cooled at 0 °C, CrO_3 (5.2 g, 52 mmol) was added. Stirring was continued at 0 °C for 30 min and the mixture was allowed to warm at room temperature over a period of 30 min. A solution of *N*-Boc-4-*trans*-hydroxy-L-proline (2 g, 8.66 mmol) in CH_2Cl_2 (30 mL) was added over 5 min and stirring was continued for 1 h at room temperature. The mixture was taken up in diethyl ether and washed with 5% citric acid and brine. The organic layer was dried, filtered and evaporated under reduced pressure to give crude compound **7** (0.610 g, 31%), as a pale yellow solid; $[a]_D$ +18° (*c* 0.5, acetone); ^{1}H NMR ($CDCl_3$): δ 1.45 [9H, s, $C(CH_3)_3$], 2.75 (2H, m, Pro C^3H_2), 3.50-3.90 (2H, m, Pro C^5H_2), 4.75 (1H, m, Pro α-CH). Anal. Calcd for $C_{10}H_{15}NO_5$: C, 52.40; H, 6.60; N, 6.11. Found: C, 52.27; H, 6.61; N, 6.09.

***N*-Boc-*cis*-(4-hydroxy)-L-proline (8).** *N*-Boc-4-oxo-L-proline **7** (0.610 g, 2.66 mmol) was dissolved in MeOH (12 mL) and the reaction flask was cooled to 0 °C. A solution of $NaBH_4$ (0.328 g, 8.67 mmol) in water (1.45 mL) was added dropwise; after 10 min the reaction was allowed to stand at 4 °C for 15 min and concentrated under reduced pressure. The residue was diluted with water, acidified to pH 3 with 10% citric acid and extracted with EtOAc. The organic layer was washed with brine, dried and concentrated to yield 0.490 g of TLC pure derivative **8** (80%) as a foam; $[a]_D$ -39° (*c* 0.66, MeOH); ^{1}H NMR ($CDCl_3$):

δ 1.45 [9H, s, $C(CH_3)_3$], 2.19-2.59 (2H, m, Pro C^3H_2), 3.44-3.56 (2H, m, Pro C^5H_2), 4.53-4.65 (2H, m, Pro α-CH and Pro C^4H). Anal. Calcd for $C_{10}H_{17}NO_5$: C, 51.94; H, 7.41; N, 6.06. Found: C, 52.09; H, 7.42; N, 6.04.

***N*-Boc-*cis*-(4-hydroxy)-L-proline methyl ester (9).** To a solution of *N*-Boc-*cis*-4-hydroxy-L-proline (0.490 g, 2.12 mmol) in MeOH (4.9 mL) an ethereal diazomethane solution was added until a yellow colour persisted. The solution was evaporated under reduced pressure to give the title compound pure on TLC (quantitative yield); $[a]_D$ -63.9° (*c* 2.3, EtOH); ^1H NMR ($CDCl_3$): δ 1.45 [9 H, s, $C(CH_3)_3$], 2.07-2.49 (2H, m, Pro C^3H_2), 3.52-3.65 (2H, m, Pro C^5H_2), 3.77 (3H, s, $COOCH_3$), 4.27-4.40 (2H, m, Pro α-CH and Pro C^4H). Anal. Calcd for $C_{11}H_{19}NO_5$: C, 53.87; H, 7.81; N, 5.71. Found: C, 53.92; H, 7.79; N, 5.72.

***N*-Boc-*cis*-(4-mesyloxy)-L-proline methyl ester (10).** To an ice-cooled solution of the methyl ester **9** (0.519 g, 2.12 mmol) in dry CH_2Cl_2 (4.9 mL) TEA (0.385 mL, 2.76 mmol) and MsCl (0.215 mL, 2.76 mmol) were added. The resulting mixture was stirred for 30 min at 0 °C. The mixture was diluted with CH_2Cl_2 and washed with 1N HCl, Na_2CO_3 ss and brine. The organic layer was dried and evaporated under reduced pressure to yield 0.65 g (95%) of pure **10** as a pale yellow oil; ^1H NMR ($CDCl_3$): δ 1.44 [9H, s, $C(CH_3)_3$], 2.48-2.60 (2H, m, Pro C^3H_2), 3.03 (3H, s, CH_3SO_2), 3.75 and 4.45 (2H, m, Pro C^5H_2), 3.77 (3H, s, $COOCH_3$), 4.44 and 5.29 (2H, m, Pro α-CH and Pro C^4H).

Anal. Calcd for $C_{12}H_{21}NO_7S$: C, 44.57; H, 6.55; N, 4.33; S, 9.92. Found: C, 44.43; H, 6.53; N, 4.31.

***N*-Boc-*trans*-(4-azido)-L-proline methyl ester (11).** A solution of **10** (0.65 g, 2.01 mmol) and NaN_3 (0.157 g, 2.41 mmol) in dry DMF (5 mL) was stirred at 55 °C overnight. After removal of the solvent under reduced pressure, the residue was dissolved in EtOAc and washed with water and NaCl ss. The organic layer was dried and evaporated under reduced pressure. The residue was purified by silica gel chromatography (CH_2Cl_2/MeOH 99.8:0.2) to give pure **11** as a colourless oil (0.434 g, 80%).

***N*-Boc-tAmp-OMe (12).** Reduction of the azido group was performed by adopting the general procedure above reported for the catalytic hydrogenolysis: **11** (0.469 g, 1.74 mmol), MeOH (15.6 mL) and Pd/C (0.0469 g) gave **12** (0.22 g, 52%) after 6 h at room temperature.

***N*-Boc-tAmp(Cbz)-OMe (13).** To an ice-cooled solution of **4** (0.22 g, 0.902 mmol) in CH_2Cl_2/DMF 9:1 (15 mL) TEA (0.33 mL, 2.706 mmol) and Cbz-Cl (0.179 mL, 1.082 mmol) were added. The resulting mixture was stirred for 2 h at 0 °C and 1 h at room temperature. After removal of the solvent under reduced pressure, the residue was dissolved in EtOAc and washed with 5% citric acid, $NaHCO_3$ ss and NaCl ss. The organic layer was dried and evaporated under reduced pressure. The residue was purified by silica gel chromatography ($CHCl_3$/EtOAc 9:1) to

give pure **13** as a colourless oil (0.11 g, 33%); $[a]_D$ -23.4° (*c* 0.4, $CHCl_3$); IR ($CHCl_3$): ν 3439, 1742, 1697 cm^{-1}; ^1H NMR ($CDCl_3$): δ 1.42 [9 H, s, $C(CH_3)_3$], 2.18-2.26 (2H, m, Pro C^3H_2), 3.36-3.43 and 3.76-3.81 (2H, m, Pro C^5H_2), 3.75 (3H, s, $COOCH_3$), 4.27-4.40 (2H, m, Pro α-CH, Pro C^4H), 4.92 (1H, m, Cbz-NH), 5.18 (2H, s, C_6H_5-CH_2-O-), 7.10-7.47 (5H, m, aromatics). Anal. Calcd for $C_{19}H_{26}N_2O_6$: C, 60.30; H, 6.93; N, 7.40. Found: C, 60.42; H, 6.91; N, 7.41.

***N*-Boc-tAmp(Cbz)-OH (14).** To an ice-cooled solution of methyl ester **13** (0.1 g, 0.264 mmol) in MeOH (5 mL) 1N NaOH (0.792 mL) was added dropwise and the mixture was stirred at 0 °C for 15 min and at room temperature overnight. The MeOH was evaporated under reduced pressure, water was added and the solution extracted with diethyl ether (2 x 25 mL). The aqueous phase was then acidified with 5% citric acid and the product extracted with EtOAc. The organic layer was washed with brine, dried and evaporated to give the TLC pure title product **14** as white foam (0.09 g, 95%).

***N*-Boc-cAmp(Cbz)-Leu-Phe-OMe (15a).** Compound **6** (0.105 g, 0.288 mmol) in CH_2Cl_2 (5 mL) was treated with TFA·H_2N-Leu-Phe-OMe (0.117 g, 0.29 mmol) according to the general procedure B. Silica gel chromatography ($CHCl_3$/EtOAc 3:1) gave a pure product **15a** as a white foam (0.119 g, 64%); $[a]_D$ -65.9° (*c* 0.3, $CHCl_3$); IR ($CHCl_3$): ν 3421, 1741, 1681 cm^{-1}; ^1H NMR ($CDCl_3$): δ 0.69-1.00 [6H, m, Leu CH(CH_3)$_2$],

1.45 [9H, s, $C(CH_3)_3$], 1.59-1.68 [3H, m, Leu CH_2-$CH(CH_3)_2$], 2.00-2.40 (2H, m, Pro C^3H_2), 3.00-3.21 (2H, m, Phe β-CH_2) 3.38-3.60 (2H, m, Pro C^5H_2), 3.71 (3H, s, $COOCH_3$), 4.20-4.42 (3H, m, Pro α-CH, Pro C^4H and Leu α-CH), 4.84 (1H, m, Phe α-CH), 5.18 (2H, s, C_6H_5-CH_2-O-), 6.50 (1H, d, J = 7.6 Hz, Cbz-NH), 6.67 (1H, d, J = 7.6 Hz, Phe-NH), 7.03 (10H, m, aromatics), 7.63 (1H, d, J = 7.6 Hz, Leu NH). Anal. Calcd for $C_{34}H_{46}N_4O_8$: C, 63.93; H, 7.26; N, 8.77. Found: C, 63.73; H, 7.23; N, 8.74.

***N*-Boc-tAmp(Cbz)-Leu-Phe-OMe (15b).** Compound **14** (0.091 g, 0.250 mmol) in CH_2Cl_2 (5 mL) was treated with TFA·H_2N-Leu-Phe-OMe (0.101 g, 0.250 mmol) according to the general procedure B. Silica gel chromatography ($CHCl_3$/EtOAc 4:1) gave a pure product **15b** as a white foam (0.115 g, 72%); $[a]_D$ -36° (*c* 1.0, $CHCl_3$); IR ($CHCl_3$): ν 436, 1722, 1682 cm^{-1}; ^1H NMR ($CDCl_3$): δ 0.90 [6H, m, Leu CH-$(CH_3)_2$], 1.47 [9H, s, $C(CH_3)_3$], 1.57 [3H, m, Leu CH_2-CH-$(CH_3)_2$], 2.10-2.40 (2H, m, Pro C^3H_2), 3.10-3.18 (2H, m, Phe β-CH_2), 3.25 (2H, m, Pro C^5H_2), 3.74 (3H, s, $COOCH_3$), 4.29-4.33 (3H, m, Pro α-CH, Pro C^4H and Leu α-CH), 4.84 (1H, m, Phe α-CH), 5.18 (2H, s, C_6H_5-CH_2-O-), 6.55 (1H, m, Cbz-NH), 6.71 (1H, m, Phe NH), 7.04-7.42 (11H, m, aromatics and Leu NH). Anal. Calcd for $C_{34}H_{46}N_4O_8$: C, 63.93; H, 7.26; N, 8.77. Found: C, 63.71; H, 7.21; N, 8.72.

***N*-Boc-cAmp-Leu-Phe-OMe (16a).** The title compound **16a** was prepared starting from compound **15a** by following the general procedure A: **15a** (0.108 g, 0.169 mmol), MeOH (10 mL) and Pd/C (0.047 g), 3 h at room temperature, quantitative yield.

***N*-Boc-tAmp-Leu-Phe-OMe (16b).** The title compound **16b** was prepared starting from compound **15b** by following the general procedure A: **15b** (0.040 g, 0.063 mmol), MeOH (5 mL), Pd/C (0.004 g), 3 h at room temperature, quantitative yield.

***N*-Boc-cAmp(Boc)-Leu-Phe-OMe (17a).** To a solution of compound **16a** (0.025 g, 0.05 mmol) in EtOAc (5 mL) Boc_2O (0.022 g, 0.10 mmol) and TEA (0.014 mL, 0.10 mmol) were added and the mixture was stirred 1 h at room temperature. The mixture was diluted with EtOAc and washed with 5% citric acid, $NaHCO_3$ ss and brine. The organic layer was dried and evaporated under reduced pressure. The residue was purified by silica gel chromatography ($CHCl_3$/EtOAc 1:1) to give pure **17a** as a white foam (0.0185 g, 62%); $[a]_D$ -76.3° (*c* 0.35, $CHCl_3$); IR ($CHCl_3$): ν 3417, 1741, 1681 cm^{-1}; ^1H NMR ($CDCl_3$): δ 0.90 [6 H, m, Leu CH-(C*H*$_3$)$_2$], 1.47 [18H, s, 2C(CH_3)$_3$], 1.59 [3H, m, Leu C*H*$_2$-C*H*-(CH_3)$_2$], 2.00-2.38 (2H, m, Pro C^3H_2), 3.00-3.11 (2H, m, Phe β-CH_2), 3.37-3.57 (2H, m, Pro C^5H_2), 3.76 (3H, s, $COOCH_3$), 4.19-4.26 (3H, m, Leu α-CH, Pro α-CH, Pro C^4H), 4.83 (1H, m, Phe α-CH), 6.25 (1H, d, *J* = 7.6 Hz, Boc-NH), 6.61 (1H, d, *J* = 7.8 Hz, Phe NH), 7.12-7.40 (5H, m, aromatics), 7.76

(1H, d, *J* = 7.6 Hz, Leu NH). Anal. Calcd for $C_{31}H_{48}N_4O_8$: C, 61.57; H, 8.00; N, 9.26. Found: C, 61.69; H, 7.98; N, 9.28.

***N*-Boc-tAmp(Boc)-Leu-Phe-OMe (17b).** To a solution of compound **16b** (0.032 g, 0.063 mmol) in EtOAc (6.3 mL) Boc_2O (0.027 g, 0.126 mmol) and TEA (0.017 mL, 0.126 mmol) were added and the mixture was stirred 1 h at room temperature. The mixture was diluted with EtOAc and washed with 5% citric acid, $NaHCO_3$ ss and brine. The organic layer was dried and evaporated under reduced pressure. The residue was purified by silica gel chromatography ($CHCl_3$/EtOAc 4:1) to give pure **17b** as a white foam (0.021 g, 55%); $[a]_D$ -34.2° (*c* 0.6, $CHCl_3$); IR ($CHCl_3$): ν 3439, 1741, 1683 cm^{-1}; ^1H NMR ($CDCl_3$): δ 0.89 [6H, m, Leu CH-(C*H*$_3$)$_2$], 1.47 [18H, s, 2 C(CH$_3$)$_3$], 1.60 [3H, m, Leu C*H*$_2$-C*H*-(CH$_3$)$_2$], 2.03-2.35 (2H, m, Pro C^3H_2), 3.08-3.14 (2H, m, Phe β-CH_2), 3.31 and 3.53 (2H, m, Pro C^5H_2), 3.70 (3H, s, $COOCH_3$), 4.19-4.26 (3H, m, Leu α-CH, Pro α-CH, Pro C^4H), 4.83 (1H, m, Phe α-CH), 6.30 (1H, m, Boc-NH), 7.08-7.35 (7H, m, Phe NH, Leu NH and aromatics). Anal. Calcd for $C_{31}H_{48}N_4O_8$: C, 61.57; H, 8.00; N, 9.26. Found: C, 61.63; H, 8.01; N, 9.25.

***N*-Boc-cAmp(For)-Leu-Phe-OMe (18a).** To a solution of HCOOH (0.018 g, 0.40 mmol) in CH_2Cl_2 (5 mL) cooled at -15 °C, *i*BuOCOCl (0.052 mL, 0.40 mmol) and NMM (0.044 mL, 0.40 mmol) were added. The mixture was stirred for 10 min at the same temperature and then a solution in CH_2Cl_2 of **16a** (0.02

g, 0.0396 mmol) and NMM (0.044 mL, 0.40 mmol) was added. Work up according to general procedure B was then followed. Preparative layer chromatography ($CHCl_3$/EtOAc 1:2) gave a pure product **18a** as a amorphous solid (0.0125 g, 59%); $[a]_D$ -75.9° (*c* 0.5, $CHCl_3$); IR ($CHCl_3$) ν: 3419, 1741, 1675 cm^{-1}; ^1H NMR ($CDCl_3$): δ 0.86 [6H, m, Leu CH-(C*H*$_3$)$_2$], 1.47 [9H, s, C(CH_3)$_3$], 1.58 [3H, m, Leu C*H*$_2$-C*H*-(CH_3)$_2$], 2.06-2.32 (2H, m, Pro C^3H_2), 3.07-3.23 (2H, m, Phe β-CH_2), 3.42-3.57 (2H, m, Pro C^5H_2), 3.76 (3H, s, $COOCH_3$), 4.32 (1H, m, Leu α-CH), 4.40 (1H, m, Pro α-CH), 4.57 (1H, m, Pro C^4H), 4.86 (1H, m, Phe α-CH), 6.58 (1H, d, *J* = 8.0 Hz, Phe NH), 7.09-7.31 (5H, m, aromatics), 7.76 (2H, m, Leu NH and For NH), 8.11 (1H, s, HCO). Anal. Calcd for $C_{27}H_{40}N_4O_7$: C, 60.88; H, 7.57; N, 10.52. Found: C, 61.00; H, 7.55; N, 10.54.

***N*-Boc-tAmp(For)-Leu-Phe-OMe (18b).** To a solution of HCOOH (0.029 g, 0.63 mmol) in CH_2Cl_2 (5 mL) cooled at -15 °C, *i*BuOCOCl (0.082 mL, 0.63 mmol) and NMM (0.069 mL, 0.63 mmol) were added. The mixture was stirred for 10 min at the same temperature and then a solution in CH_2Cl_2 of **16b** (0.032 g, 0.063 mmol) and NMM (0.069 mL, 0.63 mmol) was added. Work up according to general procedure B was then followed. Silica gel chromatography ($CHCl_3$/EtOAc 1:2) gave a pure product **18b** as a white foam (0.024 g, 73%); $[a]_D$ -32.1° (*c* 0.65, $CHCl_3$); IR ($CHCl_3$): ν 3429, 1742, 1686 cm^{-1}; ^1H NMR ($CDCl_3$): δ 0.91 [6H, m, Leu CH-(C*H*$_3$)$_2$] 1.47 [9H, s, C(CH_3)$_3$],

1.62 [3H, m, Leu C*H*$_2$-C*H*-(CH$_3$)$_2$], 2.00-2.30 (2H, m, Pro C^{3}H$_2$), 3.07-3.15 (2H, m, Phe β-CH$_2$) 3.25 and 3.77 (2H, m, Pro C^{5}H$_2$), 3.74 (3H, s, COOCH$_3$), 4.35 (2H, m, Leu α-CH and Pro α-CH), 4.53 (1H, m, Pro C^{4}H), 4.83 (1H, m, Phe α-CH), 7.06-7.32 (8H, m, Leu NH, Phe NH, For NH and aromatics), 8.15 (1H, s, HCO). Anal. Calcd for $C_{27}H_{40}N_4O_7$: C, 60.88; H, 7.57; N, 10.52. Found: C, 61.01; H, 7.56; N, 10.56.

***N*-For-cAmp(For)-Leu-Phe-OMe (19a).** HCOOH (0.066 g, 1.44 mmol) in CH_2Cl_2 (5 mL) was treated with 2HCOOH·HN-cAmp-Leu-Phe-OMe (0.024 g, 0.048 mmol) according to the general procedure B. Preparative layer chromatography (EtOAc) gave a pure product **19a** as a white foam (0.008 g, 36%); [a]$_D$ -71.9° (*c* 0.5, $CHCl_3$); IR ($CHCl_3$): ν 3427, 1740, 1687 cm^{-1}; ^{1}H NMR ($CDCl_3$): δ 0.91 [6H, m, Leu CH-(C*H*$_3$)$_2$], 1.62 [3H, m, Leu C*H*$_2$-C*H*-(CH$_3$)$_2$], 2.16-2.31 (2H, m, Pro C^{3}H$_2$), 3.10-3.24 (2H, m, Phe β-CH$_2$), 3.60 and 3.77 (2H, m, Pro C^{5}H$_2$), 3.73 (3H, s, COOCH$_3$), 4.29 (1H, m, Leu α-CH), 4.52 (1H, m, Pro α-CH), 4.55 (1H, m, Pro C^{4}H), 4.86 (1H, m, Phe α-CH), 6.52 (1H, d, *J* = 7.6 Hz, Phe NH), 7.12-7.40 (5H, m, aromatics), 7.50 (1H, d, *J* = 7.4 Hz, Leu NH), 7.75 (1H, d, *J* = 7.8 Hz, For-NH), 8.15 (1H, s, HCO), 8.25 (1H, s, HCO). Anal. Calcd for $C_{23}H_{32}N_4O_6$: C, 59.99; H, 7.00; N, 12.17. Found: C, 59.75; H, 6.97; N, 12.21.

***N*-For-tAmp(For)-Leu-Phe-OMe (19b).** HCOOH (0.0566 g, 1.23 mmol) in CH_2Cl_2 (5 mL) was treated with 2HCOOH·HN-tAmp-Leu-Phe-OMe (0.029 g, 0.059 mmol)

according to the general procedure B. Preparative layer chromatography (EtOAc/MeOH 9:1) gave the pure product **19b** as a white foam (0.005 g, 26%); $[a]_D$ -35° (*c* 0.5, $CHCl_3$); IR ($CHCl_3$): ν 3425, 1742, 1685 cm^{-1}; ^1H NMR ($CDCl_3$): δ 0.89 [6H, m, Leu CH-(C*H*$_3$)$_2$], 1.27 [3H, m, Leu C*H*$_2$-C*H*-(CH_3)$_2$], 2.10-2.40 (2H, m, Pro C^3H_2), 3.11-3.27 (2H, m, Phe β-CH_2), 3.60 and 3.77 (2H, m, Pro C^5H_2), 3.72 (3H, s, $COOCH_3$), 4.36 (1H, m, Leu α-CH), 4.58 (2H, m, Pro α-CH and Pro C^4H), 4.80 (1H, m, Phe α-CH), 6.53 (1H, d, *J* = 7.6 Hz, Phe NH), 7.00-7.50 (7H, m, Leu NH, For NH and aromatics), 8.13 (1H, s, HCO), 8.21 (1H, s, HCO). Anal. Calcd for $C_{23}H_{32}N_4O_6$: C, 59.99; H, 7.00; N, 12.17. Found: C, 59.76; H, 6.98; N, 12.20.

2.7.4.3 Biological assays

Cell preparation

Cells were obtained from the blood of healthy subjects, and human peripheral blood neutrophils were purified by using the standard techniques of dextran (Pharmacia, Uppsala, Sweden) sedimentation, centrifugation on Ficoll-Paque (Pharmacia), and hypotonic lysis of contaminating red cells. Cells were washed twice and resuspended in Krebs-Ringer phosphate (KRPG), pH 7.4, at final concentration of 50 x 10^6 cells/mL and kept at room temperature until used. Neutrophils were 98-100% viable, as determined using the Trypan Blue exclusion test. The study was

approved by the local Ethics Committee and informed consent was obtained from all participants.

Random locomotion

Random locomotion was performed with 48-well microchemotaxis chamber (Bio Probe, Milan, Italy) and migration into the filter was evaluated by the leading-front method.[96] The actual control random movement is 35 ± 3 μm SE of 10 separate experiments performed in duplicate.

Chemotaxis

Each peptide was added to the lower compartment of the chemotaxis chamber. Peptides were diluted from a stock solution with KRPG containing 1 mg/mL of bovine serum albumin (BSA; Orha Behringwerke, Germany) and used at concentrations ranging from 10^{-13} to 10^{-5} M. Data were expressed in terms of chemotactic index (C.I.), which is the ratio: (migration toward test attractant minus migration toward the buffer/migration toward the buffer); the values are the mean of six separate experiments performed in duplicate. Standard errors are in the 0.02-0.09 C.I. range.

Superoxide anion (O_2^-) production

This anion was measured by the superoxide dismutase inhibitable reduction of ferricytochrome *c* (Sigma, USA)

modified for microplate-based assays. Tests were carried out in a final volume of 200 μL containing 4 x 10^5 neutrophils, 100 nmol cytochrome *c* and KRPG. At zero time different amounts (10^{-10} -5 x 10^{-5}M) of each peptide were added and the plates were incubated into a microplate reader (Ceres 900, Bio-TeK Instruments, Inc.) with the compartment temperature set at 37 °C. Absorbance was recorded at 550 and 468 nm. The difference in absorbance at the two wavelengths was used to calculate nmol of O_2^- produced using an absorptivity for cytochrome *c* of 18.5 $mmol^{-1}$ cm^{-1}. Neutrophils were incubated with 5 μg/mL cytochalasin B (Sigma) for 5 min prior to activation by peptides. Results were expressed as net nmol of O_2^- per 1 x 10^6 cells per 5 min and are the mean of six separate experiments performed in duplicate. Standard errors are in 0.1-4 nmol O_2^- range.

Enzyme assay

The release of neutrophil granule enzymes was evaluated by determination of lysozyme activity, modified for microplate based assays. Cells, 3 x 10^6/well, were first incubated in triplicate wells of microplates with 5 μg/mL cytochalasin B at 37 °C for 15 min and then in the presence of each peptide at a final concentration of 10^{-10} -5 x 10^{-5} M for a further 15 min. The plates were then centrifuged at 400g for 5 min and the lysozyme was quantified nephelometrically by the rate of lysis of cell wall suspension of Micrococcus lysodeikticus. The reaction rate was

measured using a microplate reader at 465 nm. Enzyme release was expressed as a net percentage of total enzyme content released by 0.1% Triton X-100. Total enzyme activity was 85 ± 1 μg per 1 x 10^7 cells/min. The values are the mean of five separate experiments done in duplicate. Standard errors are in the range 1-6%.

Acknowledgments

This work was supported by grants from Fondazione Cassa di Risparmio di Ferrara. We are grateful to Banca del Sangue of Ferrara for providing fresh blood.

References

1. Becker, E. L.; Freer, R. J.; Toniolo, C.; Balaram, P. In *Membrane Receptors and Cellular Regulation*, Czech MP, Kahn CR (Eds). Liss: New York, **1985**, pp 129-134, and refs. cited therein.
2. Kobayashi, S. D.; Voyich, J. M.; De Leo, F. R. *Microbes Infect.* **2003**, *5*, 1337.
3. Schiffmann, E.; Cororan, B. A.; Wahl, S. M. *Proc. Natl. Acad. Sci. USA* **1975**, *72*, 1059.
4. Radel, S.; Genco, R. J.; De Nardin, E. *Infect. Immun.* **1994**, *62*, 1726.
5. Marasco, W. A.; Phan, S. H.; Krutzsch, H.; Showell, H. J.; Feltner, D. E.; Nairn, R.; Becker, E. L.; Ward, P. A. *J. Biol. Chem.* **1984**, *259*, 5430.
6. Delves, P. J.; Roitt, I. M. *Adv. Immunol.* **2000**, *343*, 108.
7. Niggli, V. *Int. J. Biochem. Cell Biol.* **2003**, *35*, 1619.

8. Gallin, J. I. In *Fundamental Immunology.* William, E. P. (Ed.), Raven Press, New York, **1993**, pp. 1015-1032.
9. Tramont, E. C.; Hoover, D. L. In *Principles and Practice of Infectious Diseases. Mandell*, G. L.; Bennet, J. E.; Dolin, R. (Eds.), Churchill Livingstone, Philadelphia, **2000**, pp. 31-38.
10. Hampton, M. B.; Kettle, A. J.; Winterbourn, C. *Blood* **1998**, *92*, 3007.
11. Cedergre, J.; Follin, P.; Forslund, T.; Lindmark, M.; Sundqvist, T.; Skogh, T. *Apmis* **2003**, *111*, 963.
12. Klebanoff, S. J. *J. Leukoc. Biol.* **2005**, *77*, 598.
13. Liu, Y.; Shaw, S. K.; Ma, S., Yang, L.; Luscinskas, F. W.; Parkos, C. A. *Immunol. J.* **2004**, *172*, 7.
14. Boulay, F.; Tardif, M.; Brouchon, L.; Vignais, P. *Biochem. Biophys. Res. Commun.* **1990**, *16*, 1103.
15. Ye, R. D.; Cavanag, S. L.; Quehenbergher, O.; Prossnitz, E. R.; Cohrane, C. G. *Biochem. Biophys. Res. Commun.* **1992**, *184*, 582.
16. Murphy, P. M.; Ozcelik, T.; Kenney, R. T.; Tiffany, H. I.; McDermott, D.; Francke, U. *J. Biol. Chem.* **1992**, *267*, 7637.
17. Bao, L.; Gerard, N. P.; Eddy, R. Jr.; Shows, T. B.; Gerard, C. *Genomics* **1992**, *13*, 437.
18. Dillon, S. B.; Verghese, M. W.; Snyderman, R. *Virchows Arch. B Cell. Pathol. Mol.* **1988**, *55*, 65.
19. Klinker, J. F.; Wenzel-Seifert, K.; Seifert, R. *Gen. Pharmacol.* **1996**, *27*, 33.
20. Seifert, R.; Schultz, G.; *Rev. Physiol. Biochem. Pharmac.* **1991**, *117*, 1.
21. Wenzel-Seifert, K.; Seifert, R. In *Physiology of Inflammation.* Ley, K. (Ed.), **2001**. Oxford University Press, Oxford, pp. 146-188.
22. Offermanns, S.; Simon, M. I. *J. Biol. Chem.* **1995**, *270*, 15175.

23. Sunahara, R. K.; Dessauer, C. W.; Gilman, A. G. *Ann. Rev. Pharmacol. Toxicol.* **1996**, *36*, 461.
24. Camps, M.; Carozzi, A.; Schnabel, P.; Scheer, A.; Parker, P. J.; Gierschik, P. *Nature* **1992**, *360*, 684.
25. Jiang, H.; Kuang, Y.; Wu, Y.; Smrcka, A.; Simon, M. I.; Wu, D. *J. Biol. Chem.* **1996**, *271*, 13430.
26. Leopoldt, D.; Hanck, T.; Exner, T.; Maier, U.; Wetzker, R.; Nürnberg, B. *J. Biol. Chem.* **1998**, *273*, 7024.
27. Hirsch, E.; Katanaev, V. L.; Garlanda, C.; Azzolino, O.; Pirola, L.; Silengo, L.; Sozzani, S.; Mantovani, A.; Altruda, F.; Wymann, M. P. *Science* **2000**, *287*, 1049.
28. Li, Z.; Jiang, H.; Xie, W.; Zhang, Z.; Smrcka, A. V.; Wu, D. *Science* **2000**, *287*, 1046.
29. Sasaki, T.; Irie-Sasaki, J.; Jones, R. G.; Oliveira-dos-Santos, A. J.; Stanford, W. L.; Bolon, B.; Wakeham, A.; Itie, A.; Bouchard, D.; Kozieradzki, I.; Joza, N.; Mak, T. W.; Ohashi, P. S.; Suzuki, A.; Penninger, J. M. *Science* **2000**, *287*, 1040.
30. Cavicchioni, G.; Fraulini, A.; Turchetti, M.; Varani, K.; Falzarano, S.; Pavan, B.; Spisani, S. *Eur. J. Pharmacol.* **2005**, *512*, 1.
31. Torres, M.; Hall, F. L.; O'Neill, K. *Immunol.* **1993**, *150*, 1563.
32. Rane, M. J.; Carrithers, S. L.; Arthur, J. M.; Klein, J. B.; McLeish, K. R. *J. Immunol.* **1997**, *159*, 5070.
33. Ptasznik, A.; Traynor-Kaplan, A.; Bokoch, G. M. *J. Biol. Chem.* **1995**, *270*, 19969.
34. Ali, H.; Richardson, R. M.; Tomhave, E. D.; Didsbury, J. R.; Snyderman, R. *J. Biol. Chem.* **1993**, *268*, 24247.
35. Tardif, M.; Mery, L.; Brouchon, L; Boulay, F. *J. Immunol.* **1993**, *150*, 3534.
36. Prossnitz, E. R. *J. Biol. Chem.* **1997**, *272*, 15213.

37. Hsu, M. H.; Chiang, S. C.; Ye, R. D.; Prossnitz, E. R. *J. Biol. Chem.* **1997**, 272, 29426.
38. Bennett, T. A.; Maestas. D. C.; Prossnitz, E. R. *J. Biol. Chem.* **2000**, *32*, 24590.
39. Becker, E. L.; Forouhar, F. A.; Grunnet, M. L.; Boulay, F.; Tardif, M.; Bormann, B. J.; Sodja, D.; Ye, R. D.; Woska Jr., J. R.; Murphy, P. M. *Cell Tissue Res*. **1998**, *292*, 129.
40. Le, Y.; Murphy, P. M.; Wang, J. M. *Trends Imm.* **2002**, *23*, 541.
41. Carp, H. *J. Exp. Med.* **1982**, *155*, 264.
42. Le, Y.; Yang, Y.; Cui, Y.; Yazawa, H.; Gong, W.; Qiu, C.; Wang, J. M. *Int. Immunopharm.* **2002**, *2*, 1.
43. Walther, A.; Rieheman, K.; Gerke, V. *Mol.Cell.* **2000**, *5*, 831.
44. Showell, H. J.; Freer, R. J.; Zigmond, S. H.; Schiffmann, E.; Aswanikumar, S.; Corcoran, B. A.; Becker, E. L. *J. Exp. Med.* **1976**, *143*, 1154.
45. Freer, R. J.; Day, A. R.; Radding, J. A.; Schiffmann, E.; Aswanikumar, S.; Showell, H. J.; Becker, E. L. *Biochemistry* **1980**, *19*, 2404.
46. Freer, R. J.; Day, A. R.; Muthukumaraswamy, N.; Pinon, D.; Wu, A.; Showell, H. J.; Becker, E. L. *Biochemistry* **1982**, *21*, 257.
47. Iqbal, M.; Balaram, P.; Showell, H. J.; Freer, R. J.; Becker, E. L. *FEBS Lett.* **1984**, *165*, 171.
48. Sukumar, M.; Raj, P. A.; Balaram, P.; Becker, E. L. *Biochem. Biophys. Res. Commun* **1985**, *128*, 339.
49. Rot, A.; Henderson, L. E.; Copeland, T. D.; Leonard, E. J. *Proc. Natl. Acad. Sci. USA* **1987**, *84*, 7967.
50. Toniolo, C.; Crisma, M.; Va1le, G.; Bonora, G. M.; Polinelli, S.; Becker, E. L.;Freer, R. J.; Sudhanand, R.; Balaji Rao, P.; Balaram, P.; Sukumar. M. *Peptide Res.* **1989**, *2*, 275.

51. Michel, A. G.; Lajoie, G.; Hassani, C. A. *Int. J. Pept. Protein Res.* **1990**, *36*, 489.
52. Caterina, M. J.; Devreotes, P. N. *FASEB J.* **1991**, *5*, 3078.
53. Radel, S.; Genco, R. J.; De Nardin, E. *Biochem. Int.* **1991**, *25*, 745.
54. Quehenberger, O.; Prossnitz, E. R.; Cavanagh, S. L.; Cochrane, C. G.; Ye, R. D. *J. Biol. Chem.* **1993**, *268*, 18167.
55. Lala, A.; Sharma, A.; Sojar, H. T.; Radel, S.; Genco, R. J.; De Nardin, E. *Biochim. Biophys. Acta* **1993**, *1178*, 302.
56. Klotz, K. N.; Krotec, K. L.; Gripentrog, J.; Jesaitis, A. J. *J. Immunol.* **1994**, *152*, 801.
57. Dalpiaz, A.; Spisani, S.; Biondi, C.; Fabbri, E.; Nalli, M.; Ferretti, M. E. *Curr. Drug Targets-Immune Metab.Disord.* **2003**, *3*, 33.
58. Cavicchioni, G.; Turchetti, M.; Spisani, S. *J. Pept. Res.* **2002**, *60*, 223.
59. Spisani, S.; Traniello, S.; Cavicchioni, G.; Formaggio, F.; Crisma, M.; Toniolo, C. *J. Pept. Res.* **2002**, *7*, 56.
60. Spisani, S.; Turchetti, M.; Varani, K.; Falzarano, S.; Cavicchioni, G. *Eur. J. Pharmacol.* **2003**, *469*, 13.
61. Cavicchioni, G.; Spisani, S. *J. Pept. Res.* **2001**, *58*, 257.
62. Dentino, A. R.; Antony Raj, P.; Bhandary, K. K.; Wilson, M. E.; Levine, M. J. *J. Biol. Chem.* **1991**, *266*, 18460.
63. Torrini, I.; Pagani Zecchini, G.; Paglialunga Paradisi, M.; Lucente, G.; Gavuzzo, E.; Mazza, F.; Pochetti, G.; Spisani, S.; Giuliani, A. L. *Int. J. Pept. Protein Res.* **1991**, *38*, 495.
64. Cavicchioni, G.; Varani, K.; Niccoli, S.; Rizzati, O.; Spisani, S. *J. Pept. Res.* **1999**, *54*, 336.
65. Dalpiaz, A.; Scatturin, A.; Vertuani, G.; Pecoraro, R.; Borea, P. A.; Varani, K.; Traniello, S.; Spisani, S. *Eur. J. Pharmacol.* **2001**, *411*, 327.

66. Prossnitz, E. R.; Gilbert, T. L.; Chiang, S.; Campbell, J. J.; Qin, S.; Newman, W.; Sklar, L. A.; Ye, R. D. *Biochemistry* **1999**, *38*, 2240.
67. Derian, C. K.; Solomon, H. F.; Higgins, J. D. III; Beblavy, M. J.; Santulli, R. J.; Bridger, G. J.; Pike, M. C.; Kroon, D. J.; Fischman, A. J. *Biochemistry* **1996**, *35*, 1265.
68. Higgins, J. D. III; Bridger, G. J.; Derian, C. K.; Beblavy, M. J.; Hernandez. P. E.; Gaul, F. E.; Abrams, M. J.; Pike, M. C.; Solomon, H. F. *J. Med. Chem.* **1996**, *39*, 1013.
69. Witkowska, R.; Zabrocki, J.; Spisani S.; Falzarano, M. S.; Toniolo, C.; Formaggio, F. *J. Pept. Sci.* **2003**, *9*, 354.
70. Mills, J. S.; Miettinen, H. M. Barnidge, D.; Vlases, M. J.; Wimer-Mackin, S.; Dratz, E. A.; Sunner, J.; Jesaitis, J. *J. Biol. Chem.* **1998**, *273*, 10428.
71. Mollica, A.; Paglialunga Paradisi, M.; Torino, D.; Spisani, S.; Lucente, G. *Amino Acids* **2006**, *30*, 453.
72. Lucente, G.; Paradisi Paglialunga, M.; Giordano, C.; Sansone, A.; Torino, D.; Spisani, S. *Amino Acids* **2008**, *35*, 329.
73. Giordano, C.; Lucente, G.; Masi, A; Paglialunga Paradisi, M.; Sansone, A.; Spisani, S. *Amino Acids* **2007**, *33*, 477.
74. Koksch, B.; Dahl, C.; Radics, G.; Vocks, A.; Arnold, K.; Arnhold, J.; Sieler, J.; Burger, K. *J. Pept. Sci.* **2004**, *10*, 67.
75. Prossnitz, E. R. *Pharmacol. Ther.* **1997**, *74*, 73.
76. Toniolo, C.; Bonora, G. M.; Showell, H.; Freer, R. J.; Becker, E. L. *Biochemistry* **1984**, *23*, 698.
77. Dentino, A. R.; Raj, P. A.; De Nardin, E. *Arch. Biochem. Biophys.* **1997**, *337*, 267.
78. Spisani, S.; Cavalletti, T.; Gavioli, R.; Scatturin, A.; Vertuani, G.; Traniello, S. *Inflammation* **1986**, *10*, 363.

79. Toniolo, C.; Crisma, M.; Pegoraro, S.; Valle, G.; Bonora, G. M.; Becker, E. L.; Polinelli, S.; Boesten, W. H. J.; Schoemaker, H. E.; Meijer, E. M.; Kamphuis, J.; Freer, R. *Pept. Res.* **1991**, *4*, 66.
80. Dugas, H.; Laroche, M.; Ptak, M.; Labbè, H. *Int. J. Pept. Protein Res.* **1993**, *41*, 595.
81. Prasad, S.; Rao, R. B.; Bergstrand, H.; Lundquist, B.; Becker, E. L.; Balaram, P. *Int. J. Pept. Protein Res.* **1996**, *48*, 312.
82. Formaggio, F.; Pantano, M.; Crisma, M.; Toniolo, C.; Boesten, W. H. J.; Schoemaker, H. E.; Kamphuis, J.; Becker, E. L. *Bioorg. Med. Chem. Lett.* **1993**, *3*, 953.
83. Torrini, I.; Paglialunga Paradisi, M.; Pagani Zecchini, G.; Lucente, G.; Gavazzo, E.; Mazza, F.; Pochetti, G.; Traniello, S.; Spisani, S. *Biopolymers* **1997**, *42*, 415.
84. Pagani Zecchini, G.; Morera, E.; Nalli, M.; Paglialunga Paradisi, M.; Lucente, G.; Spisani, S. *Farmaco* **2001**, *56*, 851.
85. Giordano, C.; Lucente, G.; Nalli, M.; Pagani Zecchini, G.; Paglialunga Paradisi, M.; Varani, K.; Spisani, S. *Farmaco* **2003**, *58*, 1121.
86. Giordano, C.; Lucente, G.; Mollica, A.; Nalli, M.; Pagani Zecchini, G.; Paglialunga Paradisi, M.; Gavazzo, E.; Mazza, F.; Spisani, S. *J. Pept. Sci.* **2004**, *10*, 510.
87. Seebach, D.; Abele, S.; Sifferlen, T.; Hänggi, M.; Gruner, S.; Seiler, P. *Helv. Chim. Acta* **1998**, *81*, 2218.
88. Seebach, D.; Matthews, J. L. *J. Chem. Soc. Chem. Commun.* **1997**, *21*, 2015.
89. Gellman, S. H. *Acc. Chem. Res.* **1997**, *31*, 173.
90. Karle, I. L.; Pramanik, A.; Banerjee, A.; Bhattacharjya, S.; Balaram, P. *J. Am. Chem. Soc.* **1997**, *119*, 9087.
91. Gopi, H. N.; Roy, R. S.; Raghothama, S. R.; Karle, I. L.; Balaram, P. *Helv. Chim. Acta* **2002**, *85*, 3313.

92. Lajoie, G.; Kraus, J-L. *Peptides* **1984**, *5*, 653.
93. Palomo, C.; Oiarbide, M.; Bindi, S. *J. Org. Chem.* **1998**, *63*, 2469.
94. Wu, Y-D.;Wang, D-P. *J. Am. Chem. Soc.* **1998**, *120*, 13485.
95. Schumann, F.; Müller, A.; Koksch, M.; Müller, G.; Sewald, N. *J. Am. Chem. Soc.* **2000**, *122*, 12009.
96. Zigmond, S. H.; Hirsch, J. G. *J. Exp. Med.* **1973**, *137*, 387.
97. Harvath, L. In *Cell motility factors*. Goldberg ID (Ed) Birkhäuser, Basel, **1991**, pp 35-52
98. Le, Y.; Zhou, Y.; Tao, H.; Wang, J. M. *Clin. Exp. All. Rev.* **2004**, *4*, 155.
99. Fabbri, E.; Spisani, S.; Biondi, C.; Barbin, L.; Colamussi, M. L.; Cariani, A.; Traniello, S.; Torrini, I.; Ferretti, M. E. *Biochim. Biophys. Acta* **1997**, *1359*, 233.
100. Selvatici, R.; Falzarano, S.; Mollica, A.; Spisani, S. *Eur. J. Pharmacol.* **2006**, *534*, 1.
101. Miyazaki, M.; Kodama, H.; Fujita, I.; Hamasaki, Y.; Miyazaki, S. *J. Biochem.* **1995**, *117*, 489.
102. Rathore, R. S. *Biopolymers (Pept. Sci.)* **2005**, *80*, 651.
103. Pagani Zecchini, G.; Paglialunga Paradisi, M.; Torrini, I.; Lucente, G.; Gavazzo, E.; Mazza, F.; Pochetti, G.; Paci, M.; Sette, M.; Di Nola, A.; Veglia, G.; Traniello, S.; Spisani, S. *Biopolymers* **1993**, *33*, 437.
104. Kotha, S.; Sreenivasachary, N.; Mohanraja, K.; Durani, S. *Bioorg. Med. Chem. Lett.* **2001**, *11*, 1421.
105. Aschi, M.; Lucente, G.; Mazza, F.; Mollica, A.; Morera, E.; Nalli, M.; Paglialunga Paradisi, M. *Org. Biomol. Chem.* **2003**, *1*, 1980.
106. Rao, B. N. N.; Kumar, A.; Balaram, H.; Ravi, A.; Balaram, P. *J. Am. Chem. Soc.* **1983**, *105*, 7423.
107. Millet, R.; Goossens, L.; Goossens, J-F.; Chavatte, P.; Bertrand-Caumont, K.; Houssin, R.; Henichart, J-P. *J. Pept. Sci.* **2001**, *7*, 323.

108. Hodgson, D. M.; Thompson, A. J.; Wadman, S.; Keats, C. J. *Tetrahedron* **1999**, *55*, 10815.

109. Conti, C.; De Amici, M.; Joppolo di Ventimiglia, S.; Stensbol, T. B.; Madsen, U.; Brauner-Osborne, H.; Russo, E.; De Sarro, G.; Bruno, G.; De Micheli, C. *J. Med. Chem.* **2003**, *46*, 3102.

110. Park, K-H.; Olmstead, M. M.; Kurth, J. *J. Org. Chem.* **1998**, *63*, 113.

111. Kotha, S.; Sreenivasachary, N. *Bioorg. Med. Chem. Lett.* **1998**, *8*, 257.

112. Ohfune, Y.; Shinada, T. *Eur. J. Org. Chem.* **2005**, *9*, 5127.

113. Toniolo, C.; Formaggio, F.; Kaptein, B.; Broxterman Q. B. *Synlett* **2006**, *9*, 1295.

114. Prasad, S.; Mathur, A.; Sharma, R.; Gupta, N.; Ahuja, R.; Jaggi, M.; Singh, A.; Mukherjee, R. *Int. J. Pept. Res. Ther.* **2006**, *12*, 179.

115. Cativiela, C.; Diaz-de-Villegas, M. D. *Tetrahedron Asymm.* **2000**, *11* 645.

116. Toniolo, C. *Janssen Chim. Acta* **1993**, *11*, 10.

117. Rovero, P.; Pellegrini, M.; Di Fenza, A.; Meini, S.; Quartara, L.; Maggi, C. A.; Formaggio, F.; Toniolo, C.; Mierke, D. F. *J. Med. Chem.* **2001**, *44*, 274.

118. Morera, E.; Lucente, G.; Ortar, G.; Nalli, M.; Mazza, F.; Gavuzzo, E.; Spisani, S. *Bioorg. Med. Chem.* **2002**, *10*, 147.

119. Fink, B. E.; Kym, P. R.; Katzenellenbogen, J. A. *J. Am. Chem. Soc.* **1998**, *120*, 4334.

120. Taylor, R.; Kennard, O.; Versichel, W. *Acta Cryst.* **1984**, *B40*, 280.

121. Wilmot, C. M.; Thornton, J. M. *Protein Eng.* **1990**, *3*, 479.

122. Benedetti, E.; Pedone, C.; Toniolo, C.; Nemethy, G.; Pottle, M. S.; Scheraga, H. A. *Int. J. Pept. Protein Res.* **1980**, *16*, 156.

123. Malathy Sony, S. M.; Saraboji, K.; Sukumar, N.; Ponnuswamy, M. N. *Biophys. Chem.* **2006**, *120*, 24.

124. Cirilli, M.; Coiro, V. M.; Di Nola, A.; Mazza, F. *Biopolymers* **1998**, *46*, 239.

125. The *CCP*4 suite: programs for protein crystallography. Collaborative Computational Project, Number 4. *Acta Crystallogr.* **1994**, *D50*, 760.

126. Burla, M. C.; Caliandro, L.; Camalli, M.; Carrozzini, B.; Cascarano, G. L.; De Caro, C.; Giacovazzo, C.; Polidori, G.; Siliqi, D.; Spagna, R. *J. Appl. Cryst.* **2007**, *40*, 609.

127. Le, Y.; Li, B.; Gong, W.; Shen, W.; Hu, J.; Dunlop, N. M.; Oppenheim, J. J.; Wang, J. M. *Immunol. Rev.* **2000**, *177*, 185.

128. Rabiet, M-J.; Huet, E.; Boulay, F. *Biochimie* **2007**, *89*, 1089.

129. Cavicchioni, G.; Fraulini, A.; Falzarano, S.; Spisani, S. *Bioorg. Chem.* **2006**, *34*, 298.

130. Wunsch, E. In *Methoden der organischen Chemie*, Muller, E. (Ed) Houben-Weyl: vol 15/1. Thieme,Stuttgart, **1974**, pp 46-405.

131. Mladenova-Orlinova, L.; Blaha, K.; Rudinger, J. *Coll. Czech. Chem. Commun.* **1967**, *32*, 4070.

132. Torrini, I.; Mastropietro, G.; Pagani Zecchini, G.; Paglialunga Paradisi, M.; Lucente, G.; Spisani, S. *Arch. Pharm. Pharm. Med. Chem.* **1998**, *331*, 170.

133. Leleu, S.; Penhoat, M.; Bouet, A.; Dupas, G.; Papamicaeel, C.; Marsais, F.; Levacher, V. *J. Am. Chem. Soc.* **2005**, *127*, 15668.

134. Fabbri, E.; Spisani, S.; Barbin, L.; Bondi, C.; Buzzi, M.; Traniello, S.; Pagani Zecchini, G.; Ferretti, M. E. *Cell. Signalling* **2000**, *12*, 391.

135. Mollica, A.; Paglialunga Paradisi, M.; Varani, K.; Spisani, S.; Lucente, G. *Bioorg. Med. Chem.* **2006**, *14*, 2253.

136. Karoyan, P.; Sagan, S.; Lequin, O.; Quancard, J.; Lavielle, S.; Chassaing, G. *Targets Heterocycl. Syst.* **2004**, *8*, 216.

137. Kolodziej, S. A.; Nikiforovich, G. V.; Skeean, R.; Lignon, M. F.; Martinez, J.; Marshall, G. R. *J. Med. Chem.* **1995**, *38*, 137.
138. Paglialunga Paradisi, M.; Mollica, A.; Cacciatore, I.; Di Stefano, A.; Pinnen, F.; Caccuri, A.; Ricci, G.; Duprè, S.; Spirito, A.; Lucente, G. *Bioorg. Med. Chem.* **2003**, *11*, 1667.
139. Kondo, T.; Nekado, T.; Sugimoto, I.; Ochi, K.; Takai, S.; Kinoshita, A.; Tajima, Y.; Yamamoto, S.; Kawabata, K.; Nakai, H.; Toda, M. *Bioorg. Med. Chem.* **2007**, *15*, 2631.
140. Sakashita, H.; Kitajima, H.; Nakamura, M.; Akahoshi, F.; Hayashi, Y. *Bioorg. Med. Chem. Lett.* **2005**, *15*, 2441.
141. Patchett, A. A.; Witkop, B. *J. Am. Chem. Soc.* **1957**, *79*, 185.
142. (a) Bridges, R. J.; Stanley, M. S.; Anderson, M. W.; Cotman, C. W.; Chamberlin, A. R. *J. Med. Chem.* **1991**, *34*, 717; (b) Barraclough, P.; Dieterich, P.; Spray, C. A.; Young, W. *Org. Biomol. Chem.* **2006**, *4*, 1483.
143. Spisani, S.; Giuliani, A. L.; Cavalletti, T.; Zaccarini, M.; Milani, L.; Gavioli, R.; Traniello, S. *Inflammation* **1992**, *16*, 147.
144. Ferretti, M. E.; Nalli, M.; Biondi, C.; Colamussi, M. L.; Pavan, B.; Traniello, S.; Spisani, S. *Cell. Signalling* **2001**, *13*, 233.
145. Haines, K. A.; Kolasinski, S. L.; Cronstein, B. N.; Reibman, J.; Gold, L. I.; Weissmann, G. *J. Immunol.* **1993**, *151*, 1491.

CHAPTER 3

(*S*)-Aziridine-2-carboxylic acid. A constrained and reactive amino acid unit for the synthesis of bioactive peptide analogues

3.1 Reactivity of aziridine system

The aziridine functionality, or alternatively named the azaethylene or ethylenimine unit, represents one of the most valuable three membered ring systems, because of its widely recognized versatility as a significant building block in organic synthesis for its ability to function as reactive electrofilic substrates. Aziridines are saturated three-membered heterocycles containing one nitrogen atom (Figure 1).

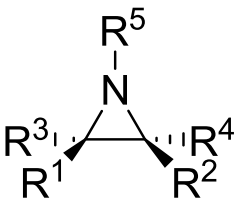

Figure 1. Structure of aziridine.

Like other three membered rings such as cyclopropanes and epoxides, aziridines are highly strained. Aziridines have a significantly higher barrier to pyramidal inversion of the nitrogen atom than acyclic amines (18.9 kcal/mol for the parent, unsubstituted aziridine, compared to 5-6 kcal/mol for most

amines).[1] This gives rise to two distinguishable invertomers: one with the nitrogen substituent *cis* to the carbon substituent and another with a *trans* relationship between the two substituents (Figure 2).[2]

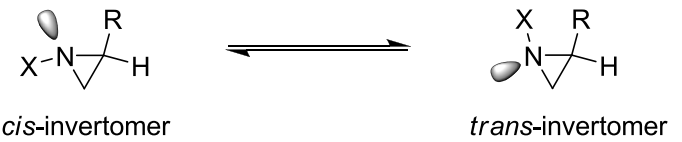

Figure 2. Due to the high nitrogen inversion barrier of aziridines, the *cis* and *trans* invertomers are two distinct species at low temperatures.

The inherent reactivity of aziridines is due, in large part, to ring strain energy which is similar to that of cyclopropane (27 kcal mol^{-1}), reflecting high bond-angle strain.[3] Ring strain renders aziridines susceptible to the ring-opening reactions. Nucleophilic ring opening (NRO) is the most thoroughly studied manipulation of aziridines.[4] Where an aziridine is unsymmetrically-substituted, reaction with a nucleophile can lead to two products of ring-opening (Scheme 1). As would be expected, most nucleophiles preferentially direct their attack to the site of lesser substitution, though electronic considerations (for instance in the ring-opening of 2-arylaziridines) may perturb this preference.

The nitrogen substituent plays a crucial role in the NRO of aziridines. In general, two types of aziridine can be considered: activated and unactivated. The former contain substituents capable of stabilising the developing negative charge on

nitrogen during NOR. The latter, also known as simple aziridines, are generally unsubstituted or with alkyl substitution on nitrogen.

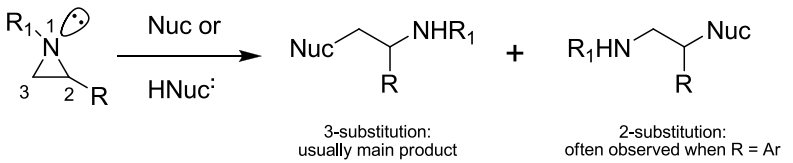

Scheme 1. Regioselective nucleophilic attack at the C-2 or C-3 positions.

Despite high ring strain energy, unactivated aziridines are generally not extremely susceptible to ring opening via nucleophilic attack. Activation by protonation, formation of a Lewis acid adduct, or replacement of the N hydrogen with an electron-withdrawing substituent (e.g. acyl, carbamoyl, sulfonyl) increases susceptibility to ring opening through nucleophilic attack.[5]

3.2 (*S*)-Aziridine-2-carboxylic acid containing peptides

(*S*)-aziridine-2-carboxylic acid (Azy) is the lowest cyclic homologue of (*S*)-proline. Among cyclic imino acids that mimic proline we can cite (*S*)-azetidin-2-carboxylic acid and (*S*)-piperidin-2-carboxylic acid. The former is a lower homologue of proline, containing a four-membered ring, the latter is a higher homologue of proline, containing a six-membered ring, in place of the five-membered ring of proline (Figure 3). Proline is

unique among naturally occurring amino acids whose C^{α}-N is a part of pyrrolidine ring. This cyclic side chain imposes strong restraints on peptide conformation, since the nitrogen is consequently unable to act as a hydrogen bond donor.

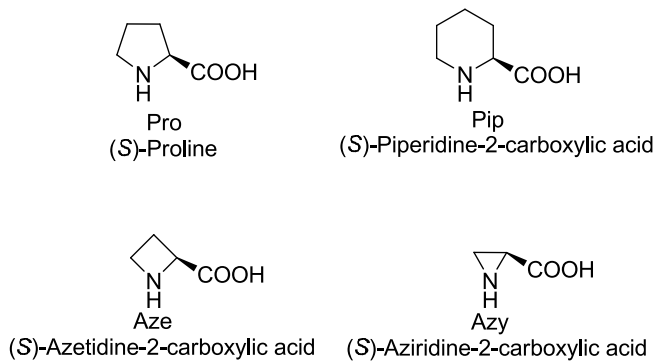

Figure 3. Structure of (*S*)-proline and its homologues.

The replacement of Pro with its homologues is of particular interest to compare the structural effect on conformation of non proteinic cyclic amino acids with that of proline which is a natural residue.

For both the structural features and chemical reactivity of aziridine system, (*S*)-aziridine-2-carboxylic acid (Azy) represents a very challenging research subject in the field of peptide chemistry. Azy, as well as Azy containing peptides, have found useful application as intermediates in the synthesis of various amino acid and peptide derivatives. They are useful for the indirect introduction into the backbone of different residues and fragments derived from Azy ring opening or

rearrangement.[6,7] This latter property of Azy containing peptides has been successfully followed for the synthesis of irreversible protease inhibitors.[8]

The acylation of the Azy nitrogen atom (i.e. the incorporation into the peptide backbone) leads to an amide bond with very peculiar structure and reactivity.

Amide bonds in peptides and proteins typically adopt planar *cis* or *trans* conformations by a partial π-electron delocalization between carbonyl and amine units which causes the four adjacent bonded atoms of the peptide linkage to become a coplanar, rigid unit (Figure 4). This produces a high barrier (16-22 kcal mol^{-1}) to rotation about the bonds within the linkage[9,10] which is required for *cis-trans* isomerization.

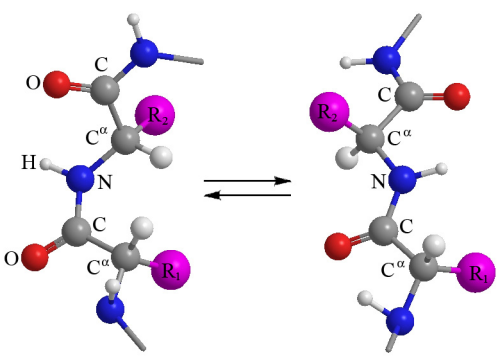

Figure 4. *Cis-trans* isomerization in a peptide bond. Left, a *cis* amide bond; right, a *trans* amide bond. The amide torsion angle ω (C^{α}-C-N-C^{α}) is 0° for the *cis* form and 180° for the *trans* form.

Amide bond isomerization is important in many processes that require alteration to protein structure, among them the transport

of polypeptides through membranes and oligomerization and folding of proteins.[11-13]

Usual amides are strongly stabilized by mesomeric effect involving an sp^2 hybridized *N*-atom; in the highly constrained 3-membered ring the amide nitrogen is practically sp^3 hybridized with high loss of the usual stability. The conjugation is maintained, but weaker than a normal amide bond. This feature deeply affects the structural and chemical properties of the R-CO-Azy- fragment as well as the conformation of Azy containing peptides: a) lengthening of the CO-N bond; b) higher reactivity toward ring opening by nucleophiles; c) higher lability of the peptide bond; d) alteration of the usual ^{1}H- and ^{13}C-NMR values. Concerning ^{13}C-NMR, the spectra are diagnostic for the presence of an acylated Azy residue. Generally, chemical shifts of amide peptide carbonyl groups are in the range 167-175 ppm. The carbonyl group attached to the aziridine nitrogen is more ketone-like. As a consequence of the acquired ketone character, the Azy amide carbonyl group appears in the range 180-184 ppm.

In order to acquire more information on the incorporation of the Azy residue into peptide backbones we chose as suitable models two bioactive oligopeptides: a) the chemotactic tripeptide For-Met-Leu-Phe-OMe with the Azy residue in place of the central Leu; b) the opioid tetrapeptide Tyr-Pro-Phe-Phe-

NH_2 (endomorphin-2) with the Azy residue replacing the native Pro at position 2 (Figure 5).

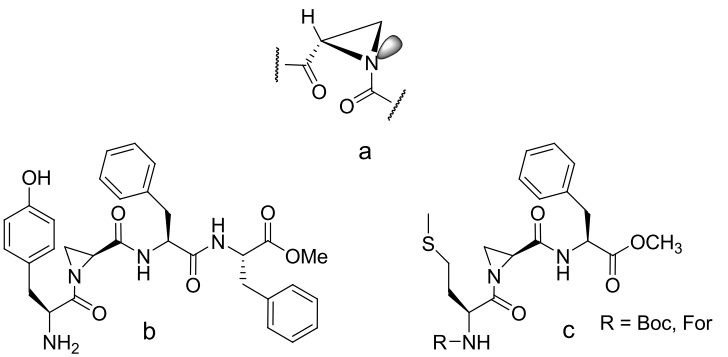

Figure 5. Structure of a) *N*-acylated Azy residue, b) Tyr-Azy-Phe-Phe-OMe, c) R-NH-Met-Azy-Phe-OMe.

3.3 On the synthesis of (*S*)-Aziridine-2-carboxylic acid containing bioactive peptides

For both the structural features and chemical reactivity, synthesis of Azy containing peptides require special attention. Concerning the synthesis of Azy residue, several methods have been considered in the past.[14-16] We chose an efficient one-pot synthesis, recently reported in literature,[17] in which *N*-trityl-aziridine-2-carboxylic acid **5** was prepared from L-serine methyl ester hydrochloride **1** (Scheme 2). The choice of trityl group as *N*-protecting alkyl group was made both to protect the α-center of amino acid from base-promoted racemization and to protect *N*-acylated serine from elimination to give didehydroalanine.

The replacement of Leu at position 2 in chemotactic tripeptide For-Met-Leu-Phe-OMe with Azy was unsuccessfull.

Synthesis of Trt-Azy-Phe-OMe and the subsequent trityl deprotection were performed following standard literature methods of solution phase synthesis of peptides (Scheme 3)[18] and compounds **6** and **7** were obtained in high yield.

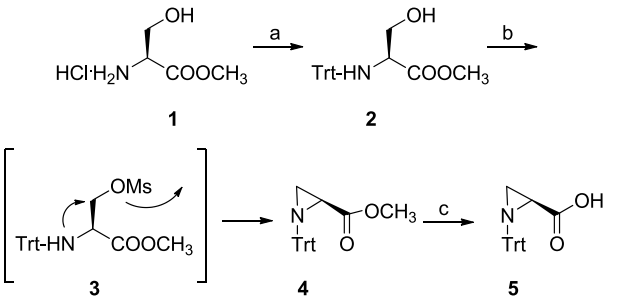

Scheme 2. Synthesis of *N*-trityl-aziridine-2-carboxylic acid **5**. *Reagents and conditions*: a) Trt-Cl, TEA, $CHCl_3$, 24h 0 °C; b) MsCl, TEA, THF, 30 min 0 °C, 48h reflux; c) 1.5N NaOH, THF, 30 min 0 °C, overnight rt.

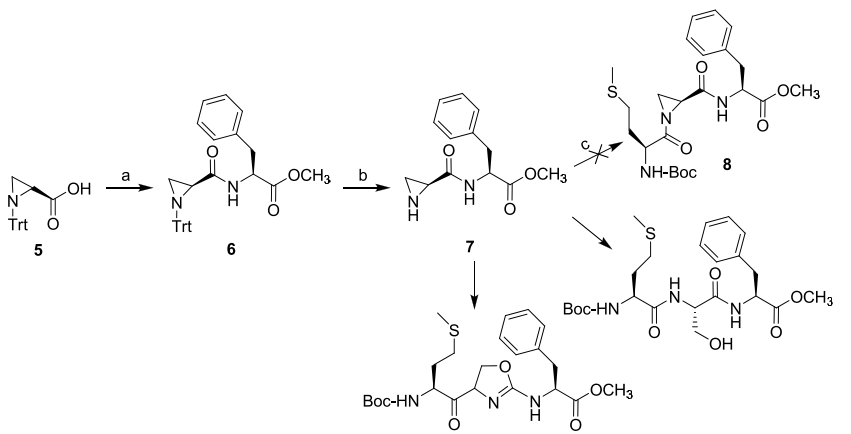

Scheme 3. Attempted synthesis of **8**. *Reagents and conditions*: a) HCl·H_2N-Phe-OMe, EDC, HOBt, NMM, CH_2Cl_2, 30 min 0 °C, 12h rt; b) TFA, CH_2Cl_2, MeOH, 0°C, overnight; c) Boc-Met-OH, BOP, DIPEA, $CHCl_3$, 30 min 0 °C, 12h rt.

Coupling of the HN-Azy-Phe-OMe with Boc-Met-OH leads to two main products instead of the expected tripeptide **8** (Scheme 3). Available spectral data suggested ring expansion of the Azy residue to an oxazoline[6] system and opening of the 3-membered ring. Then, coupling by using Boc-Nle-OH in place of Boc-Met-OH was designed (see product **9** in Scheme 4). However, notwithstanding the adoption of Boc-Nle-OH as acylating agent, the same products isolated in the reaction with Boc-Met-OH were identified.

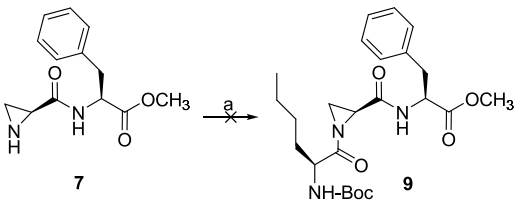

Scheme 4. Attempted synthesis of **9**. *Reagents and conditions*: a) Boc-Nle-OH, BOP, DIPEA, $CHCl_3$, 30 min 0 °C, 12h rt.

The replacement of Pro at position 2 of Boc-derivative **12** of EM-2 was performed following standard literature methods of solution phase synthesis of peptides (Scheme 5).[19]

Boc-tetrapeptide **12** was synthesized, although with low yields, without difficulty. Synthesis of EM-2 containing Azy residue in place of Pro[2] was difficult. Due to the presence of the *N*-acylated -Azy-fragment, the removal conditions usually adopted for the *N*-Boc protecting group, cannot be used in the case of Azy containing peptides. Deprotection mediated by

tetrabutyl-ammonium fluoride (TBAF)[20] was then considered. Despite the mild conditions adopted the desired Azy containing peptide H_2N-Tyr-Azy-Phe-Phe-NH_2 was not formed. The main product of the reaction was identified as the didehydroalanine (ΔAla) containing tetrapeptide Boc-Tyr-ΔAla-Phe-Phe-NH_2 (**13**, Scheme 5).

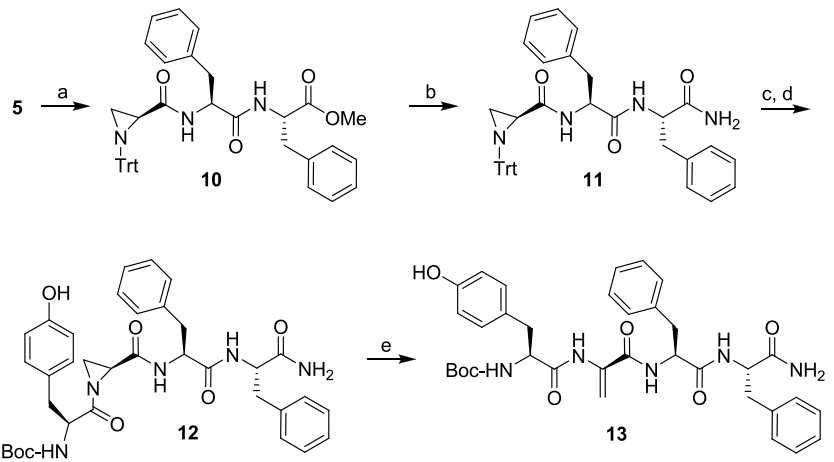

Scheme 5. Attempted synthesis of H_2N-Tyr-Azy-Phe-Phe-NH_2. *Reagents and conditions*: a) HCl·H_2N-Phe-Phe-OMe, EDC, HOBt, NMM, CH_2Cl_2, 30 min 0 °C, 12h rt; b) MeOH 0 °C/NH_3 sat., 24h rt; c) TFA, CH_2Cl_2, MeOH, 0°C overnight; d) Boc-Tyr-OH, BOP, DIPEA, $CHCl_3$, 30 min, 0 °C, 12h rt; e) TBAF, THF, 4h, reflux.

Then, we chose to adopt the carboxybenzyl (Cbz) as protecting group. Literature data[21] demonstrate in fact the compatibility of Azy containing peptides with catalytic hydrogenolysis. Contrary to the expectation, the catalytic hydrogenolysis of Z-Tyr-Azy-Phe-Phe-NH_2 led to a Tyr deprived tripeptide (Scheme 6). A reasonable explanation of this

result points toward an intermolecular deacylation. The concurrent intramolecular reaction, leading to a diketopiperazine, cannot take place since the starting tetrapeptide lacks a residue preceding the *N*-terminal Tyr.

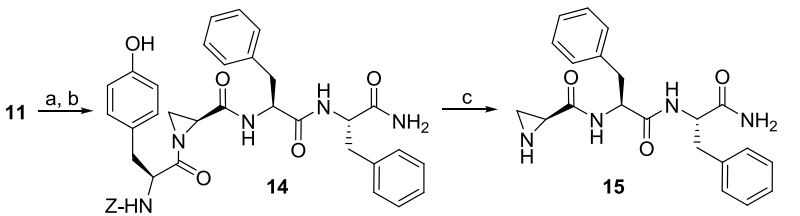

Scheme 6. Attempted synthesis of H_2N-Tyr-Azy-Phe-Phe-NH_2. *Reagents and conditions*: a) TFA, CH_2Cl_2, MeOH, 0°C overnight; b) Z-Tyr-OH, BOP, DIPEA, $CHCl_3$, 30 min 0 °C, 12h rt; c) H_2-Pd/C, MeOH, 5h rt.

In order to circumvent the above reported unexpected result, use of fluorenylmethoxycarbonyl (Fmoc) as protecting group appeared convenient. It has been in fact previously reported that the Fmoc removal, which is usually performed with piperidine, can be also advantageously achieved by replacing secondary amines (not compatible with the *N*-acyl-Azy moiety) with the non nucleophilic base 1,8-diazabicyclo[5.4.0]undec-7-ene (DBU).[22] This approach was then considered suitable and adopted in the case of the tetrapeptide model Fmoc-Tyr-Azy-Phe-Phe-OMe (**16**, Scheme 7). Furthermore, adoption of the *C*-terminal methyl ester, instead of the CO-NH_2 group, was imposed by the high insolubility shown by the tetrapeptide amide.

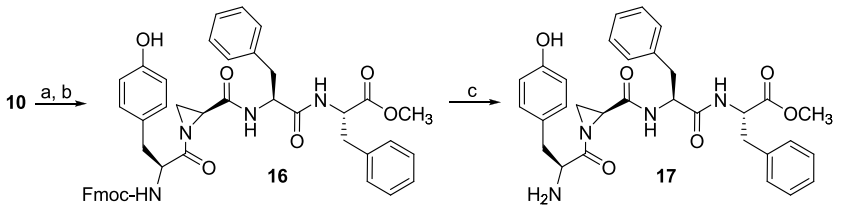

Scheme 7. Synthesis of H_2N-Tyr-Azy-Phe-Phe-OCH_3 **17**. *Reagents and conditions*: a) TFA, CH_2Cl_2, MeOH, 0°C, overnight; b) Fmoc-Tyr-OH, BOP, DIPEA, $CHCl_3$, 30 min 0 °C, 12h rt; c) DBU, CH_2Cl_2, 5 min rt.

3.3.1 X-ray crystal structure of tripeptide Trt-Azy-Phe-Phe-NH_2

Suitable X-ray crystal of the tripeptide **11** were obtained from MeOH solution.

Crystallographic analysis showed the conformation reperted in Figure 6 was studied. Table 1 reports the main torsion angles of the molecule.

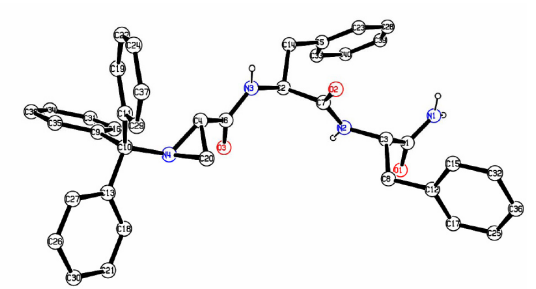

Figure 6. Crystal structure of Trt-Azy-Phe-Phe-NH_2 **(11)**. N_4 is 0.603(4) Å out of the plain defined by C_4, C_{10} and C_{20}.

This shows an highly pyramidalized Azy nitrogen atom and adopts an extended conformation which can be described by two

consecutive enlarged inverse γ-turns centered at the two Phe residues.

Table 1. Main torsion angles (°) of *N*-Trt-Azy-Phe-Phe-NH_2.

C_{10} - N_4 - C_4 - C_6	ϕ_1	-141.76
N_4 - C_4 - C_6 - N_3	ψ_1	175.01
C_2 - N_3 - C_6 - C_4	ω_1	164.21
C_6 - N_3 - C_2 - C_7	ϕ_2	-93.42
N_3 - C_2 - C_7 - N_2	ψ_2	137.26
C_3 - N_2 - C_7 - C_2	ω_2	170.68
C_7 - N_2 - C_3 - C_1	ϕ_3	-144.41
N_1 - C_1 - C_3 - N_2	ψ_3	110.29

3.4 Conclusions

A study of the Azy containing peptides synthesis, protection/deprotection conditions and reactivity has been reported. As previously reported, during the synthesis of the chemotactic tripeptide containing a central Azy residue opening and rearrangement of the Azy ring was observed. The failure of the desired reaction was initially attributed to an anchimeric assistance by the sulphur containing Met side chain.

In order to clarify this point, coupling by using Boc-Nle-OH in place of Boc-Met-OH was designed (see product **9** in Scheme 4). However, notwithstanding the adoption of Boc-Nle-OH as acylating agent, the same products isolated in the reaction with Boc-Met-OH were identified. It has been then evidenced an inherent instability to the adopted deprotection conditions of the dipeptide Trt-Azy-Phe-OMe not observed in the case of the analogue deprotection on tripeptide Trt-Azy-Phe-Phe-OMe.

Finally, a previously not known rearrangement, leading from Azy to ΔAla residues, has been evidenced and this result represents an interesting starting point for further research. Thus, it has been shown that a proper choice of *N*-protection and deprotection conditions (i.e. Fmoc/DBU) can lead to the synthesis of endomorphin-2 analogues, containing the conformationally restricted Azy residue in place of the native Pro at position 2.

In addition to this the X-ray chrystallographic analysis of the *N*-Trt-Azy-Phe-Phe-NH_2 **11** gives the first information on the conformation adopted in the crystal by an Azy containing EM-2 analogue.

3.5 Experimental section

Materials and methods. Melting points were determined with a Büchi B 540 apparatus and are uncorrected. ^{1}H NMR experiments were performed at 400 MHz on a Bruker AM 400 spectrometer in $CDCl_3$ solution (unless otherwise specified) and chemical shifts (δ) are quoted in parts per million (ppm) and were indirectly referred to TMS. TLC (thin layer chromatography) and PLC (preparative layer chromatography) were performed on silica gel Merck 60 F_{254} plates. The drying agent was sodium sulphate.

3.5.1 Chemistry. General procedures

A. Coupling with the carbodiimide method. To an ice-cooled mixture containing the required *N*-protected-amino acid (1.1 mmol), HOBt (1.1 mmol), EDC (1.1 mmol) in anhydrous CH_2Cl_2, the amino-derivative salt (1.0 mmol), and NMM (2.2 mmol), was added and the reaction mixture was allowed to warm to room temperature. After 12 h the reaction mixture was diluted with EtOAc (20 mL) and washed with 5% citric acid (2 x 15 mL), saturated aqueous $NaHCO_3$ (2 x 15 mL) and brine (15 mL). The organic phase was dried over Na_2SO_4 and evaporated under reduced pressure.

B. Coupling with BOP. To solution of amino acid (1.5 mmol), amino- peptide-derivative salt (1.0 mmol) and BOP (1.5 mmol) in CH_2Cl_2, DIPEA (2.0 mmol) was added dropwise and the reaction mixture was allowed to warm to room temperature. After 12 h the reaction mixture was diluted with CH_2Cl_2 (20 mL) and washed with 5% citric acid (15 mL), saturated aqueous $NaHCO_3$ (15 mL) and brine (15 mL). The organic phase was dried over Na_2SO_4 and evaporated under reduced pressure.

3.5.2 Synthesis

Trt-Ser-OMe (2). TEA (6.13 mL, 44 mmol) was added dropwise to a stirred suspension of L-serine methyl ester

hydrochloride **1** in $CHCl_3$ at room temperature. On dissolution, the solution was cooled to 0 °C and then triphenylmethyl chloride (5.57 g, 20 mmol) was added. The solution was stirred at 0 °C for 24 h and then washed with 10% citric acid (2 x 20 mL) and water (20 mL). The combined organic extracts were dried and evaporated in vacuo to give the title compound as white solid pure on TLC (7.01 g, 97%) that was used without further purification.

Trt-Azy-OMe (4). TEA (1.6 mL, 11.4 mmol) was added dropwise to a stirred solution of **2** (1.375 g, 3.80 mmol) in anhydrous THF (10 mL) at 0 °C. Methanesulfonyl chloride (0.44 mL, 5.7 mmol) was added dropwise and the solution was stirred at 0 °C for 30 min and then at reflux for 48 h. The solvent was removed in vacuo to give a residue which was taken up in ethyl acetate (20 mL) and washed with 5% citric acid (3 x 15 mL), $NaHCO_3$ ss (2 x 15 mL) and NaCl ss (15 mL). The combined organic extracts were dried and evaporated in vacuo. Silica gel chromatography (CH_2Cl_2) gave the title compound as white foam (1.042 g, 80%); ^{1}H NMR ($CDCl_3$): δ 1.45 (1H, m, β-*H*CH), 1.91 (1H, m, α-CH), 2.29 (1H, m, β-*H*CH), 3.79 (3H, s, $COOCH_3$), 7.18-7.61 (15 H, m, aromatics).

Trt-Azy-OH (5). To solution of **4** (1.0 g, 2.92 mmol) in THF (3 mL) was added 1.5N NaOH (2.92 mL) at 0 °C. The solution was stirred at 0 °C for 12 h. Then was evaporated under reduced pressure, diluted with water and washed with Et_2O (2 x 15 mL).

The aqueous phase was then acidified with 5% citric acid and extracted with EtOAc (3 x 20 mL). The combined organic phases were washed with brine, dried and evaporated. A white foam (0.92 g, 96%), was obtained and used without further purification.

***N*-Boc-Phe-Phe-OMe.** *N*-Boc-Phe-OH (0.895 g, 3.71 mmol) in CH_2Cl_2 (60 mL) was treated with HCl·H_2N-Phe-OMe (0.727 g, 3.37 mmol) according to the general procedure A. The title compound was obtained as a white solid, pure on TLC (1.246 g, 87%); $[a]_D$ +34.28° (*c* 1, $CHCl_3$); IR ($CHCl_3$): ν 3423, 1742, 1677 cm^{-1}; ^1H NMR ($CDCl_3$): δ 1.42 [9H, s, $C(CH_3)_3$], 3.07 (4H, m, Phe^3 and Phe^4 β-CH_2), 3.70 (3H, s, $COOCH_3$), 4.35 (1H, m, Phe^3 α-CH), 4.81 (1H, m, Phe^4 α-CH), 4.93 (1H, br s, Phe^3 NH), 6.29 (1H, br s, Phe^4 NH), 7.00-7.30 (10H, m, aromatics). Anal. Calcd for $C_{24}H_{30}N_2O_5$: C, 67.59; H, 7.09; N, 6.57. Found: C, 67.86; H, 7.11; N, 6.59.

TFA·H_2N-Phe-Phe-OMe. The Boc group was removed by treatment of *N*-Boc-Phe-Phe-OMe (0.381 g, 0.89 mmol) with TFA in CH_2Cl_2 (1:1, 6 mL) for 1 h at room temperature. Removal of solvent and precipitation of the residue with diethyl ether gave TFA·H_2N-Phe-Phe-OMe (0.392 g, quantitative yield) that was used in the next step without further purification.

Trt-Azy-Phe-Phe-OMe (10). Trt-Azy-OH (0.322 g, 0.979 mmol) in CH_2Cl_2 (10 mL) was treated with TFA·H_2N-Phe-Phe-OMe (0.392 g, 0.89 mmol) according to the general procedure

A. Silica gel chromatography ($CHCl_3$/EtOAc 95:5) gave a pure product as a white foam (0.397 g, 70%); ^{1}H NMR ($CDCl_3$): δ 1.32 (1H, m, Azy β-*H*CH), 1.47 (1H, m, Azy α-CH), 1.93 (1H, m, Azy β-*H*CH), 3.03-3.21 (4H, m, Phe^3 β-CH_2 and Phe^4 β-CH_2), 3.70 (3H, s, $COOCH_3$), 4.62 (1H, m, Phe α-CH), 4.84 (1H, m, Phe α-CH), 6.50 (1H, d, *J* = 7.6 Hz, Phe NH), 7.18 (1H, m, Phe NH), 7.01-7.48 (25 H, m, aromatics).

Trt-Azy-Phe-Phe-NH_2 (11). The peptide methyl ester **9** (0.200 g, 0.314 mmol) is allowed to stand in a pressure bottle at room temperature for 48 h in anhydrous MeOH (9.25 mL) previously saturated with ammonia gas at 0 °C for 24 h. The solution is then concentrated to dryness in vacuo at a temperature not exceeding 40 °C. The title compound was obtained as white crystal (0.18 g, 93%); mp 245.7-247.6 °C; ^{1}H NMR ($CDCl_3$): δ 1.34 (1H, m, Azy β-*H*CH), 1.48 (1H, m, Azy α-CH), 1.93 (1H, m, Azy β-*H*CH), 3.03-3.21 (4H, m, Phe^3 β-CH_2 and Phe^4 β-CH_2), 4.53 (1H, m, Phe α-CH), 4.75 (1H, m, Phe α-CH), 5.31 (1H, br s, CON*H*H), 5.95 (1H, br s, CON*H*H), 6.55 (1H, d, *J* = 8.0 Hz, Phe NH), 7.23 (1H, m, Phe NH), 7.14-7.51 (25 H, m, aromatics).

HN-Azy-Phe-Phe-NH_2. To an ice cooled solution of **11** (0.226 g, 0.363 mmol) in $CHCl_3$ (0.72 mL) and absolute MeOH (0.5 mL, used as a scavenger of trityl group), TFA (0.15 mL) was added. The solution was stirred for 12 h at 0 °C. Then the solvent was removed in vacuo and the residue was partitioned

between diethyl ether and water. $NaHCO_3$ was added to aqueous layer. The aqueous phase was extracted with EtOAc (3 x 20 mL). The combined organic phases were washed with brine, dried and evaporated. The obtained product (0.124 g, 90%), was used for the next step.

Boc-Tyr-Azy-Phe-Phe-NH_2 (12). Boc-Tyr-OH (0.100 g, 0.355 mmol) in THF (5.8 mL), was treated with HN-Azy-Phe-Phe-NH_2 (0.090 g, 0.237 mmol) according to the general procedure B. PLC (EtOAc) gave a pure product as a white foam (0.061 g, 40%); ^{1}H NMR (DMSO-d_6): δ 1.39 [9H, s, $C(CH_3)_3$], 2.19 (1H, m, Azy β-*H*CH), 2.51 (1H, m, Azy α-CH), 2.60-3.03 (6H, m, Tyr β-CH_2, Phe^3 β-CH_2 and Phe^4 β-CH_2), 3.05 (1H, m, Azy β-*H*CH), 4.09 (1H, m, Tyr α-CH), 4.38 (1H, m, Phe α-CH), 4.51 (1H, m, Phe α-CH), 6.94 (1H, d, J = 8.0 Hz, Tyr NH), 6.63-7.28 (16H, m, aromatics and $COONH_2$), 8.17 (1H, d, J = 8.4 Hz, Phe NH), 8.39 (1H, d, J = 8.0 Hz, Phe NH), 9.24 (1H, s, Tyr OH).

Attempted synthesis of H_2N-Tyr-Azy-Phe-Phe-NH_2. To a THF (5 mL) solution of **12** (0.023 g, 0.036 mmol) a solution of tetrabutylammonium fluoride (TBAF, 1M in THF, 0.072 mL) was added, and the mixture was stirred under reflux for 4 h. Then the solvent was evaporated, the residue was dissolved in EtOAc and washed with 2M $NaHCO_3$ and water. The organic layer was dried and evaporated under reduced pressure. PLC ($CHCl_3$/MeOH 9:1) gave a pure product **13** (0.013 g, 67%); ^{1}H

NMR (DMSO-d_6): δ 1.39 [9H, s, $C(CH_3)_3$], 2.60-3.03 (6H, m, Tyr β-CH_2, Phe^3 β-CH_2 and Phe^4 β-CH_2), 4.09 (1H, m, Tyr α-CH), 4.38 (1H, m, Phe α-CH), 4.51 (1H, m, Phe α-CH), 6.94 (1H, d, J = 8.0 Hz, Tyr NH), 5.48 (1H, s, ΔAla C*H*H), 6.17 (1H, s, ΔAla C*H*H), 6.62-7.38 (17H, m, aromatics, Tyr NH and $COONH_2$), 8.08 (1H, d, J = 8.0 Hz, Phe NH), 8.49 (1H, d, J = 8.4 Hz, Phe NH), 9.16 (1H, s, Tyr OH).

Z-Tyr-Azy-Phe-Phe-NH_2 (14). Z-Tyr-OH (0.092 g, 0.292 mmol) in CH_2Cl_2 (4.7 mL), was treated with HN-Azy-Phe-Phe-NH_2 (0.074 g, 0.195 mmol) according to the general procedure B. PLC (EtOAc) gave a pure product as an amorfous solid (0.035 g, 26%); ^{1}H NMR (DMSO-d_6): δ 2.22 (1H, m, Azy β-*H*CH), 2.52 (1H, m, Azy α-CH), 2.60-3.05 (6H, m, Tyr β-CH_2, Phe^3 β-CH_2 and Phe^4 β-CH_2), 3.14 (1H, m, Azy β-*H*CH), 4.19 (1H, m, Tyr α-CH), 4.43 (1H, m, Phe α-CH), 4.53 (1H, m, Phe α-CH), 5.15 (m, 2H, C_6H_5-C*H*$_2$-O), 6.61-7.35 (16H, m, aromatics and $COONH_2$), 7.53 (1H, d, J = 8.4 Hz, Tyr NH), 8.17 (1H, d, J = 8.0 Hz, Phe NH), 8.43 (1H, d, J = 8.4 Hz, Phe NH), 9.22 (1H, s, Tyr OH).

Attempted synthesis of H_2N-Tyr-Azy-Phe-Phe-NH_2. A solution of **14** (0.018 g, 0.026 mmol) in MeOH and 10% Pd on C (10%) was vigorously stirred at room temperature and atmospheric pressure for 5 h under a slow stream of hydrogen. The catalyst was removed by filtration and washed with MeOH.

The filtrate was evaporated under reduced pressure. To this compound the structure **15** was assigned.

Fmoc-Tyr-Azy-Phe-Phe-OCH_3 (16). Fmoc-Tyr-OH (0.092 g, 0.228 mmol) in CH_2Cl_2 (5 mL), was treated with HN-Azy-Phe-Phe-NH_2 (0.045 g, 0.114 mmol) according to the general procedure B. PLC ($CHCl_3$/EtOAc 8:2) gave a pure product as an amorfous solid (0.027 g, 31%); ^{1}H NMR ($CDCl_3$): δ 1.36 (1H, m, Azy β-*H*CH), 2.48 (1H, m, Azy α-CH), 2.75-3.25 (7H, m, Tyr β-CH_2, Phe^3 β-CH_2, Phe^4 β-CH_2 and Azy β-*H*CH), 3.76 (3H, s, $COOCH_3$), 4.18 (1H, m, Fmoc CH), 4.32 (1H, m, Tyr α-CH), 4.36 (2H, m, Fmoc OCH_2), 4.49 (1H, m, Phe α-CH), 4.82 (1H, m, Phe α-CH), 5.39 (1H, d, *J* = 7.6 Hz, Tyr NH), 5.49 (1H, d, *J* = 8.4 Hz, Phe NH), 6.74 (1H, d, *J* = 7.6 Hz, Phe NH), 6.69-7.88 (24H, m, aromatics).

H_2N-Tyr-Azy-Phe-Phe-OCH_3 (17). To a solution of **16** (0.050 g, 0.064 mmol) in CH_2Cl_2 (0.44 mL), DBU (0.039 g, 0.07 mmol) was added at room temperature. After 20 min the solution was evaporated to dryness. Silica gel chromatography (EtOAc/MeOH 97:3) gave a pure product **17** (0.021 g, 59%); ^{1}H NMR (DMSO-d_6): δ 1.80 (2H, br s, Tyr NH_2), 2.21 (1H, m, Azy β-*H*CH), 2.37 (1H, m, Azy α-CH), 2.63-3.11 (7H, m, Tyr β-CH_2, Phe^3 β-CH_2, Phe^4 β-CH_2 and Azy β-*H*CH), 3.61 (3H, s, $COOCH_3$), 4.49 (3H, m, Tyr α-CH, Phe^3 α-CH and Phe^4 α-CH), 6.50-7.38 (15H, m, aromatics and Phe NH), 8.50 (1H, br s, Phe NH).

Trt-Azy-Phe-OMe (6). Compound **5** (0.281 g, 0.853 mmol) in CH_2Cl_2 (10 mL) was treated with $HCl \cdot H_2N$-Phe-OMe (0.153 g, 0.711 mmol) according to the general procedure A. Silica gel chromatography (Hexane/EtOAc 8:2) gave a pure product **6** as a white foam (0.327 g, 94%); ^1H NMR ($CDCl_3$): δ 1.40 (1H, m, Azy β-*H*CH), 1.71 (1H, m, Azy α-CH), 1.97 (1H, m, Azy β-*H*CH), 3.22-3.24 (2H, m, Phe β-CH_2), 3.84 (3H, s, $COOCH_3$), 4.96 (1H, m, Phe α-CH), 7.33 (1H, br s, Phe NH), 7.19-7.46 (20 H, m, aromatics).

HN-Azy-Phe-OMe (7). To an ice cooled solution of **6** (0.267 g, 0.546 mmol) in $CHCl_3$ (9.44 mL) and absolute MeOH (6.55 mL, used as a scavenger of trityl group), TFA (1.7 mL) was added. The solution was stirred for 12 h at 0 °C. Then the solvent was removed in vacuo and the residue was partitioned between diethyl ether and water. $NaHCO_3$ was added to aqueous layer. The aqueous phase was extracted with EtOAc (3 x 20 mL). The combined organic phases were washed with brine, dried and evaporated. The obtained product was used for the next step.

References

1. Nielsen, I. M. B. *J. Phys. Chem. A.* **1998**, *102*, 3193.
2. Atkinson, R. S.; Malpass, J. R. J. *Chem. Soc., Perkin Trans.* **1977**, *1*, 2242.

3. Pearson, W. H.; Lian, B. W.; Bergmeier, S. C. In *Comprehensive Heterocyclic Chemistry II*, Katritzky, A. R.; Rees, C. W.; Scriven, E.F.V. (Eds).; Elsevier, Oxford, **1996**, vol. 1A, p.1.
4. Hu, X. *Tetrahedron* **2004**, *60*, 2701.
5. Tanner, D. *Angew. Chem. Int. Ed. Engl.* **1994**, *33*, 599.
6. Cardillo, G.; Gentilucci, L.; Tolomelli, A. *Aldrichimica Acta*, **2003**, *36*, 39.
7. Galonic, D. P.; Ide, N. D.; van der Donk, W. A.; Gin, D. Y. *J. Am. Chem. Soc.* **2005**, *127*, 7359.
8. Schirmeister, T.; Peric, M. *Bioorg. Med. Chem.* **2000**, *8*, 1281.
9. Ramachandran, G. N.; Sasisekharan, V. In *Advances in Protein Chemistry*. Anfinsen, C. B.; Anson, M. L.; Edsall, J. T.; Richards, F.M. (Eds.), Academic Press, New York. **1968** pp. 283-438.
10. Levitt, M.; Lifson, S. *J. Mol. Biol.* **1969**, *46*, 269.
11. Fischer, G. *Angew. Chem. Int. Ed. Engl.* **1994**, *33*, 1415.
12. Fischer, G.; Wittmann-Liebold, B.; Lang, K.; Kiefhaber, T.; Schmid, F.X. *Nature* **1989** *337*, 475.
13. Fischer, S.; Michnick, S.; Karplus, M. *Biochemistry* **1993**, *32*, 13830.
14. Nakajima, K.; Takai, F.; Tanaka, T.; Okawa, K. *Bull. Chem. Soc. Jpn.* **1978**, 51, 1577.
15. Sato, K.; Kozikowski, A. P. *Tetrahedron Lett.* **1989**, *30*, 4073.
16. Yeheskiely-Kuyl, E.; Lodder, M.; van der Marel, G. A.; van Boom, J. H. *Tetrahedron Lett.* **1992**, *33*, 3013.
17. McKeever, B.; Pattenden, G. *Tetrahedron* **2003**, *59*, 2713.
18. Bodansky, M. In *Principles of Peptide Synthesis*; Springer: Berlin, **1984**.
19. Bodansky, M. In *Principles of Peptide Synthesis*; Springer: Berlin, **1984**.

20. Fioravanti, S.; Massari, D.; Morreale, A.; Pellacani, L.; Tardella, P. A. *Tetrahedron* **2008**, *64*, 3204.
21. Schirmeister, T.; Peric, M. *Bioorg. Med. Chem.* **2000**, *8*, 1281.
22. Galonic, D. P.; Ide, N. D.; van der Donk, W. A.; Gin, D. Y. *J. Am. Chem. Soc.* **2005**, *127*, 7359.

Papers

1. Domenica Torino, Adriano Mollica, Francesco Pinnen, Federica Feliciani, Gino Lucente, Giancarlo Fabrizi, Gustavo Portalone, Peg Davis, Josephine Lai, Shou-Wu Ma, Frank Porreca, Victor J. Hruby. Synthesis and evaluation of new endomorphin-2 analogues containing (Z)-α,β-didehydro-phenylalanine (Δ^{Z}Phe) residues. *J. Med. Chem.* (*submitted*).

2. Adriano Mollica, Azzurra Stefanucci, Federica Feliciani, Domenica Torino, Ivana Cacciatore, Catia Cornacchia, Francesco Pinnen, Gino Lucente. Facile transformation of glutamic acid into proline residue inside a tripeptide backbone. *Tetrahedron Lett.* (*accepted* 01.06.2009).

3. Domenica Torino, Adriano Mollica, Francesco Pinnen, Gino Lucente, Federica Feliciani, Peg Davis, Josephine Lai, Shou-Wu Ma, Frank Porreca and Victor J. Hruby. Synthesis and evaluation of new endomorphin analogues modified at the Pro^2 residue. *Bioorganic and Medicinal Chemistry Letters* **2009**, *19*, 4115.

4. Pasquale Mura, Mercedes Camalli, Gaetano Campi, Gino Lucente, Cesare Giordano, Adriano Mollica, Anna Sansone and Domenica Torino. X-ray crystal structure

and conformation of *N*-(*tert*-butyloxycarbonyl)-L-methionyl-(1-aminocyclopenten-3-ene-1-cabonyl)-L-phenylalanine methyl ester (Boc^0-Met^1-Cpg^2-Phe^3-OMe). *Zeitschrift für Kristallographie* **2009**, *224*, 225.

5. Domenica Torino, Adriano Mollica, Francesco Pinnen, Federica Feliciani, Susanna Spisani and Gino Lucente. Novel chemotactic For-Met-Leu-Phe-OMe (f-MLF-OMe) analogues based on Met residue replacement by 4-amino-proline scaffold: Synthesis and bioactivity. *Bioorganic and Medicinal Chemistry* **2009**, *17*, 251.

6. Gino Lucente, Cesare Giordano, Anna Sansone, Domenica Torino and Susanna Spisani. Synthesis and bioactivity of chemotactic tetrapeptides: fMLF-OMe analogues incorporating spacer aminoacids at the lateral positions. *Amino Acids* **2009***, 37*, 285.

7. Gino Lucente, Mario Paglialunga Paradisi, Cesare Giordano, Anna Sansone, Domenica Torino and Susanna Spisani. Chemotactic tripeptides incorporating at position 2 α-aminoacid residues with unsaturated side chains. *Amino Acids* **2008**, *35*, 329.

8. Adriano Mollica, Mario Paglialunga Paradisi, Domenica Torino, Susanna Spisani and Gino Lucente. Hybrid α/β-peptides: For-Met-Leu-Phe-OMe analogues containing geminally disubstituted $\beta^{2,2}$- and $\beta^{3,3}$ amino acids at the central position. *Amino Acids* **2006**, *30*, 453.

Acknowledgments

The elaboration of this PhD Thesis has been possible thanks to the precious help given by

Prof. Gino LUCENTE
Dipartimento di Chimica e Tecnologie del Farmaco, Sapienza University of Rome, Italy

Prof. Enrico MORERA
Dipartimento di Chimica e Tecnologie del Farmaco, Sapienza University of Rome, Italy

Prof. Mario PAGLIALUNGA PARADISI
Dipartimento di Chimica e Tecnologie del Farmaco, Sapienza University of Rome, Italy

Prof. Victor J. HRUBY and his research group
Department of Chemistry and Department of Pharmacology, University of Arizona, Tucson, USA

Prof. Susanna SPISANI
Dipartimento di Biochimica e Biologia Molecolare, University of Ferrara, Italy

Prof. Francesco PINNEN
Dipartimento di Scienze del Farmaco, University of Chieti-Pescara "G. d'Annunzio", Italy

I would also like to recognize the collaboration which I had with the following researcher

Dr. Adriano MOLLICA
Dipartimento di Scienze del Farmaco, University of Chieti-Pescara "G. d'Annunzio", Italy

Dr. Anna SANSONE
Dipartimento di Scienze Chimiche, University of Padua, Italy

Dr. Cesare GIORDANO
Istituto di Chimica Biomolecolare del CNR, c/o Dipartimento di Chimica e Tecnologie del Farmaco, Sapienza University of Rome, Italy

Dr. Valentina NARDONE
Dipartimento di Chimica e Tecnologie del Farmaco, Sapienza University of Rome, Italy

Dr. Federica FELICIANI
Dipartimento di Scienze del Farmaco, University of Chieti-Pescara "G. d'Annunzio", Italy

Thanks are also due to

Prof. Gustavo PORTALONE
Dipartimento di Chimica, Sapienza University of Rome, Italy

Prof. Giancarlo FABRIZI
Dipartimento di Chimica e Tecnologie del Farmaco, Sapienza University of Rome, Italy

who gave me assistance for X-ray crystal analisys and 2D ^{1}H NMR experiments.

Special Thanks

Dr. Francesco PISCITELLI
Department of Chemistry, University of Pennsylvania, Philadelphia, USA

Peptides play an important role in the organism and highly influence all vital physiological processes *via* inter- and intra-cellular communication and signal transduction mediated by various classes of receptors. The study of the peptides has acquired a key role in medicinal chemistry and a multitude of biologically active peptides have been discovered and characterized during the last decades. Although native biologically active peptides have a great potential for therapeutical applications, their use as drugs is limited by different factors: i) low metabolic stability; ii) low level of oral absorption; iii) very scarce capacity to cross the blood-brain barrier; iv) low receptor selectivity. In order to circumvent these limitations, proper structural modifications of the natural models have been designed and realized. The family of peptidomimetics offers an advantageous solution to these problems and their chemistry and pharmacological properties are the object of continuous interest.

In this PhD thesis design and synthetical strategy leading to structural analogues of two relevant groups of biologically active peptides are treated: i) Endomorphins, the most potent μ-selective endogenous opioid peptides recently isolated from bovine brain and human cortex and ii) Chemotactic *N*-formyl peptides, the neutrophil receptor agonists active against bacterial infections.